AIIM

Association for Information and Image Management
1100 Wayne Avenue, Suite 1100
Silver Spring, Maryland 20910
301/587-8202

Centimeter

Inches

MANUFACTURED TO AIIM STANDARDS
BY APPLIED IMAGE, INC.

1 of 2

SAND93-0089
Unlimited Release
Printed April 1994

Distribution
Category UC-721

SECOND PERFORMANCE ASSESSMENT ITERATION OF THE GREATER CONFINEMENT DISPOSAL FACILITY AT THE NEVADA TEST SITE

Thomas A. Baer[1], Laura L. Price[2], James N. Emery[1], Natalie E. Olague[3]

Safety and Risk Assessment Department
Sandia National Laboratories
Albuquerque NM, 87185

Abstract

The Greater Confinement Disposal (GCD) facility was established by the Nevada Operations Office of the Department of Energy (DOE) in Area 5 at the Nevada Test Site for containment of waste inappropriate for shallow land burial. Some transuranic (TRU) waste has been disposed of at the GCD facility, and compliance of this disposal system with Environmental Protection Agency (EPA) regulation 40 CFR 191 must be evaluated by performance assessment calculations. We have adopted an iterative approach in which performance assessment results guide site data collection, which in turn influences the parameters and models used in performance assessment. The first iteration was based upon readily available data, and indicated that the GCD facility would likely comply with 40 CFR 191 and that the downward flux of water through the vadose zone (recharge) had a major influence on the results. It was seen, however, that very large recharge rates, such as might occur under a cooler, wetter climate, could result in non-compliance. As a result, a site characterization project was initiated to study recharge in Area 5 by use of three environmental tracers. This study concluded that the recharge rate is so small that the nearest groundwater aquifer will not be contaminated in less than 10,000 years. Thus upward liquid diffusion of radionuclides remained as the sole release pathway. This second performance assessment iteration refined the upward pathway models and updated the parameter distributions based upon new site information. A new plant uptake model was introduced to the upward diffusion pathway; adsorption and erosion were also incorporated into the model. Several modifications were also made to the gas phase radon transport model. Plutonium solubility and sorption coefficient distributions were changed based upon new information, and on-site measurements were used to update the moisture content distributions. The results of the performance assessment using these models indicate that the GCD facility is likely to comply with all sections of 40 CFR 191 under undisturbed conditions. A complete estimate of event and process probabilities was not done, although a simple probability model was used to estimate probabilities of human intrusion. For reasonable drilling rates, these probabilities were found to be very small.

---

[1] GRAM Inc., 8500 Menaul NE, Suite B-370, Albuquerque, NM 87112

[2] SAIC, 2109 Airpark Rd. SE, Albuquerque, NM, 87106

[3] Department 3020, Sandia National Laboratories, Albuquerque NM, 87195

Acknowledgments

The authors would like to thank several individuals and organizations who contributed to this work. Staff members of Reynolds Electrical and Engineering Company and Raytheon Services Nevada contributed considerable information on the hydrology and surface geology of the site as well as reviewing the initial draft of this report. Steve Conrad developed the new recharge value from the site data and also reviewed the initial draft. The new plutonium solubilities and sorption coefficients were obtained by Harlan Stockman who also assisted in development of the associated probability distribution functions (pdf). The geostatistical analysis of the moisture content data was done by Carol Gotway of the University of Nebraska. Jim Reitzel of GRAM was a resource for plant biology and plant rooting depths. The human intrusion analysis was based upon work done by Bob Guzowski of SAIC. Bill Fogleman also of GRAM assisted in procurement of site data and in preparation of several figures. Paul A. Davis provided valuable guidance in performing this analysis. David Gallegos assisted greatly in the preparation of the final draft of this report.

Contents

Figures

Tables

Preface

This report describes the second iteration of the 40 CFR 191 compliance assessment for the Greater Confinement Disposal facility. The results of the first iteration are contained in the three volumes of the Preliminary Performance Assessment published under SAND91-0047 [Price *et al.*, 1991]. This report is the follow-on work to the Preliminary Performance Assessment. It extends and updates the work done in the Preliminary Performance Assessment. As a result, this report will refer to this earlier work often.

Executive Summary

The Greater Confinement Disposal (GCD) facility consists of a number of deep (36 m) boreholes, 3 to 3.5 m in diameter, that have been augered into the alluvial fill deposits at the Radioactive Waste Management Site at the Nevada Test Site. The U.S. Department of Energy (DOE) has buried a small amount of transuranic (TRU) waste in several of these boreholes. Disposal of this class of waste must meet the standards established by the U.S. Environmental Protection Agency (EPA) regulation 40 CFR 191, which regulates disposal of high-level waste, TRU waste and spent fuels. Sandia National Laboratories has been contracted by DOE to perform the compliance calculations to determine whether this disposal configuration can meet these standards.

The first step in this compliance assessment was to perform a preliminary performance assessment. Using existing site-environment data, this analysis proposed a number of plausible release pathways. This performance assessment developed conceptual models for these pathways and mathematical/computational counterparts of the conceptual models. Monte Carlo analysis was employed to address the uncertainty in the models' parameters. The most important pathway was found to be downward advection of contaminants to the water table and subsequent release to the accessible environment. It was concluded from this initial analysis that the site was likely to comply with the standard for base case undisturbed conditions. A sensitivity analysis identified the downward recharge rate as the most important parameter, followed by the sorption and solubility characteristics of plutonium isotopes.

Disruptive events such as a change in climate, human intrusion, and erosion of the surface layers were also considered as part of the preliminary performance assessment. It was concluded that the last process, erosion, was found to be unimportant within the context of the prevailing downward advection conceptual model. The consequences of a human intrusion by exploratory drilling event were found to be non-trivial for the entire regulatory period (10,000 years), but since no accompanying probability was determined for this event, the effects of this event on compliance could not be addressed. To assess the consequences of this event, a very conservative model of climate change with greatly increased groundwater recharge was used, and it was found that compliance was equivocal given the likelihood of a change in climate within the regulatory period. This last result, combined with the findings from the sensitivity analysis, suggested the need to gather site-specific data on the groundwater recharge rate within Frenchman Flat.

Measurements of the concentrations of three natural environmental tracers within a number of boreholes drilled in Frenchman Flat were used to infer values of the current recharge rate. Based on these measurements, the current value of recharge is very small and would not permit transport of contaminants to the water table in the regulatory time frame. In addition to consideration of the downward recharge, some additional research was conducted to better characterize the solubility and sorption characteristics of plutonium. In general, plutonium isotopes in the GCD environment were less soluble and adsorbed more strongly to the surrounding media than originally estimated for the preliminary performance assessment.

The goal of the second performance assessment iteration was to incorporate this new site-specific information into the performance assessment. The observed lack of significant recharge prompted the analysts to alter the basic conceptual model of the site and eliminate the downward advective pathway altogether. The remaining pathway was upward diffusion of contaminants in the liquid phase to the surface, coupled with diffusion into the root zone and adsorption and transport by vegetation. Because of the increased importance of the latter mechanism, a more

refined plant transport model was developed to supplant the plant model developed for the first iteration. A simple model of erosion was also incorporated because erosional processes have a larger effect on the total release in the new conceptual model. Probability distributions for uptake factors, surface biomass densities, rooting depths, and erosion depths were also developed from available data to support these new models. In addition, on-site measurements of near-surface moisture contents were analyzed and expressed in terms of a probability density function. Finally, the increased importance of the liquid diffusion pathway suggested that the tortuosity distribution used in the first iteration be reevaluated based upon existing correlations between moisture content and tortuosity. This parameter accounts for the slowed diffusion in a convoluted sample of porous media with respect to unrestricted liquid.

The new conceptual model along with the updated and additional parameter distributions was used once again in a Monte Carlo uncertainty analysis. The model results comply with the Containment Requirements of 40 CFR 191. This result, however, did not include the effects of change in climate within the base case conceptual model. Dose calculations using the same conceptual model also showed compliance with the Individual Protection Requirements of 40 CFR 191. Compliance with the 40 CFR 191 Groundwater Protection Requirements is automatic as a consequence of the lack of significant downward recharge.

A sensitivity analysis of the Monte Carlo results indicated that the tortuosity parameter was most significant in terms of release; in particular, the largest releases were always associated with the smallest values of tortuosity. An analysis of the influence of rooting depths showed that the release was relatively insensitive to this parameter except for very deep rooting species. In this latter case, compliance of the site became equivocal. Such deep-rooted species do not currently exist at the GCD site. Also results showed that plutonium isotopes make up a very small fraction of the total integrated discharge. This finding is in direct contrast to the results from the first iteration in which plutonium isotopes account for the vast majority of the release.

Analysis of a complete set of disruptive scenarios was not within the scope of this current performance assessment. However, the consequences and probability of a human intrusion event via exploratory drilling were considered, and the release from such an intrusion event was quite significant for the entire regulatory period. However, the probabilities of such an event were quite small. A small possibility of non-compliance existed only for the worst case drilling rate established by 40 CFR 191. These results, however, did not consider the probability that drilling might not occur within the disposal area at all. Consideration of this probability and the use of a less conservative drilling rate would alter the results towards compliance.

At least one more performance assessment iteration will be required to establish the compliance of the site. This current iteration did not include the effects upon performance of a change in the climate state. Such a change is likely to occur; hence, it is necessary that to account for it in the base case conceptual model. Climate change data are being collected which will allow for this modification. In addition, the consequence and probability of disruptive scenarios must be included for a complete performance assessment. A set of potential disruptive events and processes has been developed for the GCD site. In the ensuing iteration, models for these events and processes will be developed, probabilities will be estimated, and their consequences will be included with the base case conceptual model in addressing the compliance of the site.

Nomenclature

Acronyms

CCDF	- complementary cumulative distribution function
CEDE	- committed effective dose equivalent
CFR	- code of federal regulations
DOE	- Department of Energy
DOE/NV	- Department of Energy Nevada Operations
EDTA	- ethylenediaminetetraacetic acid
EPA	- Environmental Protection Agency
GCD	- greater confinement disposal
GCDT	- greater confinement disposal test
HLW	- high-level waste
IP	- individual protection
LHS	- Latin Hypercube Sampling
LLW	- low-level waste
NCRP	- National Council on Radiation Protection
NTS	- Nevada Test Site
PDF or pdf	- probability density function
PPA	- preliminary performance assessment
QA	- quality assurance
REECo	- Reynolds Electric and Engineering Company
RSN	- Raytheon Services / Nevada
RWMS	- Radioactive Waste Management Site
SNL	- Sandia National Laboratories
SWIFT	- Sandia Waste Isolation Flow and Transport
TRU	- transuranic
VMC	- volumetric moisture content
WIPP	- Waste Isolation Pilot Plant

Symbols - Roman

A	- area [m^2]
A_b	- effective target area of GCD borehole [m^2]
B	- above ground dry biomass density [kg/m^2]
$b_j^{(i)}$	- eigenvector matrix appearing in chain decay solution [ ]
$C_{D,k}$	- diffusional portion of liquid diffusion analytic solution specific to the kth chain [$atom/m^3$]
C_i	- liquid phase concentration of the ith radionuclide [$atom/m^3$]
C_i^*	- decay portion of liquid diffusion analytic solution specific to ith species[]
C_l	- liquid phase concentration at the start of the root zone [Ci/m^3]
C_p	- concentration of a radionuclide in the above ground vegetation [Ci/g]
C_0	- initial gas phase source concentration [$atom/m^3$]
$C_{0,i}$	- initial concentration ith species in liquid phase [$atom/m^3$]
CR	- plant uptake concentration ratio [Ci/g dry vegetation / Ci/g dry soil]
D	- liquid phase molecular diffusion coefficient [m^2/s]
$D_{eff,i}$	- effective diffusion coefficient of the ith radionuclide [m^2/s]
D_v	- vapor phase effective diffusion coefficient [m^2/s]

e - depth of erosion [m]
$J_{i,surf}$ - release flux of ith radionuclide via direct diffusion at the surface [atom/m^2-s]
$J_{i,veg}$ - release flux via plant pathway [atom/m^2-s]
$K_{d,i}$ - distribution coefficient for sorption of the ith radionuclide [m^3/kg]
k - time for complete above ground biomass regeneration [yr]
L - depth of waste burial [m]
L_i - scaling factor for ith radionuclide established by 40 CFR 191 [Ci]
N - number of GCD boreholes or number realizations
n - yearly turnover fraction of above ground vegetation [ ]
P - probability of an exploratory borehole intersecting a GCD borehole [ ]
R_i - retardation coefficient of the ith radionuclide [ ]
$\mathbf{R_i}$ - normalized total integrated discharge, that is, the EPA sum [ ]
R^*_i - approximate radius of spherical diffusion front [m]
r^2 - coefficient of partial determination [ ]
S_i - concentration time history of ith species in the waste area [atom/m^3]
Q_i - total integrated discharge of the ith radionuclide [Ci]
t - time [s or yr]
$\mathbf{u}$ - gas phase velocity vector [m/s]
W - Shapiro-Wilk statistic
x - spatial coordinate [m]

Symbols - Greek

α_i - pre-exponential factor for the ith species appearing in the chain decay solution [atom/m^3]
ε - saturated porosity of the alluvium [ ]
λ_d - annual rate of human intrusion into a GCD borehole [yr^{-1}]
λ_i - radioactive decay constant [s^{-1}]
θ - volumetric moisture content of alluvium [ ]
θ_a - gas phase porosity of alluvium [ ]
ρ - bulk density of alluvium [kg/m^3]
ρ_d - density of exploratory borehole drilling [km^{-2}]
τ - tortuosity factor [ ]

1.0 INTRODUCTION

A small quantity of transuranic (TRU) waste has been disposed of by the Nevada Operations Office of the U.S. Department of Energy (DOE-NV) at the Radioactive Waste Management Site (RWMS). This site is approximately 3 km^2 within Area 5 on the Nevada Test Site (NTS) that is used primarily for shallow land burial of low-level radioactive waste. However, because shallow trench burial is not appropriate for TRU waste, an alternative disposal concept was implemented. Several deep boreholes were augered into the desert and the TRU waste was buried within them in 1984. This disposal concept was termed Greater Confinement Disposal (GCD) because it provides for better isolation of radioactive waste than shallow land burial. Because these boreholes contain TRU waste, it is necessary to demonstrate that the disposal system complies with U.S. Environmental Protection Agency (EPA) standards for disposal of transuranic waste. These standards are codified under section 40 CFR 191 of the federal regulations [EPA, 1989].

In 1989, Sandia National Laboratories (SNL) was contracted by DOE-NV to conduct the 40 CFR 191 compliance assessment calculations. Sandia's approach to assessing compliance is iterative in nature. Based upon available site data and the opinion of individuals knowledgeable about the site, release models are developed, parameters estimated, and analyses performed. In developing these models, a conservative bias is consistently introduced so that the modeled releases will always tend to exceed the actual release that is assumed to occur. After performing the assessment analysis, the results should indicate those parameters and processes with the largest effect on the performance of the site, and this information can then be used to direct further efforts in site characterization. The results of this field work can then be used in the modelling step to produce a more refined estimate of the disposal facility's performance. This process is repeated until compliance or non-compliance is demonstrated with *adequate* confidence.

In 1991, the first iteration of this performance assessment methodology was completed. It is referred to as the preliminary performance assessment (PPA) and is documented in Price *et al.* [1993]. This PPA was a comprehensive examination of the GCD site, but the information used to perform the assessment was based upon only what was existing and readily available within the literature or from site experts. Generation of new information about the site was beyond the scope of the PPA. The site models developed by the PPA, however, identified several parameters and processes that had a major influence on the site performance. Armed with this new information, several site characterization studies were set in motion to obtain site-specific data to be used in a later iteration of the performance assessment.

The information obtained from these site studies was incorporated into a second performance assessment iteration, which is the subject of this report. The intent of this second performance assessment iteration was to alter the models and parameters developed by the original PPA based upon this new site information, run the performance assessment calculations, and again assess the likelihood that the GCD site will comply with 40 CFR 191. The objectives of this iteration and their relation to the original PPA analysis will be discussed in more detail in Section 1.2.

1.1 Background Information

1.1.1 Site Description and Waste Inventories

The GCD site is located in an area known as Frenchman Flat, which is a closed, aggrading, alluvial basin in the southernmost portion of the Basin and Range geologic province of southern Nevada. The basin is filled with alluvium, which occurs in some areas to a depth of approximately 457 m. Several hydrologic units underlie the site with the shallowest being the Valley Fill aquifer, an unconfined aquifer in the alluvial sediment some 235 m below the surface. Other geologic and hydrogeologic details are reported in the PPA [Price *et al.*, 1993], and the reader is referred to that source for additional information. The climate is arid with rainfall averaging less than 12.7 cm per year. In terms of biological communities, Frenchman Flat is often considered within the northernmost reaches of the Mojave desert province. The vegetative communities in this area are those usually associated with bajada features within the Mojave desert. These communities most commonly exhibit dominance of *Larrea Tridentata* (creosote) often in association with *Ambrosia*, *Lycium-Grayia*, or *Atriplex*.

Because of the great depth to the unconfined aquifer, the aridity of the alluvial soil, and several other factors, it was thought that this site would provide a high degree of waste containment. The GCD facility consists of thirteen deep boreholes, each 36.5 m deep and either 3 or 3.7 m in diameter, augered into an alluvial fan of the Massachusetts Mountains on the northern side of Frenchman Flat. Radioactive waste containing isotopes of plutonium, americium, and uranium was disposed of in four of these boreholes (#1, #2, #3, #4), filling the lower 15.2 m of each, and native, sifted alluvium was used to backfill the remaining 21.3 m. In two other boreholes, waste containing several hundred thousand curies of ^{90}Sr and ^{137}Cs were buried, along with some ^{226}Ra and ^{227}Ac. The GCD Test hole (GCDT) is one of these latter holes. The remaining boreholes are either empty or contain waste that is not within the scope of 40 CFR 191. Aside from a small drainage berm over each borehole, no cap or other engineered barrier has been installed as of yet. Figure 1.1 is a sketch of a typical GCD borehole configuration. Figure 1.2 shows an aerial view of the RWMS and indicates the location of all the GCD boreholes.

The waste was generally contained in fiberboard or plywood boxes and steel drums. Some doubt exists about the exact amount of waste emplaced in these boreholes; Tables 11 and 12 in the PPA suggest the possible ranges. The PPA treated the inventories as uncertain variables. However, the PPA also concluded that the inventories themselves did not have a large effect on the calculated release. As a result, in this iteration, the inventories were treated as fixed variables, with the midpoint of each uncertain range as the initial inventory of a particular isotope. Reasons for choosing the midpoint instead of the maximum value are discussed in the next section. These initial radionuclide inventories in each borehole appear in Appendix A, which also contains the decay chains and those daughters that were considered in the analysis. There are other daughters not shown, but these have very short half-lives and so are not regulated under the Containment Requirements of 40 CFR 191.

1.1.2 Regulatory Driver - 40 CFR 191

The regulation governing disposal of transuranic waste is 40 CFR 191 [EPA, 1985], which contains three post-closure requirements: (1) the Containment Requirements, (2) the Individual Protection Requirements, and (3) the Groundwater Protection Requirements. The PPA

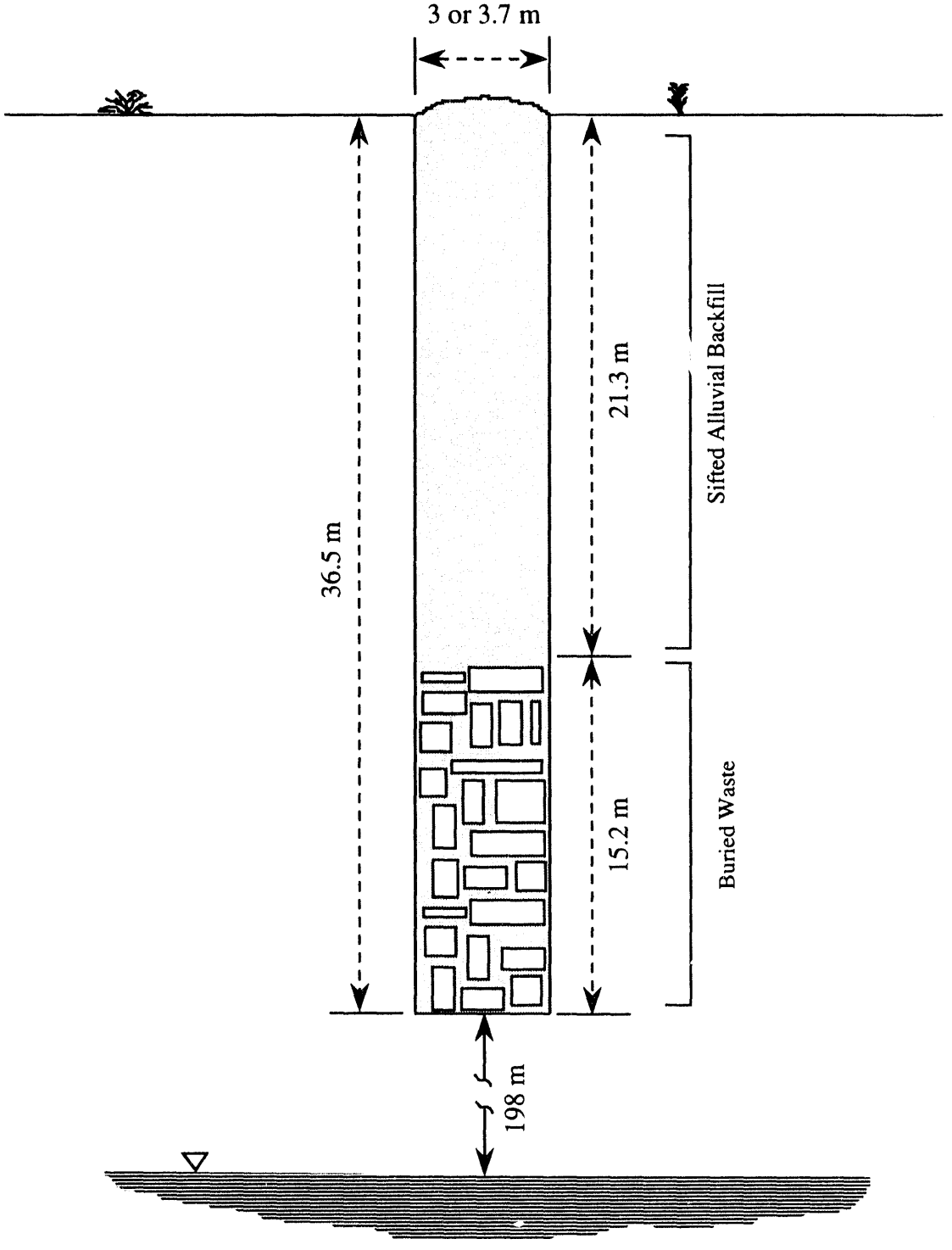

Figure 1.1 - Schematic of typical GCD borehole (not to scale)

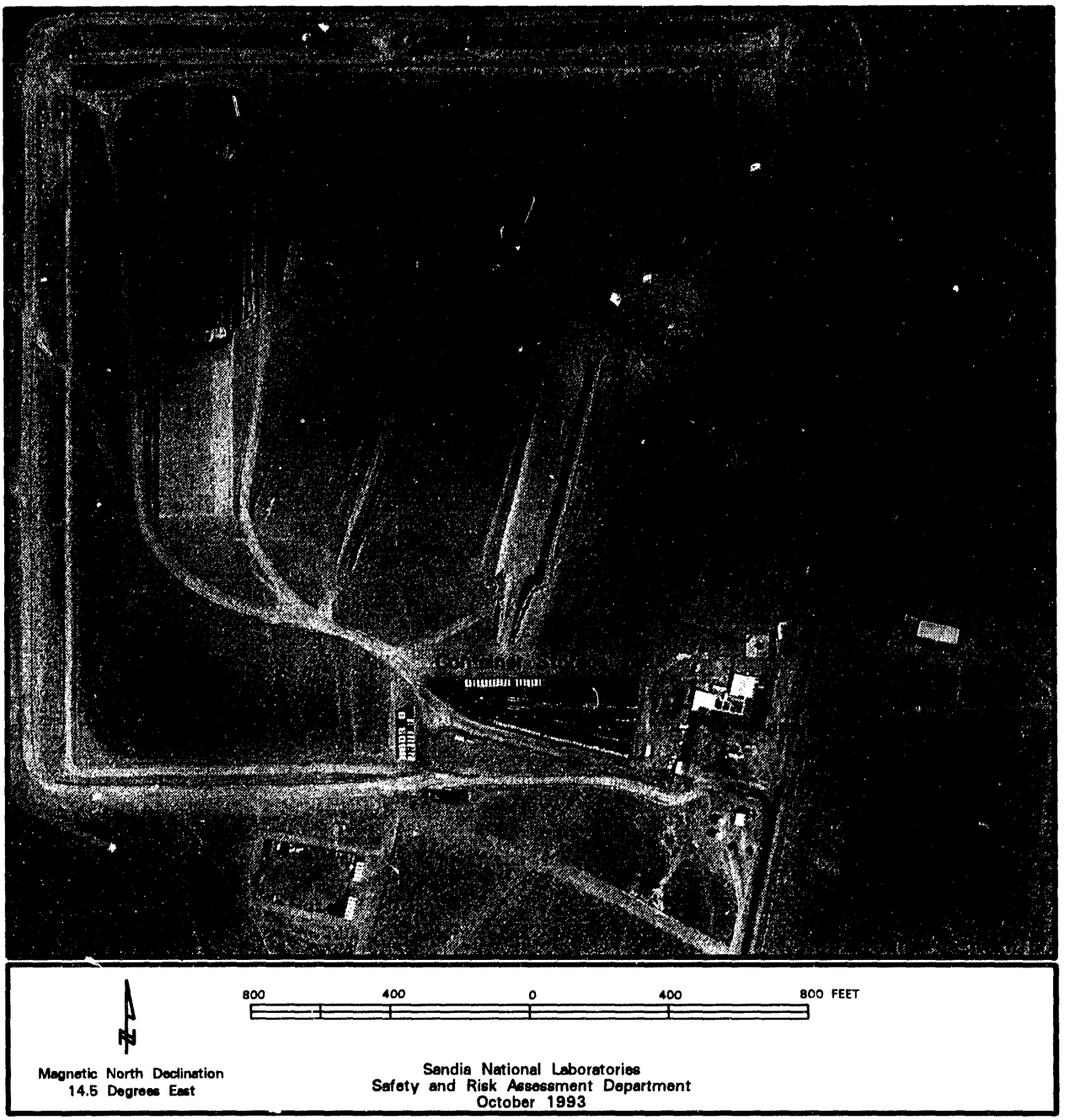

Figure 1.2 - Aerial view of RWMS showing location of GCD auger holes and exploratory site characterization boreholes

discusses each requirement in considerable detail. Therefore, only the most basic of descriptions are presented here. The most complicated of the three requirements is the Containment Requirements, which sets limits on the probability of exceeding a specified total integrated discharge of specific isotopes into the "accessible environment". The regulation is written to apply to a normalized release parameter known as the EPA sum. 40 CFR 191 defines what we refer to as the EPA sum in the following way,

$$EPA\ sum = \sum_{1}^{n} \frac{Q_i}{L_i} \qquad (1)$$

where Q_i is the total integrated discharge of the ith isotope over a 10,000-year period, L_i is the species-specific scaling factor established by the regulation, and n is the number of radionuclides present. These scaling factors are listed in Price *et al.* [1993]. It should be pointed out that L_i is directly related to the amount of waste originally emplaced. Hence, the more disposed waste, the greater the amount that can be released legally. However, this also introduces some subtle considerations in the choice of the original waste inventories for the performance assessment calculations. Intuitively, we would expect that choosing the largest amount of waste emplaced would be the most conservative choice because the absolute release is directly related to Q_i. However, in situations where a large fraction of the buried radioactivity is composed of short-lived isotopes or isotopes that are effectively immobilized by the media, choosing the largest inventory possible would increase L_i but leave Q_i essentially unaffected. This reduces the EPA sum and results in a less conservative answer. Strontium and cesium are both short-lived isotopes, and plutonium isotopes have been shown to adsorb strongly to Frenchman Flat alluvium (Section 3.1.1.3). As a compromise, we decided to use the mean values of the uncertain waste inventories as noted above.

The requirements for the EPA sum are probabilistic in nature: over 10,000 years, the probability of an EPA sum being greater than one shall not be more than 10%, nor shall the probability of its being greater than ten be larger than 0.1%. The regulation defines the "accessible environment" as (1) the land surface, (2) surface waters, (3) the atmosphere, (4) the oceans, and (5) any point in the subsurface lithosphere 5 km beyond the disposal site. For the GCD site, the only relevant accessible environment components that must be considered are the land surface, the atmosphere, and the subsurface outside the 5-km radius surrounding the site. In modeling the performance of the site, the regulation allows for an "institutional control period." This period is defined as 100 years after closure of the facility during which it can be assumed that some governmental entity will retain control over access to the site by members of the general public. At the end of the institutional control period, it is assumed that the site will revert to an unregulated state and be accessible to all.

The Containment Requirements also mandate that all "events and processes" that could affect the performance of the site for the next 10,000 years must be considered. These would include conditions such as inadvertent human intrusion into the waste sites, seismic activity, changes in land use, etc. Each set or combination of disruptive events is referred to as a scenario [Cranwell *et al.*, 1990]. For a complete performance assessment analysis, the probability of each scenario must be estimated and its consequence determined. The set of events and processes that is expected to occur in the next 10,000 years is referred to as the base case scenario. As an example, after closure of the RWMS, it is expected that vegetation will repopulate the area and as a result its presence must be included as a part of the base case scenario.

The Individual Protection Requirements limit the dose to an individual member of the public. The regulation promulgated in 1985 stated that for undisturbed performance over 1,000 years after closure of the site, no member of the public may receive an annual whole-body dose from the buried waste larger than 25 mrem or an annual individual critical-organ dose greater than 75 mrem. This standard was used in the PPA. Since then, this section of the regulation was remanded by the courts as mandated by the WIPP Land Withdrawal Act, and a proposed revision has recently been released. The revised Individual Protection Requirements increase the period of regulatory concern to 10,000 years and require that in that time period the annual committed effective dose equivalent to any individual member of the public not exceed 15 mrem. Because of the clearer dosimetric quantities used in the latter version, we have chosen to compare the performance of the GCD site to this newly promulgated revision[1].

The final section of 40 CFR 191 is the Ground Water Protection Requirements, which limits the amount of radiation that may reach a "special" groundwater source. This section was also remanded as part of the WIPP Land Withdrawal Act, and the revised section now requires that over a time frame of 10,000 years no more than 15 pCi/L may be discharged to a underground source of drinking water. As described below in Section 2.3, a study of recharge in Frenchman Flat concluded that convective transport to the water table is not likely to be significant. Thus, contamination of the unconfined Valley Fill aquifer is not a likely occurrence, and as a result, the Groundwater Protection Requirements were not considered in this analysis.

1.1.3 Performance Assessment Methodology

Determining whether the GCD site can comply with 40 CFR 191 is accomplished only through the use of mathematical models of the radionuclide release mechanisms. For the Containment Requirements, these models must simulate the behavior of the disposal system for 10,000 years throughout a 10 km diameter subsurface region surrounding the site. Given the tremendous uncertainty existing in models and parameters, the question that arises is whether it is possible to make *accurate* behavior *predictions* over time and spatial scales of this size. It is our position that accurate predictions cannot be made given the natural, economic, and practical constraints, nor are they required by 40 CFR 191.

If this is the case, how then are we to determine compliance with 40 CFR 191? The answer lies in the fact that the regulations establish and define an upper bound on the probabilities of a given release. To comply with the regulations, we need only demonstrate that the system will not exceed these probabilities to demonstrate compliance. Our goal then is *not* a model that will produce a realistic rendition of the system behavior, but a model whose release is assured of being larger than the actual release of the "true" system, given the uncertainty in the problem and our current level of knowledge. Such a model is referred to as a conservative model. For example, the worst case scenario, in which all the waste is released simultaneously, is a conservative model. It is, however, of limited utility from a regulatory compliance assessment standpoint because it almost always indicates non-compliance and therefore cannot be used to make decisions. Instead, we seek a model less extreme in its assumptions than the

[1] At press time, the newly released final version of the standard specifically indicated that GCD was to be governed by the (1985) version. This was unexpected and provided no opportunity to revise the IP analysis for consistency with the 1985 standard. Because of the longer time frames required of the newest standard, however, we feel comfortable that the IP analysis presented here depicts the GCD site in the most conservative light.

worst case scenario, but still retaining the property that the release of the real system will not exceed the release of the conservative model. Proving that a model is indeed conservative is a difficult problem given the fact that the actual behavior cannot be predicted or determined. In addressing this fact, we implicitly assume that if at each stage of the model development we consistently choose the most conservative option *except when information exists that indicates otherwise*, the resulting model will be conservative as we have defined above.

Using such models to assess compliance is done within the context of a performance assessment methodology developed for high-level waste sites by Sandia [Bonano *et al.*, 1989]. The first step is development of conservative models based upon available information about the site. The information may consist of extant literature sources and/or consultations with site experts on the most important processes associated with the site. At this point, however, no additional site characterization is done. Generally, there is considerable uncertainty, including but not limited to the values of the model parameters. Because of this uncertainty and also because the interactions of parameters and processes within a modelling framework are very often not intuitive, it is necessary to apply uncertainty analysis techniques (e.g., Monte Carlo) to assess the site, rather than simply using the most conservative parameter values in a single deterministic analysis. The results of the uncertainty analysis allow us to evaluate the site. Should the model results indicate compliance with the standard, no additional resources need be expended, and we conclude that the site is in compliance with the regulations.

Should the results indicate non-compliance, however, we are faced with a dilemma. It may be that site is indeed unsafe, but it also possible that the models we are using are overly conservative and unfairly depict the safety of the site. Because we cannot predict the actual site behavior, it is impossible to tell which of these two possibilities is correct. Therefore , we *must assume* that the non-compliance result is the result of an overly conservative model. The next step is to reduce the conservatism of the models in a defensible way based upon additional new site data.

We begin by performing a sensitivity analysis on the results of the initial analysis. This analysis identifies the parameters and/or processes that are uncertain and have the greatest effect on the performance of the site, that is, result in non-compliance. These parameters and processes determine where to direct new data collection and other research activities to reduce the uncertainty in them and provide a defensible basis for reducing the conservatism in the models. If for technical or other reasons this additional data cannot be collected, we must accept the results of our previous modeling as the best information on the safety of the site and recommend that the site be abandoned. If the data can be collected and defensible arguments can be derived for doing so, the methodology permits us to reduce the conservatism of a model, an assumption, or a parameter distribution. In this manner, we defensibly and incrementally correct the over-conservatism of our models and gradually constrict the region in which we know the actual release will occur. Thus, if the results of our modelling fall below the regulatory requirements (i.e. indicate compliance), we have a defensible basis on which to claim that the site is indeed safe.

Finally, it should be noted that the methodology outlined above has certain implications with respect to the manner in which the site is modeled. For example, apparent inconsistencies may appear among the various analyses or within a given analysis. Because our goal is to always err to the conservative side, it may become necessary to sacrifice consistency if doing otherwise would result in a less conservative analysis. For example, we might use one boundary condition when considering the performance with respect to one section of the standard, but a different boundary condition when considering a different section. The reason for doing this is

that the different performance measures dictate which boundary condition is the more conservative. The reader should, therefore, be assured that if inconsistencies appear between analyses, or if a model or parameter distribution appears to be at odds with reality, it is for purposes of ensuring conservatism.

1.1.4 First Performance Assessment Iteration

The PPA was the first step in the methodology outlined above. Its scope was to assess the possibility of compliance based only upon readily available site information. The PPA did consider the consequence of three disruptive scenarios in addition to the base case, but the scope of this iteration did not include a formalized scenario development and screening analysis, involving estimation of the probabilities of these scenarios, therefore, compliance with 40 CFR 191 could not be completely assessed.

The PPA identified two primary radionuclide transport mechanisms. The first was dissolution of the waste into the unsaturated groundwater phase, followed by convective transport downward through the vadose zone to the water table, and transport in the groundwater beyond the 5 km limit. The second pathway recognized that the aridity of the site might imply very low recharge, and the dissolved waste might diffuse upwards in the vadose zone liquid phase until it reached the surface or, after diffusion into the root zone, be absorbed into plant roots and transported to the surface by the plants. Models for both pathways were developed, and the literature and opinion of individuals knowledgeable about the site were consulted to obtain values for the model parameters. Generally, there was considerable uncertainty associated with these parameter values, which, therefore, had to be expressed in terms of probability distributions. These probabilities were propagated through the models by a Monte-Carlo simulation technique using Latin Hypercube sampling of the parameter distributions [Iman and Shortencarrier, 1984]. The upward diffusion model was used when very small values of recharge were sampled. An estimate of the upward diffusive flux was compared to an estimate of the average downward convective flux. The upward diffusion model was used in place of the downward convection model when upward diffusive flux was larger than the downward convective flux.

The PPA also identified gaseous diffusion of radon isotopes to the surface as a major pathway that could affect the dose computed for the Individual Protection Requirements. Release of radon is not regulated by the Containment Requirements, but doses received by inhalation of radon and its daughters can contribute to the overall dose determined for the Individual Protection Requirements, especially for the GCDT borehole where a great deal of radium, a radon parent, was buried.

An analysis of base case conditions indicated that the GCD site would comply with all sections of 40 CFR 191. Because a complete scenario analysis was not done, the safety of the site could not be evaluated completely. The consequences of a human intrusion event into the boreholes were considered, but no probability for this event was estimated. Erosion processes were not included in the analysis because they did not have a large affect on release via the downward convection pathway. The sensitivity analysis of the results revealed several interesting conclusions. First, the upward liquid diffusion pathway had a higher percentage of non-zero cumulative releases than the downward path, suggesting that this pathway is more important than first thought. Second, several important parameters were identified as having a large effect upon the total release. These are, in order of importance, downward recharge through the vadose zone, the sorption coefficient of dissolved plutonium, and the solubility of plutonium. A very

conservative analysis of the affects of a cooler, wetter climate on the performance of the site indicated that a non-compliance result was possible.

The PPA recommended that recharge within Frenchman Flat be addressed by site-specific characterization, especially how recharge might be influenced by variations in climate. The PPA suggests that probabilities of human intrusion be estimated and that erosional processes at Frenchman Flat be considered more closely because of the relatively large influence that upward diffusion had on the results. The PPA also recommended additional research to characterize the solubility and sorption characteristics of plutonium isotopes in the GCD system. These recommendations set in motion several site characterization projects; the results of which are discussed in Section 2 below.

1.2 Scope of Present Work

The scope of the present work is limited. According to our methodology, it is the second iteration in the process of determining whether the GCD site is likely to comply with 40 CFR 191. As such, its function is to incorporate new information developed by the site characterization projects initiated by the PPA findings, address the uncertainty in this information and its relationship to the original information used in the PPA, refine the PPA models in response to this new information, and, by a second performance assessment, evaluate once again the likelihood of compliance. As recommended by the PPA, we shall incorporate new information on the recharge rate, the solubility of plutonium isotopes, and the sorption characteristics of plutonium isotopes. In addition, site characterization generated site-specific information about moisture contents and porosities of the Frenchman Flat alluvium. This information was also included in the second iteration. Section 2.0 will summarize all of this new information. A study of erosional processes at the GCD site was undertaken by Raytheon Services of Nevada (RSN). It was still preliminary at the time of this writing, however, some general conclusions could be made. These are discussed in Section 3.1.3.

Probabilities and consequences models for scenarios are in the process of screening and development at the present time. Consequently, this iteration will not consider separate scenarios; it will deal only with the behavior of the system under base case conditions. However, as a follow on to the consequence analysis done in the PPA, a Poisson model will be used to estimate probabilities of the human intrusion event. In the PPA, a change in the climate at the GCD site was treated as a separate scenario. Guzowski and Newman [1993] indicate that it is virtually certain that the climate will change within the next 10,000 years. Thus, a model for climate change is properly a part of the base case conceptual model. Site-specific information characterizing the past climate states at the GCD is in the process of being collected and analyzed. It has not reached a point where useable climate change information can be incorporated into the performance assessment analysis. Thus, the base case model presented in this iteration is incomplete because it assumes that current climatic conditions will continue for the next 10,000 years. The third iteration will include a change of climate in the base case.

Finally, it is necessary to discuss briefly the scope of the radionuclides that are considered relevant to this performance assessment. 40 CFR 191 regulates the release of spent nuclear fuel, high-level wastes, and TRU wastes. TRU waste in turn is defined as any alpha-emitting radionuclide with an atomic number greater than 92, half-life greater than 20 years and concentration in excess of 100 nCi/g. This regulation clearly applies to the several isotopes of plutonium and ^{241}Am that were buried at GCD. However, how the regulation applies to the non-TRU isotopes of uranium, radium, strontium, cesium, and actinium is more ambiguous. None

of these latter radionuclides are TRU waste. It is true that these latter isotopes are present in both high-level waste and spent fuels, and 40 CFR 191 does establish regulatory limits on their release in the Containment Requirements. However, it is also true that none of the waste buried in the GCD boreholes was either high-level waste or spent fuel. The proportions of these non-TRU isotopes might be considerably different from what would be found in high-level waste or spent fuel. For this reason, it could be argued that strict application of 40 CFR 191 to all isotopes, including the non-TRU, might be contrary to the intent of the regulation.

We chose to deal with this uncertainty in the appropriate inventory by noting that the half-lives of the uranium isotopes are all relatively large, whereas the half-lives of the strontium, cesium, and actinium isotopes are all less than one century. Furthermore, the uranium wastes are buried in the same boreholes as the transuranic waste; whereas, the strontium, the vast majority of the cesium, and the actinium were buried in separate boreholes which contained no transuranic waste. For these reasons, it was decided to treat those uranium isotopes that had been disposed of with TRU elements as being subject to 40 CFR 191. We also assume that all daughter products resulting from decay of a TRU waste are regulated by 40 CFR 191, if release limits are given for that isotope. The strontium, cesium and actinium isotopes are refered to as non-TRU waste. For the Containment Requirements we will consider two cases: the performance when only the TRU waste is assumed present, and the performance when both TRU and non-TRU waste is present. For the Individual Protection Requirement analysis both types of waste will be assumed present.

2.0 SITE CHARACTERIZATION FOR SECOND PERFORMANCE ASSESSMENT

2.1 Exploratory Boreholes

A great deal of new site information was obtained from a series of small-diameter boreholes recently augered into the alluvium at the RWMS by Reynolds Electric and Engineering Company [REECo, 1993]. There were 10 boreholes augered with depths ranging from 4.25 m to 36.5 m. They were drilled a short distance southeast of the administration buildings shown in Figure 1.2. Table 2.1 lists the depths of each and the drilling method. Data were also taken from three pilot wells drilled to the water table throughout Frenchman Flat. Analysis of the core samples taken from these boreholes included gravimetric and volumetric moisture contents, porosities, conductivities, water potential, carbon content, chloride content, and particle size fractions. Values for recharge, porosity, and moisture content were determined using this new site characterization data, which is discussed below.

2.1.1 Moisture Contents and Porosities

The volumetric moisture content measured in the boreholes was combined with similar data used formerly in the PPA [McGrath, 1987], and this combined set of data was analyzed statistically. The details of this analysis are given in Section 3.1.1.1, but the primary conclusion was that the moisture content data could be represented by a lognormal distribution ranging between 0.001 and 0.999 quantiles of 4.75% and 18.10%. The moisture contents used in the PPA ranged between 6% and 17% and were distributed lognormally. The new distribution reflects a somewhat drier system than the distribution used in the PPA. A drier system is less conservative if diffusion is the only transport mechanism, but since site data is available to support it, we are justified in this change.

Porosity information from the borehole cores was also analyzed. The measurement used was the "saturated" porosity, which measures the void space available for flow and transport. The porosity values used in the PPA were based upon the relationship between bulk and particle densities. As such, it was not felt that the two data sets could be combined consistently. As a result, the porosity data used for the PPA were not included in the analysis of the new site data. Appendix B gives the analysis of the porosity data. It was found that data were normally distributed with mean porosity of 35.4% with a standard deviation of 3.54%. The porosities used in the PPA ranged between 24.8% to 47.5% and were uniformly distributed.

2.2 Recharge Study

The PPA identified a number of studies that reported values of recharge rate in arid southwestern environments. However, the majority of these studies were at sites far removed from Frenchman Flat or used questionable estimation methods. For the purposes of the PPA, use of this data was acceptable given the limited recharge rate data specific for Frenchman Flat. However, because of the large influence assigned to the recharge rate by the results of the PPA, it was decided to undertake a site-specific recharge study within Frenchman Flat. Because the recharge rates determined from this study would be specific to Frenchman Flat, would be obtained by the latest techniques in arid environment estimation, and we would have direct control over the qualification of this data, it was also decided that the original recharge data used

Table 2.1 - Depth and drilling method for exploratory boreholes.

Borehole	Depth (m)	Drilling Method
ST-1	35.8	ODEX[1]
ST-2 ST-2A	37.7 36.6	HSA[2] ODEX
ST-3	14.25	HSA
ST-4 ST-4A	34.7 36.6	HSA ODEX
ST-5	11.4	HSA
ST-6 ST-6A	35.4 36.6	HSA ODEX
ST-7	10.7	HSA

[1] ODEX System 140
[2] Hollow Stem Auger

by the PPA could be set aside in favor of this newest recharge information. This section describes the nature and results of this site-specific recharge study.

Estimation of groundwater recharge in arid environments is a potentially troublesome affair. Water balances cannot be estimated accurately due to high evaporation rates, and the aridity of the soil amplifies the uncertainty of the moisture content and makes it difficult to determine appropriate vadose zone flow parameters. Hence, soil water flow models are rendered inaccurate [Gee and Hillel, 1988]. In such a situation, it is necessary to rely upon depth profiles of environmental tracer species. From such information it is possible to empirically infer values of recharge.

Three methods based upon environmental tracers were chosen to estimate recharge in Frenchman Flat: a chloride mass balance, measurement of $^{36}Cl/^{35}Cl$ ratio with depth, and finding the enrichment of the ^{18}O and ^{2}H in the soil water. The first technique infers recharge by noting the increase in chloride concentration of the pore water relative to precipitation. Because chloride remains behind when precipitation evaporates, a constant buildup of chloride concentration at the surface will result unless recharge convects the chloride downwards. Hence, the elevation of the soil water chloride concentration with respect to precipitation is in effect a measure of recharge rate. The $^{36}Cl/^{35}Cl$ ratio is useful in a recharge study because it varies in time along with the magnetic field of the earth. Hence, it is a means of determining the age of water at a certain depth. Various works [Mazaud *et al.*, 1991; Blinov, 1988; Phillips *et al.*, 1991] have dealt with determining the relationship between $^{36}Cl/^{35}Cl$ and vadose water age. The age of the water at a given depth is related to the recharge rate. Finally, the stable isotopes of water (^{18}O and ^{2}H) can reflect the recharge because as water evaporates, fractionation occurs so that the remaining liquid

phase becomes enriched in these isotopes. Departures seen from the average isotope content in rain water, termed the meteoric water line, are indicative of the magnitude of recharge: the greater the departure, the more time there has been for fractionation to occur and the lower the values of recharge. These techniques are discussed in greater detail by Conrad [1993]. Two other environmental tracer techniques could have been employed: tracking of tritium and ^{36}Cl introduced by above ground nuclear explosions. However, these methods would only have given recharge values relevant to the last thirty years. Moreover, these isotopes are still within the zone of evapotranspiration where estimation of recharge is very problematic. As a result, these two latter methods were not employed in this study.

Using the first three techniques and data taken from the exploratory boreholes, Conrad was able to conclude that for current climatic conditions, the average recharge was smaller than the critical recharge rate for aquifer contamination. This critical value is the minimum recharge necessary to contaminate the groundwater aquifer in 10,000 years. The smallest pore velocity possible that will convect a fluid particle from the base of a borehole to the aquifer, a distance of 183 m if we allow for a possible rise in the water table, in a period of 10,000 years is about 1.5 cm/yr. Including dispersion in the analysis affects this value by only one or two percent. For an average moisture content of 8 percent, this velocity corresponds to a critical recharge rate of only 0.1 cm/yr. Conrad's analysis of the three environmental tracer data sets consistently resulted in current recharge values considerably smaller than this critical value. It should also be noted that this critical value does not account for groundwater travel time in the saturated zone to the 5 km limit. If this time were accounted for, the critical recharge value that would result in any release would be even larger.

This recharge study indicates that there is a very large likelihood that the recharge rate within Frenchman Flat is below the critical value for groundwater contamination, at least for current climatic conditions. The conclusion from this is that downward convection is no longer a radionuclide transport mechanism and *can be removed from further consideration for base case conditions.* Note that this means that the Groundwater Protection requirement is satisfied by default.

2.3 Geochemistry Studies

The geochemistry of the GCD site was researched in detail in three studies done by Stockman [Stockman, 1992 a,b, and c]. The first dealt with the composition of the pore water, the second with the solubility of plutonium, and the third with the sorption coefficient of plutonium onto the alluvium. The latter two studies indicated a considerable modification of these parameters from the values used in the PPA. These changes are discussed in the next two sections.

2.3.1 Plutonium Solubilities

The plutonium solubilities used in the PPA were taken from a geochemical study described by Chu and Bernard [1991]. Upon considering the composition of the groundwater and the mineralogy of the site, it was seen that this study did not consider several potentially important factors. Among these were the buffering capacity of the mineral assemblages of the native alluvium and the presence of organic compounds which could potentially form complexes

with plutonium ions. Stockman [1992b] considered the problem of plutonium solubility once again, taking these factors into account. The details of this study are summarized below in Section 3.1.1.3, but the primary conclusion was that plutonium solubilities were likely to range between 10^{-7} and $10^{-5.4}$ molal. These values are at least one and one-half orders of magnitude below the values determined for the PPA and have a dramatic effect on the modeled performance of the site. Note that these new solubilities are less conservative (in this case smaller) than those used in the PPA, but are acceptable because we have a defensible basis on which to make this change.

2.3.2 Plutonium Sorption Coefficients

In the PPA, sorption coefficients for plutonium isotopes were found in several literature studies. An upper bound of 1000 ml/g was established from these studies. The lower bound was established at 0.001 ml/g or essentially zero. For this performance assessment iteration, an additional perusal of the sorption coefficient literature was performed by Stockman [1992c]. The details of this effort are summarized in Section 3.1.1.4, but it was concluded that when colloidal transport was considered, a minimum plutonium sorption coefficient could be established at 1.56 ml/g. The arbitrary lower bound used in the PPA was a conservative value used because of a lack of data. In light of this new data, it was felt that this lower bound could be adjusted to 1.56 ml/g. In addition, other studies reviewed for this iteration suggested that the upper bound of the PPA's plutonium sorption coefficient distribution should be lowered from 1000 ml/g to 100 ml/g.

3.0 PERFORMANCE ASSESSMENT MODELS

The requirements of 40 CFR 191 consider time and spatial scales of such a large magnitude that the only way to assess the compliance of a site is by development and implementation of models of the site. Section 3.0 describes the models that were developed in this iteration for this purpose. We model the performance of the site with respect to the Containment Requirements and the Individual Protection Requirements for the base case scenario. As noted above, we do not need to develop models for the Groundwater Protection Requirements because of the low rate of recharge assumed in the base case. The base-case scenario, as noted above, is that set of events and processes that will occur at the NTS over the next 10,000 years with the exception of a change in the climate. This addition will be included in a later iteration when relevant information is available. We will also present a preliminary model for the probability and consequence of a human intrusion by exploratory drilling event.

3.1 Containment Requirements - Base Case Scenario

In this second iteration, the majority of effort was directed towards comparing the performance of the GCD facility with the Containment Requirements for the base case scenario. This section will describe the liquid-phase diffusion model, the plant uptake model, and the erosion model. The distributions used to reflect the uncertainty in the various parameters of the models will be discussed following the presentation of each model. It is implicitly assumed during the development of each model presented in this section, that institutional control no longer exists at the GCD site.

It should be noted here that radon isotopes are produced as daughters in several of the decay chains. Since radon is normally gaseous, it is transported primarily in the *gas* phase. However, we do not present a gas phase transport model in this section since the Containment Requirements do not regulate release of radon. Instead, radon is considered by the Individual Protection Requirements, and we shall present a gas phase model when this requirement is considered in Section 3.3 below.

3.1.1 Liquid Diffusion Model for Radionuclide Transport

After eliminating downward convection, the remaining transport process, upward diffusion in the unsaturated liquid phase to the ground surface, became the only viable release mechanism for the majority of the radionuclides. A model of upward diffusion was developed by the PPA, but it was employed only when the sampled recharge values were very small. However, when it was used, the releases were often quite high, indicating the importance of this mechanism. This second iteration uses a liquid diffusion model similar to the one developed previously by the PPA. However, there are numerous significant differences. The basic assumptions underlying this model are as follows:

(1) Transport is modeled as occurring in a one-dimensional, planar geometry. Some have argued that a superior alternate means of conceptualizing this transport is within a spherical geometry. That is, material diffuses away from the waste area radially in all directions. The first conceptual model is simpler and more econmical to implement and use; the second model is more realistic but more complicated and more expensive to

implement. However, which conceptual model results in the most conservative release is not a clear question. Generally speaking, at any given distance from the source, the flux in a spherical geometry is roughly 1/r times less than the flux in a planar geometry, where r is the distance from the source [Carslaw and Jaeger, 1959]. On the other hand, the spherical conceptualization affects a much larger area of the surface than the strict planar case, whose affected area is confined to the cross-sectional area of a single borehole. It is therefore conceivable that this latter fact might compensate for the smaller flux and produce a total integrated discharge for the spherical case that is comparable if not greater than the corresponding value for the planar case. Unfortunately, this question cannot be decided by heuristic arguments and requires a solution of the problem using the spherical conceptualization, which, because of the presence of the surface boundary, introduces a second spatial dimension into the problem and considerably complicates the analysis.

For this iteration, we have chosen to retain the simplicity of a one-dimensional planar geometry for computation of the transport flux. However, we acknowledge the possibility that confining this flux to the cross-section of a borehole may not be the most conservative choice in light of the above argument. As a result, we assume that the planar flux occurs over an affected area that may be larger than the borehole cross-section. How this affected area is determined will be discussed in Section 3.1.4.

(2) Diffusion is the only transport mechanism. Average downward recharge, however small, is neglected as is the occurrence of periodic unsteady infiltration events. The effect of both is to retard upward motion, and it is, therefore, more conservative to neglect them. On the other hand, advection in the opposite direction would not be conservative to neglect. Measurements of the matric potential in the near surface shows a strong trend in the pressure gradient that could sustain an upward flow [REECo, 1993]. This suggests the possibility of advection upward in the same direction as diffusion. If this advection were significant, it would not be conservative to assume diffusion as the only transport mechanism. However, the great aridity of the near surface indicates a very small value of unsaturated conductivity. It is our current opinion that this low value of conductivity will prevent any upward flow of liquid. Consequently, we do not include upward advection in the current conceptual model of the site. Subsequent work will address the potential for upward advection and whether it should be included in the base case conceptual model.

(3) Radionuclides are immediately available for transport. That is, no allowance is made for the lifetime of any waste container. We have little information on the mode of decay and rupture of the waste containers. However, as a rule, waste containers would impede the release of materials for transport. Hence, neglecting the presence of the waste containers is a conservative assumption. By making this conservative assumption, we have eliminated, for the time being, the need to characterize the dynamics of waste container rupture at the GCD site. Should the need arise (owing to a non-compliance result), however, this conservative aspect of our model could be relaxed if there were sufficient data to support a model of container rupture.

(4) A more involved source term is employed from that used in the PPA. Since no advective flow is assumed to exist, our model of the source area is limited entirely by solubility.

Implicit in this, of course, is that diffusive transport is so slow that the equilibrium between liquid and solid phases is always maintained within the source. As soon as the waste is buried, it is assumed that all species present immediately dissolve in the available pore water up to their solubility limit. At later times, the material in the source area will decay but with the restriction that the concentration of any daughter species will not exceed its solubility limit. In addition, if a concentration should fall below its solubility limit and undissolved material in the waste inventory remains, enough new material will dissolve to maintain the concentration at its solubility limit.

It is important to understand that these assumptions apply only to material within the source area. Elsewhere the concentration of species is allowed to vary irrespective of any solubility limit. It may be argued that neglecting the presence of solubility limits within the transport domain ignores a phenomena which certainly occurs. This, however, is one case where conservatism supersedes what is known to occur. If the concentration of a species exceeds its solubility limit, the result is a larger driving force for mass transfer out of the system relative to the realistic case in which the concentrations are restricted at or below the solubility limits. Also, this case is easier to model from a purely operational standpoint.

One final point about the source term model must be made. The concentrations in the source area are calculated only to supply essential boundary conditions for the transport problem in the remainder of the domain. No mass is transferred out of the source into the transport area. Hence, the amount of material within the source is depleted by decay but not by dissolution into the surrounding alluvium. It should be clear that this is another conservative aspect of the model. Ease of solution is the primary motivation behind this last assumption.

(5) The free-water molecular liquid-phase diffusion coefficient is assumed to be a constant independent of concentration. The concentration of all species considered in this analysis is sufficiently small that this is a reasonable assumption. It is also assumed that all radionuclides have the same molecular diffusion coefficient. The latter assumption has been justified by the fact that all the species tend to have very similar molecular weights and will therefore diffuse at similar rates in the absence of adsorptive effects. The value for this diffusion coefficient is given in Appendix C, and it was obtained as a typical value for species with molecular weights less than 500 g/mol, as explained in the PPA.

(6) Moisture content is uniform with depth. On-site measurements indicate that moisture content decreases near the surface. Thus, in reality, diffusion will be slower nearer the surface. Assuming a constant moisture content neglects this additional transport resistance and is conservative.

(7) The radionuclide concentration at the land surface is zero. It is presumed that there is *some* mechanism that will remove these materials once they reach the surface and prevent them from accumulating there. It has been suggested that one possible mechanism is small scale turnover of the surface layer by wind and water. The magnitude of the turnover rate and whether it is enough to maintain a zero concentration at the land surface is unknown at this point. However, since it is not possible at the present time to reject this removal mechanism, conservatism demands that we assume zero concentration at the

surface and therefore release of material from the site is equal to the rate that it reaches the surface.

(8) Species will adsorb to the alluvial matrix following a linear reversible adsorption model. Adsorption was neglected in the PPA liquid diffusion model because it was conservative to do so. However, recent research indicates that adsorption of actinide species onto the alluvium is very significant and should be a part of the conceptual model [Stockman, 1992c]. Adsorption is assumed not to occur within the source area. This was done for reasons of numerical stability. We can justify this assumption within the source area because whether a species adsorbs or not has little effect on its equilibrium liquid phase concentration.

The mathematical statement of the model is simply an unsteady diffusion process with first order loss terms accounting for radioactive decay and adsorption [Bird *et al.*, 1960; Tang *et al.*, 1981]. The model for the liquid phase concentration of the ith radionuclide of an n membered radioactive decay chain is as follows,

$$\frac{\partial C_i}{\partial t} = \frac{D}{\tau R_i}\frac{\partial^2 C_i}{\partial x^2} + \lambda_{i-1}\frac{R_{i-1}}{R_i}C_{i-1} - \lambda_i C_i \quad ; \quad i=1,2...n \tag{2}$$

where

$C_i(x,t)$ = the concentration of the ith member of a n membered chain, [atm/m^3]
D = the free-water molecular diffusion coefficient, [m^2/s]
τ = the tortuosity[dimensionless]
λ_i = the radioactive decay constant of the ith species, [sec], and
R_i = the retardation factor specific to the ith species [dimensionless].

The retardation factor accounts for adsorption of species and is related to the sorption coefficient, $K_{d,i}$[m^3/kg], by the relation [Freeze and Cherry, 1979],

$$R_i = 1 + \frac{\rho K_{d,i}}{\theta} \tag{3}$$

where θ is the moisture content and ρ the bulk soil density [1600 kg/m^3]. It should be clear that R_i is always greater than one for non-zero K_{di} and, hence, has the effect on reducing the effective diffusion coefficient,

$$D_{eff,i} = \frac{D}{\tau R_i} \tag{4}$$

The tortuosity parameter reflects the fact that the radionuclides are diffusing through a porous media. In theory, the tortuosity represents the ratio of the actual diffusion path taken through the "tortuous" pore water channels to the straight line distance between the same positions. Defined as such, it is therefore always greater than one and acts to reduce $D_{eff,i}$ as it increases.

The problem is completed by specification of the initial and boundary conditions on the transport domain that extends from the waste at x = 0 to the land surface at x = L:

$$C_i(x,0) = 0 \quad ; \quad C_i(0,t) = S_i(t) \quad ; \quad C_i(L,t) = 0 \tag{5}$$

$S_i(t)$ is the concentration history of the ith species within the source area. $S_i(t)$ is obtained by solution of the radioactive decay equations with the solubility restrictions discussed under assumption (4), above.

Solution of the problem described by Eqs. (2) and (5) is not a trivial exercise. For reasons of speed and accuracy, an analytical solution is preferable; however, we were unable to find within the literature nor could we develop on our own an analytic solution for the problem as written. An analytic solution is obtainable but only for the special case in which all species within a chain have the same retardation factor. This analytic solution is given in Appendix D for a simplified source term.

In the case where each species has a different retardation, it is necessary to solve the problem via a numerical method. We chose to use a pre-existing flow and transport code known as SWIFT II (Sandia Waste Isolation Flow and Transport). The original purpose of this code was to use the finite difference method to solve for groundwater flow and radioactive decay chain transport in three-dimensional problems. It is a relatively simple task, however, to specialize it for solution of a transient diffusion problem in one-dimension. SWIFT II also possesses a "repository" subprogram that allows us to specify the GCD source term model. In addition, SWIFT II allows for variable-sized time steps. This permits small time steps during the first few centuries as the short-lived species decay away, and progressively larger time steps at longer times when long-lived species persist. This enhances the speed and stability of the computations. The theoretical details of SWIFT II are described in Reeves *et al.* [1986a]. Reeves *et al.* [1990] provides a guide to the input data, and Reeves *et al.* [1986b] considers several example applications of SWIFT II.

The exact details of the numerical procedure are not particularly relevant to this discussion. Suffice it to say that approximately 150 finite difference grid blocks were used to discretize the transport domain. Time-stepping was done using a backward Euler technique, that is, an explicit first order solver. The discretized form of Eq. (2) used was,

$$\frac{C_{ij}^{n+1} - C_{ij}^{n}}{\Delta t} = 2D_{eff,i}\left\{\frac{C_{ij+1}^{n} - C_{ij}^{n}}{\Delta x_j^2 + \Delta x_j \Delta x_{j+1}} - \frac{C_{ij}^{n} - C_{ij-1}^{n}}{\Delta x_j^2 + \Delta x_j \Delta x_{j-1}}\right\} + \lambda_{i-1}\frac{R_{i-1}}{R_i}C_{i-1,j}^{n} - \lambda_i C_{ij}^{n} \tag{6}$$

This equation is written for the concentration of ith radionuclide in the jth grid block at the nth time step; Δx_j is the width of the jth grid block and $\Delta t = t^{n+1} - t^n$. It should be noted that SWIFT II assumes the concentration to be uniform within a grid block.

The zero concentration surface boundary condition was enforced by a special feature existing within SWIFT II. The code allows the volume of the grid block at the surface to be

increased by changing the y and z dimensions of the block. If the volume of this grid block is set to a very large value, the effect is to enforce a zero concentration condition at the land surface because no matter how much material diffuses into this grid block, the concentration within it remains at a very small value.

Computation of the release flux at the surface requires an additional step because SWIFT II solves only for the concentrations in the grid blocks. Fick's law gives the surface flux as,

$$J_{i,surf} = -\frac{\theta D}{\tau}\frac{\partial C_i}{\partial x}\bigg|_{x=L} \tag{7}$$

The derivative in Eq. (7) is approximated as a backward difference from the surface, which is assumed to be at grid block N. Hence, we get

$$J_{i,surf} = -2\frac{\theta D}{\tau}\frac{C_{i,N}-C_{i,N-1}}{\Delta x_N+\Delta x_{N-1}} \tag{8}$$

However, we have established a zero essential condition at the surface, $C_{i,N} = 0$, so Eq. (8) reduces to

$$J_{i,surf} = 2\frac{\theta D}{\tau}\frac{C_{i,N-1}}{\Delta x_N+\Delta x_{N-1}} \tag{9}$$

An example data file used to run SWIFT II is included in Appendix G to elaborate the method used. Appendix D compares the results from the analytic solution described above to the numerical solution of this specialized problem. It is clear from this comparison that the accuracy of the numerical solution is *adequate* for the purposes of performance assessment. The reader is urged to peruse this appendix for further details.

The next few sections discuss the distributions that define the uncertainty of some of the parameters in this model. Note that all parameter distributions relevant to this liquid diffusion model are given in Appendix C.

3.1.1.1 Moisture Content Distribution

One of the several measurements made on cores taken from the exploratory boreholes was θ, the volumetric moisture content (VMC). Core samples from exploratory boreholes 1, 2, 4, 5, 6, and 7 were analyzed for VMC. The depths to which sampling was done were, respectively, 35.4, 37.5, 34.1, 11.0, 35.4, and 10.4 meters. These moisture content data were then combined with data taken from the GCD boreholes themselves [McGrath, 1987] to yield the complete moisture content data set; no weighting scheme was used to reflect any differences in either group of measurements. We justify combining data taken at two different points in time on the basis that it is desirable that any distribution of moisture contents used should possess some information on temporal variability, since the end use of such a distribution is in a transient simulation.

Figure 3.1 is a scatter plot of the VMC versus depth. There is a very definite trend to moister conditions at lower depths. This trend should come as no surprise since the majority of evapotranspiration occurs at or near the soil surface. Drier conditions usually imply slowed vadose zone transport in the absence of advection. Therefore, a less conservative distribution, i.e., one skewed to drier conditions, is obtained if the entire data set is used. To avoid this problem, only moisture contents at depths greater than 12.2 m were used to generate a moisture content distribution. This value was selected from individual exploratory borehole plots of moisture content with depth that showed the moisture content reaching a more or less constant value at depths greater than about 12.2 m [REECo, 1993]

Before a complete statistical analysis of this data can be performed, it is necessary to consider the possible spatial correlation of the data to avoid developing an erroneous distribution function. This is usually done by finding the variogram plot of the data [Isaaks and Srivastava, 1989]. The variogram is a plot of the sum of the squared differences of data values separated by a distance h as a function of h. For example, if we had a set of spatial moisture content data in which the data points were separated by a constant distance of 0.5 m, we would construct a variogram plot by first summing the squared differences of all moisture content values that were separated by 0.5 m. Then, we would sum the squared differences of all data points separated by 1.0 m; after that, we would consider the data points separated by 1.5 m, and so on until we have computed a sum for all possible separation distances. By plotting the sum of the squared differences at each separation distance against the associated separation distance, we arrive at a variogram plot. In general, what is seen is that at small separation distances, referred to as lag depths, the value of the variogram will be relatively small, consistent with the notion that points that are closer together tend to have similar values. As the lag depth increases, however, the variogram also increases, consistent with the fact that points that are farther apart will tend to have dissimilar values. At some lag depth, it is generally observed that the variogram becomes independent of lag depth, consistent with the fact that points that are separated by large distances will not be correlated to any extent. The lag depth at which this occurs is called the correlation length. Data separated by distances greater than the correlation length are generally assumed to be independent.

Figure 3.2 shows the variogram for the VMC data. The variogram is actually for the residual values of VMC, that is, the values obtained when a linear regression model of the data in Figure 3.1 is subtracted out, thus removing the trend to moisture conditions at deeper depths. Note that removal of this trend was done only for the purposes of the semi-variogram analysis. This figure suggests that the variogram is more or less constant with separation distance, the implication being that the correlation length is smaller than the smallest separation distance, or, effectively, zero. Hence, all the data points are independent, and the entire set of moisture content data values below 12.2 m depth can be used in developing the probability density function for the one-dimensional diffusion model.

The frequency histogram of the VMC data is shown in Figure 3.3. Note that this figure is for the orginial moisture content values below 12.2 m. Any trend existing within this data set was retained. Even with removal of the near surface data, the distribution is still skewed slightly to drier values of moisture content. The skewing and the lack of a substantial low-end tail suggest that a lognormal distribution is an appropriate model for the distribution. Statistical analysis of the log-transformed data yields a Shapiro-Wilk statistic of approximately 0.98. Appendix E discusses the nature and interpretation of this test statistic. The ultimate point, however, is that when the statistic is of this magnitude (0.98), it can be affirmed that a normal distribution is the best representation of the data. Since the statistic was determined for the log-

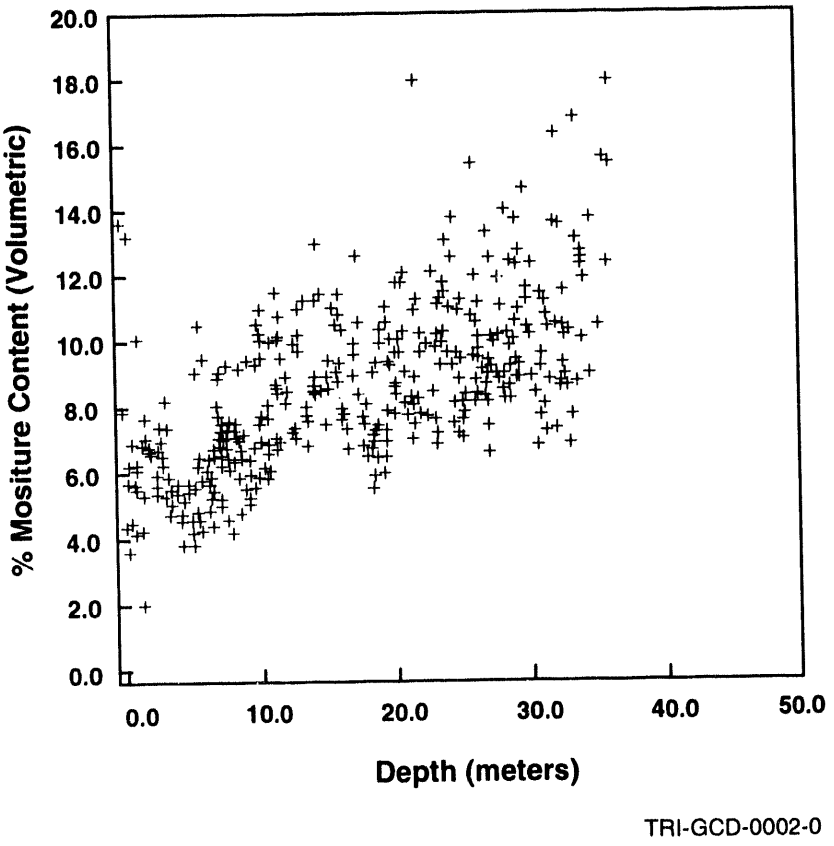

Figure 3.1 - Scatter plot of moisture contents with depth.

transformed data, the subsequent conclusion is that the original data follow a lognormal distribution. We find the expected value and variance of the log-transformed data to be 2.227 and .0469, respectively. This information can then be translated by relatively simple relations [Iman and Shortencarier, 1984] to give the sample mean and standard deviation of the original data:

$$\bar{\theta} = 9.49\% \ , \ s_{\theta} = 2.08\%$$

The 0.001 and 0.999 quantiles of the distribution can be obtained from the mean and variance of the log-transformed data by adding or subtracting approximately 3.09 standard deviations from the expected value and transforming the result back to "real" moisture contents. This yields quantiles of 4.75% and 18.10%. The corresponding values of PPA's moisture content distribution are 6% and 17% indicating that the new distribution is similar to the old, at least in range.

3.1.1.2 Tortuosity Distribution

One of the key parameters in the liquid diffusion model is the tortuosity. As noted above, its function is to account for the convoluted diffusion pathway existing in porous media. In theory, it is the ratio of the actual pathlength between two points within the medium to the

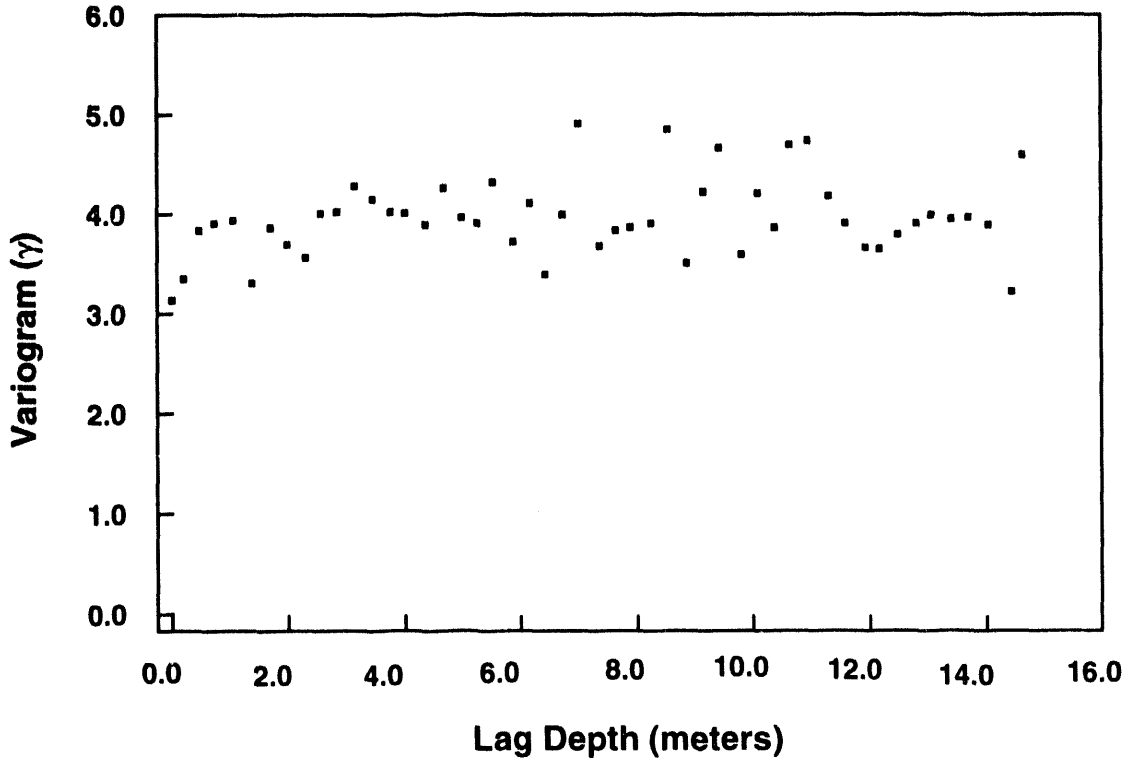

Figure 3.2 - Semi-variogram plot of moisture content residuals.

straight-line separation distance of the points. In practice, it is found by noting the amount by which diffusion is slowed in the porous medium with respect to a pure liquid phase, assuming that adsorption is negligible. In unsaturated media, it is highly dependent upon the moisture content with small moisture contents resulting in larger tortuosities.

In the PPA, a range of tortuosity was chosen between 1 and 110. The first value is the theoretical tortuosity minimum and corresponds to a particle packing situation in which there is no interference with the diffusion pathway. The latter value was arrived at using a relationship between moisture content and tortuosity suggested by Campbell [1985] and the minimum moisture content expected. Campbell's relationship suggested an upper bound of approximately 100. This was increased to 110. A uniform distribution was assumed to exist between these two extremes, as no further information existed on which tortuosity values were the most likely.

If we determine an upper bound for tortuosity in the same manner as the PPA but using a minimum moisture content of 4.75% obtained previously, we arrive at a maximum tortuosity in excess of 3000. Retaining the PPA's upper bound of 110 is therefore conservative. Hence, for this second PA iteration, re-evaluation of the tortuosity distribution focused on the lower bound. It simply *cannot* be possible that tortuosity values are at or near unity for very dry alluvium overlying the GCD boreholes. However, if we reject one as a lower bound, the problem of establishing a new lower bound still exists. We consulted the literature for other empirical relationships for tortuosity and/or experimental studies of diffusion coefficients in unsaturated media. By "polling" these sources for a minimum value of tortuosity, we hoped to arrive at a

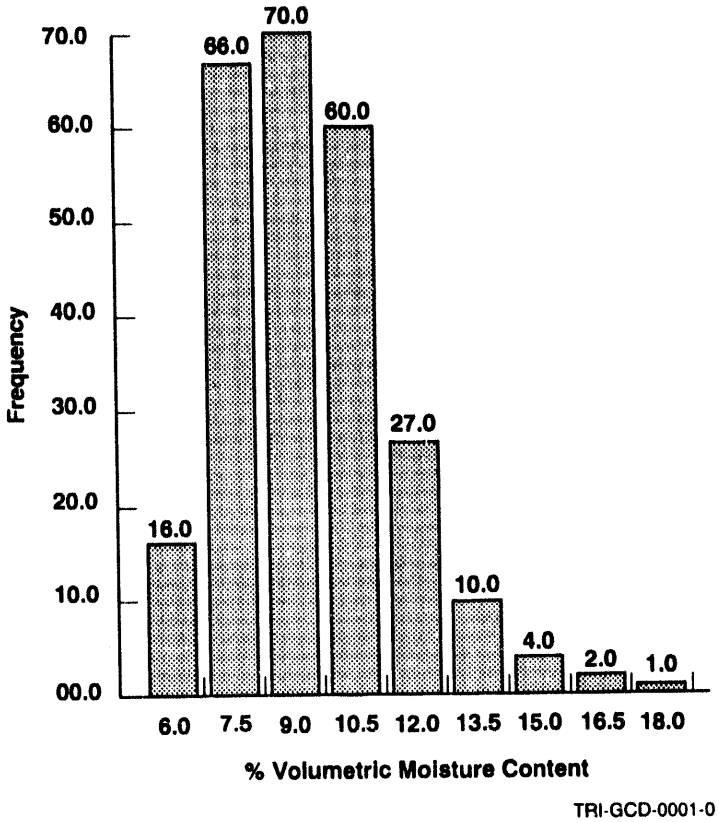

Figure 3.3 - Frequency histogram of moisture contents at depths greater than 12.2 m.

more "realistic" value than unity for the lower bound, but a value that was also defensible.

We discovered a number of correlations for tortuosity. The first was Campbell's [1985], that had been used in the PPA (it differs slightly in form from the correlation given in the PPA because of the different definition of effective diffusivity used in this iteration),

$$\tau = \frac{1}{2.8\theta^3} \tag{10}$$

A second was developed by Sadeghi *et al.*, [1989] after studying diffusion of urea in a number of different soils, none of which adsorbed urea,

$$\tau = \frac{\epsilon^{2.98}}{0.18\theta^{2.98}} \tag{11}$$

where ϵ is the porosity. Sadeghi *et al.*, [1989] also modified Campbell's original relation to better fit their data. They obtained,

$$\tau = \frac{1}{0.73\theta^{2.58}} \tag{12}$$

Finally a correlation developed by Millington and Quirk [Jury *et al.*, 1984] was selected

$$\tau = \frac{\epsilon^2}{\theta^{2.3}} \tag{13}$$

These correlations are simple in form and therefore reasonably general for many different cases. Two cases are considered for a prediction of minimum tortuosity. The first is a "realistic" case wherein the moisture content is set at 18.1%, the upper limit of the distribution described in Section 3.1.1.1, and the porosity is set at 24.48%, the lower limit of the distribution described in Appendix B. The second is a "conservative" case based upon assumed saturated conditions. Here, the moisture content is set equal to the maximum porosity value, 46.3%. The forms of the correlations indicate that these parameter choices will produce the smallest tortuosities in each case. The values obtained are shown in Table 3.1.

Table 3.1 - Minimum tortuosity predictions of several correlations.

Correlation	Minimum tortuosity predictions	
	"Conservative"	"Realistic"
Campbell	3.48	60.2
Sadeghi *et.al.*	5.56	13.6
Modified Campbell	10.0	11.23
Millington and Quirk	1.26	3.04
Conca and Wright		9.5

The additional estimate of minimum tortuosity listed as Conca and Wright [1992] was an experimental study of diffusion in bentonite. Diffusion coefficients of a dissolved, non-adsorbing electrolyte were obtained by conductivity measurements. Moisture contents in the bentonite ranged from less than 1% to over 70% at saturation. An estimate of minimum tortuosity was obtained by taking the ratio of the diffusivity at 18% moisture content (2.1×10^{-6} cm^2/s) and the value at saturation (2×10^{-5} cm^2/s).

Inspecting these results, we see that we can ignore the prediction of the first correlation for the "realistic" case on the basis of conservatism; it is simply too large relative to the other predictions to be defensible. The smallest value seen is 1.26 from the Millington and Quirk relation applied to the conservative case. However, the accuracy of this relation at moisture contents less than 30% percent has been questioned [Ryan and Cohen, 1990], so we are justified in ignoring this value. Of the remaining values obtained, all are greater than three. Therefore, it is felt that this value can be taken as a new lower bound. We still have no information about the appropriate shape of a tortuosity distribution, so we retain the form used in the PPA: a uniform distribution. Hence, the distribution used for tortuosity in this iteration is a uniform distribution ranging from a minimum of three to a maximum of 110.

3.1.1.3 Distribution of Plutonium Solubilities

In order for radionuclides to migrate, it is first necessary that they dissolve into the liquid phase. As a result, the solubility of each radionuclide in the NTS geochemical environment is

of great importance to any transport model. This point is born out by the sensitivity analysis of the PPA, which identified the Pu solubility as having a large influence on the integrated discharges. The original Pu solubility values used in the PPA were calculated using the geochemical code EQ3/6 [Wolery, 1983; Wolery and Daveler, 1992]; they are detailed in Chu and Bernard [1991]. In the previous study, however, the presence of organic complexes or the buffering capacity of the mineral matrix was not considered. As a result, Bruton's study could potentially overpredict or underpredict solubilities by one or two orders of magnitude. In view of the large influence of Pu solubilities, overprediction could result in unreasonably large discharges in light of what we know about Pu solubilities. In addition, the sorptive properties of Pu are heavily influenced by liquid phase speciation, and it is therefore necessary to better understand the solubility before an attempt is made to refine the adsorptivity. Therefore, it was well within our interests to reconsider the nature of Pu solubility.

The technique used in this iteration was numerical tracing of chemical reaction paths by the *React* code [Bethke, 1992]. Its basic function is numerically titrating a mixture of radionuclide contaminants, minerals, and organic compounds under various environmental conditions. While performing this titration, it determines the concentration of various species, in particular, those of actinide-based compounds, as well as the solid phase that controls the solubility. A considerable thermodynamic data base accompanies the code; however, data for several Pu species were not present and had to be estimated and added separately [Stockman, 1992b].

The computation proceeds under the assumption of thermodynamic equilibrium subject to certain kinetic constraints, the foremost being that plutonium dioxide solid phases do not form because it is common knowledge that these species have exceedingly slow formation rates in the environment. Also underlying this model is the assumption that Pu-rich solid phases exist within the source area that control the liquid phase solubility. The fact that material might adsorb to the surrounding soil matrix within the boreholes should have no effect on the solubility of a given species so long as these Pu-rich solids are present. There is some uncertainty regarding the initial form that the waste takes. If the initial form in the waste were far from equilibrium (e.g. Pu metal), it is likely that it would form a metastable, more soluble phase, such as Pu hydroxide, as it reacts with groundwater. If it were Pu dioxide, the thermodynamically stable form, we would be safe in lowering our solubility estimates. We chose the conservative approach of using the metastable, more soluble phases that are observed to form over a period of years in laboratories. Chu and Bernard speculated that the actinides would mainly be altered to oxides, but *adequate* evidence for this assumption has not been found.

Determining solubilities is a rather involved process. The reason being that, aside from the pore water composition, there are several variables that can influence the concentration and the speciation, including: the fugacities of CO_2 and O_2 , the activity of H^+, and the activities of organic chelating agents. The general procedure was to use the pore water composition estimated for the GCD area by Stockman [1992a] as a starting point, fix the fugacities (of pCO_2 and pO_2) to characteristic values, and then increase the pH from 3 by addition of NaOH or other basic minerals. The pCO_2 was generally set to either $10^{-3.5}$ or $10^{-2.5}$ atm, which correspond to atmospheric conditions and soil gas measurements made in Rock Valley (an area southwest of Frenchman Flat) respectively. Thus, as far as CO_2 pressure is concerned, the equilibrium is imposed externally. A difficulty arises with this procedure because the buffering capacity of the surrounding soil tends to impose an upper bound on the pH of the system. This, in turn, suppresses the solubility of carbonate-based Pu species. This limitation can only be exceeded by imposing a smaller pCO_2 on the system. The backfill in all but three of the boreholes is just

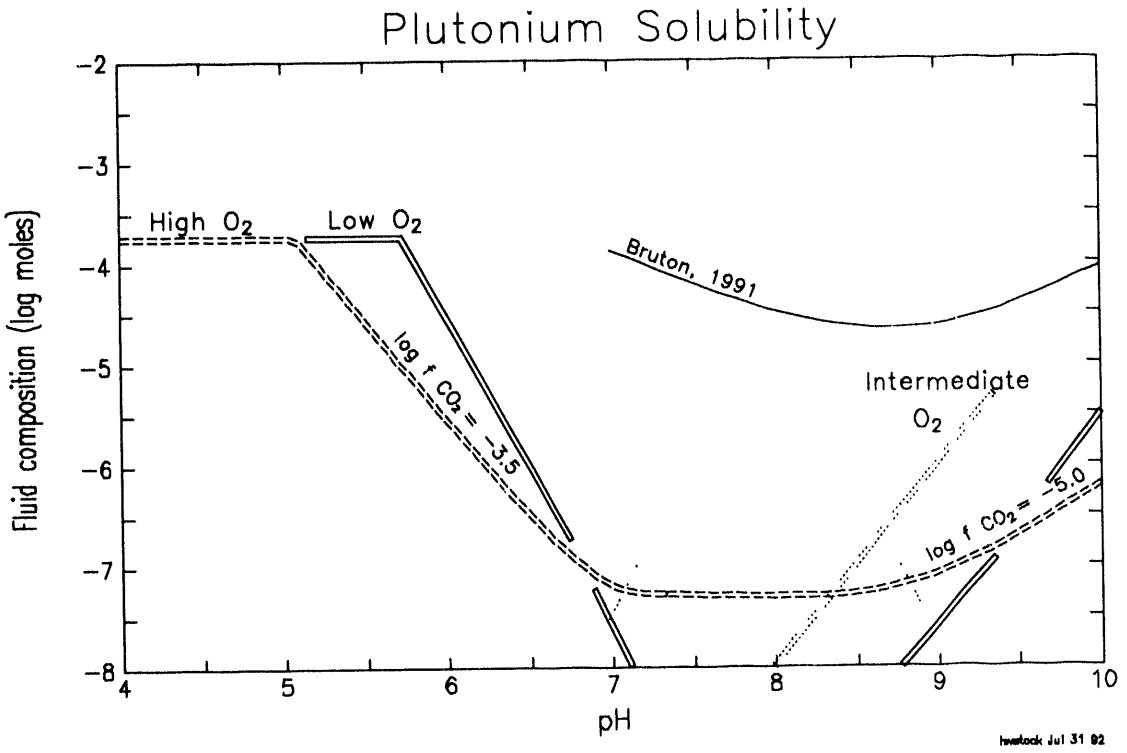

Figure 3.4 - Plot of plutonium solubility as a function of pH and oxygen potential [Stockman, 1992b]. The solid curve labeled, Bruton 1991, is the source of the PPA solubilities.

the native alluvium. As noted above, it has considerable buffering capacity. With an external pCO_2 of $10^{-3.5}$ atm, the pH could be raised to only 8.4. Thereafter, larger pH values could only be reasonably attained only at the expense of decreasing the imposed pCO_2.

The mineral environment of the three remaining boreholes is dominated by a boron-based material known as probertite, which was introduced at the time of burial to reduce the possibility of a criticality event. For our purposes, the probertite is essentially inexhaustible. Probertite also has considerable buffering capabilities and can be shown to antipathetically buffer pH and pCO_2. As CO_2 is added to the alluvium-probertite system, the pH starts in the range 9.1 to 9.3 with $pCO_2 < 10^{-6}$ atm, but as larger amounts of CO_2 are added to the system, the pH drops, first to a plateau near pH 8, and finally to a value of 6.5 at $pCO_2 \approx 1$ atm. Thus the presence of probertite makes it extremely difficult to obtain conditions of both high pH and high CO_2. The probertite does not change the speciation of the plutonium but can affect the concentration of the species in solution.

Figure 3.4 summarizes the results of the reaction path modeling. Three of the curves on this figure reflect the behavior at high (atmospheric), intermediate (10^{-25} atm), and low ($10^{-68.8}$ atm) O_2 fugacities. While the intermediate and low values seem extremely small, the intermediate values are in fact close to that of many groundwaters, and the low values are seen in bog waters and in situations dominated by rusting iron. The reason for considering these low values of fugacity for oxygen is that there has been some suggestion that complexation by organics occurs to a higher degree at low oxygen potentials. For the atmospheric O_2 curve, it is seen that at low pH values, the solubilities are quite high and are dominated by plutonium

fluor-oxides. As the pH increases, the solubility declines considerably, and the speciation becomes dominated by hydroxy-carbonate species. Up to a pH of 8.4, the CO_2 pressure is maintained at $10^{-3.5}$, but because of the buffering capacity of the alluvium beyond 8.4, it is necessary to reduce the pCO_2 to a much smaller value. A curve at $pCO_2 = 10^{-5}$ has been spliced onto the first curve at this point to indicate the solubility behavior expected when buffering is taken into account. It is seen that the solubility reaches a low value of approximately 10^{-7} molal before increasing slightly for pH greater than 9. Had the CO_2 pressure been maintained at atmospheric, a much more dramatic increase of solubility would have occurred at these high pH values. However, because of the buffering this situation is not possible.

The curve labeled intermediate O_2 shows negligible solubility at low pH, but at a pH above 8 the solubility increases dramatically. In this case the speciation is as an organic complex (modeled as saccharic acid) of plutonium. It is important to recognize that we view saccharic acid as a *representative* organic complexing agent; other (generally weaker) complexing agents may form from the oxidative breakdown of cellulose. The solubility of this species is not influenced by the presence of CO_2, and, therefore, the buffering of the solution is not a factor in its equilibrium. The fugacity of CO_2 can therefore be maintained at its atmospheric value. The choice of saccharic acid as a likely complexing compound is motivated by at least one study [Cross *et.al.*, 1989] that suggested saccharic acid would be the likely complexing agent arising from the decomposition of waste packages. Complexation by a species similar to EDTA in chelating properties produced from decomposition of the plywood glue was also considered a possibility. However, the presence of significant amounts of calcium ions in the system effectively tie up the available EDTA-like complex and reduce its effect on the solubility of plutonium.

Finally, the lowest oxygen activity curve shows very high solubility at low pH, which reflects a change in the oxidation state of plutonium to +3 in this very reducing environment. At basic pH, it decreases to an approximate low of $10^{-8.5}$ molal at about pH = 7.5 and increases once again for higher pH, but at a level generally much lower than the intermediate O_2 case. The primary species for this case is also an organic complex. The pCO_2 for this case is maintained at 10^{-5} atm.

It is notable that a recent experimental study of plutonium solubility in CO_2-rich waters from the Yucca Mountain area is in substantial agreement with the estimates given above (Nitsche *et al.*, 1993).

Developing a likely range for solubilities is based upon a reasonable range of pH. For the calcium-rich soil overlying the boreholes it is very unlikely to see a pH less than 7. The presence of calcium carbonates and other basic species imply that acidic conditions are simply not likely, and we can therefore ignore the portions of the curves that lie below this value (pH as low as 6.0 has been observed in some landfills in the eastern U.S., but these are extreme values related to anaerobic conditions with abundant organic matter). In the remainder, probably the best value for the pH upper limit is at the probertite buffer pH of 9.3. It is unlikely that the pH of the remaining alluvium would ever exceed this value under most conditions. The largest solubility seen at the upper pH limit of 9.3 is for the intermediate O_2 case, and from the figure we can determine the value as approximately $10^{-5.4}$ molal. Note that we do not attempt to determine a direct relationship between pH and solubility, which would permit us to treat pH as the uncertain variable. Additional uncertainty would accompany such a relationship, further compounding the uncertainty existing in the solubility values. We choose instead to treat the uncertainty in the solubilities directly and develop a pdf for plutonium solubility.

The lower limit of the solubility distribution might be established at the minimum on the low O_2 curve. However, it is unlikely that in the organic-poor desert environment the O_2 activity will approach values characteristic of an organic-rich bog. A more reasonable choice, which is also the conservative choice as well, for the lower solubility limit is the flat portion of the highest O_2 activity curve, approximately 10^{-7} molal. In the long run, organic chelating agents will decay, and the overall speciation will revert to the hydroxy-carbonates that dominate the solubilities at the highest O_2 activities.

Unfortunately, having established a reasonable range, there is no information available that would permit us to quantify the likelihood of one set of values within the range over another. In such a situation, a uniform probability distribution between the two extreme values is the only reasonable recourse. It should also be noted that even the most extreme solubility value suggested above is approximately one order of magnitude smaller than those used in the PPA, as shown by the fourth curve in Figure 3.4 labeled: "Bruton, 1991." This much of a difference in such an influential parameter is likely to affect the final result significantly. Note that this probability distribution applies to all boreholes, whether they contain probertite or not. Finally, it should be understood that only the solubility distribution for plutonium isotopes was altered in this iteration. The solubility distributions for the other radionuclides were those used in the PPA.

3.1.1.4 Distribution of Plutonium Sorption Coefficients

Another important parameter in the performance assessment model is the sorption or distribution coefficient, K_d. This particular parameter is used in a very simple, linear, reversible sorption model that relates liquid-phase solute concentration to the concentration on the solid phase in contact with the liquid phase. The majority of sorption studies report their results in terms of this distribution coefficient. It has a simple definition,

$$K_d = \frac{mols\ solute\ absorbed\ per\ gram\ solid\ phase}{mols\ solute\ per\ mL\ liquid\ phase} \qquad (14)$$

Adsorption phenomena are important because an ion that is adsorbed is essentially immobile for a period of time. As a result, adsorption tends to slow down the transport of contaminants in the liquid phase and reduce the average release. The retardation model assumes equilibrium partitioning between fluid and solid at all times; because the solid is unmoving, the average speed of solute transport is much lower than the average speed of fluid flow. The sensitivity analysis done by the PPA identified the plutonium distribution coefficient as having a significant influence on the overall release. For this second iteration, an effort was made towards determining plutonium distribution coefficients more specific to the geochemical environment thought to exist at the NTS.

A literature search was conducted to find distribution coefficient studies that could be applicable to the GCD site [Stockman, 1992c]. Numerous criteria were established to aid in screening these studies; among these were sufficient duration of the experiment to permit equilibration, low liquid to solid phase mass ratios to mimic the actual *in situ* situation, mineralogy similar to the NTS alluvium, similar aqueous phase chemistry, in particular comparable pH, CO_2, and O_2 potentials, and presence of organic compounds that might chelate

the solubilized ions, as the decay of packaging materials surrounding the waste might contribute such organic species to the overall geochemistry.

Of the literature considered, only a very few were deemed likely to give K_d values that could be used in the NTS environment. Higgo and Rees [1986] considered adsorption out of seawater, and their work suggests a plutonium K_d of approximately 100 ml/g for geochemical conditions similar to the GCD site. A second study by Torstenfelt *et al.*, [1988] used water from the J13 well at NTS as the liquid phase. At basic pH, they report K_d values somewhat greater than 100 ml/g. Another study by Berry *et al.*, [1991] made use of two degraded-cellulose simulants to consider the influence of organic complexing agents. The effects of colloid particles were rigorously suppressed through centrifugation because the presence of these mobile particles can introduce error in the measurement. From their results it is possible to estimate a K_d of again approximately 100 ml/g for the mineralogy at the GCD site.

There is little information on the possible role of colloids in adsorption phenomena. A study by Penrose *et al.*, [1990] considered plutonium transport at the Mortendad canyon site near Los Alamos, New Mexico. Colloidal adsorption and transport is thought to be a significant factor at this site. Based upon differences in travel time, we estimated from the Penrose *et al.*, a distribution coefficient of 1.56 ml/g, a value that is thought to reflect the influence of colloids. Caution should, however, accompany this value as rigorous laboratory techniques led to a value four orders of magnitude higher, a much more conservative value. It should also be noted that additional transport of plutonium via an intermittent stream in Mortendad canyon along with seasonal variations in groundwater velocity could result in 1.56 ml/g being an underestimate [Purtyman, 1974; Hakonson *et al.*, 1980; Nyhan *et al.*., 1982; Niklaus and Feldman, 1980; Abrahams *et al.*., 1962].

From the preceding studies, it was necessary to develop a distribution that describes the uncertainty in the plutonium distribution coefficient. The role of colloids in liquid-phase transport at the NTS is not known with any degree of certainty; however, it is quite likely that it is much less than at Mortendad canyon where the original waste stream was pre-disposed towards colloid formation. Nevertheless, we cannot discount the effect of colloid particles at the NTS. There is evidence that species adsorb less strongly to colloids. Thus, if a significant fraction of dissolved species adsorb to colloid particles, the average effective diffusivity will be higher. Therefore, until information exists that indicates that colloids are not present to a significant degree at the NTS, it is not conservative to neglect their presence.

Based upon this argument, it was felt that a reasonably conservative lower bound that would take the presence of colloids into account would be at $K_d = 1.56$ ml/g. The fact that 1.56 ml/g may be an underestimate serves only to increase the conservatism of this choice. Choosing an upper bound of 100 ml/g could be justified from the three studies that generally found K_d values on the order of this value. Because these studies also indicated that K_d values that were not influenced by colloids were much larger than 100 ml/g, this upper bound choice is also quite conservative.

The form of the distribution remains to be determined. Unfortunately, there is little that can be used to suggest the relative probability of K_d values and, therefore, the overall shape of the distribution. There is little information on the presence of colloidal particles in the liquid phase at the NTS. As a result, it is difficult to assess their relative importance when it comes to transport. However, there is reasonable evidence that 1.56 might be an underestimate of *colloidal* adsorption and therefore it is not reasonable that it should be given a large probability. The principle of maximum entropy [Harr, 1987] suggests that where information exists only for the upper and lower boundaries of distribution, a uniform distribution is the appropriate choice.

However, we have additional information that 1.56 ml/g is likely an underestimate of colloidal adsorption. Thus, we must reject a uniform distribution since it would assign too large a probability density to values near to 1.56. A lognormal distribution, on the other hand, would possess the requisite property of low probability density near the lower bound. The choice of a lognormal distribution is somewhat arbitrary; we have no information that the actual sorption coefficient uncertainty can be represented by a lognormal distribution. Since we are uncertain about the true shape of the distribution, we should like to be conservative. This requirement is also met by the choice of a lognormal distribution, which assigns the highest probability densities to relatively small sorption coefficients. It should also be noted that a lognormal distribution is completely defined by specification of the 0.001 and 0.999 quantiles (or any two quantiles). Unavailable information about the mean, standard deviation, kurtosis, etc. is not necessary when using this type of distribution. This would not be the case if a beta distribution, for example, were employed instead.

For the record, the distribution coefficients used in the PPA were assumed to be lognormally distributed between 0.001 and 0.999 quantiles of 0.001 and 1000 ml/g. Thus, the new lower bound is less conservative while the new upper bound is more conservative.

3.1.2 Plant Uptake Model

As radionuclides diffuse upwards, there are two pathways by which they can be released to the accessible environment: (1) Direct release at the surface, (2) Absorption by plant roots extending downwards into the soil, followed by transport upwards past the ground surface (and, therefore, into the accessible environment) to the vegetative portions of the plant.

The latter pathway was modelled by the PPA in a very simple fashion. The depth of the roots was assumed to be 10.7 m, and the diffusive flux was found by Eq. (7) at that depth. This value was multiplied by an uptake factor of 10^{-3} that was the same for all species and also by a root density factor of 0.1. The result was the flux released via the plant pathway. Although the uptake factor was based to some extent on measured uptake factors, this factor is highly dependent upon isotope as well as numerous other factors. Thus, it was inconsistent to use the same uptake factor for all radionuclides. The root density factor was a guess. All this was acceptable in the PPA, because the liquid diffusion pathway was not considered a dominant pathway. This is now no longer the case and a more rigorous uptake model is needed.

For plants growing in contaminated soil, the complex process of radionuclide transport into and through plant physiology is usually simplified into a factor called the concentration ratio defined as follows,

$$CR = \frac{Ci/g\ dry\ above\ ground\ vegetation}{Ci/g\ dry\ soil} \qquad (15)$$

This definition assumes equilibration between plant and soil. Measurement of the CR is quite straightforward. Plants of a given species are grown on contaminated soil of a known concentration. At some point, the vegetative portions of the plants are harvested and counted to determine the concentration of radionuclides in the plant. The ratio of these two concentrations is the concentration ratio. This relative ease in measurement is the primary advantage of using the concentration ratio to model plant uptake; a great deal of concentration ratio measurements have been made on numerous plant species.

To model plant uptake using the concentration ratio, we first assume a maximum rooting depth, r. Conservatively, the liquid concentration in contact with the roots, C_l, is assumed to be the solution value at x = r, or, $C_l = C(L - r, t)$. This liquid concentration can then be translocated to a plant concentration C_p (Ci/g dry vegetation) by the relation,

$$C_p = CR \left(\frac{\theta}{\rho} + K_d\right) C_l \tag{16}$$

where ρ is the bulk soil density [kg/m^3]. It should be noted that Eq. (16) does not have an explicit term that accounts for the density of roots below ground. Assumption of equilibration between plant and soil makes accounting for root density unnecessary. We presume a given soil concentration results in the same equilibrium plant concentration irrespective of the density of roots. This is another of the virtues of using the concentration ratio: obtaining difficult-to-measure root density data is unnecessary. Note that the definition of concentration ratio refers only to total soil concentration, which includes both materials dissolved in the liquid phase and sorbed materials. Hence, the need for the term involving the distribution coefficient, K_d, in Eq. (16).

The problem at this point is that the Containment Requirements are based upon integrated fluxes, and the concentration ratio provides only concentration information. We can, however, get around this difficulty by noting that the change in plant concentration above ground is related to release flux. If the average yearly vegetative release flux is J_{veg} [atom/m^2-yr], then over a period from t to t + k years we can write a material balance on an cross-sectional area A,

$$J_{veg}Ak = B(C_p(t+k) - C_p(t))A \tag{17}$$

where B is the above ground biomass per unit area [kg/m^2] and is assumed constant. This immediately leads to a relation for J_{veg},

$$J_{veg} = B\frac{C_p(t+k) - C_p(t)}{k} \tag{18}$$

Measurement of B is quite simple, and a pair of studies actually report values for B in Frenchman Flat and surrounding environs [Hunter and Medica, 1989; Romney *et al.*, 1973]. It is clear from these studies that B is not in fact constant but very dependent upon annual rainfall totals. However, when the biomass density data is analyzed over several years, no recognizable statistical model is evident. Use of an empirical statistical model was also deemed unsatisfactory since it would likely not be defensible over a long period of time because of the short span of years on which it was based. As a result, it was decided that B should be fixed at the largest measured data value. Because the release flux is directly proportional to the biomass density and the biomass density does not interact with any other parameters directly, it was felt that this was a conservative step. For current Frenchman Flat conditions this upper limit is approximately 0.49 kg/m^2.

While simple, there are several additional questions about the conservatism of Eq. (18). First, as the soil concentration approaches a steady state profile, Eq. (18) indicates that the flux will approach zero. Second, the model assumes that once an isotope is withdrawn into the above ground foliage it ceases to decay. Since the material in the ground continues to decay, it is not

hard to imagine that for some isotopes, Eq. (18) might actually predict a negative flux back into the subsurface. Both these failings are really reflections of a larger shortcoming: Eq. (18) ignores the fact that vegetation is constantly regenerating. It assumes no change in the vegetative environment over 10,000 years; that is, the plants that are there currently will be there in 10,000 years. This is clearly an unrealistic feature. Still, lack of realism is not a disqualifying aspect of a model within the confines of our methodology. Failing to account for regeneration, however, tends to reduce the total release, that is, make less conservative, which *is* disqualifying.

However, a simple modification allows us to approximately account for regeneration. We presume that every k years a new generation, which is uncontaminated, replaces the old. The old contaminated vegetation is discounted, because it is past the land surface and therefore into the accessible environment. We *do not*, however, presume that isotopes are introduced at the land surface by the decaying old vegetation.

Now accounting for regeneration in this way leads to the average yearly vegetative flux expressed as,

$$J_{veg} = B\frac{C_p}{k} \tag{19}$$

Eq. (19) is still incomplete, however, because it fails to account for the turnover in biomass as well as its generation. In addition to growth, plants also slough off and replace vegetation on a continual basis. For instance, in a time period k, a standing biomass density of B might be produced, but during that same time period a biomass of nB [kg/m^2] will have been dropped off and replaced. This "leaf-dropping" produces no net change in the standing biomass density, but because the material that is sloughed off is contaminated, it results in an additional release flux through the vegetation. We account for this processes simply by adding another term to Eq. (19),

$$J_{veg} = B\frac{C_p}{k} + nB\frac{C_p}{k} \tag{20}$$

or,

$$J_{veg} = B\left(\frac{1+n}{k}\right)C_p \tag{21}$$

As in the case in regeneration of the primary biomass, we do not assume that contamination is introduced at the land surface by the vegetation, which has been sloughed off.

We must now determine reasonable values for the regeneration period, k, and the biomass turnover fraction, n. It is clear that the greatest flux will occur for the smallest value of k, which would result in a conservative model. The smallest value that is still reasonable is k = 1 year. Generally speaking, vegetation regenerates either entire plants or portions of the same plant on a yearly cycle, so this choice is supported. Perennial vegetation, of course, has a much longer regeneration period for the entire plant, but it is conservative to model them as having only a yearly cycle.

Currently, we have no information on a reasonable value of the turnover fraction. It is generally easier to measure the standing biomass than how much material has passed through any individual plant. For the time being, we assume a turnover fraction of one, i.e., n = 1. Thus,

we assume that the standing biomass drops and replaces its entire weight in one year. This is a very conservative assumption because the majority of the biomass of the communities on Frenchman Flat is perennial vegetation. Most perennial plants do not regenerate entirely every year and in that same year produce additional mass equivalent to their weight. Thus, the conservatism of our final uptake model, represented by Eq. (21), should be quite evident. This conservatism is necessary because we have very little information about regeneration periods and turnover fractions beyond an intuitive sense.

3.1.2.1 Concentration Ratio Distributions

The concentration ratio is a simple if somewhat inelegant way of dealing with the problem of translocating soil concentrations to above-ground plant concentrations. The complicated manner in which plants alter the local soil chemistry surrounding their roots by alterating the pH or excreting chelating agents etc., in theory, should be reflected in some manner within the concentration ratio and therefore are not explicitly included in our uptake model. The drawback, however, is that for this very same reason the concentration ratio is highly dependent on many things: plant species, radionuclide, soil pH, type of soil, soil organic content, radionuclide concentration, etc. All this translates into considerable uncertainty when it comes to assigning values for the concentration ratios which in turn means that distributions of concentration ratios must be developed.

The approach taken to determine these distributions was to perform an initial literature search on the subject of radionuclide uptake. Values reported in these studies could then be analyzed statistically to determine suitable distributions. Many studies of plant uptakes were consulted, and, of these, values were taken from seventeen. Appendix F documents the studies used and the values extracted from them. Unfortunately, few of the studies considered desert vegetation in desert environments. The primary species studied were food or forage crops: wheat, rice, soybeans, alfalfa, tomatoes, barley, bahia grass, clover, etc. In addition, the majority of the soil types were agricultural loams or samples collected around Oak Ridge National Laboratory in Tennesse or near the Savannah River facility in Georgia. Only four of the seventeen studies used desert soils collected at the NTS [Romney *et al.*, 1982; Romney and Wallace, 1977; Adriano *et al.*, 1980; Bernhardt and Eadie, 1976]. Furthermore, tumbleweed and cheat grass were the only two desert species considered [Price, 1972]. Nonetheless, the uptake factors reported for these desert plants were within the range reported from the other studies not specific to desert conditions. There is also no reason to believe that desert plants absorb radionuclides any more readily than other species. While it is likely that desert plants are able to extract nutrients to a greater degree than other plants, it does not necessarily follow that radionuclides will be extracted to any greater extent. The difference being that radionuclides are not plant nutrients. Plants adsorb materials via two mechanisms: active transport, where the plant itself assists in transport of materials into the root, and passive transport, which is simple diffusion into the root. It follows that nutrients, such as nitrates and sulfates etc., would be the subject of active transport. It should be noted that actinides have distinctly different chemical structures than these ions and are therefore not likely to be the subjects of active transport. Materials, such as actinides, not needed by the plant would therefore enter via passive transport. Since the physics of diffusion are more or less the same for different plant species, we might suppose that the uptake factors would be similar from one species to the next. This view is supported by the fact that the concentration ratios that we do have for desert plants fall within the range of concentration ratios measured for non-desert species.

For these reasons, we concluded that distributions based upon other non desert plant species grown in non desert soils could be used to *adequately* represent the uncertainty in uptake characteristics of vegetation occurring at Frenchman Flat. In the next performance assessment iteration, this literature survey will be updated and extended with emphasis on finding additional information on desert species.

Generally, information on the uptake of only five isotopes, ^{239}Pu,^{240}Pu, ^{241}Am, ^{237}Np, and ^{90}Sr was reported in these studies. Little useful data were found for the remaining isotopes. Therefore, it was necessary to assume that the remaining plutonium isotopes had distributions identical to ^{239}Pu and ^{240}Pu. This assumption is supported by the work of Nishita [1981a], which indicated no difference between uptake factors for ^{238}Pu and ^{239}Pu. Furthermore, the remaining isotopes for which we have no information, primarily those of uranium, were conservatively assumed to have uptakes identical to ^{237}Np, which has the largest average values. ^{137}Cs was assumed to have an uptake distribution identical to that of ^{90}Sr because these two isotopes are closer in chemical structure to each other than they are to actinides or lanthanides. Little information was available concerning how different oxidation states of the same isotope affected the concentration ratio. Consequently, we must assume that all oxidation states of a given isotope have the same uptake factor. It should also be noted that different parts of the plant could potentially have differing uptake ratios. Uptake factors from the fruits and grains of a species were not included as they tended to be much smaller than other parts of the plant and would have skewed the distributions to smaller values.

The actual form of the concentration ratio distribution for each element is open to some question. However, there is some evidence [Kinnear *et al.*, 1981] that a lognormal distribution is appropriate. Our own statistical analysis is given in Table 3.2. In this table, the Shapiro-Wilk statistic is calculated for the log-transformed concentration ratios. As was mentioned previously, Appendix E discusses the nature and interpretation of the Shapiro-Wilk statistic. The relatively large values of the statistic found for the log-transformed data indicate that a lognormal distribution probably represents the uptake data best. Note that the means and standard deviations listed in Table 3.2 apply to the original data set, not to the log-transformed data.

3.1.2.2 Rooting Depth Distribution

Rooting depth is a significant parameter in the biological model. Unfortunately, we do not have a great deal of information on this subject. The trench mapping being conducted by RSN should provide some site specific data at a later date, but currently we must use the data that is available. There is some anecdotal evidence that root depths are fairly shallow at the NTS [Hunter, 1992], certainly less than 2 m, but little goodevidence on the extreme rooting depths and their relative frequencies. The most extreme depth reported is 10.7 m, which was the (fixed) rooting depth used in the PPA [Price *et al.*, 1993]. A root excavation study is described by Wallace and Romney [1972a] from which it was possible to obtain the depth data for a few individual perennial plants. These are shown in Table 3.3.

From this data, we need to construct a parameter distribution. We also possess the intuitive knowledge that the frequency of roots declines with depth; that is, most of the roots are found near the surface for the current climatic conditions. To reflect this fact in our model, it should be true that the probability of short roots should be greater than the probability of long roots. We propose, therefore, that a loguniform distribution be used that extends over the range between 1.03 and 10.7 m. When a loguniform distribution is plotted semi-log, the distribution

Table 3.2 - Concentration ratio distribution parameters.

Isotope	Sample Points	Mean [Ci/g / Ci/g]	Standard deviation [Ci/g / Ci/g]	Shapiro-Wilk statistic
^{239}Pu,^{240}Pu	40	2.82×10^{-3}	1.85×10^{-2}	.12
Other Pu isotopes	N/A	2.82×10^{-3}	1.85×10^{-2}	.12
^{241}Am	24	.0180	.119	.67
^{237}Np	17	.147	.377	.42
^{90}Sr, ^{137}Cs	25	.188	.152	.16
All other isotopes	N/A	.147	.377	.42

shows equal probability density at all values. Thus, the probability of finding a value, for example, between 0.01 and 0.1 is the same as finding a value between 1 and 10. Thus, the probability of finding a root depth near 1.03 m is the highest and near 10.7 m the lowest. It also ensures that the rooting depth will be at least 1.03 m, so that there is no possibility of a case having extremely short roots.

Table 3.3 - Observed rooting depths of several individual desert plants.

Species	**Root Depth (m)**
Eurotia lanata (winterfat)	0.99
Franseria dumosa (Burr bush)	0.86
Grayia spinosa (Spiny hop sage)	0.97
Hymenoclea salsola	0.81
Larrea divaricata (creosote bush)	1.68
Lycium andersonii	1.22
Average / standard deviation	1.03/.37

It should be noted that in developing this distribution we have made a logical leap that perhaps needs elaboration and justification. Our model of uptake assumes a constant density of roots to a uniform depth. In reality, of course, the root density varies with depth with most of the roots being near the surface with fewer present at depth. We assumed that this fact could be represented in our model by shallow roots being more likely than deep roots. This is justifiable because we are also implicitly assuming that a uniform density of roots penetrating to a uniform depth is equivalent in an average sense to the case where the root density varies with depth. In essence, we are using a mean root depth. Once this is understood, it should be clear that the form of distribution used for root depths is justified. One would expect that deep mean root depths would be less likely than shallower mean depths, in exact accordance with the actual distribution of root density in the soil.

In a subsequent iteration, more site specific data related to root depths in Frenchman Flat will be added to the analysis. It is also possible that under a change in the climate, different plant communities will inhabit Frenchman Flat with different rooting characteristics. This information will also be included in a later iteration.

3.1.3 Erosion Model

The PPA considered the possibility that erosion and deflation of material could potentially expose the waste. Based upon evidence from paleochannels observed within the trenches and the fact that Frenchman Flat is an aggrading basin, the PPA concluded that erosion was not likely to be important in eventual release. Because of the change in the conceptual model in this iteration to upward diffusion-only, erosional processes have more significance because they have the potential for reducing the diffusion path length and speed the release. The PPA also treated erosional events as being part of a separate scenario. Because erosion is currently occuring and probably will occur in the future at Frenchman Flat, erosional processes are properly part of the base case scenario where they have been included in this iteration.

Site characterization information on the erosional processes at Frenchman Flat is being collected by RSN to determine the depth and age of paleo-erosion events. By developing an erosion model, the influence of erosion can be estimated. This in turn can be used to guide site characterization and serve as a basis for deciding whether erosion processes are important.

A very simple model is used to account for loss of material from above the waste. A distance, e, is the presumed depth to which erosion occurs over all the boreholes. Diffusion is assume to proceed across the contracted region from $x = [0, L - e]$. That is, the depth of burial is reduced from L to L - e. In effect, this model imagines that at time zero an erosion event to depth e occurs over all the boreholes and the contaminants now only have to diffuse through a distance L - e to reach the surface. The plant uptakes are modelled assuming this contracted domain.

3.1.3.1 Erosion Depth Distribution

Erosional processes occuring in Frenchman Flat are being addressed by current site characterization activities. Results of this characterization are still preliminary, but it has been suggested [Rawlinson, 1993] that at the elevation of the GCD site the amount of erosion in the next 10,000 years would have very little chance of extending 2 m below present grade. We therefore establish 2 m as the upper limit of our erosion distribution. To decide upon a minimum

depth of erosion one must recognize that area in Frenchman Flat where the RWMS is located is on an *aggrading* alluvial fan. Therefore, there is a small probability that there might be a net *increase* in the alluvial overburden above the GCD waste. As a result, if we choose the lower bound of the erosion distribution to be zero meters we make a conservative choice. We have no actual data on the form this distribution should take. Intuition tells us that deep erosion events are less likely than shallow erosion events. Thus, we would expect that the distribution should be skewed to smaller values. If a uniform distribution between zero and two meters is chosen as our erosion depth distribution, we ignore this skewing and make another conservative choice.

3.1.4 Total Integrated Discharge

The Containment Requirements of 40 CFR 191 regulate the total integrated release over a period of 10,000 years into the accessible environment. One additional step is necessary to determine this quantity from the flux values computed by the liquid diffusion and plant uptake models. If J_{veg} and J_{surf} are the vegetative flux rate and the flux rate to the surface (which in the case of non-zero erosion depth is the flux to the new surface), then the total integrated release of the ith isotope, Q_i, to time t is,

$$Q_i(t) = \int_0^t (J_{veg,i} + J_{surf,i}) A_i(t') \, dt' \tag{22}$$

where $A_i(t')$ is the affected area. For a strict one-dimensional model, $A_i(t')$ is simply a constant equal to the sum of all borehole cross-sectional areas. However, as described in Section 3.1.1, we allow the affected area to vary with time in order to approximately describe the affects of two dimensional diffusion on the total release. For the purpose of determining the affected area, we imagine that contaminants diffuse away from the source as a spherical front beyond which there are no contaminants. The radius of this front, R_i^*, is taken to be one diffusion distance, found by the relation,

$$R_i^* = \sqrt{4 D_{eff,i} t'}$$

Where this spherical front intersects the surface defines the affected area. The affected area is that area on the surface that is subtended by the cone whose apex is at the source and whose longest side intersects the surface a distance R_i^* from the source. Figure 3.5 illustrates this idea. In this figure, a is the borehole radius, L is the depth of burial, and $r^*_i(t')$ is the radius of the affected area. If the affected area is less than the borehole cross-section, the affected area is assumed to be the borehole cross-section, or in mathematical terms,

$$A_i(t') = \begin{cases} N\pi a^2 \; ; \; r_i^*(t') \le a \\ N\pi (r_i^*(t'))^2 \; ; \; r_i^*(t') > a \end{cases} \tag{24}$$

where N is the number of boreholes of interest (N would equal 4 if we ignore the presence of the non-TRU waste; it would equal 6 if we did not).

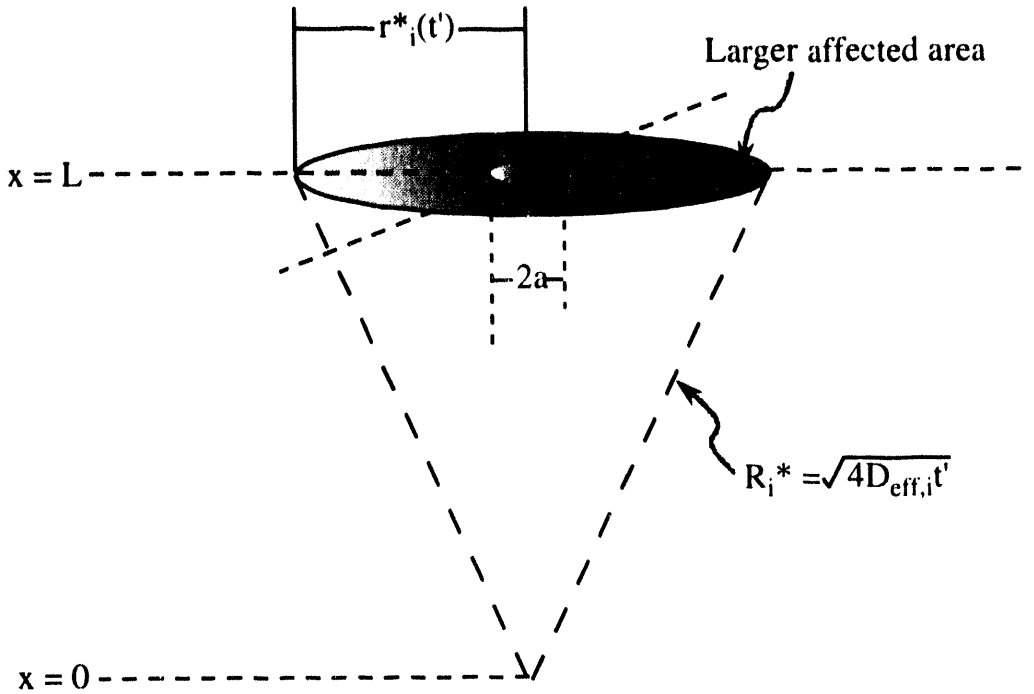

Figure 3.5 - Schematic of affected area computation.

The integral in Eq. (22) is evaluated numerically to 10,000 years for each isotope, and the results are used in computing the EPA sum. A trapezoidal rule is used for the integration because in the solution process the time step size is allowed to vary for efficiency reasons. Hence, fluxes are determined on a non-uniform temporal grid.

Note that the fluxes used in this integration are computed from the one dimensional planar diffusion model described in Section 3.1.1. Thus, these fluxes will occur, in some cases, over an area greater than is consistent with a strict one-dimensional model. It is assumed that this approximate accounting for two-dimensional diffusion is at least as conservative as the "exact" accounting of this phenomena where the smaller fluxes computed from the two-dimensional problem are integrated over the entire surface. The reasoning behind this assumption is as follows. The affected area as computed above defines the limits of the approximate region where most of the release would occur in the two-dimensional conceptualization. By and large, at a given distance from the source, the flux and concentrations computed from the planar one-dimensional conceptualization are significantly higher than those determined from a two-dimensional conceptualization. Thus, the release computed by multiplying the planar flux values by the area determined by Eq. (24) should be larger than the release obtained by integrating the spherical diffusive fluxes over the entirety of the ground surface. Unfortunately, verification of this reasoning requires solution of the two-dimensional problem. This will be done as part of the subsequent iteration.

3.1.5 Uncertainty Analysis Technique

The liquid diffusion model described in Sections 3.1.1, 3.1.2, 3.1.3 can be solved to determine the total integrated discharge (Section 3.1.4). However, the uncertainty in the model parameters means we must apply an uncertainty analysis to the problem. As was done in the PPA, we address this uncertainty by application of a Monte-Carlo approach. A total of N samples were drawn from each of the input model parameter distributions. The computer code LHS (Latin Hypercube Sampling) was employed to determine these sample values. The details of LHS have been documented elsewhere [Price *et al.*, 1993; Iman and Shortencarier, 1984]. LHS is a stratified sampling technique that generates a sample set of each parameter that spans the range of each parameter using fewer samples than conventional random sampling. An important aspect of the technique is to prevent artificial correlations between parameters from being introduced by the sampling itself. Conversely, it is possible to sample specific parameters so that a correlation will exist between them in the set of sampled parameters. In this analysis, only one such correlation was introduced. As the empirical equations presented in section 3.1.1.2 demonstrate, there is fairly strong evidence that some sort of inverse relation exists between tortuosity and moisture content. It is not justifiable that they should be completed uncorrelated. Consequently, tortuosity and moisture content were sampled so that a strong negative correlation existed between the two.

Each parameter value in each of these sampled sets is then combined randomly with values in the other parameter sets to generate a set of N parameter vectors, each of which has a single value for each parameter in the model. Each of these vectors is referred to as a realization, because each represents one possible "model reality" given the uncertainty in the parameters. The model is then repeatedly solved N times using each of these parameter vectors in succession. The result is a set of N total integrated discharges for all the isotopes of interest, which are then combined into N values for the EPA sum as described in the PPA.

From this set of EPA sums, it is possible to estimate the likelihood of compliance with the requirements of 40 CFR 191. If, under the assumption that all EPA sums are equally likely, the EPA sums are ordered from smallest to largest, $\mathbf{R}_1$, $\mathbf{R}_2$, $\mathbf{R}_3$,...,$\mathbf{R}_i$,...,$\mathbf{R}_N$, then the following is true,

$$P(R_{i-1} < R < R_i) = \frac{1}{N} \tag{25}$$

and the probability that $\mathbf{R}$ is greater than $\mathbf{R}_N$ is zero. However, 40 CFR 191 states its requirements in terms of "... probability of release greater than... ," so we are actually interested in the complementary cumulative distribution function (CCDF) of the EPA sum data. It can be found via the relation,

$$P\ (R > R_i) = \frac{N - i}{N} \tag{26}$$

Selection of the appropriate sample size N can be difficult. If N is chosen too small, there is not *adequate* coverage of the parameter space by the sample vectors, and the result is an unwarranted variability in the CCDF. That is, for a different set of sample vectors, a markedly different CCDF is the result, especially at large values of the EPA sum. On the other hand, large values of N are undesirable simply because of the impractical amount of computation-

al effort required. For problems such as ours possessing a complex model between input and output along with many uncertain parameters, there is very little theoretical guidance in choosing an appropriate value of N. We must rely upon trial and error. The sample size must be increased successively until the variability in the CCDF is reduced to an acceptable size. Put another way, we must have a large enough sample size so that there are enough samples present in the high-consequence, low-probability tail of the CCDF (that is, at large EPA sums) that we have confidence in drawing conclusions from our results.

3.2 Containment Requirements - Human Intrusion Events

The PPA identified several possible events that had the potential to severely affect the safety of the GCD site. Of these, the one with greatest adverse effect was possible inadvertent human intrusion into one of the GCD boreholes. The PPA suggested that the most likely intrusion event would be a future generation searching for oil, water, or some other resource, drilling into one of the GCD waste areas, and bringing radionuclides to the surface in the drilling mud. The PPA considered the possible release of such an intrusion and determined that it was very large for the entire regulatory period. *However, no probabilities were calculated to determine the likelihood of such an event.* As a result, no conclusions could be reached as to whether the possibility of human intrusion would lead to non-compliance. In this second iteration, these probabilities were estimated using techniques developed for the Waste Isolation Pilot Plant Project [Guzowski, 1991]. Note that a human intrusion analysis needs to be applied only to the Containment Requirements, because the Individual Protection and Groundwater Protection Requirements apply only to undisturbed conditions.

The probability of a drilling intrusion event can be represented by a Poisson model [Guzowski, 1991],

$$P = 1 - e^{-\lambda_d t} \tag{27}$$

Here P is the probability that at least one intrusion event will occur in a period of t years. The parameter λ_d is the intrusion rate and represents the number of intrusions of a drill bit into a waste area occurring per year; it is generally much less than one. This probability model assumes drilling occurs continually at a constant rate within Frenchman Flat throughout the entire 10,000-year period. This is almost certainly incorrect; presumably, drilling would occur as periods of high activity followed by periods of relatively little drilling. We approximate this periodicity as a constant drilling rate. An argument can be made that assuming a constant drilling rate is not the most conservative approach. Instead, a more conservative model would be to assume that most of the drilling occurs within a short period of time after closure, perhaps within the first two hundred years. There are two arguments to make against this model. First, based on all known information, Frenchman Flat is exceedingly poor in subsurface resources [Gustafson *et al.*, 1993]. There appears to be no great reservoir of oil or natural gas to be exploited as is the case in Oklahoma or Texas. We therefore make the assertion that there is no logical reason for a sudden rush to pockmark the basin with drill holes after institutional control of the RWMS is relinquished. Second, this very same institutional control period (the standard specifies one-hundred years) means that the very short-lived species, such as ^{241}Pu, ^{90}Sr, and ^{137}Cs, will have decayed away to a large extent prior to the possibility of any intrusion event. What is left in the waste inventory are species with half-lives on the order of thousands, tens of

thousands, and millions of years. For these radionuclides, the time of intrusion in the 9,900 years after the end of institutional control will affect only to a small degree the release from such an event.

Note that Eq. (27) also assumes that the probability that drilling *will* occur at Frenchman Flat is unity. This is a conservative assumption, because it ignores the additional conditional probabilities: P(drilling occurs in RWMS given that drilling occurs in Frenchman Flat) and P (drilling occurs in Frenchman Flat given that drilling occurs at NTS). In effect, we assume both of these probabilities are unity.

To determine λ_d requires a bit of thought. First, we presume a drilling density ρ_d that is defined as the number of boreholes per square kilometer that will be drilled in a given area over the next 10,000 years. Note that this does not mean that at any given time there will be ρ_d boreholes in any square kilometer, but over a period of 10,000 years this many boreholes will have been drilled in that square kilometer. So, if the drilling is occurring over an area A, which for convenience we might think of as the RWMS area, the total number of drill holes in 10,000 years is $\rho_d A$.

Now, if A is the area in which drilling is occurring, the probability a drillhole intrudes into a waste area is simply A_h/A, where A_h is the effective cross-sectional area of a GCD hole. The effective cross-sectional area of a borehole is the radius of a GCD borehole plus the radius of the drill hole all squared and multiplied by π. The effective radius accounts for the finite drill hole radius; drill holes dug with centers outside the effective radius will not intrude on the waste. This of course implicitly assumes that all drill holes are vertical. This we can justify based upon current drilling practice. When drilling through unconsolidated alluvium, current practice holds that there is no reason to incline the hole. Any inclination will be introduced only in the consolidated lithology far beneath the GCD facility.

Based upon this model of intrusion, the number of intrusions in 10,000 years is,

$$(\textit{No. of drillholes})x(\textit{probability of intrusion per drillhole}) = (\rho_d A)(\frac{A_h}{A}) = \rho A_h \quad (28)$$

and the yearly intrusion rate is,

$$\lambda_d = \frac{\rho_d A_h}{10{,}000} \quad (29)$$

Hence, the probability of a intrusion in a given time t is,

$$P = (1 - e^{-\rho A_h \frac{t}{10{,}000}}) \quad (30)$$

Now Eq.(30) gives the probability of intrusion into a single GCD borehole after time t. For n GCD boreholes, the probability of hitting any one of them is simply nP. Relating these intrusion probabilities to probabilities of a given radionuclide release, however, is somewhat more complicated because the boreholes generally contain different quantities of each radionuclide.

Let the human intrusion release from the ith borehole be Q_i. These releases can then be ordered from highest to lowest Q_1, Q_2, Q_3, ... , Q_n, so that for a given release Q_i, we can write the following statements,

$$
\begin{aligned}
P(Q > Q_1) &= 0, \\
P(Q > Q_2) &= P, \\
P(Q > Q_3) &= 2P, \\
&\vdots \\
P(Q > Q_n) &= (n-1)P \\
P(Q_n > Q) &= nP \\
P(Q = 0) &= 1 - nP,
\end{aligned}
$$

where P is obtained from Eq. (30). These relations allows us to construct a cumulative probability curve for comparison to the Containment Requirements of 40 CFR 191.

Computation of these releases is done in the same manner as in the PPA. It is assumed that for any intrusion event the volume of waste displaced by the intruding drillhole is brought directly to the surface. We ignore the possibility of caving. Therefore, the amount of waste released is simply the total amount of waste multiplied by the ratio of the drillhole volume to the total waste volume. This latter ratio is equal to the ratio of the drillhole cross-section to the borehole cross-section. It is true that human intrusion into the waste area as a result of drilling for water could transport a small amount of waste directly to the water table from which it would make its escape to the accessible environment. This would, however, take longer than directly transporting the material to the surface as well as dispersing and diluting the waste thereby reducing the amount of the release. Hence, assuming all the disturbed waste is brought to the surface immediately upon intrusion is the more conservative conceptualization.

In computing the release, radioactive decay of the material is considered, so time of intrusion is important; however, reduction in the waste inventory by transport (via diffusion) of material away from the waste area is not taken into account. Note also that these release calculations assume that intrusion occurs into only one borehole at a time. Elementary probability theory tells us that the probability of m boreholes being intruded upon in any 10,000-year period is approximately P^m. For any value of m greater than one, it should be clear that this probability is exceedingly small.

3.3 Individual Protection Requirements

The other requirement of 40 CFR 191 that is of concern in this iteration is the Individual Protection Requirements. This section will describe the liquid and gas phase models that were used to estimate the likelihood of complying with these requirements.

3.3.1 Liquid Phase Transport Model for Individual Protection Requirements

Unlike the Containment Requirements, the Individual Protection (IP) Requirements promulgated in 40 CFR 191 are expressed in terms of radioactive dose to a member of the public, not total integrated discharge. Dose, in turn, is generally related to integrated concentration of radioactive species, not radioactive species flux. As a result, the liquid diffusion model used for the Containment Requirements is inappropriate for the Individual Protection Requirements because of the zero concentration condition established at the surface. This would result in a zero dose from ground exposure and inhalation, which is clearly unconservative. It was necessary to modify the liquid diffusion model so that this is no longer the case.

The simplest change that will have the desired effect is to replace the zero concentration condition with a zero flux condition at the surface. Under this condition, contaminants will not be removed from the surface and will therefore collect there as time progresses. This assumption, of course, ignores the possibility of the surface layer continually turning over as was the case for the model used in the Containment Requirements. As a result, this model is inconsistent with the former model. We justify this inconsistency on the grounds that it will result in the most conservative concentration values for *evaluating compliance with the Individual Protection Requirements*.

The mathematical model is identical to that presented in Section 3.1.1; however, the boundary and initial conditions are changed to,

$$C_i(0,t) = S_i(t) \quad ; \quad \frac{\partial C_i}{\partial x}(L-e,t) = 0 \quad ; \quad C_i(x,0)=0 \tag{31}$$

In the context of the numerical solution we can impose this surface boundary condition by altering the diffusivity of the grid block at the surface to a value many orders of magnitude smaller than the diffusivity in the rest of the domain. The volume of the surface grid block is also returned to a value that is consistent with the remainder of the grid.

3.3.1.1 Dose Pathway and Parameters for Liquid Transport Individual Protection Analysis

From concentrations determined by the above model, the health physics code GENII-S [Leigh *et al.*, 1992] was employed to determine dose-to-man. GENII-S is a transport model of the human body with the capability to track radionuclides in the body and the dose from exposure to them. It also includes transport models in air, water, and biological environments. However, these models were supplanted by our own transport models. The code's plant uptake, animal ingestion, and internal transport models were then applied to the soil concentrations determined by our transport model to arrive at a value for dose.

To employ GENII-S, it is necessary to develop a dose scenario[2]; that is, develop a conceptual model of how radionuclides released could likely affect an individual human. The scenario suggested by the PPA was of an individual living continuously at the RWMS for many years, possibly raising livestock on the native vegetation. In this iteration, we have extended this scenario to include the possibility of irrigated agriculture. In this case, there are four primary pathways by which an individual may be exposed:

(1) Direct exposure from the ground surface.
(2) Inhalation of contaminated dust particles.
(3) Consumption of livestock that have consumed contaminated forage.
(4) Consumption of contaminated food crops by humans.

[2] The term "scenario" used in this context should not be confused with the scenarios that are developed as part of assessing compliance with the Containment Requirements. The two are entirely different.

Several parameters must be specified to GENII-S's internal dose models for each of these pathways. There is considerable uncertainty associated with most of them; however, because of time constraints and lack of information, no attempt was made in this analysis to address this uncertainty. This task will be considered in the next iteration.

The first two pathways are dependent upon the surface soil concentration as determined from the model described in the preceding section. The parameters used to calculate the dose from these concentrations are given in Table 3.4. For the most part, these are default values supplied by GENII-S. The inhalation exposure time assumes a continual exposure to contaminated air; no allowance is made for differences between inside and outside contamination levels. The ground contamination exposure time assumes that the individual is in contact with the soil one-half of the time. The dust mass loading factor is a GENII-S default value.

Considering the proposed revision to the Individual Protection Requirements, the committed effective dose equivalent is the dosimetric quantity that must be calculated.

Table 3.4 - Parameters for inhalation and ground exposure pathways.

Inhalation exposure hours per year	8800
Ground contamination exposure hours per year	4400
Dust mass loading factor (g/m^3)	10^{-4}

It assumes a one-year period in which the individual intakes contamination and receives exposure, followed by a fifty-year period (the commitment period) in which no additional contamination is absorbed but exposure continues from isotopes accumulated in the tissues during the one-year intake period. Exposure can occur at any time during the first 10,000 years after burial, excepting the first hundred years in which it is assumed that the public is barred from the site by active institutional control.

The third and fourth pathways constitute what can be described as an "intruder-agriculture" scenario [McKenzie *et al.*, 1982]. This scenario imagines an individual establishing a farm at the site, growing and eating crops, and raising livestock on cultivated feeds. Each of these activities involves ingestion of isotopes and consequent exposure. McKenzie *et al.*, [1982] considered this scenario for a low-level site in an arid western states setting and suggests the parameters in Table 3.5.

Note that the crop yield values appearing in the table are for cultivated plants. The biomass density value given in Section 3.1.2 is for native vegetation. In addition, the model used by GENII-S does not account for ingestion of resuspended soil adhering to the vegetation by livestock as an intake pathway. However, in a situation such as this where contaminant is transported from a buried area into the root zone and is absorbed into the vegetation, it is likely that this pathway will be the major source of livestock ingestion, not consumption of resuspended contaminated soil [Napier, 1993].

Table 3.5 - Parameters for intruder agriculture scenario.

Food	Growing Period (days)	Yield (kg/m^2)	Holdup (days)	Consumption (kg/yr)
Leafy vegetables	60	2.2	1	60
Root vegetables	90	9.0	1	182
Fruit	60	5.2	1	330
Cereals	90	2.1	1	88
Eggs	90	0.84[a]	2	30
Milk	30	1.3[a]	2	274
Beef	90	0.84[a]	15	40
Poultry	90	0.84[a]	2	18

[a] This number refers to forage crop yield

3.3.2 Gas Phase Transport Model

As was noted in the PPA, several isotopes of radon occur as daughter products of several of the radionuclides disposed in the GCD boreholes. Since radon is gaseous under normal conditions, these isotopes can transport through the vapor phase. As a result, a vapor phase transport model was developed to assess the potential for radon release to violate the Individual Protection Requirements. Radon itself is not subject to the Containment Requirements; however, ^{210}Pb, which is a daughter of ^{222}Rn, is subject to this regulation. This will be discussed below. It should also be noted that radon production and transport is primarily associated with the GCDT borehole as radon levels and temperatures in the other holes are significantly lower. For this iteration of the PA, the model for radon migration is very similar to that used in the PPA. The only differences in the two models are how radionuclide uptake by roots is modeled and what the boundary condition is for the partial differential equation describing the diffusion of radon under a concentration gradient. These two differences are discussed below. All other assumptions made in the PPA (given in Section 3.2.6 of the PPA report [Price *et al.*, 1993]) were also made for the PA analyses described below.

In the PPA, one of the boundary conditions for describing the diffusion of radon under a concentration gradient was

$$C = 0 \quad at \quad x = \infty. \tag{32}$$

For this iteration of the performance assessment, we have changed this boundary condition so that

$$C = 0 \quad at \quad x = L, \tag{33}$$

where L denotes the distance to the land surface. A no-flux surface condition, as employed in the Individual Protection Requirement liquid phase model, was not used in this model because such a condition could not be defended, because radon unquestionably diffuses from the surface soil into the atmosphere.

Therefore, the equation describing the diffusion of radon was, for the PA,

$$\frac{\partial C}{\partial t} = D_v \frac{\partial^2 C}{\partial x^2} - \lambda_2 C \ , \tag{34}$$

with boundary and initial conditions

$$\begin{aligned} C(0,t) &= C_0 e^{-\lambda_1 t} \ , \\ C(L,t) &= 0, \ and \\ C(x,0) &= 0 \ ; \end{aligned} \tag{35}$$

where

C = radon concentration in the air-filled space of the native soil (atom/m^3),
C_0 = initial concentration of radon (constant) (atom/m^3),
D_v = effective diffusion coefficient (m^2/s),
λ_1 = decay constant for parent radionuclide (s^{-1}), and
λ_2 = decay constant for radon isotope (s^{-1}).

For each radon isotope, λ_2 is greater than λ_1. Note that at the source the radon concentration is assumed to decay at a rate consistent with its *parent's* half-life. This makes the implicit assumption that the concentration of radon is directly proportional to the amount of parent species present; that is, equilibrium between parent and daughter exists at the source. Hence, the concentration of radon at the source decays at the parent decay rate. We believe this to be an acceptable assumption.

The analytic solution to this problem is

$$\begin{aligned} C = C_0 e^{-\lambda_1 t} \frac{e^{z(L-x)} - e^{-z(L-x)}}{e^{zL} - e^{-zL}} + \\ C_0 \frac{2 D_v \pi}{L^2} \sum_{n=1}^{\infty} (-1)^n \frac{n \, e^{-t\left(\lambda_2 + \frac{n^2 \pi^2 D_v}{L^2}\right)}}{\lambda_2 - \lambda_1 + \frac{n^2 \pi^2 D_v}{L^2}} \sin \frac{n \pi (L-x)}{L} \ ; \end{aligned} \tag{36}$$

where

$$z = \sqrt{\frac{\lambda_2 - \lambda_1}{D_v}} \ . \tag{37}$$

This transport model neglects any advection terms. An argument can be made that the large amount of heat producing wastes buried in the GCDT hole can create a situation conducive to formation of a natural convection cell. However, the PPA presented an analysis of natural convection and concluded that the Rayleigh number was so small that natural convection could not occur. Further, a report by Dickman [1989] detailing actual *in situ* concentration measurements within GCDT confirmed this fact when no evidence of a convection cell was apparent.

3.3.2.1 Barometric Pumping

It has been suggested that an additional gas phase transport mechanism is advective soil gas flow induced by variations in atmospheric pressure, which is often referred to as barometric pumping. In this mechanism, as the atmospheric pressure varies over the course of several weeks, convective transport will occur as the gas phase is inhaled and exhaled from the soil. The PPA suggested that this mechanism is not likely to be significant over the long term because there will be as many high pressure events as low pressure events. Thus the net flow will average out to be zero with no net transport. As a result, this mechanism was not included in the gas phase model used in the PPA. The reasoning behind the rejection of this mechanism, however, was heuristic. In this iteration, it was desired to consider the problem more closely.

To begin with, it is possible to see that barometric pumping can result in no net *bulk* flow of soil gas by a very simple argument. We first assume that the water table marks a no flow boundary for gas flow. We further assume that any induced flow occurs vertically only. This is justifiable since the horizontal scale of most low (or high) pressure systems is vastly greater than the distance to the water table. Consider now what would happen if there *was* a net bulk gas flow out of the soil. On each pressure cycle, a certain amount of air would be removed. Because there is no horizontal flow elsewhere to replenish the soil, gradually the amount of soil gas would decline. Since the void volume has not changed, this loss of mass would be accompanied by a drop in the average pressure of the soil gas. It should not be hard to see that if this situation continued, it would not take very many cycles before a considerable vacumn is created in the soil. Such a phenomena is not observed, so we are led to the conclusion that there can be no net *bulk* flow of gas out of the ground.

However, is it possible for there to be a net transport of tracer species by the forward and back flow induced by atmospheric pressure variation, even in the absence of net bulk flow? One such mechanism has been described by several authors [Peterson, Lie, and Nilson, 1987; Nilson and Lie, 1990; Nilson *et al.*, 1991]. The primary requirement is that there exists a vertical inhomogeneity that has a permeability greater than the surrounding matrix. This of course could be an open fracture. Since the permeability is greater in this area, contaminant within it will be drawn farther upward by a low-pressure event. If there is sufficient time before the next high pressure event, this material will diffuse outward into the surrounding low permeability matrix where it will be displaced downward a smaller distance in the next high pressure event than it was displaced upward. The net effect is that this material has travelled a greater distance in the same amount of time than if it had spent the entire cycle in the low permeability matrix. Hence, there is enhanced transport relative to the case in which no vertical inhomogeneity is present. However, at the GCD site there are no vertical fractures or inhomogeneities that would allow this mechanism to work. It might be argued that the backfilled borehole constitutes just such a pathway. However, it is likely that the permeability of this area is not substantially different

(certainly not an order of magnitude different) than the surrounding alluvium. Furthermore, over a period of 10,000 years any difference will become less and less. We therefore discount this particular mechanism for radon transport by barometric pumping.

Another possibility exists. The non-linear coupling between flow and transport represented by the $\mathbf{u}\cdot\nabla C$ term in the convection-diffusion equation might result in enhanced tracer transport when a periodic flow field is imposed. Recently, a model developed by REECo, which coupled gas flow and transport, was used to assess this possibility [Lindstrom, 1992]. It was found that at the GCD depths (21 m) there was no net enhanced transport, that is, net time-averaged transport [Lindstrom, 1992]. Diffusion was still the dominant process at this distance below the surface.

However, for the situation at the surface or the near-surface, there will be some region near the surface in which all the soil gas is evacuated to the atmosphere during a single low-pressure event. In the subsequent high-pressure phase, uncontaminated gas will be forced into this region. A numerical model developed by Massman and Farrier [1992] indicates that this region may extend to up to 4 m below the surface for media with gas permeabilities on the order of 10 darcies (10^{-8} cm^2). Recent gas permeability measurements at the site [Sully *et al.*, 1992] estimate permeabilities at the site in the range 8 to 50 darcies so this surface effect might extend fairly far into the alluvium. What is unclear is whether this effect has any influence on the net transport, that is, the time-averaged transport, past the surface. If the variations of atmospheric pressure occur on time scales much greater than the time scale of diffusion, this surface evacuation phenomenon might have only the effect of reducing the diffusion distance 4 or 5 m. This would be a significant number, but as yet it is unclear just how deep this "boundary region" is at the GCD site or whether there is a significant impact on the net transport because of it. Until that is determined, we cannot say that barometric pumping is a viable process for radon transport at GCD. Therefore, we do not include it within our conceptual model of gas transport.

3.3.2.2 Pathways and Parameters for Gas Phase Transport

The PPA identified four pathways for radon migration. Two involved radon diffusion upward and two involved radon diffusion downward. Only the two pathways involving radon diffusion upward will be analyzed (using the revised model discussed above) in this iteration of the PA. The two pathways involving radon diffusion downward will not be analyzed because, based on the results of the PPA [Price *et al.*, 1993], these two pathways did not result in releases or doses that violate any of the three quantitative requirements in 40 CFR 191 [EPA, 1985], even with a revised model for radon diffusion.

Of the four radon isotopes, only ^{222}Rn has a daughter (^{210}Pb) with a half-life long enough to be of concern to the Containment Requirements ($t_{1/2}$ = 22.3 years). In the case of the Individual Protection Requirements, inhalation of radon isotopes is of concern as is ingestion of ^{210}Pb. We must also concern ourselves with the dose from ^{210}Po, a short-lived (140-day half-life) daughter of ^{210}Pb that has significant biological activity. In this analysis, we assume that ^{210}Po is always in secular equilibrium with ^{210}Pb.

The two pathways of interest are: (1) diffusion of radon to the ground surface and release into the atmosphere, and (2) decay of ^{222}Rn into ^{210}Pb as radon diffuses upward, and subsequent uptake of ^{210}Pb and ^{210}Po by plant roots. The requirements of 40 CFR 191 that are of interest are the Individual Protection Requirements (inhalation of any of the four radon isotopes via pathway 1 and ingestion of ^{210}Pb and ^{210}Po via pathway 2), and the Containment Requirements (cumulative releases of ^{210}Pb to the accessible environment via pathways 1 and 2). Table 3.6

summarizes the pathways, requirements, isotopes, and exposure mechanisms that form the basis for the analyses to be described below. Each combination of pathway and requirement is discussed below.

To evaluate compliance with the Individual Protection Requirements, radon concentrations at the ground surface are needed. It is important to understand that the preceding model is used only to determine the flux at the ground surface. Differentiation of the concentration profile with respect to x yields an expression for the concentration gradient at the ground surface (x = L),

$$\left.\frac{\partial C}{\partial x}\right|_{x=L} = \frac{-2C_0 z e^{-\lambda_1 t}}{e^{zL} - e^{-zL}} - \frac{2C_0 D_v \pi^2}{L^3} \sum_{n=1}^{\infty} (-1)^n \frac{n^2 e^{-t\left(\lambda_1 + \frac{n^2\pi^2 D_v}{L^2}\right)}}{\lambda_2 - \lambda_1 + \frac{n^2\pi^2 D_v}{L^2}} \quad . \tag{38}$$

We do not obtain the surface concentration from the model but instead use an alternate approach. It is assumed that the concentration of radon approximately 1 m above the ground surface is half that at the ground surface [Nero, 1983; Porstendörfer, 1991]. Further, the gradient in the near surface atmosphere is assumed linear. This assumption is justified by the relatively higher rates of diffusion in the "free" atmosphere as compared to that in the soil gas. Equating the flux obtained from Eq. (38) with mass transfer rate from the linear profile allows determination of the radon concentration 1 m above the ground surface by

$$C(\ x=L+1\ m\ ) = -0.914\,\theta_a \left.\frac{\partial C}{\partial x}\right|_{x=L} \tag{39}$$

where θ_a is the air-filled porosity of the alluvium, assumed to be 0.30. It should be clear that the greater the surface flux, the greater the air concentration. The zero concentration boundary condition used in the model above ensures that the surface flux will be maximized and, in turn, so will the inhalation concentration.

As in the PPA, it was assumed that a member of the public inhales this outdoor concentration of radon for one year. A committed effective dose equivalent (CEDE) is obtained from this concentration through multiplication by an appropriate conversion factor. In this analysis, we use a value of 360 mRem CEDE for a one year exposure to 1 pCi/l of ^{222}Rn. This conversion factor was derived from NCRP Report #94 [NCRP, 1987; Shott, 1992]. This report suggests a committed dose equivalent conversion factor of 3 Rem per pCi/l per year. We assume a 6% effective dose weighting factor to the bronchial epithelium to arrive at a 180 mRem-l/pCi-yr effective dose equivalent conversion factor. This value, however, assumes a 50% equilibrium of radon with its daughters. We make a conservative assumption of 100% equilibrium to obtain a conversion factor of 360 mRem-l/pCi-yr. This conversion factor is multiplied by the concentration found from Eq. (39) to obtain the committed effective dose equivalent for radon inhalation. Note that this factor is specific to ^{222}Rn, but we apply it to all radon isotopes.

With respect to the diffusion of ^{222}Rn to the ground surface, the cumulative release of ^{222}Rn *is not* restricted by the Containment Requirements, nor is that of ^{210}Po, but the cumulative release of ^{210}Pb *is*. The quantity of interest, therefore, is the flux of ^{222}Rn at the ground surface, given by $-D\partial C/\partial x|_{x=L}$. Multiplying this flux by the cross-sectional area of a borehole and the air-filled porosity, θ_a, yields the atoms of ^{222}Rn released to the air per unit time. The activity of radon released in Curies is directly proportional to this value. Integrating this release rate over

Table 3.6 - Pathways, requirements, isotopes, and exposure mechanisms in the analysis of radon for the second performance assessment iteration

Pathway	Isotopes and Exposure Mechanism Modeled for Each Requirement	
	Individual Protection Requirements	**Containment Requirements**
Radon diffusion to ground surface	Inhalation of ^{218}Rn, ^{219}Rn, ^{220}Rn, and ^{222}Rn	Cumulative release of ^{210}Pb to the accessible environment
Uptake of ^{210}Pb and ^{210}Po by plant roots	Ingestion of ^{210}Pb and ^{210}Po	Cumulative release of ^{210}Pb to the accessible environment

10,000 years will yield cumulative release of ^{222}Rn in Curies, which can be converted into the cumulative release of ^{210}Pb in Curies using the activities of both isotopes (3.4134×10^7 Ci/mol for ^{222}Rn and 16.01×10^4 Ci/mol for ^{210}Pb).

So far we have discussed the pathway in which radon diffuses to the ground surface. The other pathway is one in which ^{222}Rn decays as it diffuses upward and its longest-lived daughter, ^{210}Pb, is uptaken by plant roots to the part of the plant that is above the ground surface or is edible. This pathway is of concern for both the Containment Requirements and the Individual Protection Requirements. This pathway is of concern only for ^{222}Rn because it is the only radon isotope with relatively long-lived progeny. Note that since we have assumed secular equilibrium (equal activities) between ^{210}Pb and ^{210}Po, we need only track ^{210}Pb. The amount of ^{210}Po present is easily determined from the amount of ^{210}Pb.

The amount of ^{210}Pb that will be available for uptake by plants is determined by the amount of radon that will decay in the vicinity of plant roots. As in the PPA, plant roots were assumed to reach 10.7 m below ground surface. Any radon that decays in this 10.7m is assumed to become ^{210}Pb and be available for root uptake. This last assumption is more conservative than that used in the PPA.

For the sake of simplicity, we assumed that all ^{222}Rn that diffuses above the depth of 10.7m turns into ^{210}Pb and is available for uptake by plant roots. This assumption amounts to double counting a portion of the ^{222}Rn, but it can be justified as being conservative. The ^{210}Pb is assumed to be deposited in both the pore water and the soil, which, combined, make up 70% of the volume of alluvium (30% is air). The average concentration of ^{222}Rn for the entire 10.7m root zone was assumed to equal the concentration at a depth of 10.7m , a conservative assumption. The concentration of ^{210}Pb per gram of dry soil can be obtained from the concentration of ^{222}Rn in the pore air by multiplying the latter by the air-filled porosity, dividing by the dry bulk density of the alluvium (1600 kg/m^3), and multiplying by the ratio of the activity of ^{210}Pb to the activity of ^{222}Rn. Assuming that plants regenerate on an annual basis and turnover their standing biomass once during a year, the total curies of ^{210}Pb that reach plant leaves in a

year can be calculated by multiplying the Curies of ^{210}Pb per gram of dry soil by the concentration ratio of ^{210}Pb (this is assumed to equal the mean concentration ratio of ^{237}Np, 0.147 Ci per g dry vegetation/Ci per gram dry soil), twice the biomass density (0.49 kg/m^2) (to account for plant biomass turnover), and the area of a borehole. To calculate cumulative releases over 10,000 years, as required by the Containment Requirements, the Curies of ^{210}Pb released every year will simply be integrated over 10,000 years. To calculate dose, it was assumed that a person ingests 665 kg of contaminated vegetables in a year. This consumption rate is the sum of the vegetative consumption values given in Table 3.5. It is assumed that root vegetables have the same concentration ratio as above ground vegetables. It is also assumed that each gram of ^{210}Pb results in a committed effective dose equivalent of 3.9×10^{11} mrem [DOE, 1988]. The assumption of secular equilibrium implies that equal Curies of ^{210}Po accompany the Curies of ^{210}Pb. The mass of ^{210}Po ingested can then be determined and converted to committed effective dose equivalent by the factor 7.2×10^{12} mrem/g [DOE, 1988].

All of the parameters used in the analysis of radon migration in the PA are given in Table 3.7. Most of the parameters have the same value as in the PPA. The values that are not the same as those used in the PPA are denoted with shaded boxes. An explanation as to why they are different is given in the following paragraphs. The reader is referred to the appropriate section of the PPA for the source of the unshaded values.

The effective diffusion coefficient is assumed to equal 0.21 cm^2/s for ^{222}Rn in the GCDT borehole *for the Containment Requirements.* Recall that ^{222}Rn is the only radon isotope of concern with respect to the Containment Requirements, and it is of concern only because the cumulative release of its daughter, ^{210}Pb, is limited by the Containment Requirements. This value comes from assuming a temperature of 450°C and using the relationship between effective diffusion coefficient and temperature given by Tanner [1980]. This temperature was selected because it appears to be the approximate maximum temperature within the waste emplacement zone; it occurs within the GCDT [Dickman, 1989]. Because the Containment Requirements are concerned with cumulative radionuclide releases over 10,000 years, and because our model for radon diffusion allows only one diffusion coefficient for the time period simulated, the diffusion coefficient for the entire 10,000 years equals the maximum diffusion coefficient. The Individual Protection Requirements are concerned with the dose received by a member of the public and, thus, do not apply until 100 years after closure [Price *et al.*, 1993; EPA, 1985]. For this reason, the diffusion coefficient for the GCDT borehole for the Individual Protection Requirements is 0.045 cm^2/s. This lower diffusion coefficient corresponds to a temperature of 60°C, which is assumed to be the temperature in the GCDT borehole 100 years after closure.

In this PA, the depth at which radon parents are buried is either 26 m or 21.3 m. The 26 meter depth applies to those parents disposed of in the GCDT borehole, and the 21.3 meter depth applies to those disposed of in boreholes 1, 2, 3, and 4. This procedure is different from the PPA,in which all burial depths were 21.3 m. The burial depth for the parent isotopes disposed of in GCDT has changed because Chu and Bernard [1991] report the depths at which specific parent isotopes are buried in the GCDT borehole. This information was not available for the PPA, and so the minimum burial depth (21.3 m) was assumed for the PPA. Specific depths of parent isotopes are not available for boreholes 1, 2, 3, and 4; therefore, the burial depth of the radon parents in these boreholes is assumed to be 21.3 m. Because of the greater radon production in the GCDT borehole, using a deeper source depth for this case is justified. We reiterate, however, that there are data that support this assumption.

Table 3.7 - Radon parameters used in the performance assessment.

Parameter	Value	Comments
Effective diffusion coefficient	3.6 x 10^{-6} m^2/s	Boreholes 1,2,3,4
	4.5 x 10^{-6} m^2/s	GCDT borehole
	2.1 x 10^{-5} m^2/s	GCDT, containment requirements
Initial concentration of radon	45 pCi/l	^{218}Rn in GCDT
	22,500 pCi/l	^{219}Rn in GCDT
	2.0 x 10^{-7} pCi/l	^{220}Rn in boreholes 1,2,3,4
	225,000 pCi/l	^{222}Rn in GCDT
Radon isotope half-lives	1.11 x 10^{-9} years	^{218}Rn
	1.25 x 10^{-7} years	^{219}Rn
	1.76 x 10^{-6} years	^{220}Rn
	1.05 x 10^{-2} years	^{222}Rn
Radon parent half-lives	1,600 years	^{226}Ra, parent of ^{218}Rn
	21.77 years	^{227}Ac, parent of ^{219}Rn
	1.41 x 10^{10} years	^{232}Th, parent of ^{220}Rn
	1,600 years	^{226}Ra, parent of ^{222}Rn
Dose conversion factor (CEDE to bronchial epithelium)	**360 mrem-l/year-pCi**	Continuous inhalation of 1 pCi/l of ^{222}Rn in 100% equilibrium with its short-lived progeny. Also for other radon isotopes.
Dose conversion factor (to CEDE)	**3.9 x 10^{11} mrem** **7.2 x 10^{12} mrem**	Ingestion of 1 g ^{210}Pb Ingestion of 1 g ^{210}Po
Air-filled porosity	0.30	
Radon parent burial depth	21.3 m	Boreholes 1,2,3,4
	25.8 m	GCDT borehole
Biomass density	**0.49 kg/m^2**	
Depth of plant roots	10.7 m	
Annual vegetative consumption	**665 kg/yr**	
^{210}Pb concentration ratio	**0.147**	Ci per g dry veg/Ci per g dry soil
Dry bulk density	1600 kg/m^3	
Cross-sectional area of a borehole	10.5 m^2	Boreholes 1 and 2
	7.3 m^2	All other boreholes

Shaded parameters were not used in PPA

3.4 Sensitivity Analysis Techniques

Having presented the models and parameters used in this performance assessment iteration, it is necessary to discuss the topic of sensitivity analysis. In addition to telling us whether a site is likely to meet the regulatory standards, these performance assessment modeling results can also be used to direct further research into the parameters or processes that are the most important and have the greatest uncertainty. The different techniques that were used to analyze the performance assessment results are presented in this section.

Sensitivity analysis can be divided into two major categories, qualitative and quantitative. The qualitative methods rely heavily on various types of scatter plots, the most common being a raw plot of the dependent or response variable versus each individual independent variable. Examination of these plots can reveal trends, linear or nonlinear, and also threshold values. These relations indicate which independent variables have the greatest effect on the response variable.

It is also possible to use different types of scatter plots such as semi-log, log-log, and plots of the rank transformed data. The semi-log plot is helpful in expanding the data to more easily examine the magnitude of some of the individual points. The log-log and rank plots are useful when examining trends in the data.

The quantitative method employed depends on the type of data encountered and the type of relationship that is expected to exist between the dependent and independent variables involved. As this analysis has a single dependent variable (the EPA sum) and a relatively large number of independent variables, multiple regression is the procedure of choice. Regression itself is a fairly common statistical practice, and it involves replacement of the relatively complicated physically based models that describe the relationship between dependent and independent variables with a simpler, non-physical "regression" model that generally involves only low order relationships between dependent and independent variables. Regression contains a great number of options and, although it is not the purpose of this report to describe the mathematics involved, it is appropriate to give a general overview of the models employed along with their underlying assumptions.

The more common regression model generally contains linear or quadratic terms with or without interaction. The interaction terms are used to model correlation between independent variables. Regardless of which model is chosen, the underlying assumptions remain the same; namely, the errors that result between the fitted model and the raw data are independent normally-distributed random variables having zero mean and constant variance [Draper and Smith, 1981].

With the large number of independent variables in this analysis along with the iterative nature of the regression procedure, it would be a formidable task to develop a regression equation. For these reasons the stepwise regression technique is the method of choice. Stepwise regression is an automatic search procedure that sequentially develops a subset of independent variables to be included in the model. Essentially, this method develops a sequence of regression models, at each step adding the independent variable that best explains the variability that results from fitting the model to the data. As this technique is included within the Statistical Analysis System [SAS, 1985], it is relatively simple to implement.

There are two other regression techniques that are of interest for the purpose of this analysis. These are rank regression and standardized regression. Both of the techniques apply a transformation to the raw data before performing stepwise regression. The rank transformation replaces the smallest observation with rank 1, the second smallest with rank 2, and so on. In the case of tied values, the rank assigned to each is the average of the ranks that would have been

assigned to them had they not been tied. The rank transformation tends to linearize monotone nonlinear relationships between variables and reduce the effects of extreme values [Iman and Conover, 1979]. This transformation will generally result in a better fit when a linear model is chosen. Regression on the log-transformed data, that is, considering the logarithms of the independent and dependent data, is another possibility. This technique is less acceptable for our purposes because, as is often the case, the total release will be exactly zero (within the machine precision). It is possible to truncate the data set and use only non-zero data, but this also disposes of a certain amount of important information and results in spurious correlations among the input variables.

The standardized transformation shifts the data set corresponding to the independent variable to have a mean of zero and a standard deviation of one. Although this transformation does not generally lead to a better fit, it does allow a comparison of the coefficients that result from the stepwise procedure. That is, the importance of a variable is directly related to the magnitude of its coefficient.

The regression procedure results in a number of statistics that are useful in the analysis, the first being the coefficient of determination r^2, which is a measure of the total variation explained by the regression model. r^2 can take on any value between zero and one, with one indicating the regression model fit the observed data exactly. The second statistic of value is the coefficient of partial determination, which is a measure of the marginal contribution of the latest independent variable that has been included in the model by the stepwise procedure [Neter *et al.*, 1983]. By an examination of the results of the stepwise regression model, it is possible to evaluate the overall goodness of fit, and also to tell which variables are the most important; that is, which are the most sensitive in determining the PA modeling result.

How each of these techniques was applied to the performance assessment results will be described as a part of the general discussion of results given in Section 4.1.2.

4.0 RESULTS OF SECOND PERFORMANCE ASSESSMENT ANALYSIS

Section 3.0 described the performance assessment models used for the second iteration of the PA for the GCD site. This section will detail the performance assessment analyses that were conducted with these models and the results of these analyses. We will discuss compliance assessment with the Containment Requirements, first for both base case scenario and the human intrusion event. Following that, compliance assessment with the Individual Protection Requirements will be discussed.

4.1 Containment Requirements - Base Case Scenario

This section will discuss the analysis to assess compliance with the Containment Requirements of the base case scenario. The overwhelming fraction of the integrated discharge was found by the analysis to be via the liquid diffusion pathway. Therefore, the analysis presented in this section involves only this pathway. A slight contribution to the integrated discharge is made by the gas diffusion process, but this will be discussed in the section describing the results with respect to the Individual Protection Requirements.

4.1.1 Results for the Liquid Diffusion Pathway

A total of 5,000 LHS samples were taken from the distributions described in Section 3.0 and the liquid diffusion model was evaluated 5,000 times to generate the CCDFs shown in Figure 4.1. Two cases appear in this figure: (1) only TRU waste considered in the initial inventory, and (2) TRU and non-TRU waste considered in the initial inventories. The distinction between TRU and non-TRU waste was discussed previously in Section 2.0. As discussed in the PPA, there is some ambiguity in the regulations regarding whether or not this non-TRU waste is subject to the Containment Requirements, so it was decided to consider both cases.

There are several things to note about Figure 4.1. First and foremost, neither curve passes through the shaded area. This area represents the region of non-compliance established by the Containment Requirements of 40 CFR 191. Because of the many conservative assumptions incorporated into the PA models, it is our contention that these curves are an upper bound on the actual performance of the GCD site. Given the uncertainty in the system, its "true" behavior would therefore lie somewhere below and to the left of the curves in Figure 4.1. Therefore, we are led to the conclusion that the base case scenario should meet the standards set by the Containment Requirements, whether or not non-TRU waste is considered.

Second, the curve for the case that includes the non-TRU waste is well below and to the left of the curve ignoring the non-TRU waste. This might seem at first to be incorrect with well over 500,000 additional Curies in the initial inventory considered in the case that includes the non-TRU waste. It would seem intuitive that the EPA sums would be consistently higher for this case. The reason why this is not so was discussed in detail in the PPA. We shall discuss it briefly here. The definition of EPA sum given in Section 1.1.2 shows that the EPA sum is normalized by the initial inventory. Hence, a given release will have a smaller EPA sum if a larger initial inventory is used in its computation. The non-TRU waste consists primarily of ^{90}Sr and ^{137}Cs, which have half-lives on the order of 30 years, so they generally decay away quickly and do not contribute to the total release, but their presence in the initial inventory results in a larger normalization factor. As a result, the EPA sums of the case including non-TRU are

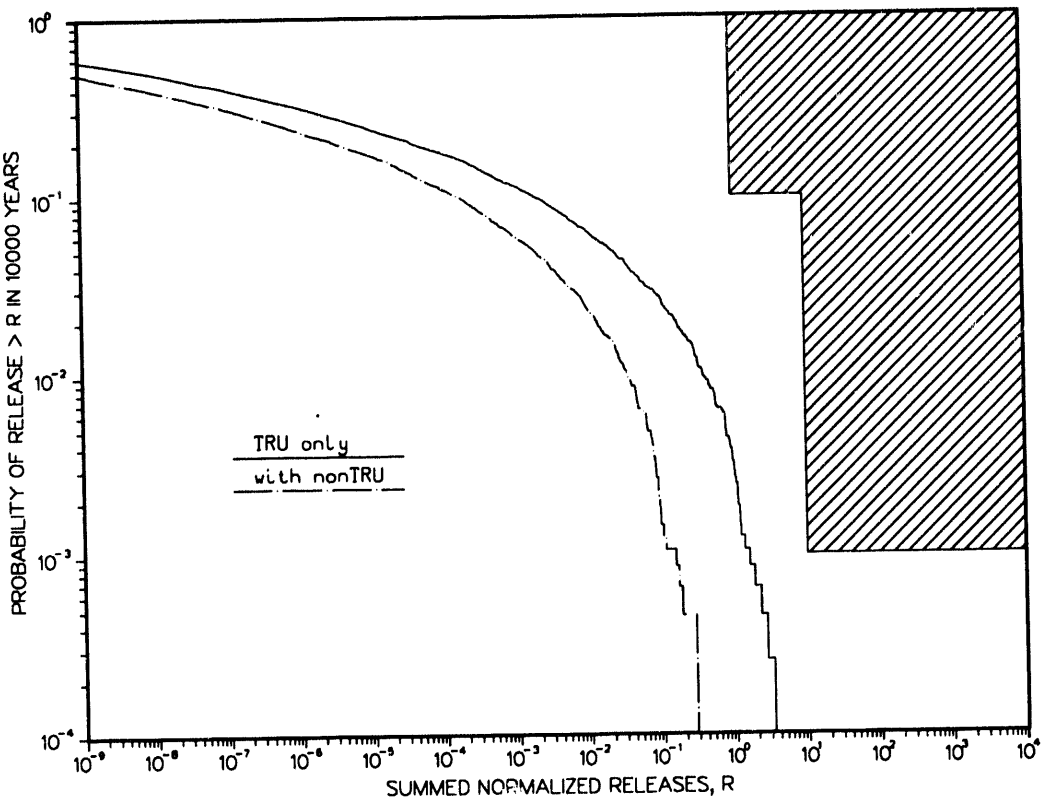

Figure 4.1 - CCDFs for base case scenario excluding and including non-TRU waste.

generally smaller.

Finally, some consideration must be given to the adequacy of the sample size in spanning the variability of the 38 random variables used in this uncertainty analysis (Appendix C). Figure 4.2 shows the CCDF of the case excluding the non-TRU waste along with three other CCDFs that differ only in the value of the random seed used to create the combinations of parameters. Thus, each curve represents a slightly different set of parameter vectors. It should be evident that there is little difference between these curves, at least from the perspective of a log-log diagram. This fact gives us confidence that 5,000 samples is large enough to ensure that all potential responses of the model system are present in our CCDF curves.

We hasten to add that the variability shown in the CCDF's in Figure 4.2 is related only to attempting to sample a continuous parameter space with a finite number of points. It is an artifact of the uncertainty analysis and has no relation whatsoever to other sources of uncertainty in the overall analysis, for instance, parameter and conceptual model uncertainty. Our intent in showing Figure 4.2 is only to show that 5000 samples is sufficiently large to capture the salient features of the parameter space. That is, the CCDF computed using 5000 samples is an *adequate* representation of the CCDF that would result from using an unlimited number of samples. We make no contention that this latter CCDF would be approximated by the "mean" of the CCDFs shown in Figure 4.2. We claim only that as the number of samples is increased to very large values, these CCDFs will coalesce into one.

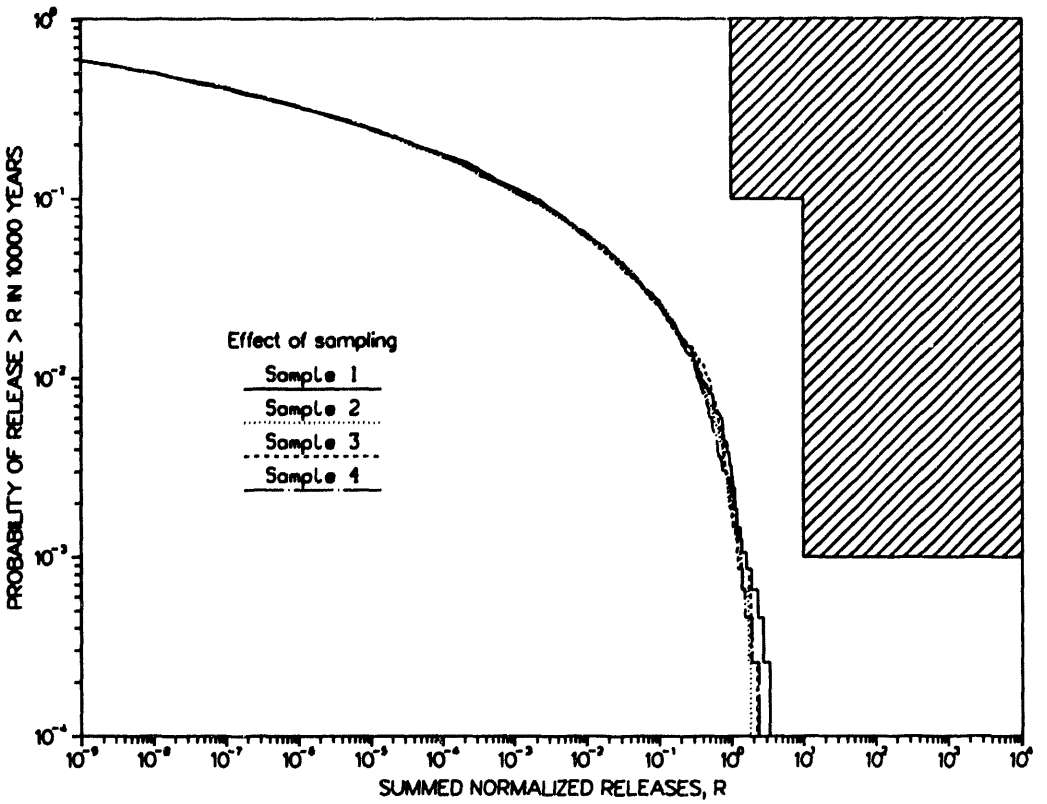

Figure 4.2 - Plot of four CCDFs differing only in the random seed used to generate the samples.

4.1.2 Sensitivity Analysis Results for Liquid Diffusion Pathway

An integral part of the performance assessment methodology is the sensitivity analysis of the results. Only via this procedure can we obtain information on those processes or parameters the models indicate to be important to the site performance. The suite of techniques described in Section 3.4 have been applied to the results from three cases. The first two are those presented in Figure 4.1: without and with non-TRU waste, respectively. The third case also excludes the non-TRU waste, but the lower bound of the tortuosity distribution has been increased from 3 to 10. This latter value was chosen based upon the results of the sensitivity analysis conducted on the first case for reasons that will become clear as this discussion continues.

Scatter plots of the nonzero EPA sums versus the independent variables were created for each variable included in the model. Examination of the plots provides limited information, with the main exception being the plot of the EPA sum versus tortuosity as shown in Figure 4.3. Examination of the tortuosity plot shows that the largest EPA sums correspond to the smallest tortuosity values, verifying our intuitive understanding of the definition of tortuosity. That is, the smaller the tortuosity, the shorter the average diffusion distance to the accessible environment and the greater the EPA sum.

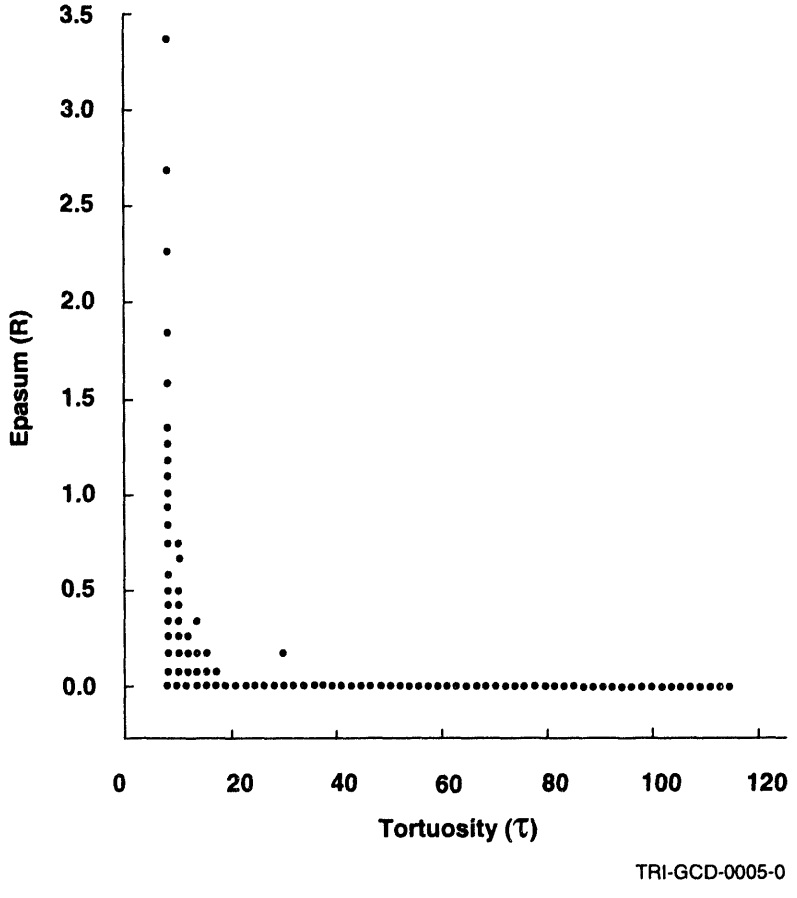

Figure 4.3 - Scatter plot of EPA sum versus tortuosity.

The scatter plot in Figure 4.3 also suggests a manual inspection of the relationship between EPA sum and tortuosity would be of value. This is a simple procedure to implement as the input vector resulting from the LHS code is assigned a number and this number is carried through the uncertainty analysis and finally assigned to the corresponding EPA sum. So, by ordering the EPA sums from smallest to largest, it is possible to find which combination of input variables results in a large EPA sum. If we consider only those realizations with EPA sums greater than one, it is observed that the values of tortuosity *do not exceed four*. That is, the highest release is always associated with shortest diffusion path. It also holds out the possibility that if it were possible to defensibly increase the lower bound of the tortuosity distribution to a value at or greater than four, then all EPA sums computed would be less than one, and the chances of non-compliance would be nil. However, this possibility would be true only for base case conditions, and as we will see below could be considerably altered depending upon the maximum depth of roots or other factors.

The stepwise regression procedure has been applied to the raw data sets, the standardized data sets, and finally the rank-transformed data sets. In each case the regression model assumes the EPA sum is simply a linear combination of the input variables. The values for the coefficient of determination (r^2), and coefficients of partial determination for each parameter are included in Table 4.1. The magnitude of r^2 is a measure of the total variation explained by the model. That is, if all values of the EPA sum resulting from a simulation fell on the fitted regression line, the regression model would explain all variation and as a result, the value of r^2 would be unity.

Table 4.1 - Regression coefficients from sensitivity analysis.

Case	Correlation Coefficient, r^2			Partial Determination Coefficient	
	Raw	Standard-ized	Ranked	Tortuosity	Root Depth
I	0.1375	0.1375	0.8905	0.7214	0.1038
II	0.1340	0.1340	0.8900	0.7213	0.1037
III	0.0743	0.0743	0.8502	0.5070	0.2774

Case I : non-TRU excluded
Case II : non-TRU waste included
Case III : non-TRU excluded, lower tortuosity bound increased to 10

Thus, r^2 is simply a convenient measure quality of fit, with a value close to one indicating the regression model fits the observed data very well, and small values indicating a poor fit. With that in mind, examination of Table 4.1 indicates that a linear model is inappropriate for the raw data and also for the standardized data but works very well for the rank transformed data (the shaded entries). These results indicate that the simulation model exhibits nonlinear behavior. Consequently, if one wished to build a surrogate regression model it would be necessary to include higher order terms and possibly terms to model interaction or correlation as well. Thus, although the results indicate the linear model is not sufficient for a surrogate, it does work very well for the purpose of sensitivity analysis if coupled with the appropriate data transformation.

The coefficients of partial determination corresponding to the rank transformation show that tortuosity and root depth explain over 92% of the variation within each of the three cases. For the first two cases, the overwhelming influence is from the tortuosity. However, it is also apparent from the third case that as the lower quantile of tortuosity increases, the tortuosity parameter becomes less significant as indicated by the decrease in the partial coefficient of determination.

Although tortuosity and root depth are by far the most significant parameters in a statistical sense, it may be helpful to indicate the parameters that followed these two in importance. These are the thorium sorption coefficient (K_d), the neptunium sorption coefficient, and finally the erosion depth. It must be kept in mind, however, that the partial correlation coefficients of these latter three are of such small size that generalizations about their importance relative to the remaining parameters should be kept to a minimum.

A final area that can be considered part of the sensitivity analysis is determining which of the radionuclides make up the majority of the release. The PPA found that plutonium isotopes made up 98% of the total activity released. It is worthwhile finding out if this is still the case. We consider the nominal situation shown in Figure 4.1 with 5000 realizations, non-TRU waste not included. Table 4.2 shows the percentage of the release attributed to each radionuclide for two cases. In the first case, the total integrated discharges for all 5000 realizations were summed to give a "grand" total release. This grand total has no physical significance, but it is useful in ranking the importance of the radionuclides in an average sense. The fraction of this grand

Table 4.2 - Percent of release for each radionuclide.

Radionuclide	Percent of "Grand" Release	Percent of Maximum Release
^{230}Th	23.6	58.6
^{234}U	22.6	19.4
^{226}Ra	20.2	12.5
^{210}Pb	17.7	5.0
^{237}Np	8.6	2.5
^{241}Am	2.9	0.25
^{231}Pa	1.8	0.59
^{227}Ac	1.7	0.49
^{236}U	0.53	0.34
^{233}U	0.24	0.11
^{229}Th	0.083	0.16
^{235}U	0.011	0.008
^{238}U	0.0012	0.0011
^{232}Th	$< 10^{-5}$	1.2×10^{-5}
^{240}Pu	$< 10^{-5}$	$< 10^{-5}$
^{239}Pu	$< 10^{-5}$	$< 10^{-5}$
^{242}Pu	$< 10^{-5}$	$< 10^{-5}$
^{238}Pu	$< 10^{-5}$	$< 10^{-5}$
^{241}Pu	$< 10^{-5}$	$< 10^{-5}$

release attributed to each species is shown in Table 4.2. In the second case, we show the fraction of the release for the realization that had the highest EPA sum. For the record, this realization has an EPA sum of 3.3 and resulted in 0.024 Curies being released to the accessible environment (only about 0.002 % of the original TRU activity emplaced). The most obvious conclusion that can be reached from Table 4.2 is the dramatic decline in the importance of the plutonium isotopes. Whereas plutonium accounted for the majority of the release computed by the PPA, in this new analysis the plutonium isotopes have fallen to the bottom of the list. This is undoubtedly the result of the new plutonium solubility and sorption information incorporated in this analysis. Based upon defensible data not available for the PPA, it was determined that plutonium dissolves to a much lesser extent and adsorbs to the alluvium to a much greater extent than originally proposed by the PPA. The new ranking in terms of majority of release is: ^{230}Th,

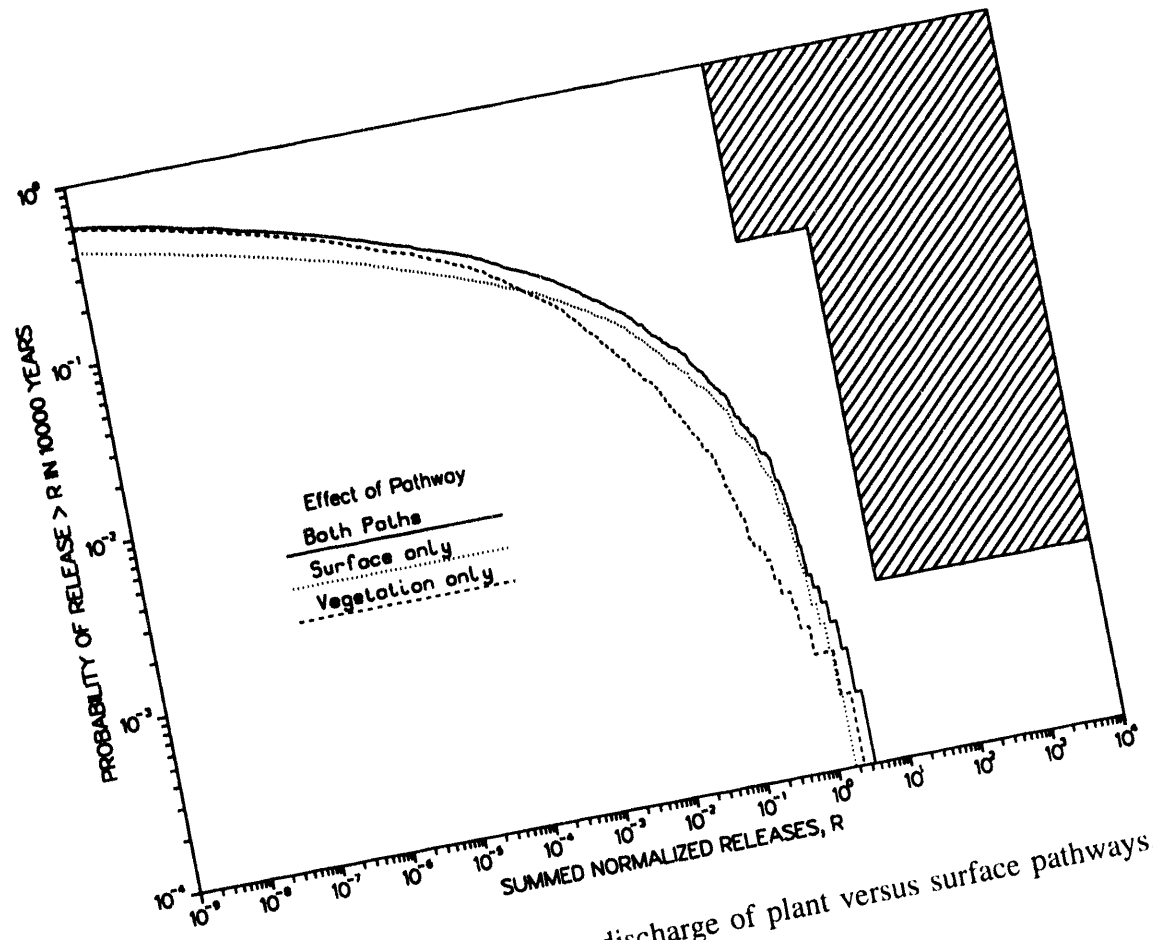

Figure 4.4 - Illustration of the relative discharge of plant versus surface pathways.

^{234}U, ^{226}Ra, and ^{210}Pb.

4.1.3 Influence of Plant Uptake

Because of the emphasis in the current conceptual model of the site on the first 21m of alluvium, the role of plants in the performance of the site is a much more important question. We can address this question in two ways. First, we can consider the changes to the CCDF if we ignore the release from either the surface flux pathway or the vegetative pathway. That is, one or the other of the pathways is ignored when computing the total integrated discharge. Figure 4.4 shows the result of this analysis. The solid curve is the CCDF already presented in Figure 4.1 for the case excluding the non-TRU inventory. The other two curves represent the CCDF that results if either the surface flux or the vegetative flux is ignored. Some care must be used in interpreting this figure because it is not necessarily the case that the same parameter realization will occur in the same location when the EPA sums are ordered from highest to lowest for the two latter cases. Put another way, it is not necessarily the case that the highest EPA sum for the case ignoring the surface flux will occur for the same realization as it does for the case ignoring the vegetative flux. As a consequence, at a given probability, the EPA sums from the two latter curves cannot be added to obtain the EPA sum at that probability for the complete case.

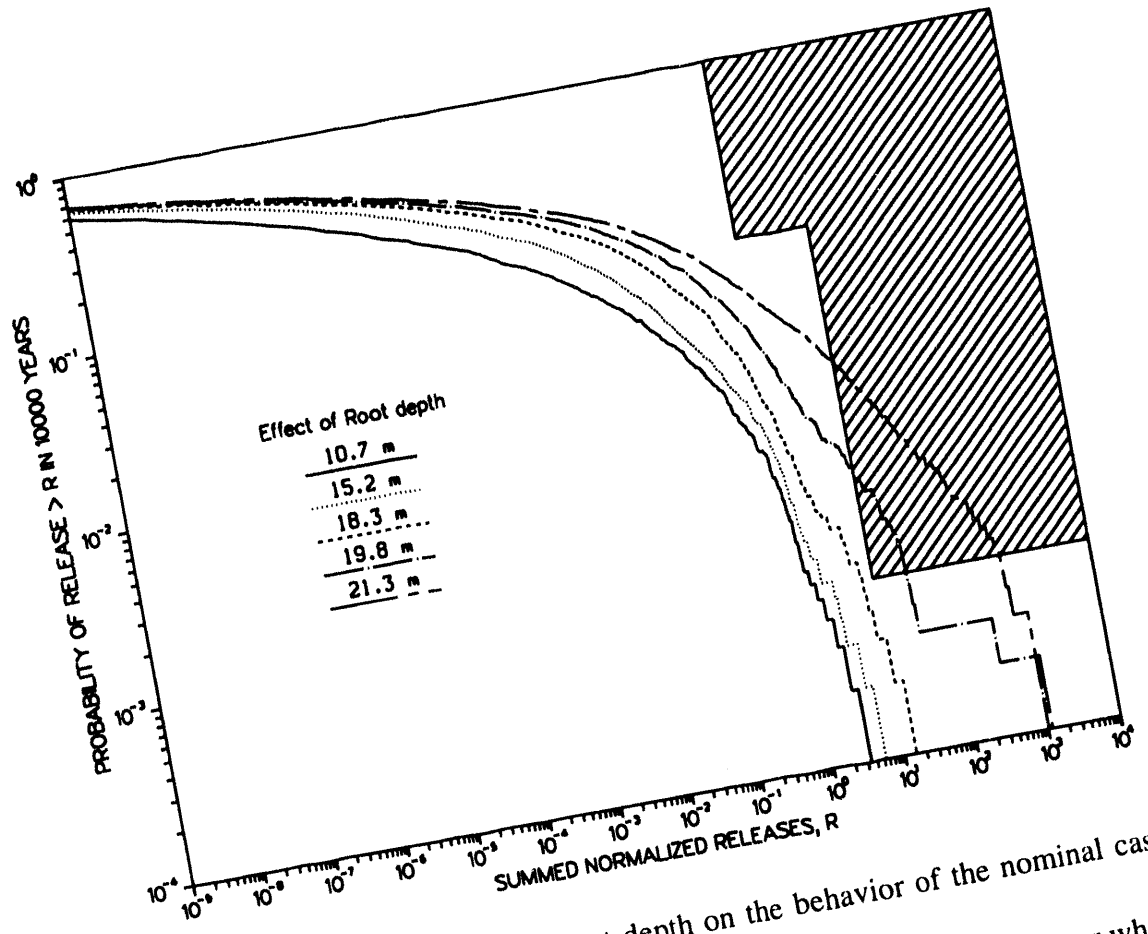

Figure 4.5 - Effect of maximum root depth on the behavior of the nominal case.

What can be seen from this figure, however, is the approximate ranges over which a given pathway dominates the release. For instance, for EPA sums less than approximately 10^{-5}, the majority of the release is via the plant pathway; whereas for EPA sums greater than about 10^{-2}, it is the surface release pathway that dominates the release. This latter generalization is not quite correct for EPA sums greater than about one, where the plant pathway starts to make an approximately equivalent contribution. Examination of the realizations for these cases reveals that this observation is a result of high values of rooting depth together with small values of tortuosity. What can be said, however, is that it should be clear that it is the release via the surface flux pathway that will likely have the greatest influence on the eventual compliance or lack of compliance that is shown.

A second means of testing the influence of the plant pathway is to change the rooting depth distribution so that the maximum root depth is progressively increased. Figure 4.5 shows the results of this analysis. The curves on this figure represent the behavior of the model at maximum rooting depths of 10.7, 15.2, 18.3, 19.8, and 21.3m. The figure indicates that increasing the maximum rooting depth from 10.7 to 15.2m does not affect the CCDF at the highest EPA sums by a very large amount. A further increase to 18.3m produces a somewhat greater shift to the right, but the CCDF is still in compliance. Increasing the rooting depth once more by 1.5 to 19.8m, however, results in a dramatic change in the CCDF. At the highest EPA sums, it is shifted to the right by at least two orders of magnitude; this CCDF passes through the shaded violation zone. A second increase of 1.5m pushes the curve even farther to the right into

Table 4.3 - Effect of root depth on coefficients of determination.

Root Depth (m)	r^2 of ranked data	Coefficient of Partial Determination		Maximum Tortuosity
		tortuosity	root depth	
10.7	.8905	.7214	.1038	4
15.2	.8529	.5772	.2206	29
18.3	.8297	.4790	.3037	47
19.8	.8193	.4333	.3431	107
21.3	.8104	.3922	.3793	110

the violation zone. In these latter two cases, there are a number of realizations in which roots actually penetrate the waste area if erosion is included. This accounts in part for the considerable shift shown in these curves. These qualitative observations are confirmed by the results of a stepwise regression analysis shown in Table 4.3. It is clear that the partial determination coefficient from tortuosity consistently decreases until it is roughly comparable to that of the root depth as the maximum depth of roots increases. The last column in Table 4.3 further illustrates this point. This column lists the maximum tortuosity observed among those realizations possessing EPA sums greater than one. We see that for relatively shallow roots (10m), the tortuosity has to take on small values in order to produce an EPA sum greater than one. As the roots become deeper in the soil, however, diffusive transport becomes assisted to a greater degree by the vegetative pathway, which is reflected in the larger values of tortuosity associated with EPA sums of more than one. Indeed, for root depths of 19.8 and 21.3 m, there are realizations in which roots enter the waste area itself. In which case, the diffusive pathway becomes irrelevant and the highest values of tortuosity can still be associated with a large release.

Generalizing these observations, it appears correct to assert that the high EPA sum response of the model remains insensitive to root depths up until they approach the waste itself. Fifteen meters is a good dividing point. If roots descend below this depth, it becomes more probable that they will contribute a significant fraction of the overall release; however, it also appears that they will become a factor in the eventual compliance of the site only for root depths greater than 18m. This generalization will be useful in screening potential plant communities that could exist at the GCD site in the next 10,000 years under a potential change in the climate; only those that have very deep roots will be hazardous to the safety of the site.

4.2 Containment Requirements - Human Intrusion Event

This section describes the results of the compliance assessment determined for a drilling-related human intrusion event. The consequence and probability models were discussed previously in Section 3.2.

4.2.1 Results of Human Intrusion Release Analysis

Calculation of the release for a given intrusion event was determined in the same manner as described in the PPA. The fraction of the waste brought to the surface was assumed equal to the fraction of the GCD borehole volume occupied by the drill hole, which happens to be the ratio of the drillhole cross-sectional area to the GCD borehole cross-sectional area. For this calculation, the GCD borehole area was based upon a 1.5m radius and the drill hole on a 15cm radius. This results in a release fraction of .01. Radioactive decay of the initial inventories was accounted for in determining the release via the Bateman relations using a numerical model developed by Gelbard [1989]. Unlike the PPA, the inventories in each borehole were not treated as being uncertain. Thus, at a given point in time, there are only four (or six) potential releases.

The only parameters in Eq. (30) are the effective area, A_b, and the drilling density, ρ_d. The former is known with reasonable precision and was based upon a 1.8m hole radius and a 15cm drill bit radius (a different borehole radius was used here from that in the previous paragraph to arrive at a more conservative answer). The latter parameter, however, is uncertain. The EPA has established as a worst case a drilling density of 30 boreholes per km^2 per 10,000 years [EPA, 1985].

All the TRU waste is confined in four of the GCD boreholes. However, considerable Curies of non-TRUs were disposed of in the GCDT and an additional borehole. Thus, there are two cases that need to be considered. If release of only TRU is considered, the probability need reflect only four boreholes. However, if the non-TRU wastes are included, then we must consider six boreholes.

It is also important to note that the Containment Requirements of 40 CFR 191 [EPA, 1985] establish a probability of 10^{-3} as a lower bound for restricting radionuclide release; no restriction is placed upon releases that have probabilities less than this value. As noted above, we have assumed the probability that drilling occurs on the RWMS is unity for this analysis so the intrusion probability computed in Eq. (30) is the release probability that is regulated by 40 CFR 191. The intrusion probabilities are based upon a Poisson model, which starts initially at zero and increases thereafter. Therefore, there is some time before which the probability of intrusion into any borehole is less than 10^{-3}. We can determine this time by setting $nP = 10^{-3}$ and determining the time from Eq. (30). In the case of four boreholes, this is approximately 7000 years, for six boreholes, it is approximately 5000 years.

Figures 4.6a and b show the CCDFs for the four and six GCD borehole cases, respectively. There are two curves on each figure; one for intrusion at 10,000 years and the other at either 5000 years for six boreholes, or 7000 years for four boreholes. Since the probability of release increases continually with time and at the same time radioactive decay alters the makeup of the waste within each borehole, it is necessary to consider two points in time to assess the effects of both of these processes.

It is clear from both figures that an intrusion event at 10,000 years shows the least safe behavior. However, it is inappropriate to consider compliance or non-compliance from these results because a full scenario analysis has not been incorporated into this iteration. In addition,

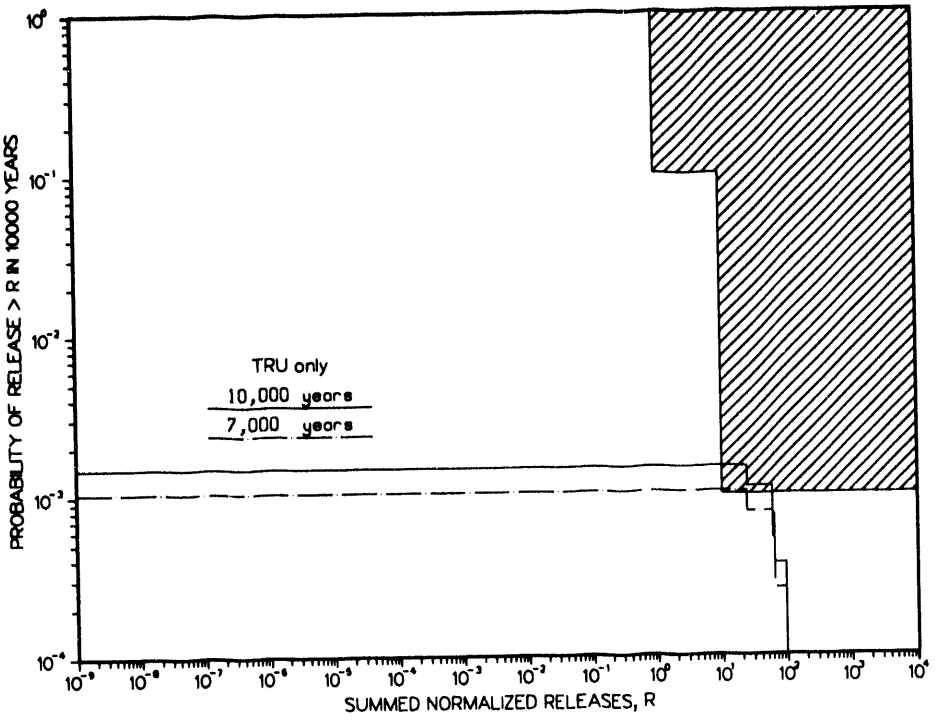

Figure 4.6a - CCDFs for human intrusion into TRU waste boreholes only.

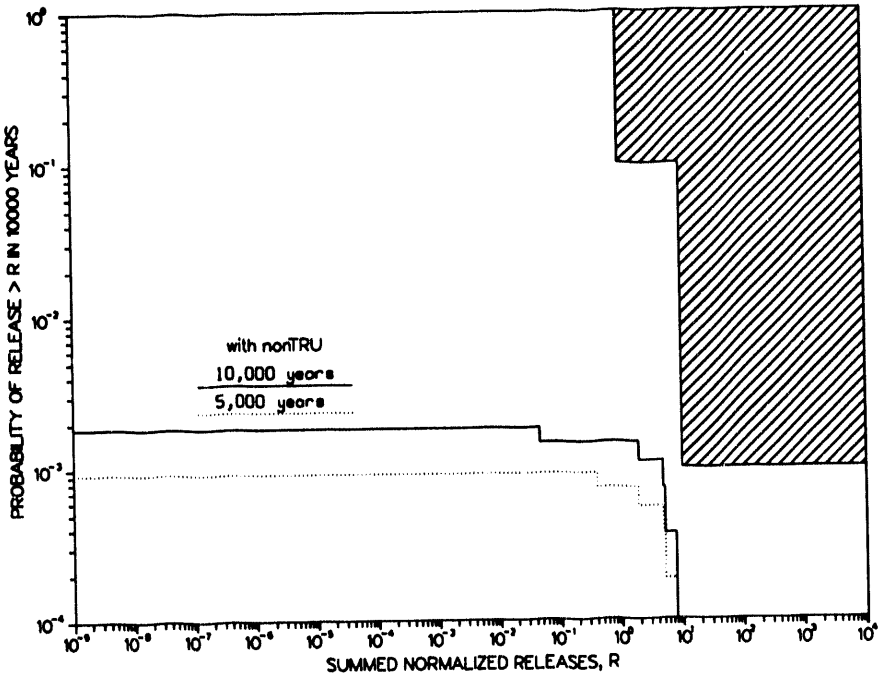

Figure 4.6b - CCDFs for human intrusion into TRU and non-TRU boreholes.

the drilling density, ρ_d, was chosen at a very conservative value. In fact, 30 wells per km^2 per 10,000 years corresponds to well over 5000 exploratory boreholes drilled into Frenchman Flat, or roughly a new borehole every two years for ten thousand years. This is an excessive number for such a resource-poor area as Frenchman Flat. For example, if a value of 1 exploratory borehole per km^2 is used, the probability of intrusion into any borehole is found to be 7×10^{-5} for the worst case of six boreholes.

4.3 Individual Protection Requirements

This section details the results of the Individual Protection analysis described in Section 3.3. Both liquid phase and gas phase pathways contribute to the dose. These will be discussed in separate sections. As noted in Section 1.1.2, the standard we use for Individual Protection is promulgated in the newest version of 40 CFR 191: the committed effective dose equivalent for a period of 10,000 years must be below 15 mrem.

4.3.1 Dose from Liquid Phase Transport

The dose from liquid phase diffusion was determined using the model described in Section 3.3.1. The parameter distributions used to evaluate compliance with the Containment Requirements were also used in this calculation with one modification: the lower limit of the root depth distribution was lowered from 1.08m to 2m. This was done to account for the tendency to deeper roots that would be expected for agricultural plants subject to irrigation. Twenty-five hundred parameter realizations were assembled from samples of these distributions, and the liquid diffusion model was solved for each realization to yield concentration histories to 10,000 years. Concentrations at two locations were tracked: the "surface" concentration, defined to be the concentration at 2m depth, and the concentration at the sampled rooting depth, referred to as the "deep soil" concentration. For each isotope, the maximum surface and deep soil concentration were extracted from the time history. Usually, these maxima would occur at 10,000 years. Short-lived species, however, tended to reach their maximum concentration at earlier times.

A mean surface and deep soil concentration for each isotope was computed from the 2500 maximum surface and deep soil values found for that isotope. This set of concentrations became the "exposure" case. That is, the concentration levels that the individual residing at Frenchman Flat was assumed exposed to for a single year. It could be argued that use of the mean value, rather than the maximum of the 2500 maximum values, is not rigorously conservative. However, it should be noted that the mean is drawn from a distribution of maximum values that were computed by an already very conservative transport model. It was felt that using the maximum of this distribution would pile conservatism upon conservatism in such a way as to unfairly depict the safety of the site. Justification for this decision can be found within the text of 40 CFR 191 itself. Appendix B of Subpart B states, "... the implementing agencies need not require that a very large percentage of the range of estimated radiation exposures or radionuclide concentrations fall below limits established in [the Individual Protection Requirements and the Groundwater Protection Requirements]. The Agency [the EPA] assumes that compliance can be determined based upon 'best estimate' predictions (e.g., the mean or the median of the appropriate distribution, whichever is higher)." We interpret this as meaning that compliance need not be demonstrated for the maximum concentration case (and therefore presumably the maximum dose),

but it is sufficient that compliance be shown for the mean of the concentration distributions. It should be noted that the median is consistently far below the mean for all isotopes.

The mean surface and deep soil concentrations were input to GENII-S. The models in GENII-S for plant uptake, animal ingestion, and human consumption were then applied to these concentrations to compute dose-to-man. The exposure and consumption parameters described in Section 3.3.1.1 were used with these models. In addition, the default concentration ratios used by GENII-S were changed to be consistent with the distributions developed for the Containment Requirements analysis. The mean values of these distributions (Appendix C) replaced the default GENII-S uptake factors in the cases were the default value was the lesser of the two. Finally, it was assumed that 99% of the root biomass was within 2m of the soil (referred to as the surface soil in GENII-S) and 1.0% was in the remainder (referred to as the deep soil in GENII-S). This was an estimate based upon examination of the measured rooting depths of common agricultural plants [Foxx, 1993].

The results of the GENII-S analysis are shown in Table 4.4. The doses shown are CEDE that assume a one-year intake of the exposure case and a fifty year commitment period. During this latter period, of course, the individual continues to receive exposure from radionuclides accumulated within body tissues, although the intake has ceased. The doses and soil concentrations are broken down into chains and specific radionuclides.

It should be noted that the concentrations shown in Table 4.4 are for conditions at or very near the GCD borehole. They do not take into account the fact that the food and forage crops grown at the RWMS in this hypothetical scenario will likely extend over a much greater area than total cross-sectional area of the GCD boreholes. Thus, only a fraction of these crops will be contaminated by radionuclides released from the GCD boreholes. Properly speaking then, some sort of dilution factor should be applied to these concentrations to account for this fact. Ignoring this factor adds further conservatism to this analysis.

The total exposure from ingestion and inhalation of radionuclides transported in the liquid phase amounts to 6.9 mRem. This is comfortably below the revised compliance limit of 15 mRem CEDE. It is interesting to note that nearly 80% of this dose is attributable to just two radionuclides, ^{237}Np and ^{210}Pb. The PPA also identified ^{237}Np as the major contributor to dose as well. All the isotopes of plutonium contribute a negligible amount to the total, which is likely a consequence of the revised solubility and retardation parameter distributions used in this iteration, as discussed in Section 4.1.3.

4.3.2 Dose from Gas Phase Transport

Seven separate analyses were performed for the various radon pathways and requirements using the model described in Section 3.3.2. The pathway, associated borehole, requirement, and radon isotope of concern for each analysis is given in Table 4.5. Note that for Analyses 1 and 6 the applicable requirement is the Containment Requirements and not the Individual Protection Requirements. As was discussed in Section 3.3.2, ^{210}Pb, which is produced by decay of ^{222}Rn, is subject to the Containment Requirements, and it is necessary to consider its release with respect to this regulation. Note also that it is the GCDT borehole that receives the majority of the attention. This is consistent with the presence of a direct radon parent (^{226}Ra) in this borehole along with a great deal of heat-producing waste.

The result of each analysis and how the result compares to the relevant requirement is given in Table 4.6. The doses obtained for any radon isotopes or from ^{210}Pb are not large enough to substantially change the doses associated with the liquid phase transport shown in Table 4.4.

Thus, we can conclude that the Individual Protection Requirements will be met by the base case. In addition, the integrated release of ^{210}Pb via gas transport is insignificant with respect to the transport of other isotopes in the liquid phase. Therefore, there is no significant affect on compliance with the Containment Requirements from release of ^{210}Pb via gas phase transport.

Table 4.4 - Concentrations and doses for each chain for the liquid diffusion pathway.

Decay Chain	Radio-nuclide	Surface Soil (pCi/kg)	Deep Soil (pCi/kg)	Annual CEDE from isotope (mRem)	Total CEDE from chain (mRem)
Chain 1	^{239}Pu	2.9×10^{-7}	1.2×10^{-3}	2.2×10^{-10}	0.7
	^{235}U	4.6×10^{-2}	0.15	1.3×10^{-5}	
	^{231}Pa	8.8	22	0.3	
	^{227}Ac	8.8	22	0.4	
Chain 2	^{240}Pu	2.4×10^{-7}	1.3×10^{-3}	9.7×10^{-12}	3.6×10^{-4}
	^{236}U	3.9	8.2	3.6×10^{-4}	
	^{232}Th	2.5×10^{-5}	5.7×10^{-5}	3.2×10^{-9}	
Chain 3	^{241}Pu	0.0	0.0	0.0	3.9
	^{241}Am	6.5	72	1.5×10^{-2}	
	^{237}Np	40	85	3.9	
	^{233}U	1.6	3.4	1.6×10^{-4}	
	^{229}Th	0.6	1.3	6.6×10^{-3}	
Chain 4	^{242}Pu	5.9×10^{-10}	1.6×10^{-6}	3.0×10^{-13}	2.3
	^{238}U	8.1×10^{-3}	1.5×10^{-2}	6.9×10^{-7}	
	^{238}Pu	0.0	0.0	0.0	
	^{234}U	150	270	0.14	
	^{230}Th	110	270	0.19	
	^{226}Ra	100	270	0.31	
	^{210}Pb	100	270	1.7	
Chain 5	^{90}Sr	1.1×10^{-7}	6.7×10^{-3}	2.0×10^{-6}	2.0×10^{-6}
Chain 6	^{137}Cs	1.3×10^{-10}	7.6×10^{-8}	1.2×10^{-12}	1.2×10^{-12}
Total CEDE, All Decay Chains (see Figure A.1), All Pathways					6.9

Table 4.5 - Pathway, requirement, and isotope for each radon analysis.

Analysis	Pathway	Borehole	Requirement	Isotope
1	Diffusion to ground surface	GCDT	Containment Requirements	^{222}Rn to ^{210}Pb, ^{210}Po
2	Diffusion to ground surface	GCDT	Individual Protection Requirements	^{222}Rn
3	Diffusion to ground surface	1,2,3,4	Individual Protection Requirements	^{220}Rn
4	Diffusion to ground surface	GCDT	Individual Protection Requirements	^{219}Rn
5	Diffusion to ground surface	GCDT	Individual Protection Requirements	^{218}Rn
6	Plant Uptake	GCDT	Containment Requirements	^{222}Rn to ^{210}Pb, ^{210}Po
7	Plant Uptake	GCDT	Individual Protection Requirements	^{222}Rn to ^{210}Pb, ^{210}Po

Table 4.6 - Results of radon analysis.

Analysis	Result	Conclusion
1	6.17×10^{-5} Ci released EPA Sum = 0.0013	No major effect on CCDF
2	0.64 mRem CEDE	Below IP limit
3	0 mRem	Insignificant
4	0 mRem	Insignificant
5	0 mRem	Insignificant
6	3.86×10^{-10} Ci released EPA Sum = 2.4×10^{-9}	Insignificant contribution to CCDF
7	4×10^{-4} mRem CEDE	Well below IP limit

5.0 SUMMARY, CONCLUSIONS, AND RECOMMENDATIONS

At the conclusion of the PPA, several recommendations were proposed. It was suggested that the recharge rate in Frenchman Flat should receive active study. Also the solubility and sorption behavior of plutonium isotopes were felt to be of considerable importance. This iteration has seen the fruition of these studies. The environmental tracer recharge study virtually eliminated recharge within the base case scenario and thereby removed the entire "down-and-out" pathway from further consideration in that scenario. As a further consequence, the Groundwater Protection Requirements were satisfied without any additional analysis. The research into plutonium solubility and sorption revealed that plutonium dissolved to a much lesser degree and adsorbed to the alluvium to a much greater degree than originally estimated in the PPA. The effect of this change is quite clear. In the PPA, 98% of the released activity was in the form of plutonium isotopes. In the current analysis, the majority of the Curies are released as ^{230}Th, ^{234}U, ^{226}Ra, and ^{210}Pb.

Elimination of the "down-and-out" pathway focused our attention in this iteration on the near surface. A more complicated plant uptake model had to be developed, and a simple erosion model was also necessary. The new analysis led us to several conclusions. First, as in the case of the PPA, we conclude that our model of the site indicates compliance with all the requirements promulgated in 40 CFR 191 and the base case scenario. In this iteration, the base case scenario was defined as those events and processes that will occur in Frenchman Flat in the next 10,000 years, with the exception of a change in the climate. Disruptive events or processes that may or may not occur were not included in this analysis. It is our contention that this model is a very conservative representation of this base case scenario. Thus, we feel that this conclusion also implies compliance of the site for these conditions. Relaxing the restriction to undisturbed conditions will be the focus of the third iteration as will be discussed below.

A second conclusion evident from this analysis is that at high EPA sums, the results are insensitive to the depth of plant roots up until the deepest roots are very close to, if not intruding into, the waste itself. We can determine a critical rooting depth to be approximately 15m at which point the CCDF starts becoming sensitive to rooting depths. This information is useful in identifying and screening plant communities that could exist at the NTS as a result of a change in climate. Those communities whose roots are substantially less than 15 m are not likely to play a major role in estimating the likelihood of compliance. On the other hand, it was seen that very deep roots can have a considerable impact on the site.

Finally, the human intrusion event was revisited. The PPA had considered the consequence but had not estimated the probability of human intrusion by exploratory drilling. In this iteration, a simple Poisson model of intrusion was used to compute the likelihood of a exploratory drill hole intruding on the waste. This analysis concluded that a human intrusion event would result in a release that would violate the regulations by only a slight amount. However, this analysis assumed a unitary probability for drilling in Frenchman Flat. It also assumed a very conservative value for the drilling density, a borehole in Frenchman Flat every two years for the next 10,000 years. Thus, we have reasons to believe that in the final analysis, the exploratory drilling intrusion event will not result in a non-compliance outcome.

At this point, we turn our attention to the direction the analysis needs to take for the third performance assessment iteration. The sensitivity analysis of the base case yielded one clear point: the tortuosity was the most significant parameter controlling radionuclide release. This is due probably in part to the very conservative nature of the distribution we applied to this parameter. For very arid environments, it would be more than likely that high values of

tortuosity would tend to occur more often than low values. The distribution used in this iteration ignores this tendency. We have seen that the greatest sensitivity to tortuosity occurs at the lower end of the distribution. We have also seen the sensitivity decrease as the lower bound of the distribution is increased. Therefore, it is the lower boundary of the distribution that is of the greatest interest. The next question is what, if anything, should or can be done about tortuosity in the next iteration. Currently, base case conditions show compliance by a comfortable margin using this conservative tortuosity distribution. Therefore, according to the performance assessment methodology, there is no reason to characterize the uncertainty in tortuosity any further. However, this conclusion does not consider the fact that several important processes have been left out of the analysis, most notably climate change, which could adversely affect compliance. As the sensitivity analysis shows, reduction in the conservatism of the tortuosity distribution is the most effective means of reducing the conservatism of the entire analysis. While not in strict keeping with out overall methodology, it seems reasonable that some effort should be expended to gain additional data in order to defensibly reduce the conservatism of the tortuoisty distribution. This would place us in a position to immediately reduce the conservatism of the entire model should inclusion of an additional process result in a non-compliance result.

There are certain questions that were brought up in this iteration that still must be resolved. We must consider the implications of a spherical diffusion model as opposed to a planar diffusion model. This can be addressed by a straightforward modeling exercise. We must also consider the possibility of upward advective flow in the near surface alluvial layer. This will require a combination of modeling and site characterization. Rooting depths must receive some site characterization attention. As part of this, some effort must be expended considering the potential for very-deep-rooting communities to exist at the GCD site. The phenomenon of bioturbation (enhanced transport near the surface owing to the mixing of soil by plants and animals in the near surface) must be researched and included in the base case model. It may not alter the behavior of the system greatly, but it is a necessary part of a defensible near-surface model. Finally, the influence of barometric pumping on radon transport should be dealt with and a definite conclusion reached on whether it is a significant process at GCD and should be included within the radon transport conceptual model.

However, the aspect of the third iteration that will likely require the greatest amount of effort is in characterizing and modeling a change in the climate. The PPA considered a change in climate as a separate disruptive event. Since that time, it has been concluded, however, that a change in climate is actually a part of the base case scenario. That is, it is a virtual certainty that the climate is going to change in the next 10,000 years. Thus, climate change must be included in the base case analysis. Data must be gathered on the possible changes in temperature and precipitation. From these, the response of infiltration rates/recharge, soil moisture content, plant and animal communities, and erosional processes must be determined or estimated. This information must then be incorporated into the performance assessment analysis.

The last important aspect of the final performance assessment iteration is consideration of disruptive events and processes. 40 CFR 191 requires that a complete analysis include the possibility of disruptive events or processes altering the behavior of the site. These processes or events are known to have a probability of occurrence that is less than one in 10,000 years; therefore, they are not a part of the base case scenario. To date, an extensive screening process of such events and processes has reduced a very large number to just four that must be considered [Guzowski and Newman, 1993] : human intrusion into the boreholes as a result of exploratory drilling in search of extractable resources, human intrusion as a result of drilling for groundwater, subsidence or caving of the boreholes owing to degradation of the waste containers

and settling of the backfill, and changes in land use that would result in irrigation farming occurring on the former RWMS. Consequence models of these events must be developed and the probabilities of their occurrence estimated. Currently, the implementation of a methodology for estimating the probabilities of these events and combinations of these events is under way [Guzowski, in progress]. This will allow the results for the base case scenario, including the effects of climate change, to be combined with the consequences and probabilities of the disrupting events and processes to generate a complete CCDF. It is this curve that will indicate the final likelihood of compliance of the site. If this curve indicates compliance, the performance assessment/site characterization phase of the GCD project will be at an end.

6.0 REFERENCES

Abrahams, J.H. jr., E.H. Baltz, W.D. Purtyman, "Movement of perched ground water in alluvium near Los Alamos, New Mexico," Short Papers in Geology, Hydrology and Topography, USGS-PP-450-B, pp. B93-B94, (1962)

Adriano, D.C., A. Wallace, E.M. Romney, "Uptake of Transuranic Nuclides from Soil by Plants Grown under Controlled Environmental Conditions," in Transuranic Elements in the Environment, DOE/TIC-22800, pp. 336-360, (1980).

Adriano D.C., K.W. McLeod, T.G. Ciravolo, "Plutonium, Curium, and Other Radionuclide Uptake by the Rice Plant from a Naturally Weathered Contaminated Soil," Soil Science, **132**(1), pp. 83-88, (1981).

Bernhardt, D.E., and G.G. Eadie, Technical Note: Parameters for Estimating the Uptake of Transuranic Elements by Terrestrial Plants, ORP/LV-76-2,(1976).

Berry, J.A., K.A. Bond, D.R. Ferguson, N.J. Pilkington, "Experimental Studies of the Effects of Organic Materials on the Sorption of Uranium and Plutonium," Radiochimica Acta, **52/53**, pp. 201-209, (1991).

Bethke, C., The Geochemist's Workbench: A Users' Guide to Rxn, Act2, Tact, React, and Gtplot, University of Illinois, IL, (1992).

Bird, R.B., W.E. Stewart, E.N. Lightfoot, Transport Phenomena, John Wiley & Sons, Inc., New York, NY, (1960).

Blinov, A., "The Dependence of Cosmogenic Isotopic Production Rate on Solar Activity and Geomagnetic Field Variations," in Secular Solar and Geomagnetic Variations in the Last 10,000 years, F.R. Stephenson and A.W. Wolfendale (eds.), Klewer Academic Pub. Co., pp. 329-340, (1988).

Bonano, E.V., R.M. Cranwell, P.A. Davis, "Performance Assessment Methodologies for the Analysis of High-Level Nuclear Waste Repositories," Radioactive Waste Management and Nuclear Fuel Cycle, **13**, pp. 229-239, (1989).

Campbell, G.S., Soil Physics with BASIC, Elsevier, New York, NY, (1985).

Carslaw, H.S., J.C. Jaeger, Conduction of Heat in Solids, Oxford Science Publications, Oxford, UK, (1959).

Chu, M.S.Y., E.A. Bernard, Waste Inventory and Source Term Model for the Greater Con finement Disposal Site at the Nevada Test Site, SAND91-0170, Sandia National Laboratories, Albuquerque, NM, (1991).

Cline, J.F., "Uptake of ^{241}Am and ^{239}Pu by Plants," USAEC Doc. BNWL-714, p 8.24-8.25, (1968).

Conca, J.L., and J. Wright, "A New Technology for Direct Measurements of Unsaturated Transport, "Proceedings of the Spectrum'92 International Topical Meeting on Nuclear and Waste Management, Boise, ID, (1992).

Conover,W.J., Practical Nonparametric Statistics, 2nd. Edition, John Wiley & Sons, New York, N.Y. (1980).

Conrad, S.H., "Using Environmental Tracers to Estimate Recharge through and Arid Basin," Proceedings of the Fourth Annual International High Level Radioactive Waste Management Conference Vol 1., American Nuclear Soc., Las Vegas, NV, (1993).

Cranwell, R.M., R.V. Guzowski, J.E. Campbell, N.R. Ortiz, Risk Methodology for Geologic Disposal of Radioactive Waste: Scenario Selection Procedure, SAND80-1429, NUREG/CR-1667, Sandia National Laboratories, Albuquerque, NM, (1990).

Cross, J.E., F.T. Ewart, B.F. Greenfield, "Modelling the Behaviour of Organic Degradation Products," In Scientific Basis for Nuclear Waste Management XII, W.Lutze and R.C. Ewing (eds.), Materials Research Society, Pittsburg, PA, pp. 715-722, (1989).

Dahlman, R.C., K.W. McLeod, "Foliar and Root Pathways of Plutonium Contamination of Vegetation," in Transuranics in Natural Environments, NVO-178, pp. 303-320, (1977).

Dickman, P. T., Greater Confinement Disposal Test at the Nevada Test Site, Final Technology Report, Reynolds Electrical and Engineering Company, Las Vegas, NV, (1989).

DOE, "Internal Dose Conversion Factors for Calculation of Dose to the Public," DOE/EH-0071, DE88-014297, (1988).

Draper, N.R., H. Smith, Applied Regression Analysis, 2nd Edition, John Wiley & Sons, New York, (1981).

EPA, "40 CFR 191: Environmental Standards for the Management and Disposal of Spent Nuclear Fuel, High-Level, and Transuranic Radioactive Waste; Final Rule," Federal Register, **50**, 38066 (1985).

Foxx T., unpublished data, Los Alamos National Laboratory, Los Alamos, NM, (1993).

Freeze, R.A., and J.A. Cherry, Groundwater, Prentice-Hall, Englewood Cliffs, NJ, (1979).

Gelbard, F., Modeling One-Dimensional Radionuclide Transport under Time-Varying Fluid-Flow Conditions, SAND89-1521, NUREG/CR-5412, Sandia National Laboratories, Albuquerque, NM, (1989).

Gee G.W., and D. Hillel, "Groundwater Recharge in Arid Regions: Review and Critique of Estimation Methods," Hydrological Processes, **2**, pp. 255-266, (1988).

Gustafson, D.L., S.E. Rawlinson, and J.J. Miller, Summary of Natural Resources that Potentially Influence Human Intrusion at the Area 5 Radioactive Waste Management DOE/Nevada Test Site, Nye County, Nevada, Raytheon Services Nevada, Las Vegas, NV, (1993)

Guzowski, R.V., Evaluation and Applicability of Probability Techniques to Determining the Probability of Occurence of Potentially Disruptive Intrusive Events at the Waste Isolation Pilot Plant, SAND90-7100, Sandia National Laboratories, Albuquerque, NM, (1991).

Guzowski, R.V., Preliminary Estimation of Probabilities of Occurence for Potentially Disruptive Scenarios at the Greater Confinement Disposal Facility, Area5 of the Nevada Test Site, in progress, Sandia National Laboratories, Albuquerque, NM

Guzowski, R.V., G. Newman, Preliminary Estimate of Probabilities of Occurence for Potentially Disruptive Scenarios at the Greater Confinement Disposal Facility, Area 5 of the Nevada Test Site, SAND93-7100, Sandia National Laboratories, Albuquerque NM, (1993).

Hakonson, T.E., G.C. White, E.S. Gladney, and M. Dreicer, "The distribution of mercury, 137Cs, and plutonium in an intermittent stream at Los Alamos," J. Environmental Quality, **9**, pp. 289-292, (1980)

Harr, M.E., Reliability-Based Design in Civil Engineering, McGraw-Hill, New York, (1987).

Higgo, J.J.W., L.V.C. Rees, "Adsorption of Actinides by Marine Sediments: Effect of the Sediment/Seawater Ratio on the Measured Distribution Ratio," Environmental Science and Technology, **20**, pp. 483-490, (1986).

Hunter, R.B., P.A. Medica, Status of the Flora and Fauna on the Nevada Test Site, DOE/NV/10630-2, Las Vegas, NV, (1989).

Hunter R.B., private communication with R.B. Hunter of Reynolds' Electrical and Engineering Co., (1992).

Iman, R.L., and M.J. Shortencarier, A FORTRAN 77 Program and User's Guide for the Generation of Latin Hypercube Samples for Use with Computer Models, SAND83-2365,Sandia National Laboratories, Albuquerque, NM, (1984).

Iman, R.L., and W.J. Conover, "The Use of Rank Transformation in Regression," Technometrics, **21**, pp. 499-509, (1979).

Isaaks, E.H., R.M. Srivastava, An Introduction to Applied Geostatistics, Oxford University Press, New York, NY, (1989).

Jacobson, L., R. Overstreet, "The Uptake by Plants of Plutonium and Some Products of Nuclear Fission Absorbed on Soil Colloids," Soil Science, **65**, pp. 129-134, (1948).

Johnson, J.E., S. Svalberg, D. Paine, The Study of Plutonium in Aquatic Systems of the Rocky Flats Environs, Progress Report of Colorado State University, Dept. of Animal Sciences, Ft. Collins, CO, (1972).

Jury, W.A., W.F. Spencer, W.J. Farmer, "Behavior Assessment Model for Trace Organics in Soil: IV. Review of Experimental Evidence," Journal of Environmental Quality, **30**, pp. 437-463, (1984).

Kinnear, J.E., A. Wallace, E.M. Romney, "Frequency Distribution of ^{241}Am in a Population of Bushbean Plants Grown in Soil in a Glasshouse," Soil Science, **132**(1), pp. 122-126, (1981).

Leigh, C.D., B.M. Thompson, J.E. Campbell, D.E. Longsine, R.A. Kennedy, and B.A. Napier, User's Guide for GENII-S: A Code for Statisitical and Deterministic Simulations of Radiation Doses to Humans from Radionuclides in the Environment, SAND91-0561A, Sandia National Laboratories, Albuquerque, NM, (1992)

Lindstrom, F.T., private communication with F.T. Lindstrom of Reynolds Electrical and Engineering Co., (1992).

Massman J., D.F. Farrier, "Effects of Atmospheric Pressures on Gas Transport in the Vadose Zone, "Water Resources Research, **28**(3), pp. 777-791, (1992).

Mazaud, A., C. Laj, E. Bard, M. Arnold, E. Tric, "Geomagnetic Field Control of ^{14}C Production over the Last 80 KY: Implications for the Radiocarbon Time Scale," Geophysical Research Letters, **18**, pp. 1885-1888, (1991).

McGrath, D.A., Monitoring of Heat and Moisture at the Greater Confinement Disposal Test from January 1983 through October 1986 - a Preliminary Analysis, RWM-7, Reynolds Electrical and Engineering Co., (1987).

McKenzie, D.H., L.L. Caldwell, L.E. Eberhardt, W.E. Kennedy, Jr., R.A. Peloquin, M.A. Simmons, Relevance of Biotic Pathways to the Long-Term Regulation of Nuclear Waste Disposal: Topical Report on Reference Western Arid Low-Level Sites, vol. 2, NUREG/-CR-2675, PNL-4241, Pacific Northwest Laboratories, Richland WA, (1982).

McLeod, K.W., D.C. Adriano, T.G. Ciravolo, "Uptake of Plutonium from Soils Contaminated by a Nuclear Fuel Chemical Separation Facility," Soil Science, **132**(1), pp. 89-98, (1981).

Napier, B.A., private communication with B.A. Napier of Pacific Northwest Laboratories, (1993).

NCRP, Report 94: Exposure of the Population of the United States and Canada from Natural Background Radiation, National Council on Radiation Protection, Bethesda, MD, (1987).

Nero, A. V., "Airborne Radionuclides and Radiation in Buildings: A Review," Health Physics, **45**(2), pp. 302-322, (1983).

Neter J., W. Wasserman, M. Kutner, Applied Linear Regression Models, Irwin, Homewood, IL, (1983).

Niklaus, P., and D.Feldman, How Safe is New Mexico's Atomic City? Southwest Research and Information Center, Albuquerque, NM, (1980)

Nilson R.H., K.H. Lie, "Double-Porosity Modelling of Oscillatory Gas Motion and Contaminant Transport in Fractured Porous Media," Inter. Journal for Numerical and Analytical Methods in Geomechanics, **14**, pp. 565-585, (1990).

Nilson, R.H., E.W. Peterson, K.H.Lie, N.R. Burkhard, J.R. Hearst, "Atmospheric Pumping: A Mechanism Causing Vertical Transport of Contaminated Gases through Fractured Permeable Media," Journal of Geophysical Research, **96**(B13), pp. 21,933-21,948, (1991).

Nishita, H., "Relative Adsorption and Plant Uptake of ^{238}Pu and ^{239}Pu in Soils," Soil Science, **132**(1), pp. 66-70, (1981).

Nishita, H., A. Wallace, E.M. Romney, J. Kinnear, "Relationship between the Chemical Extrability of Several Transuranic Elements from Soils and their Uptake by Wheat," Soil Science, **132**(1), pp. 60-65, (1981).

Nitsche, H., Roberts, K, Prussin, T., Keeney, D., Carpenter, S.A., Becraft, K. and Gatti, R.C., "Radionuclide solubility and speciation studies for the Yucca Mountain Site Characterization Project," in: Proceedings of the Fourth Annual International High Level Radioactive Waste Management Conference Vol 1. American Nuclear Society, Inc., LaGrange Park, IL, pp 1490 - 1495, (1993).

Peterson, E.W., K. Lie, R.H. Nilson, "Dispersion of Contaminant during Oscillatory Gas-Motions Driven by Atmospheric Pressure Variations," Proceedings of the Fourth Symposium on Containment of Underground Nuclear Explosions, Vol. 2, USAF Academy, Colorado Springs, CO, (1987).

Penrose, W.R., W.L. Polzer, E.H. Essington, D.M. Nelson, K.A. Orlandini, "Mobility of Plutonium and Americium through a Shallow Aquifer in a Semiarid Region," Environmental Science and Technology, **24**, pp. 228-234, (1990).

Phillips, F.M., P. Sharma, P.E. Wigand, "Deciphering Variations in Cosmic Radiation Using Cosmogenic ^{36}Cl in Ancient Rat Urine," Abstract in EOS Transactions, American Geophysical Union, **72** (44), pp. 72, (1991).

Porstendörfer, J., G. Butterweck, and A. Reineking, "Diurnal Variation of the Concentrations of Radon and its Short-Lived Daughters in the Atmosphere Near the Ground," Atmospheric Environment, **25a**(3/4), pp. 709-713, (1991).

Price, K.R.,"Uptake of ^{237}Np, ^{239}Pu, ^{241}Am, ^{244}Cm, from Soil by Tumbleweed and Cheat grass," BNWL-1688, pp. 1-14, (1972).

Price, L.L, S.H. Conrad, D.A. Zimmerman, N.E. Olague, K.C. Gaither, W.B. Cox, J.T. McCord, and C.P. Harlan, Preliminary Performance Assessment of the Greater Confinement Disposal Facility at the Nevada Test Site, Volume 1: Executive Summary, Volume 2: Technical Discussion, Volume 3: Supporting Details, SAND91-0047, Sandia National Laboratories, Albuquerque NM, (1993).

Purtymun, W.D., Dispersion and Movement of Tritium in a Shallow Aquifer in Mortendad Canyon at the Los Alamos Scientific Laboratory, LA-5716-MS, Los Alamos Scientific Laboratory, Los Alamos, NM, (1974)

Rawlinson, S.E., letter to P.A. Davis of SNL from S.E. Rawlinson of RSN, (1993).

Rediske, J.H., J.F. Cline, and A.A. Selders, The Absorption of Fission Products by Plants, HW-36734, (1955).

REECo, Hydrogeologic Data for Science Trench Boreholes at the Area 5 Radioactive Waste Management Site, Nevada Test Site, Nye County, Nevada, Reynolds Electrical and Engineering Co., report to DOE/NV, Las Vegas, NV, (1993).

Reeves, M., D.S. Ward, N.D. Johns, R.M. Cranwell, Theory and Implementation for SWIFT II: The Sandia Waste-Isolation Flow and Transport Model for Fractured Media, Release 4.84, SAND83-1159, Sandia National Laboratories, Albuquerque, NM, (1986a).

Reeves, M., D.S. Ward, P.A. Davis, E.J. Bonano, SWIFT II Self-Teaching Curriculum: Illustrative Problems for the Sandia Waste-Isolation Flow and Transport Model for Fractured Media, SAND84-1586, Sandia National Laboratories, Albuquerque, NM, (1986b).

Reeves, M., V.A. Kelley, R.H. Petrini, W.H. Statham, Revised Data Input Guide for SWIFT II, INTERA Inc., Austin, TX, (1990).

Romney, E.M., H.M. Mork, K.H. Larson, "Persistence of Plutonium in Soil, Plants, and Small Mammals," Health Physics, **19**, pp. 487-491, (1970).

Romney, E.M., V.Q. Hale, A. Wallace, O.R. Lunt, J.D. Childress, H. Kaaz, G.V. Alexander, J.E. Kinnear, T.L. Ackerman, Some Characteristics of Soil and Perennial Vegetation in Northern Mojave Desert Areas of the Nevada Test Site, UCLA 12-916, TID-4500, (1973).

Romney, E.M., A. Wallace, P.A.T. Wieland, J.E. Kinnear, "Plant Uptake of $^{239-240}$Pu and ^{241}Am through Roots Containing Aged Fallout Materials," UCLA 12-1056, pp.1-15, (1976).

Romney, E.M., A. Wallace,"Plutonium Contamination of Vegetation in Dusty Field Environments," in Transuranics in Natural Environments, NVO-178, pp. 287-302, (1977).

Romney, E.M., A. Wallace, R.K. Schulz, J. Kinnear, R.A. Wood, "Plant Uptake of ^{237}Np, $^{239,240}Pu$, ^{241}Am, ^{224}Cm from Soils Representing Major Food Production Areas of the United States," Soil Science, **132**(1), pp. 40-59, (1981a).

Romney, E.M., A. Wallace, R.T. Mueller, J.W. Cha, R.A. Wood, "Effects of DTPA on Concentration Ratios of ^{237}Np and ^{244}Cm in Vegetative Parts of Bush Bean and Barley," Soil Science, **132**(1),pp. 104-107, (1981b).

Romney, E.M., A. Wallace, J.E. Kinnear, R.A. Wood, "Plant Root Uptake of Pu and Am," in The Radioecology of Transuranics and other Radionuclides in Desert Ecosystems, NVO-224, pp. 185-200, (1982).

Ryan, P.A., Y. Cohen, "Diffusion of Sorbed Solutes in Gas and Liquid Phases of Low-Moisture Soils," Soil Sci. Soc. Am. J., **54**, pp. 341-346, (1990).

Sadeghi, A.M., D.E. Kissel, M.L. Cabrera, "Estimating Molecular Diffusion Coefficients of Urea in Unsaturated Soil," Soil Sci. Soc. Am. J., **53**, pp. 15-18, (1989).

SAS Institute Inc.,SAS User's Guide: Statistics, Version 5, SAS Institute Inc., Cary, NC, (1985).

Schulz, R.K., G.A. Tompkins, L. Levanthal, K.L. Babcock, "Uptake of Plutonium and Americium by Barley from Two Contaminated Nevada Test Site Soils," J. Environmental Quality, **5**, pp. 406-410, (1976).

Schulz, R.K, "Root Uptake of Transuranic Elements," in Transuranics in Natural Environments, NVO-178, pp.321-330, (1977).

Schulz, R.K., M.R. Ruggieri, "Uptake and Translocation of Neptunium-237, Plutonium-238, Plutonium-239,240, Americium-241, and Curium-244 by a Wheat Crop," Soil Science, **132**(1), pp. 77-82, (1981).

Shott, G.J., letter to N.E. Olague of SNL from G.J. Shott of REECo., (1992).

Stockman, H.W., "Preliminary Geochemical Characterization of Alluvium from Trench 8 at the RWMS, Area V, Nevada Test Site," Draft of an interim report to DOE/NV, Sandia National Laboratories, Albuquerque, NM, (1992a).

Stockman, H.W., "Refinement of Plutonium Solubility Estimates for the Greater Confinement Disposal Project, Area 5, Nevada Test Site," Draft of an interim report to DOE/NV, Sandia National Laboratories, Albuquerque, NM, (1992b).

Stockman, H.W., "Refinement of Plutonium K_D Estimates for the Greater Confinement Disposal Project, Area 5, Nevada Test Site," Draft of an interim report to DOE/NV, Sandia National Laboratories, Albuquerque, NM, (1992c).

AIIM

Association for Information and Image Management

1100 Wayne Avenue, Suite 1100
Silver Spring, Maryland 20910

301/587-8202

Centimeter

Inches

MANUFACTURED TO AIIM STANDARDS
BY APPLIED IMAGE, INC.

2 of 2

Sully, M.J., T.E. Detty, D.P. Hammermeister, J.C. Hauth, "Vadose Zone Air Permeability Tests in Pilot Well No.1, Area 5," Reynolds Electrical and Engineering Co., Report to DOE/NV, Las Vegas, NV, (1992).

Tang, D.H., E.O. Frind, E.A. Sudicky, "Contaminant Transport in Fractured Porous Media: Analytical Solution for a Single Fracture," Wat. Res. Research, **17**(3), pp. 555-564, (1981).

Tanner, A. B., "Radon Migration in the Ground: A Supplementary Review," in Natural Radiation Environment III, Volume I, Proceedings of a Symposium held at Houston, Texas, April 23-28, 1978, T. F. Gesell and W. M. Lowder (eds.), (1980).

Torstenfelt, B., R.S. Rundberg, A.J. Mitchell, "Actinide Sorption on Granites and Minerals as a Function of pH and Colloids/Psuedocolloids," Radiochimica Acta, **44/45**, pp. 111-117, (1988).

Wallace A., E.M. Romney, "Root Systems of Some Shrubs in the Sandy Wash Area of Rock Valley," in Radioecology and Ecophysiology of Desert Plants at the Nevada Test Site, TID-25954, pp. 271-278, (1972a).

Wallace A., E.M. Romney, "^{90}Sr Uptake by Desert Vegetation," in Radioecology and Ecophysiology of Desert Plants at the Nevada Test Site, TID-25954, pp. 69-72, (1972b).

Wallace, A., "Behavior of Certain Synthetic Chelating Agents in Biological and Soil Sys tems," UCR 34P51-37, pp. 1-12, (1974).

Wallace, A., E.M. Romney, R.T. Mueller, S.M. Soufi, "Effect of Concentration on ^{241}Am Uptake by Plants with and without DTPA Treatment," Soil Science, **132**(1), pp. 108-113, (1981).

Wildung, R.E., T.R. Garlund, "Influence of Soil Plutonium Concentration on Plutonium Uptake and Distribution in Shoots and Roots of Barley," J. Agric. and Food Chem., **22**, pp. 836-838, (1974).

Wolery, T.J., EQ3NR: A Computer Program for Geochemical Aqueous Speciation-Solubility Calculations, User's Guide and Documentation, UCRL-53414, Lawrence Livermore National Laboratory, Livermore, CA, (1983).

Wolery, T.J., S.A. Daveler, EQ6, A Computer Program for Reaction Path Modelling of Aqueous Geochemical Systems: Theoretical Manual, User's Guide, and Related Documentation (Version 7.0), UCRL-MA-110662-PT-IV, Lawrence Livermore National Laboratory, Livermore, CA, (1992).

Appendix A - Waste Inventory at GCD Site

The total mass of waste disposed of within the Greater Confinement Disposal site is not very large. Approximately, 6 to 7 kg of ^{238}Pu,^{239}Pu,^{240}Pu,^{241}Pu, and ^{242}Pu isotopes plus a small amount of ^{241}Am are buried in boreholes 1 through 4. Mixed in with this waste is approximately 700 kg of ^{234}U, ^{235}U, ^{236}U, ^{238}U isotopes. As was noted in Section 1.2, all of this waste is treated as transuranic waste. Buried in the Greater Confinement Disposal Test borehole is approximately 4 kg of ^{90}Sr, 0.25 kg of ^{137}Cs, 100 g of ^{226}Ra and a slight amount of ^{227}Ac. We classify these as non-TRU waste. Borehole 6 contains less than 10 g of ^{90}Sr and ^{137}Cs. Approximately 11 g of ^{137}Cs are buried in borehole 2. Price *et al.*, [1993] gives a more complete description of the quantities of waste involved. Table A.1 depicts the original distribution of activities among the various boreholes. It was adapted from Price *et al.*, [1993]. Decay of the initial waste inventories results in numerous daughter products. The decay chains and the corresponding daughters are depicted in Figure A.1. Note that only those daughters that have a significant half-life are considered. There are other daughters not shown because they are so short-lived that they are not governed by 40 CFR 191. Table A.2 lists the half-lives and specific activities of all the isotopes considered in this analysis.

The source of the TRU waste falls into one of two categories, nuclear weapons accidents residue (NWAR) or material that has been contaminated as a result of manufacture or disassembly of nuclear weapons. In the first case, the waste consists of weapons parts that have been deformed and contaminated as a result of fires or non-nuclear explosions involving nuclear weapons. The second waste form consists of manufacturing paraphernalia, molds, tool bits, fasteners, etc., that have a small amount of radioactive material adhering to their surface as a result of contact with either plutonium or uranium. Prior to disposal, both types of waste were packaged in either plywood or particle board boxes or within 55 gallon steel drums. Chu and Bernard [1991] described the nature of the waste forms in greater detail. Note that both waste forms are the result of classified activities; as a result, they do not meet the waste acceptance criteria for eventual disposal at the Waste Isolation Pilot Plant. They, therefore, fall into the category of special-case TRU waste. Currently, GCD is one of the few disposal concepts that can accommodate this type of waste.

Table A.1 - Inventories of radionuclides in each borehole (Adapted from Price *et al.*, [1993]),‡ indicates a non-TRU waste.

Isotope	Curies / borehole						Total curies
	#1	#2	#3	#4	#6	GCDT	
^{234}U	0.62	1.05	0.285	0.0035	-	-	1.96
^{235}U	0.045	0.032	0.006	-	-	-	0.083
^{236}U	0.065	0.0016	0.00055	-	-	-	0.0672
^{238}U	0.200	0.0024	0.003	-	-	-	0.2054
^{238}Pu	3.53	1.625	3.29	5.34	-	-	13.79
^{239}Pu	85.47	3.945	79.75	129.35			298.5
^{240}Pu	19.67	0.91	18.35	29.76			68.69
^{241}Pu	162.43	7.50	151.6	245.8			567.33
^{242}Pu	0.0014	0.00006	0.0012	0.002			0.0047
^{241}Am	21.58	0.995	20.15	32.65			75.35
^{90}Sr‡					299.2	492,048	492,347
^{137}Cs‡		99.45			190.1	20,391	20,681
^{226}Ra‡						100	100
^{227}Ac‡						9.89	9.89
TOTAL	293.61	16.06	273.43	442.91	489.3	512,549	

Table A.2 - Half-lives and specific activities of all isotopes considered in this performance assessment analysis.

	Isotope	Half-Life (years)	Specific Activity (Curies/gm)
Chain 1	^{239}Pu	2.41×10^{4}	6.20×10^{-2}
	^{235}U	7.04×10^{8}	2.16×10^{-6}
	^{231}Pa	3.28×10^{4}	4.71×10^{-2}
	^{227}Ac	21.77	72.2
Chain 2	^{240}Pu	6.56×10^{3}	0.227
	^{236}U	2.342×10^{7}	6.46×10^{-5}
	^{232}Th	1.4×10^{10}	1.10×10^{-7}
Chain 3	^{241}Pu	14.4	103
	^{241}Am	432.7	3.42
	^{237}Np	2.14×10^{6}	7.04×10^{-4}
	^{233}U	1.592×10^{5}	9.62×10^{-3}
	^{229}Th	7.3×10^{3}	0.213
Chain 4	^{242}Pu	3.75×10^{5}	3.93×10^{-3}
	^{238}U	4.47×10^{9}	3.36×10^{-7}
	^{238}Pu	87.7	17.1
	^{234}U	2.46×10^{5}	6.20×10^{-3}
	^{230}Th	7.54×10^{4}	2.06×10^{-2}
	^{226}Ra	1.6×10^{3}	1.00
	^{210}Pb	22.3	76.2
Chain 5	^{90}Sr	29.1	136
Chain 6	^{137}Cs	30.17	86.4

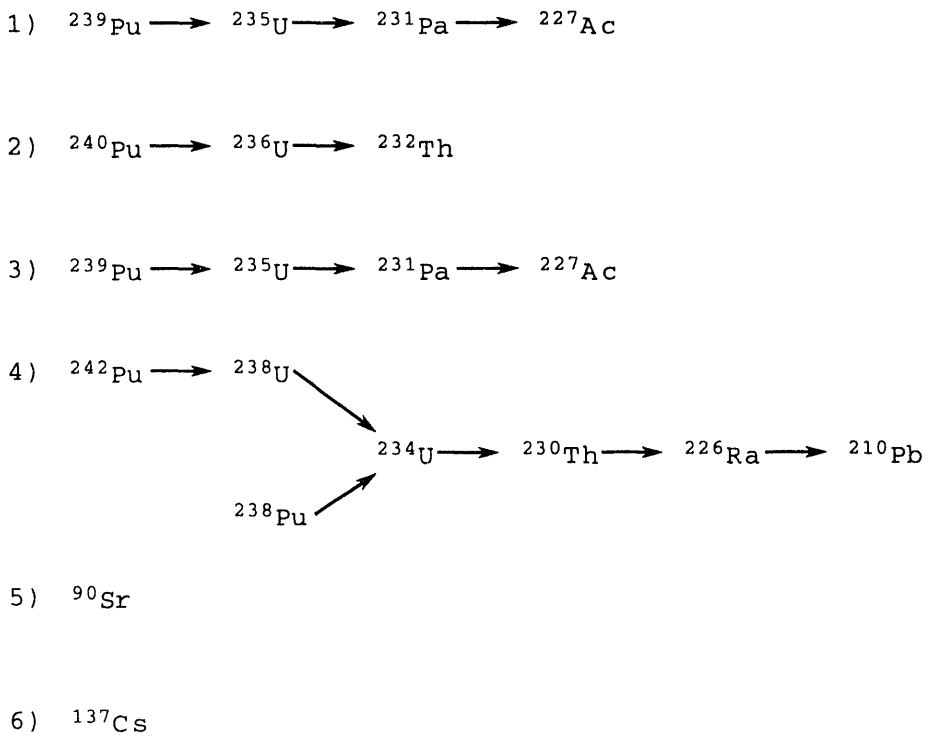

Figure A.1 - Isotopes and decay chains considered in analysis.

Appendix B - Statistical Analysis of Porosity Data from Exploratory Boreholes

Porosity does not appear as a parameter in the models used in this performance assessment iteration. However, later iterations may make use of this parameter, so the measurements from the exploratory boreholes were analyzed for porosity. Cores were sampled from exploratory boreholes 1, 2, 4, 5, 6, and 7. Porosity was determined by finding the volume of water needed to saturate each sample. The resulting porosity values, therefore, reflect the open space available to flow rather than the entire void space.

As in the case of the moisture content measurements, it is desirable to consider the possibility of spatial correlation between adjacent porosity values. The variogram of all porosity measurements is shown in Figure B.1. The variogram becomes more or less constant for lag depths greater than approximately 4.5 m. This is the correlation length.

Dealing with the influence of this correlation can be handled in several ways. One of the simplest is eliminating enough points from the data set so that the remaining points from each borehole are separated by at least the correlation length. For data from each borehole, a depth was chosen at random. Points above and below this depth that were nearer than 4.5m were removed. The two data points just beyond the correlation length were retained in the set. The next group of points removed were those at least 4.5m either above or below the two retained points. This procedure was repeated until the entire data set had been contracted. Table B.1 shows the mean and standard deviations of the full data set compared to the smaller sets,

Table B.1 - Comparing porosity distribution for different data subsets.

	Samples	Mean	standard dev.	Shapiro-Wilk
Full set	161	35.37%	3.53%	.2277
Small set #1	32	35.15%	3.43%	.5771
Small set #2	29	34.54%	3.53%	.7527

It should be quite clear that there is very little difference between the distribution parameters of the full set and of the smaller sets. The conclusion drawn from this is that effects of spatial correlation are apparently not significant. The final column shows the Shapiro-Wilk statistics. The values in the third column indicate that all sets of data are normal with the contracted data sets tending to even more normal character.

Based upon this, it was decided that a normal distribution describing the full set of porosity data should be used to represent the porosity variability. The parameters of this model are,

$$\bar{\varepsilon} = 35.37\% \ , \ s_{\varepsilon} = 3.53\%$$

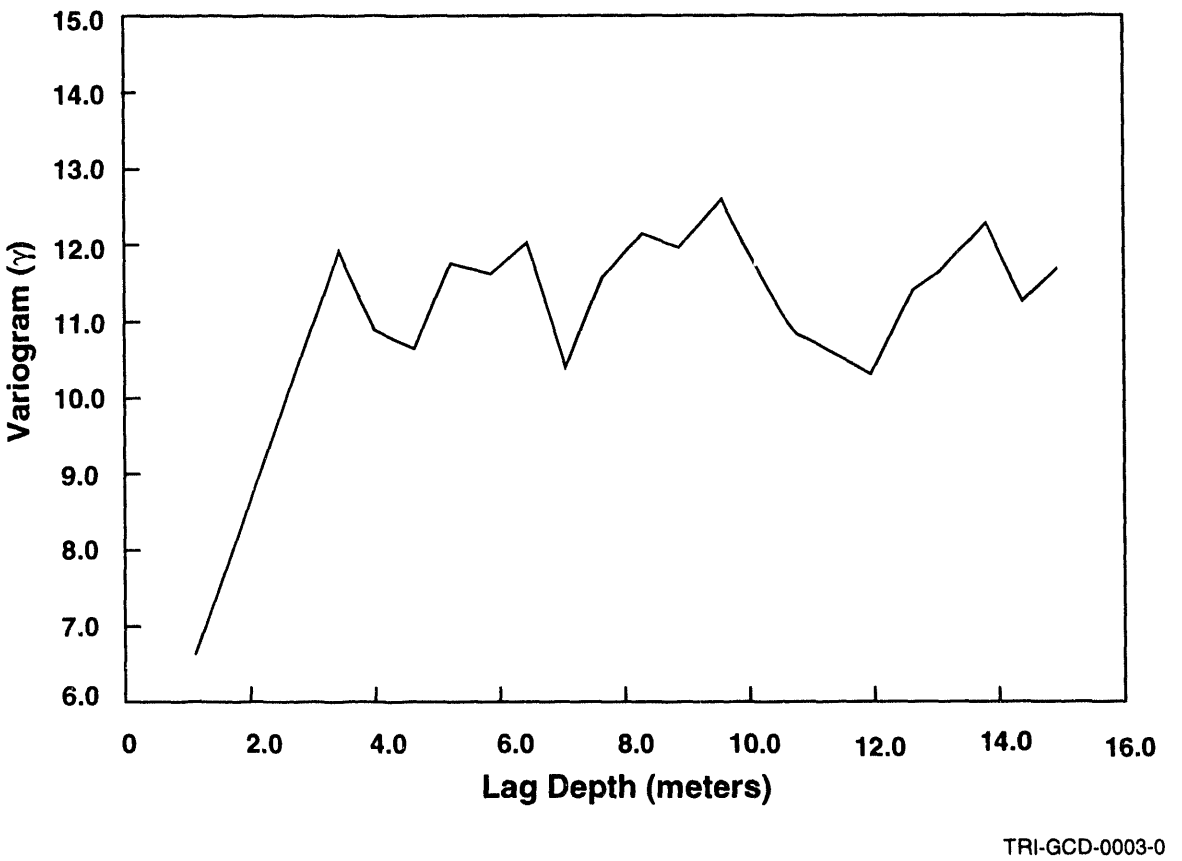

Figure B.1 - Semi-variogram of saturated porosity values

Appendix C - Parameter Distributions

When dealing with geologic systems of any sort, it is very common for considerable uncertainty to be associated with any particular parameter. It is commonplace to quantify this uncertainty in terms of a probability density function (pdf). It is often the case that these pdfs will take general forms, for example, uniform, normal, lognormal, and loguniform. The characteristics of these standard distributions can be expressed solely in terms of mean and standard deviation values or in terms of high and low quantile values. This appendix summarizes the types of distribution, mean, standard deviation, and 0.001 and 0.999 quantile values for each parameter used in the liquid diffusion models for both Containment and Individual Protection Requirements. Table C.1 lists the parameters that are not specific to any single radionuclide, e.g., tortuosity, moisture content, and erosion depth. Table C.2 lists the solubility distributions specific for each radionuclide element (that is, all plutonium isotopes have the same distribution, and all uranium isotopes have the same distribution). Table C.3 lists the sorption coefficient distributions, and Table C.4 lists the concentration ratio distributions.

Table C.1 - Distributions of general transport parameters used in liquid diffusion model.

Parameter	Distribution	Mean	Standard Dev.	0.001 quantile	0.999 quantile
Molecular Diffusivity (m^2/yr) [1]	Fixed	0.0315	N/A	N/A	N/A
Moisture Content	Lognormal	0.0949	0.0208	0.0475	0.181
Tortuosity	Uniform	56.50	30.9	3.0	110.0
Root Depth (m)	Loguniform	4.29	2.65	1.03	10.7
Biomass Density (kg/m^2)	Fixed	0.49	N/A	N/A	N/A
Biomass turnover fraction	Fixed	1.0	N/A	N/A	N/A
Erosion Depth (m)	Uniform	1.0	0.577	0.0	2.0

Table C.2 - Radionuclide solubility distribution parameters (g solute/g solvent)[2].

Radionuclide	Distribution	Mean	Standard Deviation	0.001 Quantile or Lower Bound	0.999 Quantile or Upper Bound
Sr90	Lognormal	2.073×10^{-6}	7.89×10^{-6}	9.0×10^{-9}	9.0×10^{-5}
Pu isotopes	Uniform	2.50×10^{-7}	1.31×10^{-7}	2.39×10^{-8}	9.51×10^{-7}
Pa231	Uniform	5.50	2.598	1.0	10.0
Ac227	Uniform	5.50	2.598	1.0	10.0
Th isotopes	Uniform	2.0×10^{-7}	5.77×10^{-8}	1.0×10^{-7}	3.0×10^{-7}
Np237	Uniform	2.0×10^{-4}	1.0×10^{-4}	2.0×10^{-5}	3.0×10^{-4}
Ra226	Uniform	2.75×10^{-8}	1.44×10^{-9}	2.5×10^{-8}	3.0×10^{-8}
Cs137	Uniform	5.50	2.598	1.0	10.0
U isotopes	Loguniform	8.69×10^{-8}	1.89×10^{-7}	1.0×10^{-11}	1.0×10^{-6}
Am241	Loguniform	8.03×10^{-8}	1.169×10^{-7}	1.0×10^{-9}	5.0×10^{-7}
Pb210	Loguniform	9.71×10^{-8}	1.224×10^{-7}	3.0×10^{-9}	5.0×10^{-7}

[1] See Price *et al.*, [1993] for the origins of this value

[2] Except for Pu isotopes, these distributions were taken from Price *et al.*, [1993]

Table C.3 - Sorption coefficient distribution parameters K_d $(ft^3/lb)^3$.

Radionuclide	Distribution	Mean	Standard Deviation	0.001 Quantile	0.999 Quantile
Pu isotopes	Lognormal	0.2508	1.8814	0.025	1.60
U isotopes	Lognormal	0.0032	0.0080	0.000016	0.092
Pa231	Lognormal	0.0029	0.0070	0.000016	0.08
Ac227	Lognormal	0.0029	0.0070	0.000016	0.08
Th isotopes	Lognormal	0.0029	0.0070	0.000016	0.08
Am241	Lognormal	0.0029	0.0070	0.000016	0.08
Np237	Lognormal	0.0029	0.0070	0.000016	0.08
Ra226	Lognormal	0.0029	0.0070	0.000016	0.08
Pb210	Lognormal	0.0029	0.0070	0.000016	0.08
Sr90	Lognormal	0.0029	0.2830	0.000016	2.656
Cs137	Lognormal	1.0222	25.5941	0.000016	104.0

Table C.4 - Concentration Ratio Distribution Parameters.

Radionuclide	Distribution	Mean	Standard Deviation	0.001 Quantile	0.999 Quantile
Pu isotopes	Lognormal	0.0028	0.0186	1.02×10^{-6}	0.1738
U isotopes	Lognormal	0.1472	0.3763	6.64×10^{-4}	4.3313
Am241	Lognormal	0.0180	0.1197	6.427×10^{-6}	1.116
Pa231	Lognormal	0.1472	0.3763	6.641×10^{-4}	4.331
Ac227	Lognormal	0.1472	0.3763	6.641×10^{-4}	4.331
Th isotopes	Lognormal	0.1472	0.3763	6.641×10^{-4}	4.331
Np237	Lognormal	0.1472	0.3763	6.641×10^{-4}	4.331
Ra226	Lognormal	0.1472	0.3763	6.641×10^{-4}	4.331
Pb210	Lognormal	0.1472	0.3763	6.641×10^{-4}	4.331
Sr90	Lognormal	0.188	0.152	0.01629	1.31
Cs137	Lognormal	0.188	0.152	0.01629	1.31

[3] Except for the Pu isotopes, the sorption coefficient values in this table were taken from Price *et al.*, [1993]

Appendix D - Analytic Test Case of Numerical Solution

As was discussed in Section 3.0, a numerical method was used to solve the equation set associated with the transport model. By and large, an analytic solution is preferable for reasons of speed and accuracy. However, an analytic solution could not be found for this case, represented by Eq. (2) of Section 3.1.1 where each species in a chain was retarded by a different amount. When this restriction is relaxed, however, it is possible to develop an analytic solution to the problem and use it to check the accuracy and correctness of the numerical solution. This appendix describes this analytic solution and compares it to the corresponding numerical results for verification of the latter solution.

The mathematical statement of this special case is similar to Eq. (2), presented in Section 3.1.1,

$$\frac{\partial C_i}{\partial t} = \frac{D}{\tau R_k}\frac{\partial^2 C_i}{\partial x^2} + \lambda_{i-1}C_{i-1} - \lambda_i C_i \quad ; \quad i=1,2...n \tag{D1}$$

where

$C_i(x,t)$ = the liquid phase concentration of the ith member of a n-membered chain [atom/m^3]
D = the molecular diffusion coefficient [m^2/s]
τ = the tortuosity [dimensionless]
λ_i = the radioactive decay constant of the ith species [s^{-1}]
R_k = the retardation factor of the kth chain [dimensionless]

The exception, of course, is that only one retardation coefficient is used for the kth chain. The procedure is to choose the smallest value for R_k from among the values sampled for all members of the chain. This leads to only one effective diffusion coefficient for each chain,

$$D_{eff,k} = \frac{D}{\tau R_k} \tag{D2}$$

The solution to Eq. (D1) can be expressed as the product of two parts, one accounting for diffusion and the other for radioactive decay,

$$C_i(x,t) = C_{D,k}(x,t)C_i^*(t) \tag{D3}$$

The diffusional portion, $C_{D,k}$, is the same for all members of the kth chain and satisfies a relation of the form,

$$\frac{\partial C_{D,k}}{\partial t} = D_{eff,k}\frac{\partial^2 C_{D,k}}{\partial x^2} \tag{D4}$$

with the initial and boundary conditions on the domain x = [0,L]

$$\begin{aligned} C_{D,k}(x,0) &= 0, \\ C_{D,k}(0,t) &= 1, \\ C_{D,k}(L,t) &= 0. \end{aligned} \tag{D5}$$

where the top of the waste is at x = 0, and the land surface is at x = L.

An analytic solution to Eq. (D4) satisfying the conditions, (D5), can be developed [Price *et al.*, 1993],

$$C_{D,k}(x,t) = \sum_{n=0}^{\infty} erfc\left(\frac{x+2nL}{\sqrt{4D_{eff,k}\,t}}\right) - \sum_{n=1}^{\infty} erfc\left(\frac{2nL-x}{\sqrt{4D_{eff,k}\,t}}\right) \qquad \text{(D6)}$$

Even for times as long as 10,000 years, the terms in these series decay rapidly to zero, and the summations converge quickly, often after only one or two terms.

The radioactive decay portion of Eq. (D3) satisfies a system of initial value problems of the form,

$$\frac{dC_i^*}{dt} = \lambda_{i-1}C_{i-1}^* - \lambda_i C_i^* \quad ; \quad i=1,2..n \quad ; \quad \lambda_0=0 \qquad \text{(D7)}$$

with the initial condition,

$$C_i^*(0)=C_{i,0} \quad ; \quad i=1,2..n \qquad \text{(D8)}$$

Note that since the diffusional solution goes to unity at x=0, the solution to Eqs. (D7) and (D8) constitute the source term model for this special case. For materials present in the initial inventory, $C_{i,o}$ is set to the solubility limit of that species. For radionuclides not present in the initial inventory, $C_{i,o}$ is set to zero. Thus, at the source, the concentrations of the first members of each chain will decay with time from their initial solubility limits. Daughters will decay and be produced, and their concentrations will fluctuate according to the nature of their and their parents' time constants. It should be understood that this model does not recognize the presence of undissolved species. If a species concentration falls below its solubility limit, no additional material will dissolve to maintain the concentration, even if, conceivably, there was undissolved material present. Similarly, if a species concentration rises above its solubility limit, the species will not precipitate in order to avoid this possibility. This is certainly an unrealistic aspect of this special-case model, but for the purposes to which we are applying it in this appendix, this aspect need not concern us greatly. It is mentioned here so that it is understood that this source term model is different than the one described in Section 3.1.1, where solubility limits and quantities of material in the source area are accounted for.

An analytic solution to Eqs. (D7) and (D8) can be found in Gelbard [1989]. It has the form,

$$C_i^*(t) = \sum_{j=1}^{i} \alpha_j b_i^{(j)} \exp(-\lambda_j t) \quad ; \quad i=1,2..n \qquad \text{(D9)}$$

The coefficients, α_i , and the eigenvectors, $b_j^{(i)}$, are as follows,

$$\alpha_i = \begin{cases} C_i^*(0) \ , \ i=1 \\ C_i^*(0) - \sum_{j=1}^{i-1} \alpha_j b_i^{(j)} \ , \ i=2,3...n \end{cases} \quad \text{(D10)}$$

and

$$b_i^{(j)} = \begin{cases} 0 \ , & i<j \\ 1 \ , & i=j \\ \prod_{k=j}^{i-1} \dfrac{\lambda_k}{\lambda_{k+1} - \lambda_j} & i>j \end{cases} \quad \text{(D11)}$$

Note that for i=1 (parent species), Eqs. (D10) and (D11) reduce to a standard radioactive decay law,

$$C_1^* = C_1^*(0)\exp(-\lambda_1 t) \quad \text{(D12)}$$

The release flux at the surface is obtained from Fick's law.

$$J_i = -\theta D_{eff,k} \frac{\partial C_i}{\partial x} \quad \text{(D13)}$$

Substituting Eq. (D6) yields the surface release flux,

$$J_i(L,t) = \frac{\theta D_{eff,k}}{\sqrt{\pi D_{eff,k}\, t}} \left[\sum_{n=0}^{\infty} \exp\left(\frac{-((2n+1)L)^2}{4 D_{eff,k}\, t} \right) + \sum_{n=1}^{\infty} \exp\left(\frac{-((2n-1)L)^2}{4 D_{eff,k}\, t} \right) \right] C_i^*(t) \quad \text{(D14)}$$

Computation of the release flux via the plant pathway uses the concentration obtained from Eq. (D6) at the rooting depth and the model developed in Section 3.1.2. This analytic model was implemented in a FORTRAN code called LIQDIF3E_QA. A copy of this code is included at the end of Appendix G.

In order to compare the numerical solution to this analytic result, certain modifications are necessary to the input file so that the numerical method solves the same problem as the analytic solution. First, the absorption coefficients (K_ds) of the species in a given chain must be set to the same value. We used the smallest K_d among the members of a chain. Second, the actual initial inventories were ignored. Instead, the inventories supplied to SWIFT II were obtained from the sampled solubility values of each isotope so that each species present in the initial inventory would dissolve at once in the pore water present in the repository block to its solubility limit. That is, the initial waste inventory divided by the pore water contained in the source volume (assuming that the source area can be treated identically to the native alluvium) would equal the sampled solubility value. This effectively mimics the nature of the source term in the analytic solution. Finally, the values of solubility that are actually supplied to SWIFT II are set to very high values to account for the fact that no accounting of solubility limits is taken within the analytic solution, except when setting the initial concentrations.

The test case used a sample size of 1,000 and the parameter distributions shown in Appendix C. For this test case, the total integrated discharges were based only upon the total

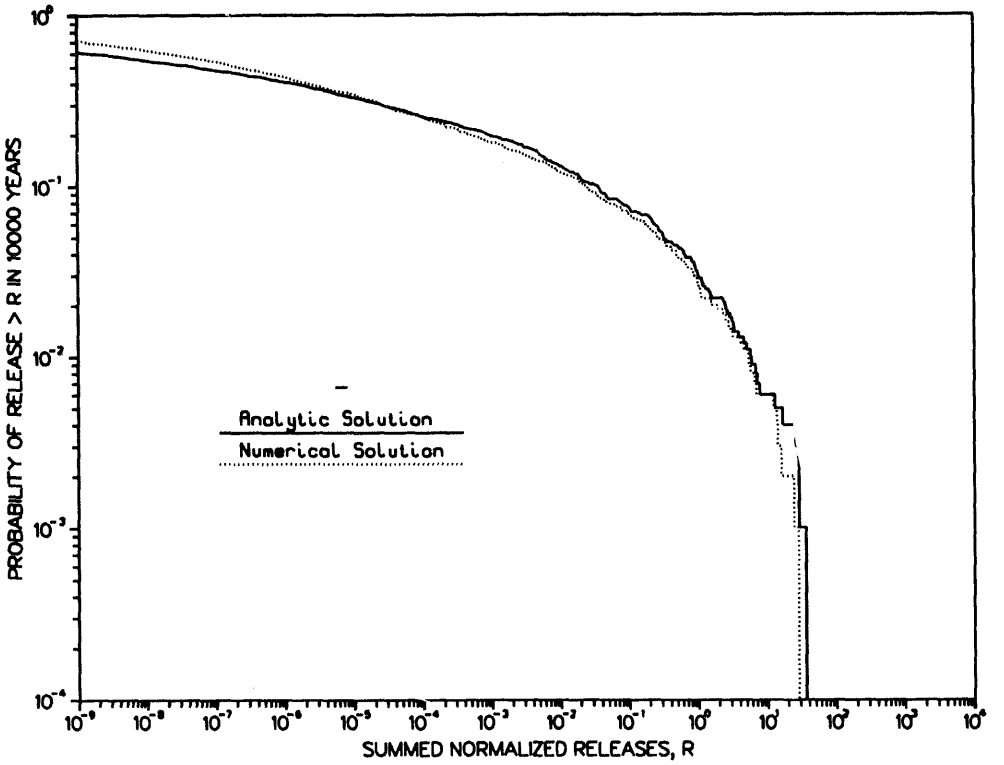

Figure D.1 - Comparison of numerical and analytic solutions.

borehole cross-sectional area instead of the manner described in Section 3.1.4. Figure D.1 compares the CCDF determined via the numerical method to that from the analytic solution. We note general agreement between analytic and numerical solution for the entire range of EPA sums shown. This agreement is sufficiently close that we can have confidence in the compliance conclusions conjectured for the cases considered by the numerical method in this performance assessment.

Figure D.1 also shows us that the codes for both the analytic solution and those associated with putting SWIFT II in a Monte Carlo context are likely correct. It is unlikely that two erroneous codes will produce exactly the same deviation; hence, agreement of the results of two entirely different codes strongly suggests that the original codes themselves are correct.

Appendix E - Shapiro-Wilk Test for Normality

Very often uncertainties in data can be represented by normal or lognormal distributions. Deciding if this is the case can be done by using frequency histograms or normality plots. The frequency histogram allows a visual examination of the shape of the data distribution, while the normality plot test results in a linear plot if the sample data are from a normal probability distribution. The difficulty with both of these methods is that they rely heavily on the subjective opinion of the viewer; what looks normal to one person does not look normal to another. It is therefore desirable to use a test for normality that possesses more quantitative objectivity. One option is the Shapiro-Wilk test statistic for normality described in Conover [1980] and implemented as part of the Statistical Analysis System (SAS) univariate analysis procedure.

From the data, the Shapiro-Wilk test computes a test statistic, W, whose value is between zero and one. We make the initial assumption that the data is derived from a normal population, in statistical parlance, the null hypothesis. The value computed for W tells us if this assumption is correct or not. Small values of W imply that the data were obtained from a non-normal distribution. Large values of W indicate that there is not sufficient evidence to conclude that the data were not obtained from a normal distribution. W itself, however, follows its own probability distribution. This distribution is skewed very substantially to the high end of the range between zero and one. The SAS procedure computes both the value of W and the probability of finding a value of W less than this value based upon the W distribution. Whether the value of W is to be considered "big" (normal) or "small" (non-normal) is based upon this computed probability. If this probability is less than some specified value of α (5% is a common choice), then it is possible to conclude that there is statistical evidence (to a 95% confidence level) that the distribution from which the data were taken is not normal, that is, we can reject the null hypothesis. However, if the probability determined is greater than α, we conclude that there is insufficient evidence to reject the assumption that the distribution is normal. We therefore assume that in this case the data follow a normal distribution. Note that the statistic is designed to indicate non-normally distributed data. We cannot tell from it how "normal" the data are, merely that no other type of distribution is a better fit to the data. If the frequency histograms indicate the sample data may be from a lognormal population, it is still possible to use the same procedures outlined above by simply taking the natural logarithm of the sample data and applying these tests to the log-transformed data.

To lend a better understanding of the Shapiro-Wilk statistic, three examples were developed. Fifty data points were randomly sampled from three probability distribution functions of a known type: normal, lognormal, and uniform. The Shapiro-Wilk test statistic was computed for each random sample set. Table E.1 gives the Shapiro-Wilk statistics, the associated probability, and our conclusion about the distribution from which the sample was drawn.

It should be clear that the test indicates which samples are from a non-normal distribution. The point should be made, however, that even for the sample that was drawn from a known normal distribution, the probability determined is not particularly large (34.8%). This fact should be borne in mind when considering the probability values determined for the statistics computed from the moisture content and concentration ratio distribution samples. Some of these are as low as 10%. However, as can be seen from the value computed for the standard normal distribution this does not necessarily mean a normal distribution is not the best fit to the sampled data. If it were indeed true that a distribution of another type was a better representation of this data, then we would expect that the probability computed by the SAS procedure would be on the order of those in the table for the lognormal and uniform distributions.

Table E.1 - Shapiro-Wilk statistic for three known distribution types.

Simulated Distribution	Shapiro-Wilk Statistic, W	Probability of less than W	Conclusion
Standard Normal	0.969	0.3480	Cannot reject the null hypothesis.
Log-Normal	0.703	0.0001	Reject the null hypothesis and conclude the data is not from a Normal population.
Uniform (0,1)	0.924	0.0035	Reject the null hypothesis and conclude the data is not from a Normal population.

Appendix F - Literature Sources of Concentration Ratio Information

STUDY	CR (Ci/ g plant/ Ci/ g soil)	ISOTOPE	PLANT TYPE	SOIL TYPE	SOIL PH	COMMENTS
(1) Romney *et. al.*, [1982]	mean= 4.60e-4 s.d. = 1.06e-4 (mean of 16 means)	Pu-239, Pu-240	Alfalfa (from 1976 and 1978 study, 8 soil samples each)	NTS fallout areas	None reported	Possible contamination
	mean= 3.44e-4 s.d. = 1.66e-4 (mean of 16 means)	Am-241				Without DTPA
	mean= 2.95e-4 s.d. = 0.79e-4 (mean of 8 means)	Pu-239, PuU-240	Wheat Straw (8 soil samples, wheat grains excluded)			
	mean= 7.75e-3 s.d. = 7.42e-3 (mean of 8 means)	Am-241				
	mean=1.67e-3 s.d. = 2.82e-3 (mean of 6 means)	Pu-239, Pu-240	Bushbean Leaves and Stems (4 soil samples for leaves, 2 for stems, fruit excluded)			

STUDY	CR (Ci/g plant/-Ci/g soil)	ISOTOPE	PLANT TYPE	SOIL TYPE	SOIL PH	COMMENTS
(1) Romney *et. al.*, [1982]	mean= 3.94e-2 s.d. = 6.58e-2 (mean of 6 means)	Am-241	Bushbean leaves and stems (4 soil samples leaves, 2 for stems, fruit excluded)	NTS fallout areas	None reported	Possible resuspension contamination Without DTPA
	mean= 2.73e-3 s.d. = 1.48e-3 (mean of 4 means)	Pu-239, Pu-240	Carrot tops (4 soil samples, peel and core excluded)			
	mean= 1.55e-2 s.d. = 3.38e-3 (mean of 4 means)	Am-241				
(2) Price, [1972]	mean= 1.12e-1 s.d. = 2.0e-2 (mean of 5 exp.)	Np-237	Tumbleweed (Salsola kali)	Hanford soil	No pH reported	Nitrate solution used to complex species
	mean= 4.6e-5 s.d. = 0.7e-5 (mean of 5 exp.)	Pu-239				

STUDY	CR (Ci/g plant/-Ci/g soil)	ISOTOPE	PLANT TYPE	SOIL TYPE	SOIL PH	COMMENTS
(2) Price, [1972]	mean= 1.12e-1 s.d. = 2.0e-2	Np-237	Tumbleweed (Salsola kali)	Hanford soil	No pH reported	Nitrate solution used to complex species Mean of 5 experiments
	mean=4.6e-5 s.d. = 0.7e-5	Pu-239				
	mean=1.4e-3 s.d. = 0.16e-3	Am-241				
	mean= 1.26e-2 s.d. = 0.5e-3	Np-237	Cheat Grass (Bromus tectorum)			
	mean= 1.7e-5 s.d. = 0.2e-5	Pu-239				
	mean=6.0e-4 s.d. = 1.0e-4	Am-241				
(3) Cline, [1968]	3.0e-3	Am-241	Barley	Cinebar	4.5	Nitrate complex spike
	2.0e-4	Pu-239				
	2.0e-3	Am-241	Barley	Ephrata	7.5	
	1.0e-4	Pu-239				

STUDY	CR(Ci/g plant/Ci/g soil)	ISOTOPE	PLANT TYPE	SOIL TYPE	SOIL PH	COMMENTS
(4) Schulz, [1977]	10e-5 - 10e-4	Plutonium	Ladino clover	NTS soil	Not reported	From Romney, *et.al.* [1976]
	10e-5 - 10e-4		Alfalfa			
	10e-5 - 10e-3		Barley Straw			
	10e-4 - 10e-3		Soybean forage			
	10e-5 - 10e-3	Americium	Barley Straw			
	10e-5	Plutonium	Barley leaves			From Schulz [1976]
	10e-5 - 10e-3		Barley leaves and stems	Unknown		From Wildung, *et al.*, [1974]
	10e-6 - 10e-3	Americium	Wheat leaves	NTS soil		From Schulz [1976]
	10e-4 - 10e-3		Alfalfa			
	10e-4		Barley leaves			

STUDY	CR (Ci/g plant/Ci/g soil)	ISOTOPE	PLANT TYPE	SOIL TYPE	SOIL PH	COMMENTS
(4) Schulz, [1977]	10e-2	Americium	Corn	Unknown	6	From Wallace [1974]
	10e-1				8.5	
	10e-1		Barley		7.5	
	10e-1				6	
	10e-1		Bushbean		7	
	10e-1			Sand texture	Not reported	
	10e-1			Clay texture		
	10e-1		Corn	Sand texture		
	10e-1			Clay texture		

STUDY	CR (Ci/g-plant/-Ci/g-soil)	ISOTOPE	PLANT TYPE	SOIL TYPE	SOIL PH	COMMENTS
(5) Dahlman and McLeod, [1977]	6e-5	Plutonium	Native tree	Vicinitiy of Oak Ridge National Laboratory	No pH reported	-
	2e-4		Native shrub			
	2e-3		Native herbaceous plant			
	2e-3		Bushbean foliage			
	2e-3		Soybean foliage			
	5e-3		Tomato foliage			
(6) Romney and Wallace, [1977]	mean= 3.85e-4 s.d. = 4.78e-4	Pu-239, Pu-240	Soybean foliage	4 NTS soil samples	Not reported	Greenhouse measurements (field measurements contaminated by fallout)
	mean= 5e-4 s.d. = 2e-4			4 Tonopah Test Range soil samples		

STUDY	CR (Ci/g-plant/Ci/g-soil)	ISOTOPE	PLANT TYPE	SOIL TYPE	SOIL PH	COMMENTS
7) Kinnear *et. al.*, [1981]	mean= 5.6e-3 s.d. = 3.4e-3	Am-241	Bushbean 3rd and 4th trifoilate leaves	Yolo loam soil	No pH reported	1. Conservative to take 3rd and 4th trifoilate leaves
8) Romney *et. al.*, [1981a]	mean=1.17e-1 s.d. = 1.6e-1	Np-237	Soybean leaves	7 agricultural soil samples	5.3 - 7.8	
	mean=3.14e-4 s.d. = 2.8e-4	Pu-239, Pu-240				
	mean=5.84e-3 s.d. = 6.7e-3	Am-241				
	mean=1.8e-2 s.d. = 2.3e-2	Np-237	Soybean stems			
	mean=9.4e-5 s.d. = 1.0e-4	Pu-239, Pu-240				
	mean= 1.25e-3 s.d. = 1.6e-3	Am-241				
	mean= 3.16e-1 s.d. = 2.2e-1	Np-237	Pea leaves			

STUDY	CR (Ci/g-plant/-Ci/g-soil)	ISOTOPE	PLANT TYPE	SOIL TYPE	SOIL PH	COMMENTS
(8) Romney *et. al.*, [1981a]	mean=6.21e-4 s.d. = 4.3e-4	Pu-239, Pu-240	Pea leaves	7 agricultural soil samples	5.3 - 7.8	
	mean=2.61e-2 s.d. = 3.9e-2	Am-241				
	mean=1.65e-1 s.d. = 3.1e-1	Np-237	Pea stems			
	mean=2.64e-4 s.d. = 3.3e-4	Pu-239, Pu-240				
	mean= 1.94e-3 s.d. = 2.7e-3	Am-241				
	mean= 2.06e-2 s.d. = 1.5e-2	Np-237	Wheat straw			
	mean=5.82e-5 s.d. = 8.1e-5	Pu-239, Pu-240				
	mean=2.74e-4 s.d. = 2.74e-4	Am-241				
	mean=8.85e-2 s.d. = 8e-2	Np-237	Tomato leaves			
	mean=1.4e-4 s.d. = 1.4e-4	Pu-239, Pu-240				

STUDY	CR (Ci/g-plant/-Ci/g-soil)	ISOTOPE	PLANT TYPE	SOIL TYPE	SOIL PH	COMMENTS
(8) Romney *et. al.*, [1981a]	mean=1.60e-3 s.d. = 1.3e-3	Am-241	Tomato leaves	7 agricultural soil samples	5.3 - 7.8	
	mean=9.90e-3 s.d. = 6.7e-3	Np-237	Tomato stems			
	mean=3.51e-5 s.d. = 2.4e-5	Pu-239, Pu-240				
	mean= 3.82e-4 s.d. = 3.3e-4	Am-241				
(9) Nishita, [1981]	mean=2.1e-5 s.d. = 4.90e-6	Pu-238	Wheat leaves	Three loamy soil samples (clay, sandy, silt)	5.3 - 7.8	Demonstrated that uptake was the same for each PU isotope Mean of 3 means
	mean=2.0e-5 s.d. = 5.0e-6	Pu-239				
10) Nishita *et. al.*, [1981]	mean=1.70e-2 s.d.=1.45e-2	Np-237	Wheat leaves and stems	7 loamy soil samples	5 - 7.2	
	mean=7.21e-5 s.d. = 6.32e-5	Pu-239, Pu-240				
	mean=6.06e-4 s.d. = 7.43e-4	Am-241				

STUDY	CR(Ci/g-plant/-Ci/g-soil)	ISOTOPE	PLANT TYPE	SOIL TYPE	SOIL PH	COMMENTS
(11) Adriano, *et. al.*, [1981]	mean = 3.3e-4	Pu-238	4 rice varieties	Savannah River, GA floodplain soil sample	5.2	Rice foliage
	mean = 1.5e-2	Pu-239, Pu-240				
(12) McLeod, *et. al.*, [1981]	mean = 5.5e-2 s.d. = 3.5e-2	Pu-238	Soybean stems and leaves	3 Savannah River, GA soil samples (floodplain and fields)	4.9 - 6.4	Increased pH by adding lime which suppresses metal uptake
	mean = 5.0e-3 s.d. = 2.3e-3		Wheat stems and leaves			Mean of 3 means
	mean= 9.47e-3 s.d. = 1.5e-2		Corn stalks and leaves			Mean of 6 means (3 soils, 2 corn parts)
	mean= 3.39e-2 s.d. = 1.18e-2	Pu-239, Pu-240	Soybean stems and leaves			Mean of 3 means
	mean= 7.87e-3 s.d. = 3.51e-3		Wheat stems and leaves			
	mean= 7.9e-3 s.d. = 6.5e-3		Corn stalks and leaves			Mean of 6 means

STUDY	CR (Ci/g-plant/-Ci/g-soil)	ISOTOPE	PLANT TYPE	SOIL TYPE	SOIL PH	COMMENTS
(13) Romney, *et. al.*, [1981b]	7.56e-1	Np-237	Bushbean primary leaves	Yolo loam soil	6	
	1.90e-1			Hacienda loam soil	7.5	
	1.08e-1		Barley leaves	Yolo loam soil	6	
	2.2e-2			Hacienda loam soil	7.5	
	1.6e-1		Rice	Yolo loam soil	6	
	2.2e-2			Hacienda loam soil	7.5	
(14) Wallace *et. al*, [1981]	mean = 2.9e-2 s.d. = 4.0e-3	Am-241	Bushbeans stems and leaves	Yolo loam soil	6	Report for varying soil concentrations, used largest Report for leaves and stems, used largest

STUDY	CR (Ci/g-plant/Ci-/g-soil)	ISOTOPE	PLANT TYPE	SOIL TYPE	SOIL PH	COMMENTS
(15) Schulz and Ruggieri, [1981]	4.4e-3	Np-237	Wheat (lower half of stem)	Yolo silt loam soil	6.7	Used largest reported values
	7.2e-5	Pu-238				
	7.5e-5	Pu-239/Pu-240				
	4.2e-5	Am-241				
(16) Adrianno, *et. al.*, [1980]	mean = 8.6e-2 s.d. = 1.4e-2	Am-241	Bahia grass	Dothean soil	4.2	Mean of 3 means from 5 replicates
	mean = 4.8e-2 s.d. = 8.0e-3			Troup soil	5.0	Southeastern agricultural soil
	1.9e-4	Pu-239/Pu-240	Barley	NTS Area 13 soil	approximately 8	
	4.8e-4	Am-241				
	3.8e-5	Pu-239/Pu-240	Alfalfa			
	4.8e-4	Am-241				
	mean = 4.4e-4 s.d. = 3.4e-4	Pu-239, Pu-240	Soybean leaves and stems			mean of 8 means, s.d. of 8 means (no s.d. information reported)

STUDY	CR(Ci/g-plant-/Ci/g-soil)	ISOTOPE	PLANT TYPE	SOIL TYPE	SOIL PH	COMMENTS
(16) Adrianno, *et. al.*, [1980]	mean = 9.3e-3 s.d. = 8.5e-3	Am-241	Soybean leaves and stems	NTS soil samples	approx. 8	Mean of 8 means, s.d. of means
(17) Wallace and Romney,[1972b]	range = 0.4 0.048	Sr-90	Desert vegetation	Frenchmen Flat soil	Not reported	
(18) Rediske, J.H., *et. al.*, [1955]	9.0e-4	Pu-239	Barley	Ephrata Loamy Sand	7.3	
	mean = 2.05 s.d. = 1.13	Sr-90		9 soil samples	7.3 - 8.2	average of 9
	mean = 7.1e-2 s.d. = 3e-2	Cs-137		3 soil samples	7.3 - 7.7	average of 3
(19) Bernhardt and Eadie, [1976]	mean = 6.3e-5 s.d. = 4.7e-5	Pu-239	Ladino Clover	NTS soil	Not reported	from Romney *et. al.*, [1970], mean of 5 values
	mean = 6.4e-4	Plutonium	Barley	Not reported		Johnson *et. al.*, [1972]
	2.0e-5					Jacobson and Overstreet, [1948]

STUDY	CR (Ci/g-plant-/Ci/g-soil)	ISOTOPE	PLANT TYPE	SOIL TYPE	SOIL PH	COMMENTS
(20) Wallace and Romney, [1972b]	leaf: 9.88e-02 stem: 9.05e-02	Sr-90	Artemisia tridentata	Grown on west Frenchman Flat soil samples	Not Reported	All species native to desert areas. Growing time between 60 and 300 days. Soil and plant activity reported as dis/g/s. CR values inferred from these.
	leaf: 0.155 stem:0.146		Astragalus lentignosus			
	leaf: 0.4 stem: 0.196		Atriplex canescens			
	leaf: 0.387 stem:0.428		Atriplex confertifolia			
	leaf: 0.143 stem: 0.322		Atriplex hymenelytra			
	leaf:0.112 stem:0.0692		Ariplex polycarpa			
	leaf: 0.0592 stem: 0.0483		Chrysothmanus nauseosus			
	top: .220		Descurainia pinnata			
	leaf: 0.193 stem: 0.0506		Eurotia lanata			

STUDY	UPTAKE FACTOR (Ci/g-plant/-Ci/g-soil)	ISOTOPE	PLANT TYPE	SOIL TYPE	SOIL PH	COMMENTS
20) Wallace and Romney, 1972b	leaf: 0.311 stem: 0.220	SR-90	Franseria dumosa	Grown on west Frenchman Flat soil samples	Not Reported	
	leaf: 0.0853 stem: 0.0820		Larrea divaricata			
	leaf: 0.393 stem: 0.110		Lycium andersonii			
	top: 0.0484		Orysopsis hymenoides			
	top: 0.228		Yucca schidigera			

From the preceding studies, values of concentration ratio were extracted as follows. Numbers in parenthesis indicate which study in the preceding list the value was obtained.

^{239,240}Pu uptake factors :

All Conditions		Grown on NTS-Like Soil		Desert Plants	
4.6e-4	(1)	4.6e-4	(1)	4.6e-5	(2)
2.95e-4	(1)	2.95e-4	(1)	1.7e-5	(2)
1.67e-3	(1)	1.67e-3	(1)		
2.73e-10	(1)	2.7e-10	(1)		
4.6e-5	(2)	3.85e-4	(6)		
2.0e-4	(3)	5.0e-4	(6)		
1.0e-4	(3)	1.9e-4	(16)		
6.0e-5	(5)	3.8e-5	(16)		
2.0e-4	(5)	4.4e-4	(16)		
2.0e-3	(5)	6.3e-5	(19)		
2.0e-3	(5)				
2.0e-3	(5)				
5.0e-3	(5)				
3.8e-4	(6)				
5.0e-4	(6)				
3.14e-4	(8)				
9.4e-5	(8)				
6.21e-4	(8)				
2.64e-4	(8)				
5.82e-5	(8)				
1.4e-4	(8)				
3.51e-5	(8)				
2.1e-5	(9)				
2.0e-5	(9)				
7.21e-5	(10)				
3.3e-4	(11)				
1.5e-2	(11)				
5.0e-3	(12)				
9.47e-3	(12)				
3.39e-2	(12)				
7.78e-3	(12)				
7.9e-3	(12)				
7.2e-5	(15)				
7.5e-5	(15)				
1.9e-4	(16)				
3.8e-5	(16)				
4.4e-4	(16)				
9.0e-4	(18)				
6.3e-5	(19)				
6.4e-4	(19)				

^{241}Am uptake factors:

All Conditions		Grown on NTS-like Soil		Desert Plants	
3.44e-4	(1)	3.44e-4	(1)	1.44e-3	(2)
7.75e-3	(1)	7.75e-3	(1)	6.0e-4	(2)
3.94e-2	(1)	3.94e-2	(1)		
1.55e-2	(1)	1.55e-2	(1)		
1.4e-3	(2)	4.8e-4	(16)		
6.0e-4	(2)	4.8e-4	(16)		
3.0e-3	(3)	9.3e-3	(16)		
2.0e-3	(3)				
5.6e-3	(7)				
5.84e-3	(8)				
1.25e-3	(8)				
2.61e-2	(8)				
1.94e-3	(8)				
2.74e-4	(8)				
1.6e-3	(8)				
3.82e-4	(8)				
6.06e-4	(10)				
2.9e-2	(14)				
4.2e-5	(15)				
8.6e-2	(16)				
4.8e-2	(16)				
4.8e-4	(16)				
4.8e-4	(16)				
9.3e-3	(16)				

^{237}Np uptake factors:

All Conditions		Grown on NTS - Like Soil	Desert Plants
1.12e-1	(2)		1.12e-2(2)
1.26e-2	(2)		1.26e-2(2)
1.17e-1	(8)		
1.8e-2	(8)		
3.16e-1	(8)		
1.65e-1	(8)		
2.06e-2	(8)		
8.85e-2	(8)		
9.9e-3	(8)		
1.7e-2	(10)		
7.56e-1	(13)		
1.90e-1	(13)		
1.08e-1	(13)		
2.2e-2	(13)		
1.6e-1	(13)		

2.2e-2 (13)
4.4e-3 (13)

^{90}Sr uptake factors:

All Conditions		Grown on NTS - Like Soil		Desert Plants	
0.0988	(20)	0.0988	(20)	0.0988	(20)
0.0905	(20)	0.0905	(20)	0.0905	(20)
0.155	(20)	0.155	(20)	0.155	(20)
0.146	(20)	0.146	(20)	0.146	(20)
0.400	(20)	0.400	(20)	0.400	(20)
0.196	(20)	0.196	(20)	0.196	(20)
0.387	(20)	0.387	(20)	0.387	(20)
0.428	(20)	0.428	(20)	0.428	(20)
0.143	(20)	0.143	(20)	0.143	(20)
0.322	(20)	0.322	(20)	0.322	(20)
0.112	(20)	0.112	(20)	0.112	(20)
0.0692	(20)	0.0692	(20)	0.0692	(20)
0.0592	(20)	0.0592	(20)	0.0592	(20)
0.0483	(20)	0.0483	(20)	0.0483	(20)
0.2200	(20)	0.2200	(20)	0.2200	(20)
0.1930	(20)	0.1930	(20)	0.1930	(20)
0.0506	(20)	0.0506	(20)	0.0506	(20)
0.3110	(20)	0.3110	(20)	0.3110	(20)
0.2200	(20)	0.2200	(20)	0.2200	(20)
0.0853	(20)	0.0853	(20)	0.0853	(20)
0.0820	(20)	0.0820	(20)	0.0820	(20)
0.3930	(20)	0.3930	(20)	0.3930	(20)
0.1100	(20)	0.1100	(20)	0.1100	(20)
0.0484	(20)	0.0484	(20)	0.0484	(20)
0.2280	(20)	0.2280	(20)	0.2280	(20)

Appendix G - Implementation and Description of Computer Codes

The modeling and uncertainty analyses presented in this work were all generated by computer. This appendix describes the operational procedure for running the computer codes, data file input, and the codes themselves. First, we shall describe the overall code sequence used in performing the uncertainty analysis that includes a brief description of the codes themselves. After that, we shall discuss how this procedure is modified to perform the analyses for the Individual Protection Requirements. Finally, a compilation of data input files and FORTRAN codes developed for this performance assessment will be given.

Computational Procedure for Uncertainty Analysis

Table G.1 lists the codes used in the analysis along with their corresponding input and output files. The arrows in the Output file column indicate that the file name is changed to that shown (*tid2.dat* is appended to *intdis2.dat*). Note that the sequence WRSWIFT, SWIFT, and TID2 is repeated for as many realizations as there are, as indicated by the flowchart in Figure G.1. We now discuss the individual codes shown in the table.

Latin Hypercube Sampling

As noted in the text, the uncertainty in the input model parameters was accounted for by a Monte Carlo uncertainty analysis. The purpose of the LHS code is to generate samples of the input parameter probability distributions and combine them into a set of N parameter realizations. It does this using a technique called Latin Hypercube Sampling (LHS). Essentially, this is a stratified sampling procedure to ensure that even coverage of the entire range of uncertainty is obtained while sampling. This is in contrast to random sampling which in theory could potentially result in samples taken from only a specific region in the range. This technique is described in much greater detail in [Iman and Shortencarrier, 1984]

LHS requires only one input file, *lhs.inp*. This file contains the type and range of each probability distribution assigned to each parameter. It also specifies the magnitude of any correlation that is desired between parameters (the default is no correlation). An example of an *lhs.inp* file is included at the end of this appendix. The file lhs.inp must be read from standard input.

LHS writes the file containing the parameter vectors in a file called *fort.1*. It contains N parameter vectors that are combinations of the samples taken from the input parameter distributions in *lhs.inp*. The name of this file is changed to *nefii.smp* for the next step in the procedure.

Multiple Realizations

Unlike NEFTRAN II, SWIFT II is not intrinsically enabled to performed uncertainty analysis. To be more specific, it cannot consider a set of multiple realizations from one command line input. It becomes necessary therefore to develop pre- and post- processing programs that will enable SWIFT II to be used in a Monte Carlo context.

Table G.1 - Sequence and description of code operation.

	Code Name	Description	Input Files	Output files
1	LHS	Sample parameter distributions and create realization vectors	lhs.inp	fort.1 -> nefii.smp
2	WRSWIFT	Read nefii.smp and write input files for SWIFT and TID2	swift.inp zot.dat nefii.smp	SWIFTINP tid.inp wrswift.out
3	SWIFT II	Solve diffusion problem to surface	SWIFTINP	SWIFTNMD
4	TID2	Reduce concentration history in SWIFTNMD to total integrated discharge	SWIFTNMD tid.inp	tid2.dat->> intdis2.dat tid2.out
5	COMBINEII	Filter intdis2.dat in a form readable by CCDFTRUIIFI	nefii.dis intdis2.dat	cumrel.dat -> fort.11
6	CCDFTRUIIFI	Calculate the CCDF from the total integrated discharge in fort.11	fort.11 Gcdinv.dat ccdftruin.dat eparlslim.dat	ccdftrxypts.dat epasumtru.dat ccdftrout.dat

WRSWIFT

The pre-processor is called WRSWIFT, and its function is to read a specific parameter realization from *nefii.smp* and translate the parameter information into an input file that is readable by SWIFT. It reads the realization number from the file *zot.dat*. It then reads a "boilerplate" SWIFT input file called *swift.inp* which it then rewrites into a file called *SWIFTINP* that is almost identical to *swift.inp* but with the parameters of the current realization inserted in the appropriate places. To save on speed and complexity, lines in *swift.inp* that do not need to be changed are read wholesale as 80 column character strings and written to *SWIFTINP* in the same format. This technique has advantages in terms of simplicity but also means WRSWIFT is very problem specific. For instance, the original version of WRSWIFT is specific to the case that ignores the non transuranic (TRU) waste. A different version of the code called WRSWIFT56 had to be developed when the two additional strontium and cesium decay chains were included in the case that did include non-TRU waste. Due to space considerations, only WRSWIFT is included at the end of this appendix. WRSWIFT also writes an additional file called *tid.inp* that transmits the parameters of the current realization to the post-processor, TID2.

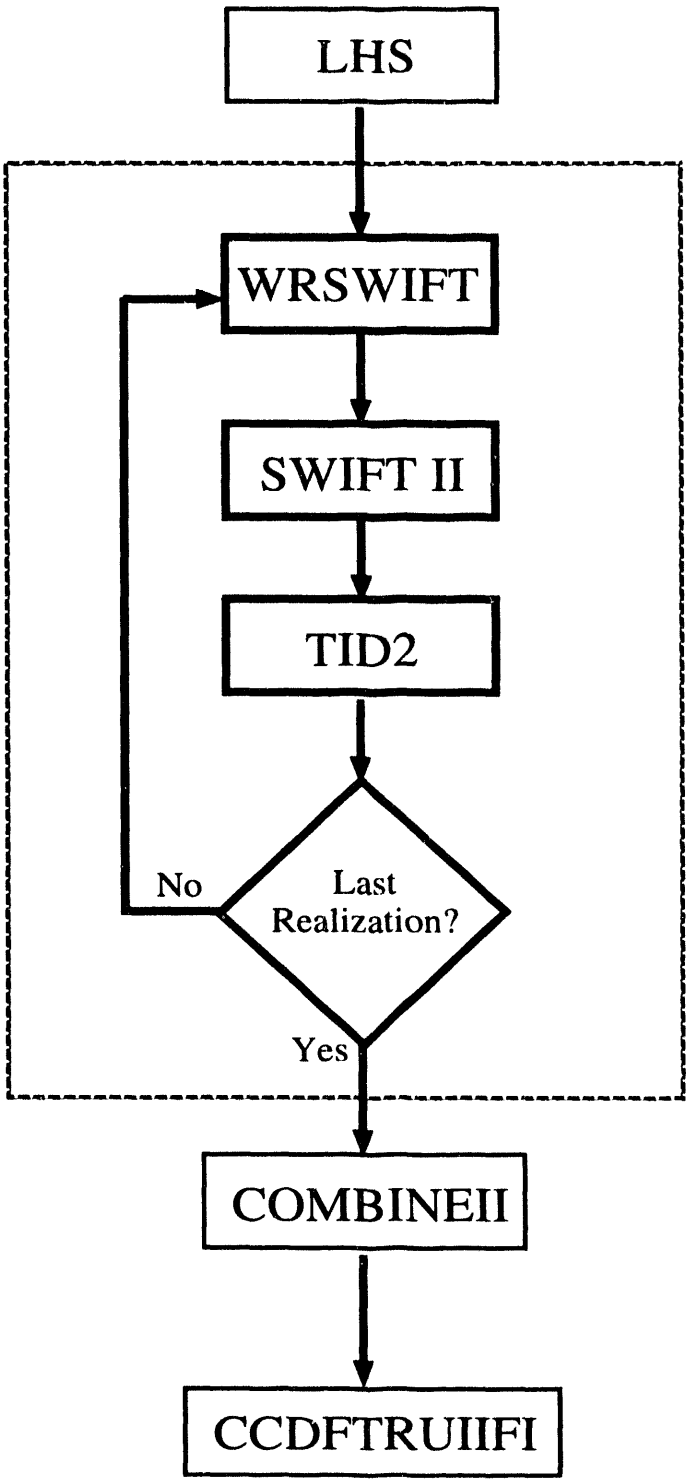

Figure G.1 - Flowchart showing sequence of code operation. Dashed box indicates that those codes are executed once for every realization.

SWIFT II

The actual transport calculations are done using a preexisting code called SWIFT II. This code's primary purpose is compútation of groundwater flow and associated transport. However, it is possible to allow the code to calculate diffusive transport alone by simply specifying a zero gradient in hydraulic head along with very small values of conductivity. We also makes use of the repository subprogram to simulate the source term. This requires determination of the volume of the source area and its inclusion in the input file. This volume is just the lower 15 meters of all the boreholes considered (four for TRU waste only, six if non-TRU waste is included). The repository subprogram also requires the waste density in lb/ft^3 and the solubility limits of each isotope. The former parameter is computed assuming uniform distribution of the mass of each isotope throughout the volume. The latter value is supplied as a mass fraction. We, in fact, use the samples from the solubility distributions directly since these are in units of grams isotope per gram solvent. Two examples of input files for SWIFT are included at the end of this appendix. The first considers only decay of the TRU waste; the second includes the strontium and ceisum decay chains.

The output of SWIFT that is of concern to us is in the file *SWIFTNMD*. This file contains the computed concentration history of all isotopes at three points with the transport domain: the repository block, at the rooting depth, and in the block adjacent to the surface block. These concentrations are in units of mass fraction and are written in the preceding order at each time point. Note the time points are not uniform. In order to promote efficient solution, the time step was allowed to vary from small values at early times when short-lived species, such as ^{241}Pu are present, to larger values at long times when the only remaining isotopes are those with half-lives on the order of millenia.

TID2

TID2 is the post-processing portion of the code procedure. Its function is to read the concentration histories in *SWIFTNMD* and compute a value of total integrated discharge for each isotope. The surface flux is computed from the concentration in the block adjacent to the surface by use of a backward difference as described Section 3.1.1. The plant flux is directly related to the concentration at the rooting depth. The time integration is done using a trapezoidal numerical integration algorithm since the temporal spacing of the data is not uniform. The program reads the file *tid.inp* for essential parameters such as diffusivities, plant uptake factors, moisture contents, etc. The total integrated discharges of each radionuclide are written to a file called *tid2.dat*. TID2 is included at the end of this appendix

The UNIX shell script

As noted above, the three codes must be run successively for each realization. A UNIX shell script was written to perform this task. The entire script, referred to as *monte2*, is as follows:

```
#!/usr/bin/sh
#
START=zotstart
```

```
SWIFT=SWIFTINP
#
# set the number chains and the realization number at which to cease
#
NCHN=4
NSIM=$2
#
#  ISIM + 1 is the current
#   realization number
#
ISIM=`expr $1 - 1`
#
date >> runtime
#
#  Set up a do while loop to proceed
#   over all the realizations
#
while [ "$ISIM" -lt "$NSIM" ]
do
ISIM=`expr $ISIM + 1`
#
#  The next set of commands writes  a set of sed
#   commands to the file sed.inp
#
cat > sed.inp << stop
1c\\
  $ISIM    $NCHN
stop
#
#  This sed command reads sed.inp and puts the output into
#  zot.dat.  The effect is to change the realization number
#  in zot.dat.  This is the most important aspect of this script
#
sed -f sed.inp  $START > zot.dat
#rm sed.inp
#
#  The codes are run in order
#
/m/tab/swift/run/wrswift/wrswift > /dev/null

/m/tab/swift/swift > /dev/null

/m/tab/swift/run/tid/TID2

#  The output from TID2 is appended to intdis2.dat.  And the
#   realization number is recorded in runtime
#
cat tid2.dat >> intdis2.dat
cat zot.dat >> runtime
#
done
rm SWIFTDAT SWIFTGRS SWIFTINP SWIFTOUT SWIFTVEL SWIFTWEL tid.dat tid.inp tid.out

date >> runtime
```

The command line command to perform the analysis between realization n and realization m, inclusive, is

> monte2 n m

This script successively increments a realization counter (ISIM) and uses the sed UNIX utility to write this realization number into the file *zot.dat*. Recall that WRSWIFT reads the current realization number from this file. The script then runs WRSWIFT, SWIFT II, and TID2 in sequence for every realization between n and m. At the conclusion of each realization, the total integrated discharges in *tid2.dat* are appended to the file *intdis2.dat*. Thus at the conclusion of the procedure *intdis2.dat* contains the total integrated discharges for all realizations.

COMBINEII

COMBINEII is a remnant of the code operation procedure developed for the preliminary performance assessment (PPA). Its function in that context was to combine the integrated discharges determined by NEFTRAN for the "down-and-out" pathway realizations with the integrated discharges determined for those realizations in which upward diffusion dominated the process that had been saved in *intdis2.dat*. In the current iteration, of course, there are no longer any realizations that consider the down-and-out direction. Consequently, the file that would have contained these values, *nefii.dis*, is empty save for two header lines at the top. Thus, in the current context COMBINEII acts as a simple translator program that takes the discharges in the *intdis2.dat* format and writes them into a file call *cumrel.dat* that is in the format that is readable by CCDFTRUIIFI. COMBINEII is included at the end of this appendix.

CCDFTRUIIFI

CCDFTRUIIFI is a modified version of CCDFTRU that was described in the PPA. Its function is to read the total integrated discharges from a file called *fort.11* (formerly *cumrel.dat*) and compute the associated complementary cumulative distribution function (CCDF). The code also contains appropriate calls to the DISSPLA© graphics package so the curve can be displayed directly on the monitor or written to a POSTSCRIPT® file and printed. Aside from the discharge file, CCDF also requires the initial Curies of all radionuclides that are subject to regulation in a file called *Gcdinv.dat*. There is only one set of initial inventories in this file, and this is one of the ways in which this code differs from CCDFTRU, which expected different inventories for each realization (the FI in the name signifies "fixed inventory"). The other input files to CCDFTRUIIFI include *ccdftruin.dat*, which contains the number of isotopes, and the number of scenarios and their probabilities, along with the number of chains and number in each chain. The file *eparlslim.dat* contains the release limits established for each isotope by 40 CFR 191. In addition to a graphic representation of the CCDF, the code returns the numerical values of the CCDF curve in the file *ccdftrxypts.dat* and the correspondence between EPA sum and vector number in the file *epasumtru.dat*.

Code Operation for Individual Protection Requirements

In performing the Individual Protection analysis, the code operation procedure is very similar to that outlined above. Virtually the same codes are run in the same sequence by virtually the same script. The pre- and post-processors were modified somewhat. The code WRSWIFT56_IP is a modification of WRSWIFT56, and TID2_IP is a modification of TID2. Both new codes are included at the end of this appendix. The major difference in doing this analysis is that concentration values instead of integrated discharges are what are sought from the sequence of SWIFT runs. TID2_IP is modified so that instead of integrating fluxes, it searches for the maximum concentration over time of each radionuclide at two locations, the surface soil and at the root depth (the deep soil). These maximum concentrations are recorded for all realizations in two files soilconc and deepsoilconc. In turn, these files serve as input to another UNIX shell script called findmean which is as follows,

```
#!/bin/sh
grep 'PU239' $1 | sorter > out
grep 'U235' $1 | sorter >> out
grep 'PA231' $1 | sorter >> out
grep 'AC227' $1 | sorter >> out
grep 'PU240' $1 | sorter >> out
grep 'U236' $1 | sorter >> out
grep 'TH232' $1 | sorter >> out
grep 'PU241' $1 | sorter >> out
grep 'AM241' $1 | sorter >> out
grep 'NP237' $1 | sorter >> out
grep 'U233' $1 | sorter >> out
grep 'TH229' $1 | sorter >> out
grep 'PU242' $1 | sorter >> out
grep 'U238' $1 | grep -v 'PU' | sorter >> out
grep 'PU238' $1 | sorter >> out
grep 'U234' $1 | sorter >> out
grep 'TH230' $1 | sorter >> out
grep 'RA226' $1 | sorter >> out
grep 'PB210' $1 | sorter >> out
grep 'SR90' $1 | sorter >> out
grep 'CS137' $1 | sorter >> out
```

The command to execute this script on soilconc is,

> findmean soilconc

The script successively filters the file for each radionuclide and pipes these concentration values to a code called *sorter*. This program determines the mean of the concentration values and appends them to a file called out. A copy of the *sorter* code is included at the end of this appendix.

The last step in this analysis is to take these concentration values and the pathway parameters described in Section 3.3.1 to the GENII code and determine individual doses from them. Because of code constraints it was necessary to break up this run into six separate runs,

one for each decay chain. A sample GENII input file for the first chain is included at the end of this Appendix. Similar input files were developed for the other chains.

Gas Phase Computations: VAPDIF2

The gas phase diffusion model described in Section 3.3.2 was implemented in a code called VAPDIF2. The input file to this code is called vapdif2.inp. It contains a pair of flags for controlling the mode of computation, Containment or Individual Protection Requirements, and the mode of release; surface release or plant uptake. This file also contains additional information such as depth of burial, initial concentration at the waste source, and parent and daughter half-lives. As such, it can be used to compute the dose from all radon isotopes and their daughters along with the total integrated release of ^{210}Pb. A copy of the code is included at the end of this appendix.

Input file for LHS: nominal case

```
TITLE LHS FILE- RUN PAII.5-5
NOBS 5000
RANDOM SEED 548788715
CORRELATION MATRIX
1  2 25 -.9
OUTPUT CORR DATA
NORMAL          (1 - porosity in saturated alluvium)
0.2455 0.4576    (lower and upper endpoints)
LOGNORMAL        (2 - moisture cont in alluvium, modified for PAII.5)
0.04745 .1810    (.001 and .999 quantiles)
LOGNORMAL        (3 - Kd for Pu238, 239, 240, 241, 242, ft3/lb)
0.025 1.6       (.001 and .999 quantiles)
LOGNORMAL        (4 - Kd for U233, 234, 235, 236, 238, ft3/lb)
0.000016 0.092   (.001 and .999 quantiles)
LOGNORMAL        (5 - Kd for Pa231, ft3/lb)
0.000016 0.08    (.001 and .999 quantiles)
LOGNORMAL        (6 - Kd for Ac227, ft3/lb)
0.000016 0.08    (.001 and .999 qualtiles)
LOGNORMAL        (7 - Kd for Th229, 230, 232)
0.000016 0.08    (.001 and .999 quantiles)
LOGNORMAL        (8 - Kd for Am241, ft3/lb)
0.000016 0.08    (.001 and .999 quantiles)
LOGNORMAL        (9 - Kd for Np237, ft3/lb)
0.000016 0.08    (.001 and .999 quantiles)
LOGNORMAL        (10 - Kd for Ra226, ft3/lb)
0.000016 0.08    (.001 and .999 quantiles)
LOGNORMAL        (11 - Kd for Pb210, ft3/lb)
0.000016 0.08    (.001 and .999 quantiles)
LOGNORMAL        (12 - Kd for Sr90, ft3/lb)
0.000016 2.656   (.001 and .999 quantiles)
LOGNORMAL        (13- Kd for Cs137, ft3/lb)
0.000016 104     (.001 and .999 quantiles)
UNIFORM          (14 - Pu238,239,240,241,242 solubility, g/g)
2.39E-8 9.51E-7  (lower and upper endpoints)
LOGUNIFORM       (15 - U233,234,235,236,238 solubility, g/g)
1.E-11 1.E-6     (.001 and .999 quantiles)
UNIFORM          (16 - Pa231 solubility, g/g)
1  10           (lower and upper endpoints)
UNIFORM          (17- Ac227 solubility, g/g)
1  10           (lower and upper endpoints)
UNIFORM          (18 - Th229, 230, 232 solubility, g/g)
1.E-7 3.E-7      (lower and upper endpoints)
LOGUNIFORM       (19 - Am241 solubility, g/g)
1.E-9  5.E-7     (.001 and .000 quantiles)
UNIFORM          (20 - Np237 solubility, g/g)
2.E-5  3.E-4     (lower and upper endpoints)
UNIFORM          (21 - Ra226 solubility, g/g)
2.5E-8 3.E-8     (lower and upper endpoints)
LOGUNIFORM       (22 - Pb210 solubility, g/g)
3.E-9  5.E-7     (.001 and .999 quantiles)
LOGNORMAL        (23 - Sr90 solubility, g/g)
9.E-9  9.E-5     (.001 and .999 quantiles)
UNIFORM          (24 - Cs137 solubility, g/g)
1  10           (lower and upper endpoints)
UNIFORM          (25 - tortuosity, modified for PAII.5)
3 110           (lower and upper endpoints)
LOGNORMAL        (26 - Pu238,239,240,241,242 isotope uptakes )
1.02e-6 .17382   (lower and upper endpoints)
LOGNORMAL        (27 - U233,234,235,236,238 isotope uptakes )
6.641e-4 4.3313  (lower and upper endpoints)
```

```
LOGNORMAL          (28 - Am241 uptakes )
6.427e-6 1.116     (lower and upper endpoints)
LOGNORMAL          (29 - Pa231 uptake factor)
6.641e-4 4.3313    (lower and upper endpoints)
LOGNORMAL          (30 - Ac227 uptake factor)
6.641e-4 4.3313    (lower and upper endpoints)
LOGNORMAL          (31 - Th229,230,232 uptake factors)
6.641e-4 4.3313    (lower and upper endpoints)
LOGNORMAL          (32 - Np237 uptake factor)
6.641e-4 4.3313    (lower and upper endpoints)
LOGNORMAL          (33 - Ra226 uptake factor)
6.641e-4 4.3313    (lower and upper endpoints)
LOGNORMAL          (34 - Pb210 uptake factor)
6.641e-4 4.3313    (lower and upper endpoints)
LOGNORMAL          (35 - Sr90 uptake factor, modified for PAII.5)
.01629 1.31069     (lower and upper endpoints,)
LOGNORMAL          (36 - Cs137 uptake factor, modified for PAII.5)
.01629 1.31069     (lower and upper endpoints)
UNIFORM            (37 - Erosion depth (ft), modified for PAII.5 )
0. 6.56          (lower and upper endpoints)
LOGUNIFORM         (38 - Root depth (ft) modified for PAII.5)
3.4  35.0        (lower and upper endpoints)
```

Input file for SWIFT II: 4 decay chains, nonTRU waste not included

```
ONE-DIMENSIONAL DIFFUSION ONLY
FOUR DECAY CHAINS, NONTRU WASTE
   4   0   0   0   0   0   0   0   1   0
 146   1   1   1  19   3   0   1   0   0   0   0   1   1
   1   0   1   0   0   0
239 PU239        1   0   0 2.410E04
235 U235         2   1   0 7.040E08
   1    1.0
231 PA231        3   1   0 3.280E04
   2    1.0
227 AC227        4   1   0 2.177E01
   3    1.0
240 PU240        5   0   0 6.560E03
236 U236         6   1   0 2.342E07
   5    1.0
232 TH232        7   1   0 1.400E10
   6    1.0
241 PU241        8   0   1 1.440E01
241 AM241        9   1   0 4.327E02
   8    1.0
237 NP237       10   1   0 2.140E06
   9    1.0
233 U233        11   1   0 1.590E05
  10    1.0
229 TH229       12   1   0 7.300E03
  11    1.0
242 PU242       13   0   0 3.750E05
238 U238        14   1   0 4.470E09
  13    1.0
238 PU238       15   0   0 8.770E01
234 U234        16   2   0 2.460E05
  14    1.0      15     1.0
230 TH230       17   1   0 7.540E04
  16    1.0
226 RA226       18   1   0 1.600E03
  17    1.0
210 PB210       19   1   0 2.230E01
  18    1.0
```

```
   0.00     0.00     0.00     0.00     0.00     0.00     0.00
   0.00     0.00     0.00     0.00     0.00     0.00     0.00
   0.00     0.00     0.00     0.00     0.00
7.139E-3 7.139E-3 7.139E-3 7.139E-3 7.139E-3 7.139E-3 7.139E-3
6.790E-4 6.790E-4 6.790E-4 6.790E-4 6.790E-4 7.139E-3 7.139E-3
7.139E-3 7.139E-3 7.139E-3 7.139E-3 7.139E-3
7.139E-3 7.139E-3 7.139E-3 7.139E-3 7.139E-3 7.139E-3 7.139E-3
6.790E-4 6.790E-4 6.790E-4 6.790E-4 6.790E-4 7.139E-3 7.139E-3
7.139E-3 7.139E-3 7.139E-3 7.139E-3 7.139E-3
    1.0      1.0      1.0      1.0      1.0      1.0      1.0
    1.0      1.0      1.0      1.0      1.0      1.0      1.0
    1.0      1.0      1.0      1.0      1.0
    1.0      1.0      1.0      1.0      1.0      1.0      1.0
    1.0      1.0      1.0      1.0      1.0      1.0      1.0
    1.0      1.0      1.0      1.0      1.0
    1.0      1.0      1.0      1.0      1.0      1.0      1.0
    1.0      1.0      1.0      1.0      1.0      1.0      1.0
    1.0      1.0      1.0      1.0      1.0
2.948E-10 2.948E-10 2.948E-10 2.948E-10 2.948E-10 2.948E-10 2.948E-10
2.948E-10 2.948E-10 2.948E-10 2.948E-10 2.948E-10 2.948E-10 2.948E-10
2.948E-10 2.948E-10 2.948E-10 2.948E-10 2.948E-10
6.668E-5 6.668E-5 6.668E-5 6.668E-5 6.668E-5 6.668E-5 6.668E-5
6.668E-5 6.668E-5 6.668E-5 6.668E-5 6.668E-5 6.668E-5 6.668E-5
6.668E-5 6.668E-5 6.668E-5 6.668E-5 6.668E-5
6.668E-5 6.668E-5 6.668E-5 6.668E-5 6.668E-5 6.668E-5 6.668E-5
6.668E-5 6.668E-5 6.668E-5 6.668E-5 6.668E-5 6.668E-5 6.668E-5
6.668E-5 6.668E-5 6.668E-5 6.668E-5 6.668E-5
    0.0      0.0      0.0      1.0      1.0      0.0
    1.0      1.0      1.0      0.0      0.0      0.0      0.0
    1.0      1.0      1.0      0.0
    0.0      0.0      0.0      0.0
    1.0      1.0      1.0      0.0
    0.0      0.0      0.0      0.0
    1.0      1.0      1.0      0.0
    0.0      0.0      0.0      0.0
  100.0     14.7     60.0     62.34    62.34
  0   0   0   2
   60.0      1.0     60.0      1.0
    0.0     60.0
   10.0     60.0
  0   0
   60.0     14.7      0.0      0.0
0.1  0.1  0.2  0.3  0.4 136*0.297794  0.4  0.3  0.2  0.1  0.1
1.0
1.0
 1.0E-14   1.0E-14   1.0E-14  0.136980      0.0      0.0      0.00
  1   1   1   1   1   1
    1.0      1.0      1.0      1.0      0.0      0.0 2.262E+05
    0.0      0.0      0.0
146  146   1   1   1   1
    1.0      1.0      1.0      1.0      0.0      0.0    1.0E8
    0.0      0.0      0.0
  0   0   0   0   0   0
  0   0
  0   0   0
  1   1   1   1   1   1   1
  2  145   1   1   1   1   2
146  146   1   1   1   1   3
  0
    0.0
  0
    0.0      0.0      1.0      0.0
    1.0      1.0      1.0      1.0
  1   1   1   1   1   1
    0.
PU239     4.689E-04
```

```
U235      3.743E-03
PA231     0.000E+00
AC227     0.000E+00
PU240     2.949E-05
U236      1.011E-04
TH232     0.000E+00
PU241     5.360E-07
AM241     2.139E-06
NP237     0.000E+00
U233      0.000E+00
TH229     0.000E+00
PU242     1.163E-07
U238      5.960E-02
PU238     7.848E-08
U234      3.092E-05
TH230     0.000E+00
RA226     0.000E+00
PB210     0.000E+00
8.760E-00 4.803E-00 4.803E-00 4.803E-00 8.760E-00 4.803E-00 4.803E-00
8.764E-00 8.570E-00 8.570E-00 8.570E-00 8.570E-00 8.769E-00 4.780E-00
8.769E-00 4.780E-00 4.803E-00 4.803E-00 4.803E-00
  1   1   1
 140   1   1
 145   1   1
  0
  0   0   0   0   1   0   0   0   0   0
 1.0E-12   0.0E+00
   73000      3650       0.0       0.0       0.0       0.0       0.0   0.0
  1   -1   -1   -1   -1   -1  000    0 0000    0   00   0    0   0
 -1 0000 0000 0000 1111    1
  1  146    1    1    1    1
  1  146    1    1    1    1
  1  146    1    1    1    1
  1  146    1    1    1    1
  0   0   0   0   1   0   0   0   0   0
 1.0E-12   0.0E+00
  365000     18250       0.0       0.0       0.0       0.0       0.0   0.0
  1   -1   -1   -1   -1   -1  000    0 0000    0   00   0    0   0
 -1 0000 0000 0000 1111    0
  0   0   0   0   1   0   0   0   0   0
 1.0E-12   0.0E+00
  912500     36500       0.0       0.0       0.0       0.0       0.0   0.0
  1   -1   -1   -1   -1   -1  000    0 0000    0   00   0    0   0
 -1 0000 0000 0000 1111    0
  0   0   0   0   1   0   0   0   0   0
 1.0E-12   0.0E+00
 1825000     91250       0.0       0.0       0.0       0.0       0.0   0.0
  1   -1   -1   -1   -1   -1  000    0 0000    0   00   0    0   0
 -1 0000 0000 0000 1111    0
  0   0   0   0   1   0   0   0   0   0
 1.0E-12   0.0E+00
 2555000    182500       0.0       0.0       0.0       0.0       0.0   0.0
  1   -1   -1   -1   -1   -1  000    0 0000    0   00   0    0   0
 -1 0000 0000 0000 1111    0
  0   0   0   0   1   0   0   0   0   0
 1.0E-12   0.0E+00
 3650000    365000       0.0       0.0       0.0       0.0       0.0   0.0
  1   -1   -1   -1   -1   -1  000    0 0000    0   00   0    0   0
 -1 0000 0000 0000 1111    0
  0   0   0   1
```

Input file for SWIFT II: 6 decay chains, nonTRU waste included

```
ONE-DIMENSIONAL DIFFUSION ONLY
```

6 DECAY CHAINS, NONTRU WASTE INCLUDED

```
  4   0   0   0   0   0   0   0   1   0
 146   1   1   1  21   3   0   1   0   0   0   0   1   1
 1   0   1   0   0   0
239 PU239        1   0   0 2.410E04
235 U235         2   1   0 7.040E08
  1    1.0
231 PA231        3   1   0 3.280E04
  2    1.0
227 AC227        4   1   0 2.177E01
  3    1.0
240 PU240        5   0   0 6.560E03
236 U236         6   1   0 2.342E07
  5    1.0
232 TH232        7   1   0 1.400E10
  6    1.0
241 PU241        8   0   1 1.440E01
241 AM241        9   1   0 4.327E02
  8    1.0
237 NP237       10   1   0 2.140E06
  9    1.0
233 U233        11   1   0 1.590E05
 10    1.0
229 TH229       12   1   0 7.300E03
 11    1.0
242 PU242       13   0   0 3.750E05
238 U238        14   1   0 4.470E09
 13    1.0
238 PU238       15   0   0 8.770E01
234 U234        16   2   0 2.460E05
 14    1.0      15       1.0
230 TH230       17   1   0 7.540E04
 16    1.0
226 RA226       18   1   0 1.600E03
 17    1.0
210 PB210       19   1   0 2.230E01
 18    1.0
 90 SR90        20   0   0 2.910E01
137 CS137       21   0   0 3.017E01
    0.00      0.00      0.00      0.00      0.00      0.00      0.00
    0.00      0.00      0.00      0.00      0.00      0.00      0.00
    0.00      0.00      0.00      0.00      0.00      0.00      0.00
 7.139E-3  7.139E-3  7.139E-3  7.139E-3  7.139E-3  7.139E-3  7.139E-3
 6.790E-4  6.790E-4  6.790E-4  6.790E-4  6.790E-4  7.139E-3  7.139E-3
 7.139E-3  7.139E-3  7.139E-3  7.139E-3  7.139E-3  7.139E-3  7.139E-3
 7.139E-3  7.139E-3  7.139E-3  7.139E-3  7.139E-3  7.139E-3  7.139E-3
 6.790E-4  6.790E-4  6.790E-4  6.790E-4  6.790E-4  7.139E-3  7.139E-3
 7.139E-3  7.139E-3  7.139E-3  7.139E-3  7.139E-3  7.139E-3  7.139E-3
     1.0       1.0       1.0       1.0       1.0       1.0       1.0
     1.0       1.0       1.0       1.0       1.0       1.0       1.0
     1.0       1.0       1.0       1.0       1.0       1.0       1.0
     1.0       1.0       1.0       1.0       1.0       1.0       1.0
     1.0       1.0       1.0       1.0       1.0       1.0       1.0
     1.0       1.0       1.0       1.0       1.0       1.0       1.0
     1.0       1.0       1.0       1.0       1.0       1.0       1.0
     1.0       1.0       1.0       1.0       1.0       1.0       1.0
     1.0       1.0       1.0       1.0       1.0       1.0       1.0
2.948E-10 2.948E-10 2.948E-10 2.948E-10 2.948E-10 2.948E-10 2.948E-10
2.948E-10 2.948E-10 2.948E-10 2.948E-10 2.948E-10 2.948E-10 2.948E-10
2.948E-10 2.948E-10 2.948E-10 2.948E-10 2.948E-10 2.948E-10 2.948E-10
 6.668E-5  6.668E-5  6.668E-5  6.668E-5  6.668E-5  6.668E-5  6.668E-5
 6.668E-5  6.668E-5  6.668E-5  6.668E-5  6.668E-5  6.668E-5  6.668E-5
 6.668E-5  6.668E-5  6.668E-5  6.668E-5  6.668E-5  6.668E-5  6.668E-5
 6.668E-5  6.668E-5  6.668E-5  6.668E-5  6.668E-5  6.668E-5  6.668E-5
 6.668E-5  6.668E-5  6.668E-5  6.668E-5  6.668E-5  6.668E-5  6.668E-5
 6.668E-5  6.668E-5  6.668E-5  6.668E-5  6.668E-5  6.668E-5  6.668E-5
```

```
    0.0       0.0       0.0       1.0       1.0       0.0
    1.0       1.0       1.0       0.0       0.0       0.0       0.0
    1.0       1.0       1.0       0.0
    0.0       0.0       0.0       0.0
    1.0       1.0       1.0       0.0
    0.0       0.0       0.0       0.0
    1.0       1.0       1.0       0.0
    0.0       0.0       0.0       0.0
  100.0      14.7      60.0      62.34     62.34
 0   0   0   2
   60.0       1.0      60.0       1.0
    0.0      60.0
   10.0      60.0
 0   0
   60.0      14.7       0.0       0.0
0.1  0.1  0.2  0.3  0.4 136*0.297794  0.4  0.3  0.2  0.1  0.1
1.0
1.0
 1.0E-14   1.0E-14   1.0E-14  0.136980       0.0       0.0       0.00
  1    1    1    1    1    1
    1.0       1.0       1.0       1.0       0.0       0.0 3.390E+05
    0.0       0.0       0.0
146  146    1    1    1    1
    1.0       1.0       1.0       1.0       0.0       0.0     1.0E8
    0.0       0.0       0.0
 0   0   0   0   0   0
 0   0
 0   0   0
 1   1   1   1   1   1   1
 2  145   1   1   1   1   2
146  146   1   1   1   1   3
 0
    0.0
 0
    0.0       0.0       1.0       0.0
    1.0       1.0       1.0       1.0
 1   1   1   1   1   1
    0.
PU239     3.126E-04
U235      2.495E-03
PA231     0.000E+00
AC227     0.000E+00
PU240     1.966E-05
U236      6.740E-05
TH232     0.000E+00
PU241     3.573E-07
AM241     1.426E-06
NP237     0.000E+00
U233      0.000E+00
TH229     0.000E+00
PU242     7.753E-08
U238      3.973E-02
PU238     5.232E-08
U234      2.061E-05
TH230     0.000E+00
RA226     0.000E+00
PB210     0.000E+00
SR90      2.352E-04
CS137     1.555E-05
8.760E-00 4.803E-00 4.803E-00 4.803E-00 8.760E-00 4.803E-00 4.803E-00
8.764E-00 8.570E-00 8.570E-00 8.570E-00 8.570E-00 8.769E-00 4.780E-00
8.769E-00 4.780E-00 4.803E-00 4.803E-00 4.803E-00 4.803E-00 4.803E-00
  1   1   1
 140   1   1
 145   1   1
  0
```

```
 0   0   0   0   1   0   0   0   0   0
1.0E-12   0.0E+00
  18250      1825       0.0       0.0       0.0       0.0       0.0   0.0
 1   -1   -1   -1   -1   -1  000    0 0000    0   00    0    0    0
-1 0000 0000 0000 1111    1
 1  146    1    1    1    1
 1  146    1    1    1    1
 1  146    1    1    1    1
 1  146    1    1    1    1
 0   0   0   0   1   0   0   0   0   0
1.0E-12   0.0E+00
  73000      3650       0.0       0.0       0.0       0.0       0.0   0.0
 1   -1   -1   -1   -1   -1  000    0 0000    0   00    0    0    0
-1 0000 0000 0000 1111    0
 0   0   0   0   1   0   0   0   0   0
1.0E-12   0.0E+00
 365000     18250       0.0       0.0       0.0       0.0       0.0   0.0
 1   -1   -1   -1   -1   -1  000    0 0000    0   00    0    0    0
-1 0000 0000 0000 1111    0
 0   0   0   0   1   0   0   0   0   0
1.0E-12   0.0E+00
 912500     36500       0.0       0.0       0.0       0.0       0.0   0.0
 1   -1   -1   -1   -1   -1  000    0 0000    0   00    0    0    0
-1 0000 0000 0000 1111    0
 0   0   0   0   1   0   0   0   0   0
1.0E-12   0.0E+00
1825000     91250       0.0       0.0       0.0       0.0       0.0   0.0
 1   -1   -1   -1   -1   -1  000    0 0000    0   00    0    0    0
-1 0000 0000 0000 1111    0
 0   0   0   0   1   0   0   0   0   0
1.0E-12   0.0E+00
2555000    182500       0.0       0.0       0.0       0.0       0.0   0.0
 1   -1   -1   -1   -1   -1  000    0 0000    0   00    0    0    0
-1 0000 0000 0000 1111    0
 0   0   0   0   1   0   0   0   0   0
1.0E-12   0.0E+00
3650000    365000       0.0       0.0       0.0       0.0       0.0   0.0
 1   -1   -1   -1   -1   -1  000    0 0000    0   00    0    0    0
-1 0000 0000 0000 1111    0
 0   0   0   1
```

Input data for GENII: Chain 1

GENIIS Dose Calculation Program
(Version 1.485 15-Jan-91)

Case title: Dose from basic soil concentrations

Executed on: 09/13/93 at 10:49:12 Page 2

This is a near field (narrowly-focused, single site) scenario.
Release is chronic
Individual dose

THE FOLLOWING EXPOSURE PATHS ARE CONSIDERED:
Ground, external
Inhalation uptake
Terrestrial foods ingestion
Animal product ingestion

THE FOLLOWING TIMES ARE USED:
Intake ends after (yr): 1.0
Dose calculations ends after (yr): 50.0

========== FILENAMES AND TITLES OF FILES/LIBRARIES USED ==========

GENII Default Parameter Values (28-Mar-90 RAP)
Radionuclide Master Library (11/28/90 RAP)
Food Transfer Factor Library - (RAP 29-Aug-88) (UPDATED LEACHING FA
External Dose Factors for GENII-Sphere source modification BAN 5/19/
Internal Yearly Dose Increments (Sv/Bq) 29-Aug-88 RAP

==========

3 Surface soil input unit: (1-m2, 2-m3, 3-kg)

Release Radio-nuclide	Air pCi/L	Surface Soil pCi/kg	Deep Soil pCi/m3	Ground Water pCi/L	Surface Water pCi/L
U 235	0.0E+00	4.6E-02	2.5E+02	0.0E+00	0.0E+00
PA231	0.0E+00	8.8E+00	3.5E+04	0.0E+00	0.0E+00
AC227	0.0E+00	8.8E+00	3.5E+04	0.0E+00	0.0E+00
PU239	0.0E+00	2.9E-07	1.9E+00	0.0E+00	0.0E+00

========== NEAR-FIELD PARAMETERS ==========

0.0 Inventory disposed n years prior to beginning of intake period
0 LOIC occurred n years prior to beginning of intake period
9.9E-01 Fraction of roots in upper soil (top 15 cm)
1.0E-02 Fraction of roots in deep soil
0.0E+00 Manual redistribution: deep soil/surface soil dilution factor

========== WASTE FORM AVAILABILITY ==========

0.0E+00 Waste form/package half life, yr
2.0E+01 Thickness of buried waste, m
1.0E+00 Depth of soil overburden, m

========== EXTERNAL EXPOSURE ==========

4.4E+03 Hours of exposure to ground contamination

========== INHALATION ==========

8.8E+03 Hours of inhalation exposure per year
1 Resuspension model: 1-Mass Loading, 2-Anspaugh
1.0E-04 Mass loading factor (g/m3)

========== TERRESTRIAL FOOD INGESTION ==========

FOOD TYPE	GROW TIME d	S RATE *	IRRIGATION-- TIME in/yr	IRRIGATION-- mo/yr	PROD- UCTION kg/m2	YIELD kg/yr	HOLDUP d	CONSUMPTION-- RATE kg/yr
Leaf Veg	60.0	0	0.0	0.0	2.2	6.00E+01	1.0	6.0E+01
Oth. Veg	90.0	0	0.0	0.0	9.0	1.82E+02	1.0	1.8E+02
Fruit	60.0	0	0.0	0.0	5.2	3.35E+02	1.0	3.3E+02
Cereals	90.0	0	0.0	0.0	2.1	8.80E+01	1.0	8.8E+01

========== ANIMAL FOOD INGESTION ==========

FOOD TYPE	---HUMAN---- CONSUMPTION RATE kg/yr	TOTAL PROD- HOLDUP d	DRINK WATER UCTION kg/yr	DIET CONTAM FRACT.	GROW TION	STORED FEED---------- TIME d	IRRIGATION-- S RATE * in/yr	IRRIGATION-- TIME mo/yr	STOR- YIELD kg/m3	AGE d
Meat	4.0E+01	15.04.0E+01	0.00	1.0	90.00	0	0.0	0.0	0.84	0.0
Poultry	1.8E+01	2.01.8E+01	0.00	1.0	90.00	0	0.0	0.0	0.84	0.0
Cow Milk	2.7E+02	2.02.7E+02	0.00	1.0	30.00	0	0.0	0.0	1.30	0.0
Eggs	3.0E+01	2.03.0E+01	0.00	1.0	90.00	0	0.0	0.0	0.84	0.0

	----------FRESH FORAGE----------						
Meat	0.00	0.0	0	0.0	0.0	0.00	0.0
Cow Milk	0.00	0.0	0	0.0	0.0	0.00	0.0

CODES

```
      PROGRAM WRSWFT
c
C  The purpose of this program is to read the current realizaiton
c  parameter vector from nefii.smp and write out an input file
c  for SWIFT with these values inserted in the appropriate place.
c  To do so it reads a standard input file called swift.inp
c  and changes the appropriate parts of it and writes out the
c  new file as SWIFTINP
c
c  DATE WRITTEN: March, April 1993 for used with SWIFT II VERSION 2B
c  AUTHOR:    THOMAS A. Baer
c
c
c Variable names:
c          NOVEC - current realization number
c          NOISO - number of isotopes
c          POROS - porosity
c       THETA - moisture content
c       CTHETA - 1 - THETA
c          TAU - tortuosity
c          ROOTD - root depth (ft)
c       ERN - erosion depth (ft)
c       DEFF - effective alluvium diffusion coefficient ( ft**2/yr)
c       DM - molecular diffusion coefficient (ft**2/yr)
c          TUB - simulation time (yr)
c          AREAL - crossectional area of one borehole (ft**2)
c          BIODENS - above ground plant biomass density (lb/ft**2)
c          RDENS - bulk density of alluvium (lb/ft**3)
c
c Array names:
c          AKD - distribution coefficient ( ft**3/lb )
c          CSALL - solubility (g/g)
c          UPTAKE - plant uptake factor
c          HLFALL - half life (yr)
c          DIFF - diffusion coefficient of each isotope accounting for
c                retardation (ft**2/yr)
c       GRID - the x location of the centers of each grid block (ft)
c       ENDS - the width of the first five and last five grid blocks (ft)
c
      IMPLICIT DOUBLE PRECISION (A-H,O-Z)
C
      DIMENSION UPTAKE(25), AKD(25), DIFF(25), RV(150)
      DIMENSION NI(7), AMALL(21), CSALL(25), INV(21), ENDS(5)
      DIMENSION GRID(146),NI(6), HLFALL(21), DU(21)
      CHARACTER*6 NAMALL(21)
c
      DATA NAMALL/'PU239','U235','PA231','AC227',
     +          'PU240','U236','TH232',
     +          'PU241','AM241','NP237','U233','TH229',
     +    'PU242','U238','PU238','U234','TH230','RA226','PB210',
     +          'SR90',
     +          'CS137'/
C
      DATA HLFALL/2.41E+04,7.04E+08,3.28E+04,2.177E+01,
     +          6.56E+03,2.342E+07,1.4E+10,
     +          1.44E+01,4.327E+02,2.14E+06,1.59E+05,7.3E+03,
     +   3.75E+05,4.47E+09,8.77E+01,2.46E+05,7.54E+04,1.60E+03,2.23E+01,
     +          2.91E+01,
     +          3.017E+01/
C
      DATA AMALL/239.,235.,231.,227.,240.,236.,232.,241.,241.,
     +          237.,233.,229.,242.,238.,238.,234.,230.,226.,
     +          210.,90.,137./
      DATA INV/1,1,0,0,1,1,0,1,1,0,0,0,1,1,1,1,0,0,0,0,0/
```

```
      DATA ENDS/.1,.1,.2,.3,.4/
      DATA NI/4,3,5,7,1,1/
C
      OPEN(UNIT=9,FILE='zot.dat',STATUS='OLD')
      OPEN(UNIT=11,FILE='nefii.smp',STATUS='OLD')
      OPEN(UNIT=12,FILE='swift.inp',STATUS='OLD')
      OPEN(UNIT=14,FILE='SWIFTINP',STATUS='UNKNOWN')
      OPEN(UNIT=40,FILE='tid.inp',STATUS='UNKNOWN')
C
c  The current realization number is read from zot.dat
c
      READ(9,*)NOVEC,NCHNS
c
      NRT = 3
c
c  The parameter vector corresponding to NOVEC is read in from nefii.smp
C
      DO WHILE( JTRIAL .NE. NOVEC )
C
       READ(11,*,END=1000) JTRIAL, NVAR, (RV(I),I = 1,NVAR)
C
      ENDDO
c
       WRITE(*,'(I5,E15.7)')(I,RV(I),I=1,NVAR )
c
 1000 CONTINUE
C
c  The values of parameters are transferred into the appropriate
c    variables or arrays
c
      POROS = RV(1)
      THETA = RV(2)
      CTHETA = 1.0 - THETA
      TAU = RV(25)
      ROOTD = RV(38)
      ERN = RV(37)
C
C  Chain 1
c
      AKD(1) = RV(3)
      AKD(2) = RV(4)
      AKD(3) = RV(5)
      AKD(4) = RV(6)
c
      FACT = 453.593 * 62.4 * 6.02 * 10. ** 23
c
c                       !* if this inline comment is removed
c                         the solubilities are converted to atm/ft**3
c
      CSALL(1) = RV(14)      !*FACT/AMALL(1)
      CSALL(2) = RV(15)      !*FACT/AMALL(2)
      CSALL(3) = RV(16)      !*FACT/AMALL(3)
      CSALL(4) = RV(17)      !*FACT/AMALL(4)
c
      UPTAKE(1) = RV(26)
      UPTAKE(2) = RV(27)
      UPTAKE(3) = RV(29)
      UPTAKE(4) = RV(30)
C
c  Chain 2
c
      AKD(5) = RV(3)
      AKD(6) = RV(4)
      AKD(7) = RV(7)
c
      CSALL(5) = RV(14)      !*FACT/AMALL(5)
```

```
      CSALL(6) = RV(15)      !*FACT/AMALL(6)
      CSALL(7) = RV(18)      !*FACT/AMALL(7)
C
      UPTAKE(5) = RV(26)
      UPTAKE(6) = RV(27)
      UPTAKE(7) = RV(31)
c
C
c  Chain 3
c
      AKD(8) = RV(3)
      AKD(9) = RV(8)
      AKD(10) = RV(9)
      AKD(11) = RV(4)
      AKD(12) = RV(7)
c
      CSALL(8) = RV(14)      !*FACT/AMALL(8)
      CSALL(9) = RV(19)      !*FACT/AMALL(9)
      CSALL(10) = RV(20)     !*FACT/AMALL(10)
      CSALL(11) = RV(15)     !*FACT/AMALL(11)
      CSALL(12) = RV(18)     !*FACT/AMALL(12)
c
      UPTAKE(8) = RV(26)
      UPTAKE(9) = RV(28)
      UPTAKE(10) = RV(32)
      UPTAKE(11) = RV(27)
      UPTAKE(12) = RV(31)
C
c  Chain 4
c
      AKD(13) = RV(3)
      AKD(14) = RV(4)
      AKD(15) = RV(3)
c      AKD(15) = RV(4)
      AKD(16) = RV(4)
      AKD(17) = RV(7)
      AKD(18) = RV(10)
      AKD(19) = RV(11)
c
      CSALL(13) = RV(14)     !*FACT/AMALL(13)
      CSALL(14) = RV(15)     !*FACT/AMALL(14)
      CSALL(15) = RV(14)     !*FACT/AMALL(15)
      CSALL(16) = RV(15)     !*FACT/AMALL(16)
      CSALL(17) = RV(18)     !*FACT/AMALL(17)
      CSALL(18) = RV(21)     !*FACT/AMALL(18)
      CSALL(19) = RV(22)     !*FACT/AMALL(19)
c
c     IF ( CSALL(16) .LT. CSALL(15)/10. ) CSALL(16) = CSALL(15)/10.
C
      UPTAKE(13) = RV(26)
      UPTAKE(14) = RV(27)
      UPTAKE(15) = RV(26)
      UPTAKE(16) = RV(27)
      UPTAKE(17) = RV(31)
      UPTAKE(18) = RV(33)
      UPTAKE(19) = RV(34)
c
c  Chain 5
c
      AKD(20) = RV(12)
      CSALL(20) = RV(23)         !*FACT/AMALL(20)
      UPTAKE(20) = RV(35)
c
c  Chain 6
c
      AKD(21) = RV(13)
```

```
      CSALL(21) = RV(24)          !*FACT/AMALL(21)
      UPTAKE(21) = RV(36)
c
      DM = .34
C
      DEFF = THETA*DM/TAU/365.0
C
      NOISO = 0
C
      DO 100 J = 1,NCHNS
       NOISO = NOISO + NI(J)
 100  CONTINUE
C
c  At this point, the code writes the input file SWIFTINP
c   by referring to the standard input file swift.inp
c
      CALL WRITLN(5)
c
      CALL WRITLN(33)
C
c  Insert distribution coefficients into SWIFTINP file
c
      READ(12,'(7F10.0)')( DU(I),I=1,NOISO)
c      WRITE(14,'(7E10.3)')(AKD(I)/CTHETA,I=1,NOISO)
      WRITE(14,'(7F10.2)')( DU(I),I=1,NOISO)
c
      READ(12,'(7E10.0)')(DU(I),I=1,NOISO)
      WRITE(14,'(7E10.3)')(AKD(I)/CTHETA,I=1,NOISO)
C
      READ(12,'(7E10.0)')(DU(I),I=1,NOISO)
      WRITE(14,'(7E10.3)')(AKD(I)/CTHETA,I=1,NOISO)
c
      DO 101 J = 1,NRT
       READ(12,'(7F10.0)')( DU(I),I=1,NOISO)
       WRITE(14,'(7F10.2)')( DU(I),I=1,NOISO)
 101  CONTINUE
C
c  Insert diffusion coefficients into SWIFTINP
c
      REPTHICK = 2.262E+5
C
      DO 102 J = 1,NRT
C
       READ(12,'(7E10.0)')(DU(I),I=1,NOISO)
C
      IF ( J.EQ.1) THEN
       WRITE(14,'(7E10.3)')(DEFF/REPTHICK,I=1,NOISO)
      ELSE
       WRITE(14,'(7E10.3)')(DEFF,I=1,NOISO)
      ENDIF
C
 102  CONTINUE
C
      CALL WRITLN(15)
c
c  Write the finite difference grid parameters into SWIFTINP
c    Contraction of the domain due to erosion must be accounted for
c
      DOB = 70.0 - ERN
      DELX = ( DOB - 2.0 )/136.0
C
      WRITE(14,50)( ENDS(I),I=1,5),' 136*',DELX,( ENDS(I),I=5,1,-1)
 50   FORMAT(5F5.2,A5,F6.4,5F5.2)
c
      CALL READLN(1)
C
```

```
      CALL WRITLN(2)
C
c   Insert moisture content into SWIFTINP
c
      READ(12,*) D1,D2,D3,D4,D5,D6,D7
      WRITE(14,'(3E10.1,4F10.5)') D1,D2,D3,THETA,D5,D6,D7
C
      CALL WRITLN(19)
c
c  This writes the inventory information to SWIFTINP
c
      DO 33 K = 1,NOISO
C
       CALL WRITLN(1)
c
 33    CONTINUE
c
      READ(12,'(7. .0.0)')( DU(I),I=1,NOISO)
      WRITE(14,'(7E10.3)')( CSALL(I),I=1,NOISO)

       CALL WRITLN(1)
c
c  The next section determines which grid block the
c   roots penetrate to.
c
c  The first step is to set up GRID
c
       GRID(1) = ENDS(2)
       GRID(2) = GRID(1) + ENDS(3)
       GRID(3) = GRID(2) + ENDS(4)
       GRID(4) = GRID(3) + ENDS(5)
C
        DO 60 J = 5,140
C
        GRID(J) = GRID(J-1) + DELX
C
 60     CONTINUE
C
      GRID(141) = GRID(140) + ENDS(5)
      GRID(142) = GRID(141) + ENDS(4)
      GRID(143) = GRID(142) + ENDS(3)
      GRID(144) = GRID(143) + ENDS(2)
C
c      WRITE(*,'(I5,E15.7)')(J,GRID(J), J=1,145)
c
c  Find the x location of the bottom of the roots
c
      ROOT = DOB - ROOTD
C
      NBLOCK = 1
C
      IF ( ROOT .LE. 0.0 ) GO TO 80
C
c  Search for the grid block with coordinate greater than the root depth
c
      DO 70 K = 144,1,-1
C
       IF ( ROOT .GT. GRID(K) ) THEN
         NBLOCK = K + 2
         GO TO 80
       ENDIF
 70    CONTINUE
C
 80    CONTINUE
C
      CALL READLN(1)
```

```
c
c  Write this grid block to SWIFTINP
C
      WRITE(14,'(3I5)')NBLOCK,1,1
C
      CALL WRITLN(37)
c
c  Write the tid.inp file
c
       PI = 3.141592653589793238D0
C
       TUB = 10000.
       AREAL = PI*(6.0)**2
       BIODENS = .1
       RDENS = 100.0
C
              WRITE(40,*)NOVEC, ' - LHS VECTOR #'
              WRITE(40,*)TUB, ' - SIMULATION TIME (YRS)'
              WRITE(40,*) NCHNS, ' - # OF CHAINS'
              DO 30 I = 1,NCHNS
                WRITE(40,*) NI(I), ' - # OF MEMBERS OF CHAIN', I
30            CONTINUE
              WRITE(40,'(E15.5,A35,E15.5,A20)')
     *      DEFF*365./THETA, ' - EFFECTIVE DIFFUSIVITY (FT**2/YR)',
     *      THETA,' - MOISTURE CONTENT '
          WRITE(40,*) AREAL, ' - AREA (FT**2) PER BOREHOLE'
          WRITE(40,*)ERN,' - EROSION DEPTH (FT) '
          WRITE(40,*)ROOTD, ' - ROOTING DEPTH (FT) '
          WRITE(40,*)BIODENS, ' - BIOMASS DENSITY (LB/FT**2) '
              WRITE(40,7200)
7200          FORMAT(1X,'ISOTOPE', 8X, 'HALF-LIFE(YR)', 2X,
     *        'S.L.( G/G )',' TRANS. FACTOR ',' ISOTOPE DIFFUSIVITY ')
              DO 40 I = 1,NOISO
C
c  CR is the tranlocation factor from atm/ft**3 solvent to atm/lb dry above
c    ground vegetation.
C
          CR = UPTAKE(I)*( THETA/RDENS + AKD(I) )
c
c  Compute retardation coefficient
c
          RET = 1.0 + ( AKD(I) * RDENS ) / THETA
c
          DIFF(I) = DEFF*365./THETA/RET
C
              CS = CSALL(I)
C
              WRITE(40,7500) NAMALL(I),HLFALL(I),CS, CR, DIFF(I)
7500          FORMAT(1X,A6,6X,1P8E15.6,8X,1P8E15.6)
40        CONTINUE


      END
C
      SUBROUTINE READLN(N)
c
c  This subroutine reads N 80 character lines from UNIT 12 ( swift.inp)
C
      CHARACTER*80 LINE
C
      DO 20 J = 1,N
C
       READ(12,10) LINE
C
  20  CONTINUE
C
```

```
 10   FORMAT ( A80 )
C
      RETURN
      END
C
      SUBROUTINE WRITLN(N)
c
c  This subroutine reads N 80 character lines from UNIT 12 ( swift.inp)
c   and writes them to UNIT 14 (SWIFTINP )
C
      CHARACTER*80 LINE
C
      DO 20 J = 1,N
C
       READ(12,10) LINE
       WRITE(14,10) LINE
C
  20  CONTINUE
C
 10   FORMAT ( A80 )
C
      RETURN
      END
```

```
      PROGRAM TID2
c
c  TID2 reads SWIFTNMD and from this computes the flux at
c   the surface and the vegetative flux.  These are integrated
c   to give the total integrated release. In this version of the code
c   the affected area is allowed to be greater than the borehole
c   cross section for the appropriate diffusion coefficient and point in
c   time.
c
c WRITTEN: MARCH, APRIL 1993 FOR USED WITH SWIFT II VERSION 2B
C MODIFIED: AUGUST, 1993
C
C  AUTHOR: THOMAS A. BAER
c
c
c Variable names:
c
c          TUB  - simulation time (yr)
c          NOTV - current realization number
c          NCHNS - number of chains
c          NOISO - number of radionuclides
c          DEFF - No retardation effective diffusivity (ft**2/yr)
C          THETA - moisture content
C          AREAB - cross-sectional area of a single borehole
C          ERN - erosion depth (ft)
C          ROOTD - rooting depth (ft)
C          BIODENS - above ground plant biomass density (lb/ft**2)
C          NBORE - number of boreholes in analysis
C          DOB - depth of waste burial ( 70 ft - ERN )
C          DIFLEN - the approximate extend of diffusion after a given time
C          FLUX1TOT - total discharge via the surface pathway ( Ci)
C          FLUX2TOT - total discharge via the plant pathway ( Ci)
c
c
c Array names:
c
c          CSALL - solubility limits ( g/g)
c          NI - number of isotopes in each chain
c          T - array of time values at which concentrations are determined (yr)
c          DIFF - diffusivity of each isotope ( includes retardation ) (ft**2/yr)
C          AMALL - molecular weight of each isotope ( g/mol)
C          UPTAKE - plant uptake factor
C          RATALL - decay time constant of each isotope (1/yr)
C          HLFALL - half life of each isotope (yr)
C          FLUX1 - array of surface flux values (atm/ft**2-yr)
C          FLUX2 - array of plant flux values (atm/ft**2-yr)
C          FLUXI1 - integrated surface flux (atm)
C          FLUXI2 - integrated plant flux (atm)
C          FLUXI - total integrated flux (Ci)
C          NAMALL - array of isotope name strings
C
      IMPLICIT REAL*8 (A-H,O-Z)
      DIMENSION CSALL(25),NI(7)
      DIMENSION T(5000), DIFF(25), AMALL(21)
      DIMENSION UPTAKE(25),RATALL(25),HLFALL(25)
      DIMENSION FLUXI1(5000,25),FLUXI2(5000,25)
      DIMENSION FLUXI(5000,25), FLUX1(5000,25)
      DIMENSION FLUX2(5000,25)
c
      CHARACTER*6 NAMALL(25)
      CHARACTER*7 ISOTOP
      CHARACTER*15 HLFLIF
      CHARACTER*20 SOLLIM
c
      LOGICAL DF
```

```
C
      DATA AMALL/239.,235.,231.,227.,240.,236.,232.,241.,241.,
     +          237.,233.,229.,242.,238.,238.,234.,230.,226.,
     +          210.,90.,137./
C
      OPEN(10,FILE='tid.inp',STATUS='OLD')
      OPEN(11,FILE='tid2.dat',STATUS='UNKNOWN')
      OPEN(12,FILE='tid2.out',STATUS='UNKNOWN')
      OPEN(14,FILE='SWIFTNMD',STATUS='OLD')
C
C
C  INPUT DATE, TIME AND TITLE
C
C
C  INPUT VECTOR NUMBER
C
        READ(10,*)NOTV
        WRITE(12,*)'LHS VECTOR #',NOTV
C
C  INPUT SIMULATION TIME (YEARS)
C
        READ(10,*)TUB
        WRITE(12,*)'SIMULATION TIME(YRS) = ', TUB
C
C
C  INPUT # OF RADIOACTIVE CHAINS TO BE INCLUDED IN THE ANALYSIS
C
        READ(10,*)NCHNS
        WRITE(12,*)'# OF RADIOACTIVE CHAINS = ', NCHNS
C
C  INPUT THE NUMBER OF ISOTOPES IN EACH CHAIN
C
        NOISO = 0
        DO 10 I = 1,NCHNS
          READ(10,*)NI(I)
          WRITE(12,*)'FOR CHAIN ', I
          WRITE(12,*)'# OF MEMBERS = ', NI(I)
C
C  SUM TOTAL NUMBER OF ISOTOPES, NEEDED TO READ IN HLFALL AND CSALL ARRAY
C
          NOISO = NOISO + NI(I)
10      CONTINUE
        WRITE(12,*)'TOTAL # ISOTOPES = ', NOISO
C
C  READ IN EFFECTIVE DIFFUSION COEFFICIENT (FT**2/YEAR)
        READ(10,'(E15.5,A35,E15.5)') DEFF, ADUM, THETA
        WRITE(12,*)'EFFECTIVE DIFFUSION COEFF. = ',DEFF
        WRITE(12,*)'MOISTURE CONTENT = ',THETA
C
C  READ IN THE AREA
        READ(10,*)AREAB
        WRITE(12,*)'AREA (FT**2) = ', AREAB
C
C  READ IN EROSION DEPTH, ROOT DEPTH AND BIOMASS DENSISTY
        READ(10,*) ERN
        WRITE(12,*)' EROSION DEPTH (FT) = ',ERN
        READ(10,*) ROOTD
        WRITE(12,*)' ROOTING DEPTH (FT) = ',ROOTD
        READ(10,*)BIODENS
        WRITE(12,*)' BIOMASS DENSITY (LB/FT**2) = ', BIODENS
C
C  READ IN HALF-LIFES, NAMES, DIFFUSIVITIES, AND UPTAKE FACTORS
C   OF EACH ISOTOPE
C
        WRITE(12,*)'ISOTOPE    HALF-LIFE (YRS)    S. L.(AT/FT**3)   ',
     +     ' TRANS. FACTOR  ISOTOPE DIFFUSIVITY '
```

```
      READ(10,3) ISOTOP,HLFLIF,SOLLIM
3     FORMAT(1X,A7,8X,13A,2X,A17)
C
      DO 20 I = 1,NOISO
        READ(10,2)NAMALL(I),HLFALL(I),CSALL(I),UPTAKE(I),DIFF(I)
        RATALL(I) = 0.693/HLFALL(I)
        WRITE(12,2)NAMALL(I),HLFALL(I),CSALL(I),UPTAKE(I),DIFF(I)
2       FORMAT(1X,A6,6X,1P8E15.6,8X,1P8E15.6)
20    CONTINUE
c
c
c
c     NCHNS = 4
C
C
      DF = .TRUE.
      N = 1
      DIY = 365.
      DELX = .05
      NBORE = 4
c
c     NBORE = 6
c
      AREA = AREAB*NBORE
      DOB = 70.0 - ERN
      NFLAG = 0
      PI = 3.14159265358979323 8D0
c
C  THIS LOOP READS SWIFTNMD AND COMPUTES THE TID FOR EACH ISOTOPE
C
      DO WHILE (DF)
C
C
      READ(14, *, END = 117 )  T(N)
      WRITE(12,*) T(N)
      T(N) = T(N)/DIY
C
      ISTART = 1
C
      IEND = NI(1)
C
C  THIS LOOP READS IN THE DATA AND CONVERTS IT TO THE APPROPRIATE UNITS
c
      DO 40 I = 1,NCHNS
C
      DO 30 K = ISTART,IEND
C
      FACT = 6.02 * (10. ** 23) *453.593*62.4/AMALL(K)
C
C   READ CONCENTRATION HISTORIES FROM SWIFTNMD
C
C   FLUX2 = ROOT FLUX : FLUX1 = SURFACE FLUX
C
       READ(14,*)I1,NAMALL(K),D1,FLUX2(N,K),FLUX1(N,K)
c       WRITE(12,*)NAMALL(K),D1,FLUX2(N,K),FLUX1(N,K)
c
C   CHECK FOR ERRORS IN THE RUN
C
       IF ( ( D1 .LT. 0.0 ) .AND. ( DABS(D1) .GT. 1.0D-50 ) ) NFLAG = 1
C
C  CONVERT FROM MASS FRACTION TO ATM/FT**3
C
       FLUX1(N,K) = FLUX1(N,K)*FACT
C
C  FLUX1 IS COMPUTED HERE
C  FLUX2 IS NOT YET VEGETATIVE FLUX, IT WILL BE MADE SO LATER ON
```

```
C  BY MULTIPLICATION BY APPROPRIATE FACTORS
C
      FLUX1(N,K) = FLUX1(N,K)*DEFF*THETA/DELX
      FLUX2(N,K) = FLUX2(N,K)*FACT
C
C  NOTE THAT COMPUTATION THE SURFACE FLUX VIA THE PRECEDING RELATION
C   ASSUMES THAT THE LAST( THE SURFACE BLOCK )AND THE NEXT TO LAST GRID BLOCK
C   HAVE THE SAME WIDTH
C
c
  30   CONTINUE
C
      IF( I .NE. NCHNS ) THEN
       ISTART = ISTART + NI(I)
       IEND = ISTART + NI(I+1) - 1
      ENDIF
C
  40   CONTINUE
      N = N + 1

      ENDDO
C
 117   CONTINUE

C
      NTIME = N - 1
      ISTART = 1
      IEND = NI(1)
c
      WRITE(11,*)NCHNS
C
        FLUXI1TOT = 0.
        FLUXI2TOT = 0.
C
C  THIS SEQUENCE OF NESTED DO LOOPS INTEGRATES THE FLUXES
c
      DO 70 J = 1,NCHNS
C
      DO 50 I = 1,NTIME
c
       DO 60 K = ISTART,IEND
c
c       DIFLEN = DSQRT( 4.0*DEFF*T(I) )
       DIFLEN = DSQRT( 4.0*DIFF(K)*T(I) )
C
C THE FOLLOWING IF THEN LOOP COMPUTES THE AFFECTED AREA
C  IF THE DIFFUSION DISTANCE (DIFLEN) IS LESS THAT THE DISTANCE TO
C   THE SURFACE, THE AFFECTED AREA IS JUST THE NOMINAL AREA OF THE
C    BOREHOLE.  IF IT IS GREATER THAN THE DISTANCE TO SURFACE
C    THE AFFECTED AREA IS TAKEN TO THE CIRCULAR AREA ON THE SURFACE
C    WHICH IS SUBTENDED BY A CONE WITH APEX AT THE WASTE PILE AND
C    LONGEST SIDE EQUAL TO DIFLEN.  IF THIS AREA IS LESS THAN THE
C    THE NOMINAL BOREHOLE AREA, THE AFFECTED AREA IS SET TO THE NOMINAL AREA.
C
       IF( DIFLEN .LT. DOB ) THEN
c
         AREA = AREAB
c
       ELSE
C
          SQR = DIFLEN*DIFLEN - DOB*DOB
C
         IF( SQR .GT. 36.0 ) AREA = PI*SQR
         IF( SQR .LE. 36.0 ) AREA = AREAB
C
       ENDIF
```

```
c
      AREA = AREA*NBORE
c
c      WRITE(*,'(4E15.6)') T(I), FLUX1(I,4)*AREA, FLUX2(I,4)*AREA,AREA
c
C  INTEGRATE NUMERICALLY USING THE TRAPEZOIDAL RULE
C
      FLUX1(I,K) = FLUX1(I,K)*AREA
      FLUX2(I,K) = FLUX2(I,K)*AREA
C
      IF( I.EQ.1 ) THEN
        FLUXI1(I,K) = FLUX1(I,K)*T(I)/2.0
        FLUXI2(I,K) = FLUX2(I,K)*T(I)/2.0
      ELSE
        FLUXI1(I,K) = FLUXI1(I-1,K) + (FLUX1(I,K) + FLUX1(I-1,K))*
     +                          (T(I) - T(I-1))/2.0
        FLUXI2(I,K) = FLUXI2(I-1,K) + (FLUX2(I,K) + FLUX2(I-1,K))*
     +                          (T(I) - T(I-1))/2.0
      ENDIF
C
 60   CONTINUE
 50   CONTINUE
C
C
      DO 80 M = ISTART, IEND
C
C  THIS FACTOR CONVERTS FROM ATOMS TO CURIES
C
      FACT = 1.684E18 * HLFALL(M)
C
C  HERE WE MULTIPLY THE CONCENTRATION AT THE ROOTING DEPTH BY
C   THE UPTAKE FACTOR AND THE BIOMASS DENSITY TO ARRIVE AT A
C    VEGETATIVE FLUX
C
C  THE FACTOR OF 2.0 IN THE FOLLOWING ACCOUNTS FOR TURNOVER
C   IN THE BIOMASS DENSITY.  IN A ONE YEAR PERIOD IT IS ASSUMED
C   THAT THE BIOMASS IS TURNED OVER TWICE.
c
      FLUXI2(NTIME,M) = FLUXI2(NTIME,M)*UPTAKE(M)*BIODENS*2.0
c
      FLUXI2(NTIME,M) = FLUXI2(NTIME,M)*2.0
      FLUXI2(NTIME,M) = FLUXI2(NTIME,M)/FACT
C
      FLUXI1(NTIME,M) = FLUXI1(NTIME,M)/FACT
      FLUXI(NTIME,M)  = FLUXI1(NTIME,M) + FLUXI2(NTIME,M)
C
      FLUXI1TOT = FLUXI1TOT + FLUXI1(NTIME,M)
      FLUXI2TOT = FLUXI2TOT + FLUXI2(NTIME,M)
C
C  DE-BUG WRITE TO OUTPUTFILE
C
c     WRITE(12,*)M,'FLUXI1=',FLUXI1(NTIME,M),'FLUXI2=',FLUXI2(NTIME,M)
C
80       CONTINUE
C
C  OUTPUT TO TID2.DAT
C
      WRITE(11,*)NI(J),(NAMALL(K),K=ISTART,IEND)
      WRITE(11,*)NOTV,(FLUXI(NTIME,K),K=ISTART,IEND)
c
     IF( J .NE. NCHNS ) THEN
      ISTART = ISTART + NI(J)
      IEND = ISTART + NI(J+1) - 1
     ENDIF
c
70   CONTINUE
```

```
C
      IF ( NFLAG .EQ. 1 ) THEN
        WRITE(11,*)' ### WARNING: NEGATIVE CONCENTRATION DETECTED ###'
        WRITE(11,*) 'VECTOR NUMBER : ',NOTV
      ENDIF
C
        WRITE(12,*)' TOTAL INTEGRATED DISCHARGES: '
        WRITE(12,'(3(A,E15.6))')' PAST EROSION DEPTH : ',
     *    FLUXI1TOT,' VIA PLANT PATH : ',FLUXI2TOT,
     *              ' PAST SURFACE   : ',FLUXI3TOT

C
      END
```

```
      PROGRAM COMBINEII
C
C  This program combines the output from NEFTRANII, which is contained
C  in nefii.dis, and the output from LIQDIF2, which
C  is contained in intdis2.dat.  It produces a file that is ready
C  to be read by CCDFTRUIIFI to produce ccdf plots
C
      INTEGER I,J,K,L,N,NI,NID,NCHNS,NCHNSD,NSAMP,LHSVN,LHSVND,NUMDIF
      DIMENSION NI(7),NID(7)
      DOUBLE PRECISION REL(24),RELD(7,7)
      CHARACTER*80 TITLE,ADUMMY
      CHARACTER*6 NAM(24)
      CHARACTER*6 NAMD(7,7)
      OPEN(10,FILE='intdis2.dat',STATUS='OLD')
      OPEN(15,FILE='cumrel.dat',STATUS='UNKNOWN')
      OPEN(20,FILE='nefii.dis',STATUS='OLD')

C
C
C  Read the title from nefii.dis
C
      READ(20,1) TITLE
      WRITE(15,1) TITLE
      READ(20,1)ADUMMY
      WRITE(15,1)ADUMMY
1     FORMAT(A)
C
C  Read the number of LHS vectors for which the diffusion program was run
C  and the total number of LHS vectors.
C
      READ(10,*) NUMDIF, NSAMP
C
C  Begin a loop to read the output vectors from intdis2.dat.  These vectors
C  are in order, except for when liquid phase diffusion dominates.  When
C  this occurs, NEFTRAN is not run and the output for that LHS vector is
C  skipped.  When NEFTRAN is finished, a file has been created that is the
C  input file for the liquid phase diffusion program.  Once LIQDIF2 is run,
C  the output from LIQDIF2 needs to be added to the output from NEFTRAN, with
C  the results in the right LHS-sample order.
C
      IF (NUMDIF .EQ. 0) THEN
        LHSVND = 0
      ELSE
        L=0
            NOISO = 0
        READ(10,*)NCHNSD
        DO 10 J=1,NCHNSD
          READ(10,*)NID(J),(NAMD(J,K),K=1,NID(J))
2         FORMAT (I3,7(A6))
          READ(10,*)LHSVND,(RELD(J,K),K=1,NID(J))
          NOISO = NOISO + NID(J)
10      CONTINUE
      ENDIF
      DO 20 I = 1,NSAMP
        IF (LHSVND .EQ. I) THEN
            IPASS = 1
            NRATE = 0
            JTRIAL = I
            NC = NOISO + 1
            WRITE(15,9070)IPASS,JTRIAL,NRATE,NC
            WRITE(15,9050)((NAMD(J,K),K=1,NID(J)),J=1,NCHNSD)
            WRITE(15,*)TUB,((RELD(J,K),K=1,NID(J)),J=1,NCHNSD)
          L=L+1
          IF (L .LT. NUMDIF) THEN
            READ(10,*)NCHNSD
            DO 35 J=1,NCHNSD
```

```
            READ(10,*)NID(J),(NAMD(J,K),K=1,NID(J))
            READ(10,*)LHSVND,(RELD(J,K),K=1,NID(J))
35          CONTINUE
          ENDIF
        ELSE
            READ(20,9060)ADUMMY,IPASS,ADUMMY,
     +                  JTRIAL,ADUMMY,NRATE,ADUMMY,NC
         WRITE(15,9070)IPASS,JTRIAL,NRATE,NC
C
            READ(20,9050)(NAM(K),K=1,NC-1)
         WRITE(15,9050)(NAM(K),K=1,NC-1)
         READ(20,*)TUB,(REL(K),K=1,NC-1)
         WRITE(15,*)TUB,(REL(K),K=1,NC-1)
C
          DO 40 J = 1,NRATE
            READ(20,*)TUB,(REL(K),K=1,NC-1)
            WRITE(15,*)TUB,(REL(K),K=1,NC-1)
40          CONTINUE
        ENDIF
20    CONTINUE
C
 9050 FORMAT(4(15(1X,A6),/))
 9060 FORMAT(A9,I3,A7,I5,A8,I4,A10,I4)
 9070 FORMAT(' DATA SET',I3,', TRIAL',I5,', #RATES',I4,', #COLUMNS',I4)
comt 2     FORMAT (I12,7(A6))
C3     FORMAT (I4,7(2X,E24.16))
      STOP
      END
```

```
      PROGRAM SORTER
c
c  This program sorts an input one-dimensional array
c   from maximum to minimum.  It also computes the
c   the mean, median, and 95th percentile values
c
      EXTERNAL COMPAR
C
      DIMENSION X(10000),Y(10000)
      CHARACTER*6 NAM(10000), NAME(21)
c
C     open(unit=10,file='out.75',status='append')
C     open(unit=11,file='out.95',status='append')
C
      J = 1
C
c  Read the data arrays from standard input
c
      DO WHILE ( J .GT. 0 )
       READ(5,*,END=100)NAM(J),X(J),Y(J)
       J = J + 1
      END DO
C
 100  CONTINUE
C
c  QSORT is SUN FORTRAN utility subroutine that automatically
c   sorots an array supplied to it.
c
      CALL QSORT(X,J-1,4,COMPAR)
C
c      WRITE(6,*)'Maximum ',NAM(1),' concentration : ',X(1)
c
c   J is the number of entries in X
c
      J = J - 1
C
c   K is the location of the median
c
      K = INT(J/2) + 1
C
c      WRITE(6,*)' Median ',NAM(1),' concentration : ',X(K)
c
c  The mean is computed as would be expected
c
       CMEAN = 0.
C
      DO 20 K = 1,J
       CMEAN = CMEAN + X(K)
 20    CONTINUE
       CMEAN = CMEAN / J
c
      L = 1
c
c  Compute the location of the 95th percentile
C
      KQUA2 = ( J - INT ( .95*J ) ) + 1
C
      WRITE(6,*)' Mean ',NAM(1),' concentration : ',CMEAN
      WRITE(6,*)'                 95th quantile : ',X(KQUA2)

C
      END
C
      INTEGER*2 FUNCTION COMPAR(A,B)
C
      REAL A,B
```

```
      IF ( A .GT. B ) COMPAR = -1
      IF ( A .EQ. B ) COMPAR = 0
      IF ( A .LT. B ) COMPAR = 1
      RETURN
C
      END
```

```
c
      PROGRAM VAPDIF2
C     NOVEMBER, 1992
C     CREATED BY LAURA PRICE
C     ANALYTICAL SOLUTION FOR TIME-VARYING VAPOR PHASE
C     DIFFUSION FOR GCD PA
C
C     GOVERNING EQUATION: dC = DEFF d**2C - kbC
C                         dt       dx**2
C
C     BOUNDARY CONDITIONS: C = 0 AT x = L.
C                          C = CO*EXP(-ka*t) AT X = 0
C     INITIAL CONDITION:   C = 0 AT t = 0
C
C
      REAL NUM,KA,KB,I,L, MASSPB, MASSPO
      OPEN(UNIT=10,FILE='vapdif2.inp',STATUS='OLD')
      OPEN(UNIT=11,FILE='vapdif2.out',STATUS='UNKNOWN')
C
C     INPUT REQUIRED FOR SOLUTION
C
C     INPUT SWITCH FOR PATHWAY TO ANALYZE
C        1 - DIFFUSION OF RADON TO GROUND SURFACE
C        2 - DECAY OF 222RN AT ROOT ZONE AND UPTAKE OF 210PB
      READ (10,*)PS
C
C     INPUT SWITCH FOR REQUIREMENT TO ANALYZE
C        1 - CONTAINMENT REQUIREMENTS
C        2 - INDIVIDUAL PROTECTION REQUIREMENTS
      READ (10,*)RS
C
C     INPUT INITIAL CONCENTRATION, CO (PICOCURIES/LITER)
      READ(10,*)CO
C
C     INPUT EFFECTIVE DIFFUSIVITY (CM**2/SEC)
      READ(10,*)DEFF
C
C     CONVERT DEFF FROM CM**2/SEC TO FT**2/YR
      DEFF = DEFF*(60.0*60.0*24.0*365.25)/(30.48*30.48)
C
C     INPUT DISTANCE (FEET) ABOVE RADON SOURCE AT WHICH
C     CALCULATIONS ARE TO BE PERFORMED.
      READ(10,*)X
C
C     INPUT DISTANCE (FEET) FROM RADON SOURCE TO GROUND SURFACE
      READ (10,*)L
C
C     INPUT TIME (YEARS) FOR WHICH ANALYSIS TO BE DONE
      READ(10,*)TIME
C
C     INPUT NUMBER OF TIME STEPS
      READ(10,*) NTS
C
C     INPUT HALF-LIFE OF PARENT (YEARS)
      READ(10,*) HA
C
C     INPUT HALF-LIFE OF DAUGHTER (YEARS)
      READ(10,*) HB
C
      KA = 0.6931/HA
      KB = 0.6931/HB
C
C     ECHO TO OUTPUT FILE THE INPUT VALUES
      WRITE(11,*)'INITIAL CONCENTRATION =',CO,' PICOCURIES/LITER'
      WRITE(11,*)'EFFECTIVE DIFFUSION COEFF =',DEFF,' FEET**2/YEAR'
```

```
      WRITE(11,*)'CALCULATIONS PERFORMED ',X,' FEET ABOVE SOURCE'
      WRITE(11,*)'DISTANCE FROM SOURCE TO GROUND SURFACE = ',L,' FEET'
      WRITE(11,*)'DECAY CONSTANT FOR PARENT, K1, =',KA,' 1/YEAR'
      WRITE(11,*)'DECAY CONSTANT FOR DAUGHTER, K2, =',KB,' 1/YEAR'
      WRITE(11,*)'CALCULATION PERFORMED FOR ',TIME,' YEARS'
      WRITE(11,*)' '
      IF (PS.EQ.1) THEN
        WRITE(11,*)'PATHWAY: RADON DIFFUSION TO GROUND SURFACE'
      ENDIF
      IF (PS.EQ.2) THEN
        WRITE(11,*)'PATHWAY: UPTAKE OF 210PB BY PLANT ROOTS'
      ENDIF
      IF (RS.EQ.2) THEN
        WRITE(11,*)'REQUIREMENT: INDIVIDUAL PROTECTION REQUIREMENTS'
        WRITE(11,*)'    C.E.D.E. (MREM/YR)   TIME(YEAR)'
      ENDIF
C     INITIALIZE CONSTANTS
      PI=3.1415926
C     ASSUME AIR-FILLED POROSITY (THETA SUB A) EQUALS 0.30.
      THETAA=0.30
      Z=SQRT((KB-KA)/DEFF)
C     WRITE(*,*)'Z= ',Z
      CUMULPB=0.
C
C     BEGIN TIME LOOP
      DO 10 J = 1,NTS
        I=J*TIME/NTS
C
C       BEGIN CALCULATIONS FOR PATHWAY 1, RADON DIFFUSION TO GROUND
C       SURFACE.  FOR BOTH THE INDIVIDUAL PROTECTION AND CONTAINMENT
C       REQUIREMENTS, THE CONCENTRATION GRADIENT OF RADON AT THE
C       GROUND SURFACE IS NEEDED.
C
        IF (PS.EQ.1) THEN
          SUM=0
          DO 20 K = 1,20
            F=DEFF*(K**2)*(PI**2)/(L**2)
C             WRITE(*,*)'F= ',F
            NUM=EXP(-I*(F+KB))*COS(K*PI*(L-X)/L)
            DEN=KB-KA+F
            SUM=SUM+(((-1)**K)*K*K*NUM/DEN)
C             WRITE(*,*)'SUM= ',SUM
20          CONTINUE
          FIRST=CO*Z*EXP(-KA*I)*(EXP(Z*(L-X))+EXP(-Z*(L-X)))/
     *          (EXP(Z*L)-EXP(-Z*L))
          SECOND=2*CO*DEFF*PI*PI*SUM/(L**3)
          GRAD=-FIRST-SECOND
C         WRITE(*,*)'FIRST TERM = ',FIRST
C         WRITE(*,*)'SECOND TERM = ',SECOND
C         WRITE(*,*)'CONCENTRATION GRADIENT = ',GRAD
C
C     CALCULATE EITHER THE DOSE FROM INHALING ANY ISOTOPE OF RADON (RS=2)
C     OR THE CUMULATIVE RELEASE OF PB210 TO THE ACCESSIBLE ENVIRONMENT
C     (RS=1) RESULTING FROM THE RELEASE OF 222RN AT THE GROUND SURFACE
C
          IF (RS.EQ.1) THEN
            RNFLUX=(-DEFF)*GRAD*THETAA*25*PI*28.317
c
c   Note there are 28.317 L / ft ** 3
c
            PBFLUX=RNFLUX*76.23*210./1.5376E17/222.
            CUMULPB=CUMULPB+(PBFLUX*TIME/NTS)
C             WRITE(*,*)'CUMULATIVE PB RELEASED (CURIES) = ',CUMULPB
          ENDIF
C
          IF (RS.EQ.2) THEN
```

```
            RNCONC=(-3)*THETAA*GRAD
c           WRITE(*,*) 'RADON CONC 3 FT ABOVE GROUND = ',RNCONC
c
c  This conversion factor was used in the draft version of PAII
c
            DOSCON = 3000.
c
c  This conversion factor was used in the final version of PAII
c   If gives dose in terms of commited effective dose equivalent
c   It is based upon numbers described in NCRP Report #94 which
c   where interpreted by G.J. Shott of REECo.  This interpretationc
c   was communicated to N.E. Olague in a formal letter that should
c   be present in the GCD Record Center.
c   The value is 360 mrem/yr CEDE for a one year exposure to 1 pCi/L
c   of Rn222
c
c
            DOSCON = 360.
            DOSE=RNCONC*DOSCON
            WRITE(11,*)DOSE,I
          ENDIF
        ENDIF
C
C     BEGIN CALCULATIONS FOR PATHWAY 2, 222RN DECAYING AT THE
C     ROOT ZONE AND BEING TAKEN UP BY PLANTS AS 210PB.
C     FIRST, FIND THE CONCENTRATION AT THE DISTANCE
C     GIVEN AS THE ROOT ZONE, X
C
        IF (PS.EQ.2) THEN
          SUM=0
          DO 30 K = 1,20
            F=DEFF*(K**2)*(PI**2)/(L**2)
            NUM=EXP(-I*(F+KB))*SIN(K*PI*(L-X)/L)
            DEN=KB-KA+F
            SUM=SUM+(((-1)**K)*K*NUM/DEN)
C            WRITE(*,*)'SUM= ',SUM
30         CONTINUE
          FIRST=CO*EXP(-KA*I)*(EXP(Z*(L-X))-EXP(-Z*(L-X)))/
     *          (EXP(Z*L)-EXP(-Z*L))
          SECOND=2*CO*DEFF*PI*SUM/(L**2)
          CONC=FIRST+SECOND
C         WRITE(*,*)'CONCENTRATION FIRST TERM = ',FIRST
C         WRITE(*,*)'CONCENTRATION SECOND TERM = ',SECOND
C         WRITE(*,*)'CONCENTRATION (pCi/L) = ',CONC
C
C         CALCULATE THE CUMULATIVE RELEASE OF 210PB TO THE
C         ACCESSIBLE ENVIRONMENT VIA ROOT UPTAKE OR THE
C         DOSE TO A MEMBER OF THE PUBLIC RESULTING FROM
C         INGESTING 210PB.
C
          PBCONC=CONC*THETAA*76.23*210.*28.317/
     *           (99.26*454*1.5376E17*222.)
c
c
c
C         WRITE(*,*)'ANNUAL CURIES OF 210PB RELEASED = ',ANNUALPB
C
          IF (RS.EQ.1) THEN
            ANNUALPB=PBCONC*0.147*PI*25.*0.1*2.0*454.
            CUMULPB=CUMULPB+(ANNUALPB*TIME/NTS)
c           WRITE(*,*)'CUMUL CURIES OF 210PB REL = ',CUMULPB
          ENDIF
C
          IF (RS.EQ.2) THEN
c
c  annual consumption of vegetables: McKenzie et.al. NUREG/CR-2675
```

```
c
        VEGCONS = 665.     ! kg/year

        ANNUALPB=PBCONC*0.147*VEGCONS*1000.
        ANNUALPO=ANNUALPB
c
        MASSPB = ANNUALPB/76.23
        MASSPO = ANNUALPO/4483.3
c
        DOSE= MASSPB*3.9E11 + MASSPO*7.2E12
C
C  DOSE IS CEDE
C

C            WRITE(*,*)'DOSE = ',DOSE
            WRITE(11,*)DOSE,I
          ENDIF
        ENDIF
10    CONTINUE
C
C     WRITE OUT RESULTS FOR CONTAINMENT REQUIREMENTS
C
      IF (RS.EQ.1) THEN
       WRITE(11,*)'REQUIREMENT:  CONTAINMENT REQUIREMENTS'
       WRITE(11,*)'TOTAL CURIES OF 210PB RELEASED = ',CUMULPB
      ENDIF
C
      STOP
      END
```

```
C
      PROGRAM LIQDIF3E_QA
c
c  Special version of LIQDIF3E.  It is used to compute an
c   analytic solution for comparison to SWIFT
c
      IMPLICIT REAL*8 (A-H,O-Z)
      DIMENSION CSALL(25),NI(7), IND(25)
      DIMENSION FLUXD1(500),FLUXD2(500), FLUXD3(500)
      DIMENSION T(500),CDECAY(500,25), DIFF(25), DEF(25), SIG(25)
      DIMENSION UPTAKE(25),RATALL(25),CDUMMY(25),HLFALL(25)
      DIMENSION FLUXI1(500,25),FLUXI2(500,25), AINV(25)
      DIMENSION FLUXI3(500,25),FLUXI(500,25), FLUX1(500,25)
      DIMENSION FLUX2(500,25), FLUX3(500,25), CAVE(500)
      DIMENSION CPLOT(1500,5)
      DATA (UPTAKE(I),I=1,25) /25*1E-3/
c
      DATA (AINV(I),I=1,16) / 298.5,
     +          .083 ,
     +          0.0  ,
     +          0.0  ,
     +          68.69,
     +          .0671,
     +          0.00 ,
     +         567.25,
     +         75.35 ,
     +          0.0 ,
     +          0.0 ,
     +          0.0 ,
     +          .0047,
     +          .2055,
     +          13.79,
     +           1.97/
c
      CHARACTER*9 DAT
      CHARACTER*9 TIM
      CHARACTER*40 TITLE
      CHARACTER*6 NAMALL(25)
      CHARACTER*7 ISOTOP
      CHARACTER*15 HLFLIF
      CHARACTER*20 SOLLIM
      LOGICAL DF
      OPEN(9,FILE='numdif.dat',STATUS='OLD')
      OPEN(10,FILE='liqdif.inp',STATUS='OLD')
      OPEN(11,FILE='intdis2.dat',STATUS='UNKNOWN')
      OPEN(12,FILE='liqdif3e_QA.out',STATUS='UNKNOWN')
C
C  SUB-PROGRAM: LIQUID DIFFUSION
C  WRITTEN BY: N.E. OLAGUE AND L.L. PRICE      DATE:7/90
C  MODIFIED BY: T.A. BAER                      DATE:9/92
C  MODIFIED BY: T.A. BAER                      DATE:8/93
C  THIS PROGRAM IS AN ANALYTIC SOLUTION TO THE LIQUID DIFFUSION
C  BASE CASE FOR THE GCD PPA, ASSUMING THAT THE *CONCENTRATION* EQUALS ZERO
C  AT THE GROUND SURFACE (70 FEET).  * ABSORPTION, PLANT UPTAKES AND EROSION
C   INCLUDED IN MODEL *
c  CHANGES TO THE MODEL TO MAKE IT CONSISTENT WITH THE REVISED 2ND PA HAVE
C   BEEN DONE.
C
c  THE PERFORMANCE MEASURE IS THE INTEGRATED
C  FLUX AT THE ACCESSIBLE ENVIRONMENT FOR EACH ISOTOPE.  THIS CODE
C  SIMULATES DIFFUSION AND RADIOACTIVE DECAY FOR RADIOACTIVE DECAY
C  CHAINS WITH MULTIPLE MEMBERS.  THE PURPOSE OF THIS SUB-PROGRAM
C  IS TO BE INCLUDED WITH THE GETRV SUBROUTINE IN NEFTRAN.  DEPENDING
C  ON THE RECHARGE VARIABLE THAT IS SAMPLED BY LHS, THIS MODEL MAY OR
C  MAY NOT BE USED.  IT IS MEANT FOR THE VARIABLES TO BE NAMED
C  CONSISTENTLY WITH VARIABLES FROM NEFTRAN WHEN IT IS POSSIBLE.  THE
```

```
C  OUTPUT FROM THIS MODEL WILL BE WRITTEN TO THE SAME OUTPUT FILE THAT
C  NEFTRAN USES(TAPE20).
C
C LIST OF VARIABLES:
C
C     NCHNS  = NUMBER OF CHAINS TO BE INCLUDED IN THE ANALYSIS
C     TUB    = SIMULATION TIME (COMMON WITH NEFTRAN), YEARS
C     NTIME  = NUMBER OF TIMES FLUX IS CALCULATED DURING
C              SIMULATION TIME (DECLARED IN SUBPROGRAM)
C     DEFF   = EFFECTIVE DIFFUSION COEFFICIENT(DECLARED IN
C              SUBPROGRAM IN TERMS OF SAMPLED VARIABLES), FT**2/YR
C     H1     = DISTANCE TO THE ROOT ZONE (DELCARED IN SUBPROGRAM), FT
C     H2     = DISTANCE TO THE LAND SURFACE, FT
C     PI     = CONSTANT DECLARED IN SUBPROGRAM
C     T      = ARRAY OF TIMES THAT FLUX IS FOUND, YEARS
C     FLUXD1 = ARRAY OF PART OF THE DIFFUSION FLUX AT THE ROOT
C              ZONE, DIMENSIONLESS
C     FLUXD2 = ARRAY OF PART OF THE DIFFUSION FLUX AT THE GROUND
C              SURFACE, DIMENSIONLESS
C     CDECAY = ARRAY OF DECAY PART OF FLUX, ATOMS/FT**3
C     CDUMMY = ARRAY OF DECAY PART OF SOLUTION SENT FROM SUBROUTINE
C              RADECAY AND ASSIGNED TO THE CDECAY ARRAY
C     HLFALL = ARRAY OF HALF-LIVES OF EACH ISOTOPE (COMMON WITH NEFTRAN)
C              THIS IS A 1-D ARRAY WHERE THE ISOTOPES ARE IN SEQUENTIAL
C              ORDER FROM CHAIN 1 TO CHAIN NCHNS
C     RATALL = ARRAY OF DECAY RATES (0.693/HALF-LIFE), 1/YEAR)  THIS
C              IS A 1-D ARRAY WHERE THE ISOTOPES ARE INSEQUENTIAL ORDER
C              FROM CHAIN 1 TO CHAIN NCHNS.
C     CSALL  = ARRAY OF SOLUBILITY LIMITS (COMMON WITH NEFTRAN)
C              ASSUMED TO BE INITIAL CONCENTRATIONS FOR DECAY
C              INITIAL CONDITION, ATOMS/FT**3.  THE ISOTOPES ARE IN
C              THE SAME ORDER AS THE HLFALL ARRAY DESCRIBED ABOVE
C     ERN    = EROSION DEPTH. DEPTH OF ALLUVIUM REMOVED IN 10,000 YRS. (FT)
C     DOB    = DEPTH OF BURIAL, ORIGINAL SURFACE HEIGHT ABOVE WASTE
C               LESS THE EROSION DEPTH (FT)
C     CAVE   = ARRAY OF AVERAGE CONCENTRATION WITHIN THE ROOT ZONE
C     UPTAKE = ARRAY OF UPTAKE FACTORS IN PLANTS FOR EACH RADIONUCLIDE
C               ACTUALLY THIS IS THE CONCENTRATION RATIO MULTIPLIED BY:
C                  A CONVERSION FACTOR FROM LIQUID PHASE TO SOLID PHASE
C                           CONCENTRATIONS
C                THE ABOVE GROUND BIOMASS DENSITY
C     FLUX1  = ARRAY OF FLUX FOR EACH ISOTOPE AT EACH TIME AT THE
C              ROOT ZONE, ATOMS/FT**3
C     FLUX2  = ARRAY OF OF FLUX FOR EACH ISOTOPE AT EACH TIME AT THE
C              GROUND SURFACE, ATOMS/FT**3
C     FLUXI1 = ARRAY OF INTEGRATED FLUX FOR EACH ISOTOPE AT THE
C              ROOT ZONE, CI
C     FLUXI2 = ARRAY OF INTEGRATED FLUX FOR EACH ISOTOPE AT THE
C              GROUND SURFACE, CI
C     FLUXI  = ARRAY OF INTEGRATED FLUX FOR EACH ISOTOPE, CI
C     ISTART = BEGINNING POINTER FOR HLFALL AND CSALL ARRAY
C     IEND   = ENDING POINTER FOR HLFALL AND CSALL ARRAY
C     NOISO  = TOTAL NUMBER OF ISOTOPES
C     TAU    = TORTUOSITY, SAMPLED IN LHS, USED TO CALCULATE DEFF,
C              DIMENSIONLESS
C     THETA  = MOISTURE CONTENT, SAMPLED IN LHS, USED TO CALCULATE DEFF,
C              DIMENSIONLESS
C     DEFF   = EFFECTIVE DIFFUSION COEFFICIENT ASSUMED TO BE CONSTANT
C              FOR ALL RADIONUCLIDES, FT**2/YR
c     DIFF   = VECTOR OF DIFFUSIVITIES OF EACH ISOTOPE
C     NOTV   = # OF THE CURRENT VECTOR FROM LHS, COMMON WITH NEFTRAN
C     NAMALL = CHARACTER ARRAY WITH THE NAME OF EACH ISOTOPE
C     ROOTDN = ROOT DENSITY, DIMENSIONLESS
C     DAT    = DATE CHARACTER STRING INPUT BY USER
C     TIM    = TIME CHARACTER STRING INPUT BY USER
C     TITLE  = TITLE CHARACTER STRING INPUT BY USER
```

```
C
C  INPUT STATEMENTS
C
C  INPUT THE NUMBER OF LHS VECTORS FOR WHICH THE DIFFUSIVE FLUX
C  IS GREATER THAN THE RECHARGE FLUX AND THE TOTAL NUMBER OF LHS VECTORS
C
      READ(9,*) NUMDIF, NOVEC
      WRITE(11,*) NUMDIF, NOVEC
      DO 200 ND = 1,NUMDIF
      WRITE(*,*) ND
C
C  INPUT DATE, TIME AND TITLE
C
      READ(10,1)DAT
      READ(10,1)TIM
      READ(10,1)TITLE
      WRITE(12,*)DAT,TIM,TITLE
1     FORMAT(A20)
C
C  INPUT VECTOR NUMBER
C
      READ(10,*)NOTV
      WRITE(12,*)'LHS VECTOR #',NOTV
C
C  INPUT SIMULATION TIME (YEARS)
C
      READ(10,*)TUB
      WRITE(12,*)'SIMULATION TIME(YRS) = ', TUB
C
C  INPUT NUMBER OF TIMES FLUX IS CALCULATED DURING SIMULATION TIME (YRS)
C
      NTIME=40
      WRITE(12,*)'NUMBER OF POINTS = ', NTIME

C
C  CALCULATE TIME INCREMENTS BASED ON TUB AND NTIME
C
      DELTAT = TUB/FLOAT(NTIME)
      WRITE(12,*)'TIME INCREMENT (YR) = ', DELTAT
C
C  DISTANCE TO ROOT ZONE AND TO GROUND SURFACE (FT)
C
      H1 = 35.0
      H2 = 70.0
      WRITE(12,*)'DISTANCE TO ROOT ZONE (FT) = ', H1
      WRITE(12,*)'DISTANCE TO GROUND SURFACE (FT) = ', H2
C
C  INPUT # OF RADIOACTIVE CHAINS TO BE INCLUDED IN THE ANALYSIS
C
      READ(10,*)NCHNS
      WRITE(12,*)'# OF RADIOACTIVE CHAINS = ', NCHNS
C
C  INPUT THE NUMBER OF ISOTOPES IN EACH CHAIN
C
      NOISO = 0
      DO 10 I = 1,NCHNS
        READ(10,*)NI(I)
        WRITE(12,*)'FOR CHAIN ', I
        WRITE(12,*)'# OF MEMBERS = ', NI(I)
C
C  SUM TOTAL NUMBER OF ISOTOPES, NEEDED TO READ IN HLFALL AND CSALL ARRAY
C
        NOISO = NOISO + NI(I)
10    CONTINUE
      WRITE(12,*)'TOTAL # ISOTOPES = ', NOISO
C
```

```
C  READ IN EFFECTIVE DIFFUSION COEFFICIENT (FT**2/YEAR)
      READ(10,'(E15.5,A35,E15.5)') DEFF, ADUM, THETA
      WRITE(12,*)'EFFECTIVE DIFFUSION COEFF. = ',DEFF
      WRITE(12,*)'MOISTURE CONTENT = ',THETA
C
C  READ IN THE AREA
      READ(10,*)AREA
      WRITE(12,*)'AREA (FT**2) = ', AREA
      READ(10,*) ERN
      WRITE(12,*)' EROSION DEPTH (FT) = ',ERN
      READ(10,*) ROOTD
      WRITE(12,*)' ROOTING DEPTH (FT) = ',ROOTD
      READ(10,*)BIODENS
      WRITE(12,*)' BIOMASS DENSITY (LB/FT**2) = ', BIODENS
c
      IF( H2 - ERN - ROOTD .LT. 0.0)THEN
C
        WRITE(12,*) ' *WARNING* ROOTS ENTERING WASTE '
C
      ENDIF

C
C  READ IN HALF-LIFES AND NAME OF EACH ISOTOPE (YRS)
C
c       WRITE(12,*)'ISOTOPE    HALF-LIFE (YRS)    S. L.(AT/FT**3)   ',
c    +      ' TRANS. FACTOR  ISOTOPE DIFFUSIVITY '
      READ(10,3) ISOTOP,HLFLIF,SOLLIM
3      FORMAT(1X,A7,8X,13A,2X,A17)
C
      DO 20 I = 1,NOISO
        READ(10,2)NAMALL(I),HLFALL(I),CSALL(I),UPTAKE(I),DIFF(I)
        RATALL(I) = 0.693/HLFALL(I)
C         WRITE(12,2)NAMALL(I),HLFALL(I),CSALL(I),UPTAKE(I),DIFF(I)
2       FORMAT(1X,A6,6X,1P8E15.6,8X,1P8E15.6)
20     CONTINUE
C
C  INITIALIZE CONSTANTS
C
      PI = 3.141592653589793238D0
      ISTART = 1
      IEND = NI(1)
      NBORE = 4
      AREA = AREA*NBORE
C
C  GIVEN BELOW ARE THE RADIONUCLIDE CHAINS THAT ARE CONSIDERED
C  IN THE ANALYSIS ALONG WITH THE NUMBER ASSIGNED TO EACH RADIONUCLIDE
C
C  CHAIN 1:
C
C     1      2      3      4
C    PU239 -> U235 -> PA231 -> AC227
C
C  CHAIN 2:
C
C     5      6      7
C    PU240 -> U236 -> TH232
C
C  CHAIN 3:
C
C     8      9      10     11     12
C    PU241 -> AM241 -> NP237 -> U233 -> TH229
C
C  CHAIN 4:
C
C   13     14     16     17     18     19
C  PU242 -> U238 -> U234-> TH230 -> RA226 -> PB210
```

```
C                 |
C             15  |
C           PU238 ->
C
C  CHAIN 5:
C
C    20
C   SR90
C
C  CHAIN 6:
C
C    21
C   CS137
C
C
C
C  BECAUSE CHAIN 4 HAS A BRANCH, IT IS DIFFICULT TO CALCULATE DECAY.
C  THIS CHAIN BECOMES TWO CHAINS, CHAIN 4:
C
C        13      14     15       16       17      18
C      PU242 -> U238 -> U234 -> TH230 -> RA226 -> PB210
C
C   AND CHAIN 5:
C
C        19      20      21       22      23
C      PU238 -> U234 -> TH230 -> RA226 -> PB210.
C
C  SR90 AND CS137 BECOME NUMBER 24 AND 25, RESPECTIVELY.
C  CUMULATIVE RELEASES ARE CALCULATED, AND THEN THE RELEASES OF THE
C  RADIONUCLIDES THAT ARE COMMON BETWEEN THE TWO CHAINS (15 AND 20,
C  16 AND 21, 17 AND 22, AND 18 AND 23) ARE SUMMED BEFORE PRINTING
C  OUT TO THE OUTPUT FILE OF CUMULATIVE RELEASE.
C
C  BEGIN REDEFINING VARIABLES TO ACCOUNT FOR THE NEW CHAIN
C
       NI(4) = 6
       NI(5) = 5
       NI(6) = 1
       Ni(7) = 1
       NCHNS = NCHNS + 1
       NOISO = NOISO + 4
       DO 30 I = 1,(NOISO - 18)
         J = NOISO + 1 - I
         K = J - 4
         CSALL(J) = CSALL(K)
         NAMALL(J) = NAMALL(K)
         RATALL(J) = RATALL(K)
         HLFALL(J) = HLFALL(K)
         UPTAKE(J) = UPTAKE(K)
         DIFF(j)   = DIFF(K)
30      CONTINUE
       DO 35 I = 1,4
         J = I + 14
         K = J + 5
         CSALL(J) = CSALL(K)
         NAMALL(J) = NAMALL(K)
         RATALL(J) = RATALL(K)
         HLFALL(J) = HLFALL(K)
         UPTAKE(J) = UPTAKE(K)
         DIFF(J)   = DIFF(K)
35      CONTINUE
C
c   The concentration of U234 in the second chain must be zeroed.
c    Otherwise, it amounts to doubling the amount of U234 present
c    in the inventory.  SWIFT accounts for a branched chain automatically
c    so this change is necessary if we are to compare comparable cases.
```

```
c
        CSALL(20) = 0.0
c
c
        I1 = ISTART
        I2 = IEND
        DEF(1) = 0.
        IDEF = 1
C
       DO 400 ICHN = 1,NCHNS
c
        DEF(ICHN) = 0.
C
c  The following IF-THEN loop computes the chain diffusivity from
c   the isotope diffusivities by one of two methods.  First, the
c   the maximum isotope diffusivity is assigned to the chain.  Second
c   the chain diffusivity is computed as an average of all isotope
c   diffusivities weighted by half-lives and initial inventories.
c
       IF( IDEF .EQ. 1 ) THEN
C
        DO 502 K = I1,I2
         IF( DIFF(K).GT.DEF(ICHN) ) DEF(ICHN) = DIFF(K)
         IF( K .NE. I2 ) SIG(K) = DIFF(K+1)/DIFF(K)
         SIG(K) = 1.0
 502     CONTINUE
c
       ELSE
C
        SCALE = 0.0
c
        DO 500 K = I1,I2
         SCALE = SCALE + HLFALL(K)*AINV(K)
 500     CONTINUE
c
        IF( SCALE .EQ. 0.) THEN
C
         DEF(ICHN) =  DIFF(I1)
C
        ELSE
C
        DEF(ICHN) = 0.0
C
        DO 600 K = I1,I2
C
         DEF(ICHN) = DEF(ICHN) + DIFF(K)*HLFALL(K)*AINV(K)/SCALE
         IF( K .NE. I2 ) SIG(K) = DIFF(K+1)/DIFF(K)
C
 600     CONTINUE
C
        ENDIF
C
       ENDIF
C
       IF( ICHN .NE. NCHNS ) THEN
         I1 = I1 + NI(ICHN)
         I2 = I2 + NI(ICHN + 1)
       ENDIF
c
 400     CONTINUE
c
C  DEBUG WRITE STATEMENTS
C
C       WRITE(*,*) (NAMALL(I),I=1,25)
C       WRITE(*,*) (CSALL(I),I=1,25)
C        WRITE(*,*) (DEF(I),I=1,NCHNS)
```

```
C       WRITE(*,*) ( K,SIG(K),K=1,NOISO)
C
C  END OF INPUT STATEMENTS
C
C  BEGIN CALCULATIONS
C
C  FOR DIFFUSION PART OF SOLUTION, NOT DEPENDENT ON WHICH
C  ISOTOPE SINCE DEFF IS NOT ISOTOPE SPECIFIC, THEREFORE
C  CAN CALCULATE PART OF THE FLUX (FROM DIFFUSION)
C
C
C  DEBUG WRITE TO OUTPUT FILE
C
      WRITE(12,*)'ISTART = ',ISTART
      WRITE(12,*)'IEND =', IEND
c
C
C  LOOP OVER EACH CHAIN MEMBER FOR DECAY PART OF SOLUTION
C
      WRITE(11,*)(NCHNS-1)
c
      FLUXI1TOT = 0.
      FLUXI2TOT = 0.
c      FLUXI3TOT = 0.
C
      DO 100 I = 1,NCHNS
        DO 70 K = ISTART,IEND
          DO 60 J = 1, NTIME

        T(J) = DELTAT*FLOAT(J)
c
        DOB = H2 - ERN
C
C  DETERMINE NORMALIZED FLUX AT EROSION DEPTH ZONE ( H2 - ERN )
C
        CALL GETFLUX( DEF(I), DOB, H2 - ERN, T(J), TFLUX1, N1 )
C
C
C  COMPUTE THE DIMENSIONAL FLUX AT EROSION DEPTH
C
          FLUXD1(J) = 1.0/SQRT(PI*DEF(I)*T(J))*TFLUX1
C
C  COMPUTE AVERAGE CONCENTRATION IN THE ROOT ZONE
C
        IF( DOB - ROOTD .GT. 0.0)THEN
C
        CALL GETCONC( DEF(I), DOB, DOB - ROOTD, T(J), CONC1, N3 )
c
        ENDIF
c
        CAVE(J) =   CONC1
C
C  DE-BUG WRITE TO OUTPUT FILE
C
c          WRITE(12,*)'TIME,YRS=', T(J),'FLUXD1=', FLUXD1(J)
c          WRITE(12,*)'TIME,YRS=', T(J),'FLUXD2=', FLUXD2(J)
c          WRITE(12,*)'TIME,YRS=', T(J),'CAVE=', CAVE(J)
C
c          WRITE(12,*)' ITERATIONS ' , N1, N2
C

          CALL RADDEC(T(J),ISTART,IEND,RATALL,CSALL,SIG,CDUMMY)
          CDECAY(J,K) = CDUMMY(K)
C
C  DE-BUG WRITE TO OUTPUT FILE
C
```

```
C              WRITE(12,*)'TIME =',T(J), 'CDECAY =', CDECAY(J,K)
C
C  CALCULATE FLUX FOR EACH ISOTOPE
C
               FLUX1(J,K) = THETA*DEFF*CDECAY(J,K)*FLUXD1(J)
c              FLUX3(J,K) = THETA*DEFF*CDECAY(J,K)*FLUXD3(J)
C
               CDECAY(J,K) = CDECAY(J,K)*CAVE(J)
C
C
c  COMPUTATION OF THE BIO FLUX IS DONE ASSUMING A YEARLY REGENERATION
C   CYCLE.  THAT IS, EVERY YEAR THE PLANT CONCENTRATION RETURNS TO
C    ZERO TO REPRESENT A NEW GENERATION OF VEGETATION.
c
            IF( DOB - ROOTD .LT. 0.0)THEN
C
C         IF ROOTS ENTER THE WASTE PACKAGE, THE UPTAKE CONCENTRATION
C           IS ASSUMED TO BE AT THE SOLUBILITY LIMIT
C
              FLUX2(J,K) = CSALL(K)
C
            ELSE
C
              FLUX2(J,K) =   CDECAY(J,K)
C
            ENDIF
c
c  TRANSPORT OF RN BACKWARD ALONG THE PLANT UPTAKE PATHWAY IS NOT ALLOWED
C
              IF( FLUX2(J,K) .LT. 0.0 ) FLUX2(J,K) = 0.
C
C  DE-BUG WRITE TO OUTPUT FILE
C
c             WRITE(12,*)'TIME = ',T(J), 'FLUX1 = ', FLUX1(J,K)
c             WRITE(12,*)'TIME = ',T(J), 'FLUX2 = ', FLUX2(J,K)
c             WRITE(12,*)'TIME = ',T(J), 'FLUX3 = ', FLUX3(J,K)
C
C  CALCULATE INTEGRATED FLUX FOR EACH ISOTOPE USING SIMPSON RULE
C
              IF (J.EQ.2) THEN
C
               FLUXI1(J,K) = ( FLUX1(J,K) + 4.0*FLUX1(J-1,K) )
               FLUXI2(J,K) = ( FLUX2(J,K) + 4.0*FLUX2(J-1,K) )
c               FLUXI3(J,K) = ( FLUX3(J,K) + 4.0*FLUX3(J-1,K) )
               FLUXI1(J,K) = FLUXI1(J,K)*DELTAT/3.0
               FLUXI2(J,K) = FLUXI2(J,K)*DELTAT/3.0
c               FLUXI3(J,K) = FLUXI3(J,K)*DELTAT/3.0
c
C
              ELSEIF ( MOD(J,2) .EQ. 0 ) THEN
C
               A1 = FLUX1(J,K) + 4.0*FLUX1(J-1,K) + FLUX1(J-2,K)
               A2 = FLUX2(J,K) + 4.0*FLUX2(J-1,K) + FLUX2(J-2,K)
c               A3 = FLUX3(J,K) + 4.0*FLUX3(J-1,K) + FLUX3(J-2,K)
C
               FLUXI1(J,K)=FLUXI1(J-2,K)+ A1*DELTAT/3.0
               FLUXI2(J,K)=FLUXI2(J-2,K)+ A2*DELTAT/3.0
c               FLUXI3(J,K)=FLUXI3(J-2,K)+ A3*DELTAT/3.0
C
C  DE-BUG WRITE TO OUTPUT FILE
C
c             WRITE(12,*)'TIME = ', T(J), 'FLUXI1 = ', FLUXI1(J,K)
c             WRITE(12,*)'TIME = ', T(J), 'FLUXI2 = ', FLUXI2(J,K)
c             WRITE(12,*)'TIME = ', T(J), 'FLUXI3 = ', FLUXI3(J,K)
c
            ENDIF
```

```
C
60          CONTINUE
70        CONTINUE
C
C  CONVERT INTEGRATED FLUX AT TUB FROM ATOMS TO CURIIES
C
        DO 80 M = ISTART, IEND
        FACT = 1.684E18 * HLFALL(M)
        FLUXI2(NTIME,M) = FLUXI2(NTIME,M)*UPTAKE(M)*BIODENS
c
c    The factor DEFF/DIFF(M) = R_M accounts for sorption in the biomodel
c      The factor of 2.0 accounts for turnover of the biomass
c
        FLUXI2(NTIME,M) = FLUXI2(NTIME,M)*(DEFF/DIFF(M) ) *2.0
c
        FLUXI2(NTIME,M) = FLUXI2(NTIME,M)/FACT*AREA
        FLUXI1(NTIME,M) = FLUXI1(NTIME,M)/FACT*AREA
c        FLUXI3(NTIME,M) = FLUXI3(NTIME,M)/FACT*AREA
        FLUXI(NTIME,M)  = FLUXI1(NTIME,M) + FLUXI2(NTIME,M)
c     +                                + FLUXI3(NTIME,M)
C
        FLUXI1TOT = FLUXI1TOT + FLUXI1(NTIME,M)
        FLUXI2TOT = FLUXI2TOT + FLUXI2(NTIME,M)
c        FLUXI3TOT = FLUXI3TOT + FLUXI3(NTIME,M)
C
C  DE-BUG WRITE TO OUTPUTFILE
C
c     WRITE(12,*)M,'FLUXI1=',FLUXI1(NTIME,M),'FLUXI2=',FLUXI2(NTIME,M)
C
80        CONTINUE
C
C  WRITE RESULTS TO OUTPUT FILE
C
          IF ((I .NE. 4) .AND. (I .NE. 5)) THEN
            WRITE(11,*)NI(I),(NAMALL(J),J=ISTART,IEND)
            WRITE(11,*)NOTV,(FLUXI(NTIME,J),J=ISTART,IEND)
          ENDIF
          IF (I .EQ. 5) THEN
            FLUXI(NTIME,20) = FLUXI(NTIME,20) + FLUXI(NTIME,15)
            FLUXI(NTIME,21) = FLUXI(NTIME,21) + FLUXI(NTIME,16)
            FLUXI(NTIME,22) = FLUXI(NTIME,22) + FLUXI(NTIME,17)
            FLUXI(NTIME,23) = FLUXI(NTIME,23) + FLUXI(NTIME,18)
            WRITE(11,*)7,NAMALL(13),NAMALL(14),(NAMALL(J),J=19,23)
            WRITE(11,*)NOTV,FLUXI(NTIME,13),FLUXI(NTIME,14),
     *                 (FLUXI(NTIME,J),J=19,23)
          ENDIF
          IF (I .NE. NCHNS) THEN
            ISTART = ISTART + NI(I)
            IEND = IEND + NI(I+1)
          ENDIF
100     CONTINUE
C
C  OUTPUT TOTAL INTEGRATED FLUX OF ALL ISOTOPES TO ROOTS
C   AND SURFACE
C
        WRITE(12,*)' TOTAL INTEGRATED DISCHARGES: '
        WRITE(12,'(3(A,E15.6))')' PAST EROSION DEPTH : ',
     *     FLUXI1TOT,' VIA PLANT PATH : ',FLUXI2TOT,
     *             ' PAST SURFACE   : ',FLUXI3TOT
200   CONTINUE
C
C
C
C
C
```

```
c
c       ISTART = 1
c c      IEND = NI(1)
C
c       dt = 1000.
c       DO 501 ICHN = 1,NCHNS
c       DO 301 J = 1,10
c        TT = dt*float(j)
c       DO 401 X = 0.,70.,10.
c
c       CALL CHECKIT(ISTART,IEND,X,TT,DOB,DEF(ICHN),RATALL,SIG,CSALL)
c
c 401    CONTINUE
c 301    CONTINUE
C
c          IF (ICHN .NE. NCHNS) THEN
c            ISTART = ISTART + NI(ICHN)
c            IEND = IEND + NI(ICHN+1)
c          ENDIF
c
c 501    CONTINUE
c
c      ISTART = 1
c      IEND = NI(1)
c
c      IND(1) = 1
c
c     DO 401 I = 1,NCHNS
C
c     IF (I .NE. NCHNS) THEN
c       IND(I+1) = ISTART + NI(I)
c       ISTART = IND(I+1)
c       IEND = IEND + NI(I+1)
c     ENDIF
C
c 401   CONTINUE
C
c     READ(10,*)ICHN,ISPACE
cC
c     ISTART = IND(ICHN)
c     IEND   = IND(ICHN) + NI(ICHN) - 1
C
c     K = 1
c     DOB = 70.0
c     X = 0.
c     NSTP = 4
c c    DT = TUB/FLOAT(NSTP)
c
c     DO WHILE ( X .LE. 70.)
C
c      DO 501 J = 0,NSTP
C
c        TT = FLOAT(J)*DT
c        CALL GETCONC(DEF(ICHN),DOB, X, TT,CONC1,N3)
c        CALL RADDEC(TT,ISTART,IEND,RATALL,CSALL,SIG,CDUMMY)
C
c        DO 601 I = 0,NI(ICHN) - 1
c          CPLOT( J + (NSTP+1)*I,K) = CDUMMY( ISTART + I )*CONC1
c          CPLOT( J + (NSTP+1)*I,K) = CPLOT( J + (NSTP+1)*I,K)
c    +                              CSALL( ISTART + I )
c 601      CONTINUE
C
c 501      CONTINUE
C
c c       X = K*35.
c       K = K + 1
```

```
C
c      ENDDO
C
C      ITIME = 5
C
c      DO 701 K = 0,NI(ICHN) - 1
c       DO 801 J = 0,NSTP
cc         WRITE(11+K,*)DT*FLOAT(J), CPLOT(J + (NSTP+1)*K,ISPACE)
c 801     CONTINUE
c 701    CONTINUE

      STOP
      END



      SUBROUTINE RADDEC(T,I1,I2,DECAY,C0,S,C)
      IMPLICIT REAL*8 (A-H,O-Z)
C
C  THIS SUBROUTINE HAS BEEN MODIFIED FROM ONE THAT WAS
C  WRITTEN BY FRED GELBARD TO SOLVE THE BATEMAN EQUATIONS
C  USING A MATRIX SOLUTION.  SEE NUREG/CR-5412(SAND89-1521)
C  FOR A DESCRIPTION OF THE EQUATIONS USED.
c
c  Modified by : T.A. Baer
C
C  LIST OF VARIABLES
C
C      T     = TIME (YEARS)
C      I1    = BEGINING POINTER FOR C0 AND DECAY ARRAY
C      I2    = ENDING POINTER FOR C0 AND DECAY ARRAY
C      DECAY = ARRAY OF DECAY RATES (1/YEAR)
C      C0    = ARRAY OF INITIAL CONCENTRATIONS (ATOMS/FT**3)
C      C     = OUTPUT ARRAY OF CONCENTRATIONS (ATOMS/VOLUME)
C              FOR EACH ISOTOPE AT TIME T
C      A     = ARRAY OF ALPHA'S
C      S     = ARRAY OF RATIOS OF RETARDATION FACTORS
C      B     = EIGENVECTORS
C
      DIMENSION DECAY(25),C0(25),C(25), S(25)
      DIMENSION A(25),B(25,25)
C
      DO 2 I = I1,I2
        DO 2 J = I1,I2
          IF(I.LT.J)THEN
            B(I,J)=0.
          ENDIF
          IF(J.EQ.I)THEN
            B(I,J)=1.0
          ENDIF
          IF(I.GT.J)THEN
            IM1=I-1
            PROD=1.
          DO 3 K=J,IM1
            PROD=PROD*DECAY(K)*S(K)/(DECAY(K+1)-DECAY(J))
3         CONTINUE
          B(I,J)=PROD
        ENDIF
2     CONTINUE
C
      A(I1)=C0(I1)
      DO 4 I=I1+1,I2
        IM1=I-1
        SUM=C0(I)
        DO 5 J=1,IM1
          SUM=SUM-A(J)*B(I,J)
```

```
5      CONTINUE
       A(I)=SUM
4     CONTINUE
C
      DO 6 I=I1,I2
        SUM=0.
        DO 7 J=1,I
          SUM=SUM+A(J)*B(I,J)*EXP(-DECAY(J)*T)
7       CONTINUE
        C(I)=SUM
6     CONTINUE
C
      RETURN
      END
c
      SUBROUTINE GETFLUX ( DEFF, DOB, X, T, FLUX, N )
C
      IMPLICIT REAL*8 (A-H,O-Z)
      LOGICAL DF
C
C   CASE: ZERO ESSENTIAL CONDITION AT THE LAND SURFACE
C
C  THIS SUBROUTINE RETURNS A VALUE FOR THE NORMALIZED FLUX
C   ( FLUX*SQRT( PI*DEFF*T) AT X AND T.  THE SOLUTION WAS
C   OBTAINED FROM CRANK(* ).  HOWEVER, THE SPATIAL COORDINATE WAS
C   MODIFIED FROM THAT USED BY CRANK SO THAT X = 0 OCCURS AT THE
C   TOP OF THE WASTE.
C
C * J. CRANK, *THE MATHEMATICS OF DIFFUSION*, OXFORD SCI. PUB., 1975
C
          SUM1A = 0.
          SUM1B = 0
          SUM2A = 0
          SUM2B = 0
C
          TERM1A = 0.
          TERM2A = 0.
          TERM1B = 0.
          TERM2B = 0.
C
          N = 0
          DF = .TRUE.
C
        DO WHILE ( DF )
C
          RN = N
C
          TERM1A = EXP(-( 2.*RN*DOB+ X )**2/(4.*DEFF*T ))
C
          SUM1A = SUM1A + TERM1A
C
          TERM1B = EXP(-(2.*RN*DOB- X)**2/(4.*DEFF*T ))
C
          IF( N .EQ. 0 ) TERM1B = 0.

          SUM1B = SUM1B + TERM1B
c
              RELERR = ABS ( TERM1A + TERM1B ) / ABS( SUM1A + SUM1B )
C
C  CHECK TO SEE IF NEW TERM IS INSIGNIFICANT WITH RESPECT TO
C   SUMMATION AND IF SO SIGNAL LOOP TO TERMINATE.  ALSO FLUX MAYBE
C   EXACTLY ZERO AND LOOP WILL TERMINATE UNDER THIS CONDITION AS WELL
C
          IF( ( RELERR .LT. 1.E-5 )
     +    .OR. ( N .GT. 10 )
     +    .OR. ( ( SUM1A + SUM1B ) .EQ. 0.0 ) ) THEN
```

```
            DF = .FALSE.

          ENDIF

        N = N + 1
C
      END DO
C
      FLUX = SUM1A + SUM1B
      N  = N - 1
C
    RETURN
    END
c
    SUBROUTINE GETCONC ( DEFF, DOB, X, T, CONC, N)
    IMPLICIT REAL*8 (A-H,O-Z)
    LOGICAL DF
C
C  CASE: ZERO ESSENTIAL CONDITION AT THE LAND SURFACE
C
C  RETURNS NORMALIZED CONCENTRATION ( C/C0 ) AT X AND T
C   THE ANALYTIC SOLUTION WAS OBTAINED FROM CRANK(*).  HOWEVER,
C   THE SPATIAL COORDINATE WAS MODIFIED FROM THAT USED BY CRANK
C   SO THAT X = 0 OCCURS AT THE TOP OF THE WASTE.
C
C * J. CRANK, *THE MATHEMATICS OF DIFFUSION*, OXFORD SCI. PUB., 1975

C
    SUM1A  = 0.
    TERM1A = 0.
    SUM1B  = 0.
    TERM1B = 0.
c
    DF = .TRUE.
    N = 0
C
    DO WHILE ( DF )
C
     RN = N
C
     GROUP1 =  ( 2.0*RN*DOB + X )/DSQRT( 4.0*DEFF*T)
     GROUP2 =  ( 2.0*RN*DOB - X )/ DSQRT(4.0*DEFF*T)
C
     TERM1A = ERFCC( GROUP1 )
     TERM1B = ERFCC( GROUP2 )
C
     IF( N .EQ. 0 ) TERM1B = 0.
C
     SUM1A = SUM1A + TERM1A
     SUM1B = SUM1B + TERM1B
C
     RELERR = ABS ( TERM1A - TERM1B ) / ABS ( SUM1A - SUM1B )
C
C  CHECK TO SEE IF NEW TERM IS INSIGNIFICANT WITH RESPECT TO
C   SUMMATION AND IF SO SIGNAL LOOP TO TERMINATE.  ALSO CONC MAYBE
C   EXACTLY ZERO AND LOOP WILL TERMINATE UNDER THIS CONDITION AS WELL
c
     IF ( ( RELERR .LT. 1.E-5 )
    + .OR. ( N .GT. 10 )
    + .OR. ( ( SUM1A - SUM1B ) .EQ. 0.0 ) ) THEN

        DF = .FALSE.

     ENDIF
C
     N = N + 1
```

```
C
      END DO
C
      CONC = SUM1A - SUM1B
C
      RETURN
      END
C
     FUNCTION ERFCC(X)
c
c  This subroutine returns the complementary error function at X
c
      IMPLICIT REAL*8 (A-H,O-Z)
      Z = ABS(X)
      V = 1.0/(1.0 + 0.5*Z)
      ERFCC=V*EXP(-Z*Z-1.26551223+V*(1.00002368+V*(.37409196+
     *     V*(.09678418+V*(-.18628806+V*(.27886807+V*(-1.13520398+
     *     V*(1.48851587+V*(-.82215223+V*.17087277)))))))) .
      IF (X.LT.0) ERFCC=2.-ERFCC
      RETURN
      END
C
      SUBROUTINE CHECKIT(I1,I2,X,T,DOB,DEFF,RATALL,S, CSALL)
c
c  This subroutine was used in checking the correct operation
c   of the program and the solution subroutines.
c
      IMPLICIT REAL*8 ( A-H, O-Z)
      DIMENSION RATALL(25), CSALL(25), D2X(25), DCDT(25)
      DIMENSION CDUM(25), CDUM1(25), CDUM2(25),S(25)
C
      PI = 3.141592653589793238D0
c
      WRITE(12,*)' X = ',X, ' T = ',T
c
      CALL GETFLUX( DEFF, DOB, X, T, FLUX, N)
C
      DX = 1.e-4
      DT = .01
C
      CALL GETFLUX( DEFF, DOB, X + DX, T, FLUX1, N )
      CALL GETFLUX( DEFF, DOB, X - DX, T, FLUX2, N )
C
      FLUX1 = -1.0*FLUX1/(DSQRT(PI*DEFF*T))
      FLUX2 = -1.0*FLUX2/(DSQRT(PI*DEFF*T))
C
      CALL GETCONC( DEFF, DOB, X     , T, CONC1, N )
      CALL RADDEC(T,I1,I2,RATALL,CSALL,S,CDUM )
C
      CALL GETCONC( DEFF, DOB, X + DX, T, CONC2, N )
      CALL GETCONC( DEFF, DOB, X - DX, T, CONC3, N )
      CALL GETCONC( DEFF, DOB, X + 2.*DX, T, CONC4, N )
      CALL GETCONC( DEFF, DOB, X - 2.*DX, T, CONC5, N )
C
      D2XB = ( CONC2 - 2.0*CONC1 + CONC3 ) /DX/DX
C
      FLUX4 = ( CONC4 - CONC1 ) /2./DX
      FLUX5 = ( CONC1 - CONC5 )/2./DX
C
      D2XC  = ( FLUX1 - FLUX2 )/2./DX
C
      CALL GETCONC( DEFF, DOB, X, T, CONC0, N )
      CALL GETCONC( DEFF, DOB, X, T - DT, CONC1, N )
      CALL GETCONC( DEFF, DOB, X, T + DT, CONC2, N )
      CALL RADDEC(T+DT,I1,I2,RATALL,CSALL,S,CDUM1 )
      CALL RADDEC(T-DT,I1,I2,RATALL,CSALL,S,CDUM2 )
```

```
C
      DO 30 K = I1,I2
C
      D2X(K) = D2XC*CDUM(K)
      DCDT(K) = ( CONC2*CDUM1(K) - CONC1*CDUM2(K) ) / 2.0 / DT
C
      RES = DCDT(K) - DEFF*D2X(K)+ RATALL(K)*CONC0*CDUM(K)
      IF(K .NE. I1 ) RES = RES - RATALL(K-1)*CONC0*CDUM(K-1)*S(K-1)
C
      SCALE = .33*( DABS(DCDT(K) ) + DABS ( DEFF* D2X(K) ) +
     +              DABS( RATALL(K)*CONC0*CDUM(K) ) )

      RERR = ABS ( RES ) / SCALE
C
      WRITE(12,*) 'ISOTOPE ',K
      WRITE(12,*) '  ABSOLUTE RESIDUAL',ABS(RES),
     +      ' RELATIVE RESIDUAL ', RERR
C
 30   CONTINUE
C
      RETURN
      END
```

Distribution

Federal Agencies

U.S. Department of Energy
Office of Environmental Restoration and
Waste Management
Attn: T. P. Grumbly, EM-1
Forrestal Building
Washington, DC 20585-0002

U.S. Department of Energy
Office of Environmental Restoration and
Waste Management
Attn: M. Frie, EM-34, Trevion II
Director, Waste Management Projects
Washington, DC 20585-0002

U.S. Department of Energy [8]
Office of Environmental Restoration and
Waste Management
Attn: David Huizenga, EM-30
Jill E. Lytle EM-30
Warren Black, EM-322
Joseph Boda, EM-322
Wayne Nobles, EM-332
Joe Coleman, EM-35
Betty Shackleford, EM-331
Leanne Smith, EM-60
Jay Rhoderick, EM-351
Washington, DC 20585-0002

U.S. Department of Energy [6]
Nevada Operations Office
Attn: Doug Duncan
Joe Fiore
Joe Ginanni [2]
Layton O'Neill
Technical Information Office
2743 S. Highland Drive
Las Vegas, NV 89193-8518

U.S. Department of Energy
WIPP Project Integration Office
Attn: Paul Dickman
One Park Square, Suite 903
6501 Americas Parkway NE
Albuquerque, NM 87110

U.S. Department of Energy
WIPP Task Force
Attn: B. Bower
12800 Middlebrook Road, Suite 400
Germantown, MD 20874

U.S. Department of Energy
Carlsbad Area Office
Attn: George Dials, Manager
P.O. Box 3090
Carlsbad, NM 88221-3090

U.S. Department of Energy
National TRU Program Office
Carlsbad Area Office
Attn: Mark Matthews
P.O. Box 3090
Carlsbad, NM 88221-3090

Linda M. Smith
Associate Director for Geologic Disposal
Department of Energy
Yucca Mountain Site Characterization
Project Office
P. O. Box 98608
Las Vegas, NV 89193-8608

U.S. Department of Energy
Office of Geologic Disposal
Yucca Mountain Project Office
Attn: Associate Director RW-20
P.O. Box 98608
Las Vegas, NV 89193-8608

U.S. Environmental Protection Agency
Attn: Reid Rosnick
Mail Code 5303 W
401 M Street SW
Washington, DC 20460

U.S. Environmental Protection Agency
Office of Radiation/Indoor Air
Criteria and Standards [3]
Attn: Ray Clark
William Gunter, Jr.
Lawrence Weinstock
Mail Code 6602J
401 M Street SW
Washington, DC 20460

U.S. Nuclear Regulatory Commission [4]
Advisory Committee on Nuclear Waste
Attn: D. Moeller
M. J. Steindler
R. W. Pomeroy
W. J. Hinze
7920 Norfolk Avenue
Bethesda, MD 20814

Defense Nuclear Facilities Safety Board
Attn: D. Winters
625 Indiana Ave NW
Suite 700
Washington, DC 20004

Nuclear Waste Technical Review Board
Attn: Library [2]
1100 Wilson Blvd
Suite 910
Arlington, VA 22209-2297

Office of Management and Budget
Energy and Science Division
Attn: K. Yuracko
725 17th Street NW
Washington, DC 20503

Yucca Mountain Project Office
U.S. Department of Energy
Attn: Russell Dyer
P.O. Box 98608
Las Vegas, NV 89103

U.S. Nuclear Regulatory Commission [6]
Attn: R. Codell
L. Deering
N. Eisenberg
M. Federlina
T. McCartin
J. Randall
Mail Stop 4-H-3
Washington, DC 20555

National Laboratories

Battelle Pacific Northwest Laboratories
Attn: P.W. Eslinger
MS K2-32
P.O. Box 999
Richland, WA 99352

Idaho National Engineering Laboratory[3]
Attn: H. Loo
R. Klinger
Darryl Siemer
Mail Stop 5108
P.O. Box 1625
Idaho Falls, ID 83403-4000

Idaho National Engineering Laboratory
EG & G Idaho Inc.
Attn: Sven Magnusson
P.O. Box 1625
Idaho Falls, ID 83415

Corporations/Members of the Public

John F. Ahearne
Executive Director, Sigma Xi
99 Alexander Drive
Research Triangle Park, NC 27709

Center for Nuclear Waste Regulatory Analysis (CNWRA)
Southwest Research Institute
Attn: B. Sagar
P.O. Drawer 28510
6220 Culebra Road
San Antonio, TX 78284

R.L. Bras Consulting Engineers
Attn: Rafael L. Bras
44 Percy Road
Lexington, MA 02173

Desert Research Institute - North
Attn: Scott Tyler
P.O. Box 60220
Reno, NV 89506

Desert Research Institute - South
Attn: Jenny Chapman
P.O. Box 19040
Las Vegas, NV 89132-0040

Disposal Safety, Inc
Attn: B. Ross
1660 L. Street NW, Suite 314
Washington, SC 20036

Golder Associates, Inc. [2]
Attn: R. Kossik
I. Miller
4104 148th Avenue NE
Redmond, WA 98052

INTERA, Inc.
Attn: W. Nelson
A. E. Van Luik
Valley Bank Building
101 Convention Center Drive
Suite 540
Las Vegas, NV 89109

Raytheon/Environmental Operations [3]
Attn: Dennis Gustafson
Julie Miller
Stuart Rawlinson
222 S. Rainbow, Suite 115
Las Vegas, NV 89128

Reynolds Electrical and Engineering Company, Inc. [9]
Attn: Dale Daffern
Bob Dodge
Max Dolenc
Brian Dozier
Dudley Emer
Dale Hammermeister
Tom Lindstrom
Greg Shott
Mike Sully
Mail Stop 738
P.O. Box 98521
Las Vegas, NV 89193-8521

Science Applications International Corporation (SAIC)
Attn: H. R. Pratt
10260 Campus Point Drive
San Diego, CA 92121

Science Applications International Corporation (SAIC)
Attn: C. G. Pflum
101 Convention Center Drive
Las Vegas, NV 89109

Science Applications International
Corporation (SAIC)
Attn: K. Brinster
2109 Air Park Road SE
Albuquerque, NM 87106

Westinghouse Hanford Co.
Attn: Don Wood
MS HO-33
P.O. Box 1970
Richland, WA 99352

Foreign Agencies

International Atomic Energy Agency [2]
Division of Nuclear Fuel Cycle and
Waste Management
Attn: Shaheed Hossain
Gordon S. Linsley
Wagramerstrasse 5
P.O. Box 100
A-1400 Vienna, AUSTRIA

Atomic Energy of Canada Limited [3]
Whiteshell Research Establishment
Attn: M. E. Stevens
B. W. Goodwin
D. Wushke
Pinawa, Manitoba ROE 1L0, CANADA

Miroslav Kucerka
Botevova 3104
143 00 Praha 4
CZECH REPUBLIC

Timo Vieno
Technical Research Centre of Finland
(VTT)
Nuclear Energy Laboratory
P.O. Box 208
SF-02151 Espoo, FINLAND

OECD Nuclear Energy Agency [2]
Attn: Claudio Pescatore
Jean-Pierre Olivier
Le Seine-Saint Germain
12 Boulevard des Iles
F-92130 Issy-les-Moulineaux, FRANCE

Gesellschaft für Reaktorsicherheit (GRS)
MBH
Attn: P. Bogorinski
Schwertnergasse 1
D-5000 Köln 1, GERMANY

Netherlands Energy Research Foundation
(ECN) [2]
Attn: J. Prij
L.H. Vons
3 Westerduinweg
P.O. Box 1
NL-1755 ZG Petten
THE NETHERLANDS

CIEMAT [2]
Instituto de Tecnología Nuclear
Attn: P. Prado
C. Ruiz
Avenida Complutense, 22
E-28040 Madrid, SPAIN

ENRESA [2]
Attn: P. Carboneras Martinez
Calle Emilio Vargas 7
R-28043 Madrid, SPAIN

Royal Institute of Technology
Automatic Control
Attn: Björn Cronhjort
S-100 44 Stockholm, SWEDEN

Svensk Kärnbränsleforjning AB
Project KBS
Attn: Fred Karlsson
Box 5864
S-102 40 Stockholm, SWEDEN

Swedish Nuclear Fuel and Waste Management Company (SKB) [3]
Attn: Torsten Eng
Nils A. Kjellbert
Tonis Papp
Box 5864
S-102 48 Stockholm, SWEDEN

Swedish Nuclear Power Inspectorate
Statens Kärnkraftinspektion (SKI)
Attn: Johan Andersson
Box 27106
S-102 52 Stockholm, SWEDEN

HSK-Swiss Nuclear Safety Inspectorate
Federal Office of Energy
Attn: J. Vigfusson
CH-5232 Villigen-HSK, SWITZERLAND

Nationale Genossenschaft für die Lagerung Radioaktiver Abfälle [3]
Attn: C. McCombie
F. Van Dorp
P. Zuidema
Hardstrasse 73
CH-5430 Wettingen, SWITZERLAND

Paul Scherrer Institute [2]
Waste Management Programme
Attn: Richard A. Klos
J. Hadermann
CH-5232 Villigen PSI, SWITZERLAND

Department of the Environment
Her Majesty's Inspectorate of Pollution
Attn: Brian G.J. Thompson
Room A5.33, Romney House
43 Marsham Street
London SW1P 2PY
UNITED KINGDOM

Galson Sciences Ltd.
Attn: Daniel A. Galson
35 Market Place
Oakham, Leicestershire LE15 6DT
UNITED KINGDOM

Intera Information Technologies
Attn: N.A. Chapman
Park View House
14B Burton Street
Melton Mowbray, Leicestershire
LE131AE
UNITED KINGDOM

Intera Information Technologies
Attn: David P. Hodgkinson
45 Station Road, Chiltern House
Henley-on-Thames
Oxfordshire RG9 1AT
UNITED KINGDOM

UK Nirex LTD
Attn: Alan J. Hooper
Harwell, Didcot
Oxfordshire OX11 ORH
UNITED KINGDOM

Internal

MS	ORG	
1351	3020	N. E. Olague
0750	6118	H. W. Stockman
1337	6300	D. E. Ellis
1335	6301	F. W. Bingham
1335	6302	L. E. Shephard
1335	6303	W. D.Weart
1335	6305	S. A. Goldstein
1341	6306	A. L. Stevens
1345	6307	P. A. Davis
1326	6312	H. A. Dockery
1326	6313	L. S. Costin
1335	6319	D. Brosseau
1330	6352	GCD Records Center/S34
1345	6331	T. A. Baer
1345	6331	T. Brown

1345	6331	J. Cochran
1345	6331	S. H. Conrad
1345	6331	B. Delker
1345	6331	L. Dubes
1345	6331	F. A. Durán
1345	6331	J. N. Emery
1345	6331	T. Feeney
1345	6331	B. Fogleman
1345	6331	D. P. Gallegos [30]
1345	6331	R. V. Guzowski
1345	6331	E. Kalinina
1345	6331	M. W. Kozak
1345	6331	G. C. Newman
1345	6331	L. L. Price
1345	6331	L. Snyder
1345	6331	J. Reitzel
1345	6331	C. D. Updegraff
1345	6331	B. Vocke
1345	6331	E. K. Webb
1328	6342	D. R. Anderson
1328	6342	M. Marietta
1330	6352	Nuclear Waste Management Library [2]
0727	6622	M. S. Y. Chu
0727	6622	J. T. McCord
1339	6903	G. W. Barr
0743	6907	M. Harrington
0743	6907	C. P. Harlan
1347	7581	W. B. Cox
1347	7585	K. C. Gaither

1	MS	9018	Central Technical Files, 8523-2
5	MS	0899	Technical Library, 7141
1	MS	0619	Technical Publications, 7151
10	MS	0100	Document Processing for DOE/OSTI, 7613-2

END DATE
9-14-94

*U.S. GOVERNMENT PRINTING OFFICE 1994-0-573-026/00009